# A network of bHLHZip transcription factors in melanoma: Interactions of MITF, TFEB and TFE3

**Josué A. Ballesteros Álvarez**

**Thesis for the degree of Philosophiae Doctor**

January 2019

UNIVERSITY OF ICELAND
SCHOOL OF HEALTH SCIENCES
FACULTY OF MEDICINE

# Net bHLHZip umritunarþátta í sortuæxlum: Samstarf milli MITF, TFEB og TFE3

**Josué A. Ballesteros Álvarez**

**Ritgerð til doktorsgráðu**

**Leiðbeinandi/leiðbeinendur:**
Eiríkur Steingrímsson

**Doktorsnefnd:**
Margrét H. Ögmundsdóttir

Þórarinn Guðjónsson

Jórunn E. Eyfjörð

Lars Rönnstrand

Janúar 2019

UNIVERSITY OF ICELAND
SCHOOL OF HEALTH SCIENCES
FACULTY OF MEDICINE

ISBN 978-9935-9421-4-2

Printing by Háskólaprent

Reykjavik, Iceland 2019

# Ágrip

Stjórnpróteinin MITF , TFEB, TFE3 og TFEC (stundum nefnd MiT-TFE þættirnir) tilheyra bHLHZip fjölskyldu umritunarþátta sem bindast DNA og stjórna tjáningu gena. MITF er mikilvægt fyrir myndun og starfsemi litfruma en ættingjar þess, TFEB og TFE3, stjórna myndun og starfsemi lysósóma og sjálfsáti. Sjálfsát er líffræðilegt ferli sem gegnir mikilvægu hlutverki í starfsemi fruma en getur einnig haft áhrif á myndun og meðhöndlun sjúkdóma.

Í verkefni þessu var samstarf MITF, TFE3 og TFEB próteinanna skoðað í sortuæxlisfrumum og hvaða áhrif þau hafa á tjáningu hvers annars. Eins og MITF eru TFEB og TFE3 genin tjáð í sortuæxlisfrumum og sortuæxlum; TFEC er ekki tjáð í þessum frumum og var því ekki skoðað í þessu verkefni. Með notkun sérvirkra hindra var sýnt að boðleiðir hafa áhrif á staðsetningu próteinanna þriggja í sortuæxlisfrumum. Umritunarþættir þessir geta bundist skyldum DNA-bindisetum og haft áhrif á tjáningu gena sem eru nauðsynleg fyrir myndun bæði lýsósóma og melanósóma. Áhugavert er að hver umritunarþáttanna þriggja stjórnar tjáningu gena sem hinir hafa engin áhrif á en ekki er ljóst hvernig þessari takmörkun er stjórnað. Þessi þættir stjórna tjáningu hvers annars, bæði beint og óbeint. Með mótefnisfellingu kom í ljós að MITF, TFEB og TFE3 geta myndað mistvenndir í æxlisfrumum en geta ekki myndað mistvenndir með öðrum bHLHZip próteinum eins og MAX. Þriggja amínósýru-svæði, sem er til staðar í HLH-Zip svæðinu, er nauðsynlegt fyrir þessa sértæku tvenndarmyndun. Hlutverk þessara amínósýra var greint frekar og, með tilfærslu þessara þriggja amínósýra, var reynt að útbúa MITF prótein sem einungis geta myndað einstvenndir. Það tókst ekki en áhugaverðar upplýsingar fengust um hvernig tvenndarmyndun MITF fer fram.

Niðurstaðan er að sambandið milli MITF, TFEB og TFE3 í sortuæxlisfrumum er flókið og felst í áhrifum á stjórnun genatjáningar, samstarfi próteina með myndun mistvennda og áhrifum boðleiða á staðsetningu í frumulíffærum. Mikilvægt er að greina og skilja þetta samband í sortuæxlum til að öðlast betri skilning á því hvernig unnt er að hafa áhrif á þau ferli sem umritunarþættir þessir stjórna.



**Lykilorð:**

Sortuæxli, MITF, TFEB, TFE3, sjálfsát

## Abstract

The MITF, TFEB, TFE3 and TFEC (MiT-TFE) proteins belong to a larger family of basic helix-loop-helix leucine zipper transcription factors that are able to bind DNA and regulate gene expression. MITF is crucial for melanocyte development and has been called a lineage specific oncogene in melanoma whereas its relatives, TFEB and TFE3 are involved in the biogenesis and function of lysosomes and autophagosomes, regulating cellular clearance pathways. Autophagy is a biological process that plays a prominent role in human disease and can also have an impact on the outcome of therapeutic approaches. Whether MITF, TFEB and TFE3 regulate each others expression and whether they cooperate in the regulation of gene expression is presently unknown.

I have investigated the interactions and cross-regulatory relationship of MITF, TFE3 and TFEB in melanoma cells. Like MITF, the TFEB and TFE3 genes are expressed in melanoma cells and tissues. I show that these factors regulate each other's expression. Also, using co-immunoprecipitation studies, I demonstrate that MITF, TFEB and TFE3 are able to heterodimerize in melanoma cells. However, they fail to interact with other members of the bHLH family such as MAX. Furthermore, I show that a three amino acid region present in the HLH-Zip region is responsible for dimerization specificity. In addition, several signaling pathways can post-translationally modify these factors, affecting their nuclear localization, activity and stability. Reporter gene and ChIP assays show that the three factors are able to bind and activate similar DNA regulatory motifs and drive the expression of genes involved in autophagy and pigmentation. Interestingly, some genes are exclusively regulated by one of the factors.

The relationship between MITF, TFEB and TFE3 is complex and involves regulation of gene expression, protein-protein interactions resulting in complementary functions. It is important to further unravel this relationship in melanoma to gain a better understanding of the cross-regulatory mechanisms involved and how these factors regulate lysosomal function.



**Keywords:**

Melanoma, MITF, TFEB, TFE3, autophagy

# Acknowledgements

All the work presented in this dissertation has been performed in the laboratory of Prof. Eiríkur Steingrímsson, the supervisor of this PhD project. Eiríkur's lab is part of the Department of Biochemistry and Molecular Biology at the BioMedical Center of the University of Iceland in Reykjavík, Iceland. This work could not have been carried out without the financial support of the Icelandic Research Fund (Rannís).

Thank you so much Eiríkur for making this possible. When I first visited your lab back in 2013 asking for a job I could not imagine how much I would learn throughout these years, and how this entire experience would shape me, not only professionally as a scientist, but also the way I think and how I understand the reality around me.

Thank you Margrét for all the scientific discussions that took place on a regular basis and were crucial to the development of my entire PhD project. Also, you conveyed to me your deep interest in autophagy, and I really think I would like to continue this subject in the future. I wish you success in your growing "autophagy lab".

Thank you to the remaining members of my doctoral committee, Prof. Þórarinn Guðjónsson, Prof. Jórunn Erla Eyfjörð and Prof. Lars Rönnstrand. They provided critical assessment of my project during the regular PhD committee meetings held to discuss the project. There is no way to build a solid piece of research without the constructive criticism that allows you to be your own biggest critic. Also, a big thank you to Drs. Vivian Pogenberg and Mathias Wilmanns at the EMBL in Hamburg. It was (still is) an honor to collaborate with such experts in understanding the structure of MITF. And how much more there is yet to discover.

Thank you to Ramile Dilshat, Ludwig Karl, Ingibjörg Sigvaldadóttir, Katrín Möller, Ásgeir Örn Árnþórsson and Kimberley Anderson for your direct contribution to this thesis with your hard work. You are greatly talented people. My gratitude to Lionel Larue for contributing to this thesis with the microarray expression data. Also, thank you Prof. Colin Goding and Dr. Erna Magnusdóttir for the plasmid constructs thoroughly used in this work. Thank you Dr. Sævar Ingþórsson for all your assistance with the confocal microscope at the imaging core of the BioMedical Center.

To all the lab members not yet mentioned, Valerie Fock, Sara Sigurbjörnsdóttir, Diahann Atacho, Sigurður Rúnar Guðmundsson, Kristín Bergsteinsdóttir, Hilmar Gunnlaugsson, Lára Stefansson, Linda Sooman, Freyja Imsland and Berglind Einarsdóttir. I learned a lot from each one of you during your lab meetings and day to day interactions. I am looking forward to the next chapter in my life but I will definitely miss you. I wish you all the best!

A heartfelt thank you to Prof. Guðmundur Hrafn Guðmundsson for introducing me to Iceland and planting the first seed of my scientific career.

Thank you so much Borys for your support and for the fun times that made easier to go through the slightly stressful final stages of my PhD. Thank you Alba for our everyday conversations about my research and your research in Naples. We never stop laughing and it is great to have a friend for so long that exactly understands you.

Finally, but most importantly, thank you to my loving parents Chelo and Luis and my siblings Alberto, Elda and Zoila. It is the biggest blessing to have a family that loves you and supports you unconditionally and without reservations. Mum and dad, you have always encouraged me since I was a kid to study and to pursue my career of choice. For this, you gave me all the emotional and material support I would need, and I could never thank you enough for this. I love you.

# Contents

# List of abbreviations

| | |
|---|---|
| °C | Degrees Celsius |
| 4EBP1 | 4E-binding protein 1 |
| A | Alanine |
| AC | Adenylate cyclase |
| AD | Alzheimer disease |
| Ala | Alanine |
| AME | Analysis of motif enrichment |
| AMP | Adenosine monophosphate |
| AMPK | Adenosine monophosphate kinase |
| ANOVA | Analysis of the variance |
| APS | Ammonium persulfate |
| Arg | Arginine |
| ATF4 | Activating transcription factor 4 |
| ATG | Autophagy related |
| ATP | Adenosine triphosphate |
| AXL | Tyrosine-protein kinase receptor UFO |
| BECN1 | Beclin-1 |
| bHLH | Basic helix-loop-helix |
| BHLHZip | Basic helix-loop-helix leucine zipper |
| BMP4 | Bone morphogenetic protein 4 |
| bp | Base pairs |
| BRG1 | Brahma-related gene 1 |
| BRN2 | N-Oct-3 |
| BSA | Bovine serum albumin |
| C | Cytosine |
| Ca | Calcium |
| cAMP | Cyclic-adenosine-monophosphate |
| Cas9 | CRISPR associated protein 9 |

| | |
|---|---|
| CBP | CREB binding protein |
| CDK2A | Cyclin-dependent kinase inhibitor 2A |
| ChIP-seq | Chromatin immunoprecipitation-sequencing |
| CHX | Cycloheximide |
| CLEAR | Coordinated Lysosomal Expression and Regulation |
| CMA | Chaperone-mediated autophagy |
| CMN | Common acquired melanocytic nevus |
| COMMAD | Coloboma, osteopetrosis, microphthalmia, macrocephaly, albinism and deafness |
| CREB | cAMP responsive-element binding protein |
| CRISPR | Clustered Regularly Interspaced Short Palindromic Repeats |
| CTSD | Cathepsin protease D |
| CTSZ | Cathepsin protease Z |
| Cys | Cysteine |
| Da | Dalton |
| DAPI | 4′,6-diamidino-2-phenylindole |
| DEC1 | Differentially expressed in chondrocytes protein 1 |
| DEP | Dishevelled, Egl-10 and Pleckstrin |
| DEPTOR | DEP domain-containing mTOR-interacting protein |
| DEPC | Diethyl pyrocarbonate-treated |
| DMEM | Dulbecco's Modified Eagle Medium |
| DMN | Dysplastic melanocytic nevus |
| DMSO | Dimethyl sulfoxide |
| E | Glutamate |
| E-box | Ephrussi box |
| EDN3 | Endothelin-3 |
| EDNRB | Endothelin B receptor |
| EDTA | Ethylenediaminetetraacetic acid |
| EGFR | Epidermal growth factor receptor |
| ER | Endoplasmic reticulum |

| | |
|---|---|
| ERK | Extracellular-signal regulated kinase |
| ESC | Embryonic stem cells |
| EV | Empty vector |
| FKBP12 | FK506-binding protein 12 |
| FOXD3 | Forkhead box D3 |
| FUS | Fused in sarcoma protein |
| G | Glycine |
| GALC | Galactosylceramidase |
| GDP | Guanosine diphosphate |
| GFP | Green fluorescent protein |
| GLB1L | Galactosidase Beta 1 Like |
| GNS | N-acetylglucosamine-6-sulfatase |
| GO | Gene Ontology |
| GSK3β | Glycogen synthase kinase-3β |
| GTP | Guanosine triphosphate |
| h | Hour |
| HA | Human influenza hemagglutinin |
| HAT | Histone acetyl transferase |
| HBSS | Hank's balanced saline solution |
| HDAC | Histone deacetylase |
| HIF-1 | Hypoxia inducible factor 1 |
| HLH | Helix-loop-helix |
| hsc70 | Heat shock cognate 71 kDa protein |
| hUBC9 | Human ubiquitin carrier protein 9 |
| IFN-γ | Interferon γ |
| K | Lysine |
| kDa | Kilodalton |
| KIT | Tyrosine kinase receptor |
| KSR | Kinase suppressor of Ras |
| LAMP | Lysosome-associated membrane protein |
| LB | Lysogeny broth |
| LC3 | Microtubule-associated protein light chain 3 |

| | |
|---|---|
| LEF-1 | Lymphoid enhancer-binding factor 1 |
| Leu | Leucine |
| LMN | Lentiginous melanocytic nevus |
| LSD | Lysosomal storage disease |
| MAD | MAX dimerization protein 1 |
| MAPK | Mitogen-activated protein kinase |
| MAPKK | Mitogen-activated protein kinase kinase |
| MAP1LC3B2 | Microtubule-associated protein 1 light chain 3 beta 2 |
| MAX | Myc-associated factor X |
| MCOLN1 | Mucolipin-1 |
| MC1R | Melanocortin-1-receptor |
| MHC | Major histocompatibility complex |
| min | Minute |
| miRNA | MicroRNA |
| MITF | Microphthalmia-associated transcription factor |
| mL | Milliliter |
| MLANA | Melan-A protein |
| mM | Millimolar |
| MMCP6 | Mouse mast cell protease 6 |
| mRNA | Messenger RNA |
| mSIN1 | Mammalian stress-activated MAP kinase-interacting protein 1 |
| mTOR | Mammalian target of rapamycin |
| mTORC | Mammalian target of rapamycin complex |
| MYC | Myelocytomatosis oncogene |
| NC | Neural crest |
| NCC | Neural crest cells |
| NF1 | Neurofibromin 1 |
| NHEM | Normal human epidermal melanocytes |
| NK | Natural killer |
| NLS | Nuclear localization signal |

| | |
|---|---|
| NSF | N-ethylmaleimide-sensitive factor |
| nsSNVs | Non-synonymous single nucleotide variants |
| OIS | Oncogene-induced senescence |
| OS | Overall survival |
| $p14^{ARF}$ | p14 alternate reading frame protein |
| $p16^{INK4A}$ | p16 cell cycle inhibitor of kinase 4A |
| p90RSK | p90 ribosomal s6 kinase |
| PAX3 | Paired box gene 3 |
| pBac | Piggybac |
| PBS | Phosphate-buffered saline |
| PCR | Polymerase chain reaction |
| PDA | Pancreatic ductal adenocarcinoma |
| PD-1 | Programmed death-1 |
| PE | Phosphatidylethanolamine |
| PFA | Paraformaldehyde |
| PI3K | Phosphatidylinositol 3-kinase |
| PIAS3 | Protein inhibitor of the activated STAT3 |
| PKA | Protein kinase A |
| PKCβ | Protein kinase C β |
| PMEL | Premelanosome protein |
| PMSF | Phenylmethylsulfonyl fluoride |
| PNK | Polynucleotide kinase |
| POMC | Pro-opiomelanocortin |
| PP1α | Protein phosphatase 1 alpha |
| PRAS40 | 40-kDa proline-rich Akt substrate |
| PTEN | Phosphatase and tensin homolog |
| PVDF | Polyvinylidene fluoride |
| $R^2$ | Coefficient of determination |
| RAF | Rapidly accelerated fibrosarcoma protein |
| RANKL | Receptor activator NF-kappa B ligand |
| RAPTOR | Regulatory-associated protein of mTOR |
| RAS | Rat sarcoma protein |

| | |
|---|---|
| RGP | Radial growth phase |
| Rho | Spearman's rank correlation coefficient |
| RICTOR | Rapamycin-insensitive companion of mTOR |
| ROS | Reactive oxygen species |
| RPE | Retinal pigmented epithelium |
| RPS6 | Ribosomal protein S6 |
| RSK | 40S ribosomal protein S6 kinase |
| RTK | Receptor tyrosine kinase |
| RT-qPCR | Real Time quantitative PCR |
| S6K1 | S6 kinase beta-1 |
| SCF | Stem cell factor |
| SDS | Sodium dodecyl sulfate |
| SDS-PAGE | Sodium dodecyl sulfate–polyacrylamide gel electrophoresis |
| sec | Second |
| SEM | Standard error of the mean |
| Ser | Serine |
| siRNA | Small interference RNA |
| Sl | Steel factor |
| SLC17A5 | Solute carrier family 17, member 5 |
| SMARCA2 | SWI/SNF related, matrix-associated, actin-dependent regulator of chromatin A2 |
| SNARE | Soluble NSF attachment protein receptor |
| SNCA | Alpha-synuclein |
| SOC | Super optimal broth with catabolite repression |
| SOX10 | SRY-box 10 |
| SPNS2 | Sphingolipid transporter 2 |
| SRY | Sex-determining region Y |
| STAT | Signal transducer and activator of transcription |
| SUMO | Small ubiquitin-like modifier |
| T | Thymine |

| | |
|---|---|
| TBS | Tris-buffered saline |
| TCGA | The Cancer Genome Atlas |
| TEMED | N,N,N′,N′-Tetramethylethylenediamine |
| TFE3 | Transcription factor 3 |
| TFEB | Transcription factor EB |
| TFEC | Transcription factor EC |
| TP53 | Tumor protein 53 |
| TRE | Tetracycline response element |
| Trp | Tryptophan |
| TPA | 12-O-Tetradecanoylphorbol-13-acetate |
| TRPML | Transient receptor potential cation channel mucolipin |
| TS | Tietz's Syndrome |
| TSC | Tuberous sclerosis complex |
| TSS | Transcription start site |
| TYR | Tyrosinase |
| TYRP1 | Tyrosinase-related protein 1 |
| ULK1 | UNC51-like kinase 1 |
| ULK2 | UNC51-like kinase 2 |
| USF | Upstream stimulatory factor |
| UV | Ultra-violet |
| UVRAG | UV radiation resistance-associated gene protein |
| V | Valine |
| V | Volt |
| Val | Valine |
| vATPase | V-type ATPase |
| VGP | Vertical growth phase |
| WNT | Wingless type |
| WS2A | Waardenburg Syndrome type 2A |
| Zip | Leucine zipper |
| ZNF263 | Zinc finger protein 263 |
| α-MSH | Alpha-melanocyte-stimulating-hormone |

| | |
|---|---|
| µl | Microliter |
| µm | Micrometer |
| µM | Micromolar |

# List of figures

# List of tables

## List of original papers

I. *MITF, TFEB and TFE3 interact and regulate each other's expression in melanoma*
**Josué Ballesteros Álvarez**, Ramile Dilshat, Ásgeir Örn Arnþórsson, Kimberley Anderson, Margrét Helga Ögmundsdóttir, Lionel Larue, Eiríkur Steingrímsson
Manuscript in preparation

II. *Mechanism of restricted partner selectivity in MiT/TFE family transcription factors with a conserved coiled-coil stammer motif*
Vivian Pogenberg, **Josué Ballesteros Álvarez**, Romana Schober, Ingibjörg Sigvaldadóttir, Morlin Milewski, Margrét Helga Ögmundsdóttir, Rainer Schindl, Eiríkur Steingrímsson and Matthias Wilmanns
Manuscript in preparation

## Declaration of contribution

All the experiments described in this study were designed and performed with the supervision of my supervisor Prof. Eiríkur Steingrímsson and Dr. Margrét Helga Ögmundsdóttir. I have written the manuscript which is currently in preparation, listed as **Paper I** above. In addition, I performed all the analysis and figures included in this thesis and performed the co-immunoprecipitation experiments included in **Paper II** in the list of original papers shown above.

The generation of the inducible cell lines included in the Materials and methods section was performed by Ramile Dilshat, a PhD student, and Dr. Sara Sigurbjörnsdóttir, a postdoctoral fellow in the lab. The analysis of the nuclear localization and transactivation ability of the MITF(Δ259-261) mutant shown in **Figure 18**, described in section **4.3.1 The role of a three-residue insertion in the leucine zipper of the MiT-TFE transcription factors**, was performed by Ingibjörg Sigvaldadóttir as part of her BSc project, under supervision of Dr. Margrét Helga Ögmundsdóttir. In addition, **Figure 19D** in this same section, which shows the structural coiled-coil arrangement of mutant MITF(Δ259-261) in opposition to wild type MITF, was performed by Vivian Pogenberg at the EMBL in Hamburg Germany. **Figure 19D** is part of the manuscript listed as **Paper II**.

Ramile Dilshat generated the TFEB chromatin immunoprecipitation sequencing data in human melanoma cells, and assisted me in data analysis. The analysis of expression of MITF, TFEB, TFE3 and TFEC in melanoma samples described in **Figure 7A**, and the analysis of the correlation of MITF, TFEB and TFE3 with a list of lysosomal genes presented in **Table 13**, were performed by Katrín Möller. These analyses were part of her MSc project under the supervision of Dr. Margrét Helga Ögmundsdóttir and Eiríkur Steingrímsson, and is currently subject of a submitted manuscript that is undergoing the reviewing process. The analysis of the ability of MITF, TFEB and TFE3 to transactivate the wild type tyrosinase promoter or variations thereof containing E-boxes, M-boxes or CLEAR boxes were performed by Ásgeir Örn Arnþórsson as part of his MSc

project, under the supervision of Dr. Margrét Helga Ögmundsdóttir and Eiríkur Steingrímsson.

# 1 Introduction

## 1.1 Melanocytes

### 1.1.1 Development

Melanocytes are responsible for the production and distribution of the pigment melanin in vertebrates. The melanocyte precursor cells are called melanoblasts and are derived by lineage specification from neural crest cells (NCC) during embryogenesis. NCC arise from the embryonic ectoderm. These cells are originally multipotent and can differentiate into neurons, glial cells, muscle cells, fibroblasts, chondrocytes and melanocytes. They gradually undergo determination of their lineage fate, influenced by their anatomical localization along the cranial-caudal axis. Melanoblast-committed NCC expand and migrate to the dermis, epidermis and hair follicles. During development, most melanoblasts follow a dorsolateral migration trajectory from the neural crest (NC). However, there is evidence that a number of melanoblasts originate from Schwann cell precursors that have migrated ventrally but have not committed to the neural lineage (Adameyko et al., 2009). As melanoblasts travel through the dermis and proliferate, they begin to progressively express melanocyte-specific genes (Cichorek et al., 2013). Cutaneous melanocytes that are responsible for the pigmentation of skin or hair and have followed the dorsolateral migration pathway from the NC, are described as classical melanocytes. Non-classical melanocytes do not fulfill these three criteria, and can be found in the inner ear, retina and iris, meninges, adipose tissue, heart and bone. The function of non-classical melanocytes remains unclear (Borovanský & Riley, 2011).

Melanocyte differentiation is dependent upon initiation of the expression of required transcription factors, such as paired box gene 3 (PAX3) (Potterf et al., 2000; Tassabehji et al., 1992), sex-determining region Y (SRY)-box 10 (SOX10) (Potterf et al., 2000; Stolt et al., 2008) and microphthalmia-associated transcription factor (MITF) (Adameyko et al., 2012; Opdecamp et al., 1997). Furthermore, the activity of signaling pathways is important, including wingless type (WNT) (Dunn et al., 2005), where increase of WNT3A expression and reduced expression of bone morphogenetic protein 4 (BMP4) induce melanoblast formation in avian embryo neural crest cultures (E. J. Jin et al., 2001). The transcription factors PAX3 and SOX10 are crucial for the

development of melanoblasts by activating *MITF* transcription (Potterf et al., 2000; Stolt et al., 2008; Tassabehji et al., 1992). Interestingly, PAX3 and SOX10 also contribute to initial glial cell development, suggesting that other factors are also involved in the differentiation pathway specific to melanocytes. Forkhead box D3 (FOXD3) is found in glia progenitors but not in melanocyte precursors. It is able to repress MITF expression in melanoma cells, even in the presence of PAX3 and SOX10 (Thomas & Erickson, 2009). In line with this, SOX2 is able to induce neural crest cells to switch to glial differentiation by binding to the promoter of MITF and repressing its expression (Adameyko et al., 2012). Mutations in PAX3 or SOX10 result in melanocytic loss in vertebrates, similar to mutations in MITF (Tachibana et al., 2003). Other pathways that are required for the development of the melanocytic lineage are the G-coupled endothelin B receptor (EDNRB), its ligand endothelin-3 (EDN3) (Stanchina et al., 2006); and the tyrosine kinase receptor KIT (Aoki et al., 2005; Karafiat et al., 2007). The KIT receptor has been shown to be required during the migration of melanocytes through the dermis and for post-natal hair pigmentation (Hachiya et al., 2009; Yoshida et al., 2001).

In summary, melanocytic differentiation is based on a combination of silenced transcription factors, such as FOXD3 and SOX2 that are required for glial development from NC cells, coupled with an increase in expression of PAX3 and SOX10 and subsequent upregulation of MITF.

### 1.1.2 Function

Melanocytes are the cells responsible for the synthesis of melanin, by enzymatic oxidation and polymerization of the amino acid tyrosine. Each skin melanocyte is approximately 7 μm in length and contacts 30-40 neighboring keratinocytes through melanocytic pseudopodia called dendrites. The distribution of melanocytes varies across species. In humans they constitute about 5-10% of the cells in the basal layer of the epidermis, whereas in rodents they are mostly found in the hair follicles and epidermis of hairless skin (Borovanský & Riley, 2011).

Melanogenesis is the process through which melanocytes produce melanin. There are two major types of melanin: the dark brown/black eumelanin and the red/yellow pheomelanin. Melanin is produced and transported in specific membrane-bound organelles, called melanosomes, which are delivered to the adjacent keratinocytes through the melanocytic dendrites (**Figure 1**). Keratinocytes function as a barrier against pathogens and ultra-violet (UV) radiation, the latter being absorbed by melanin and thereby, minimizing cellular damage due to reactive oxygen species (ROS)

and DNA mutagenesis. Melanosomes are lysosome-related organelles that go through four different stages of maturation. Stage I premelanosomes are found perinuclearly and have been suggested to derive from endosomes originated

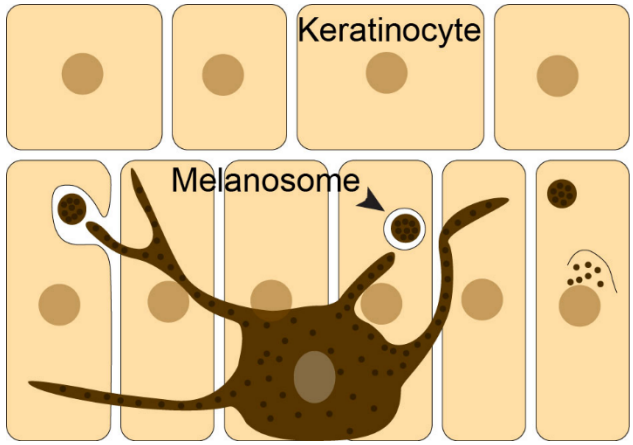


**Figure 1. Classical melanocyte in the basal layer of the skin.** Melanocytes produce melanin pigment and deliver it to neighboring keratinocytes.

from the *trans* Golgi network and go through several steps of maturation. Mature melanosomes produce and accumulate melanin and appear as solid dark pigmented vesicles (Raposo & Marks, 2007).

The differences in skin color among the human population are not determined by the number of melanocytes in the individual's skin, rather the size and amount of melanosomes they contain, and the quantitative and relative abundance of eumelanin and pheomelanin produced in the cell. Pheomelanin is less efficient at blocking UV radiation and has been shown to promote melanoma, independent of UV radiation (Mitra et al., 2012). Melanin biosynthesis is a process under hormonal control, arising from the cross-talk of melanocytes and keratinocytes. Exposure of skin to UV radiation triggers DNA damage and subsequent activation of TP53 which enhances the expression of pro-opiomelanocortin (POMC) in keratinocytes (Cui et al., 2007; Fields & Jang, 1990). POMC is the precursor of the alpha-melanocyte-stimulating-hormone α-MSH, a full agonist of the melanocortin-1-receptor (MC1R). Binding of α-MSH to MC1R activates adenylate cyclase (AC),

increasing the production of the second messenger cyclic-adenosine-monophosphate (cAMP) (Pawelek et al., 1973). Increased levels of cAMP activates protein kinase A (PKA), leading to phosphorylation of the transcription factor cAMP responsive-element binding protein (CREB) and CREB-mediated upregulation of MITF (Bertolotto et al., 1998; Price, Horstmann, et al., 1998). MITF, in turn, activates the transcription of several genes that are required for the melanin biosynthesis machinery.

## 1.2 Melanoma

### 1.2.1 Epidemiology and molecular mechanisms

Skin cancer is the most common of all cancers. The three main types are basal-cell carcinoma, cutaneous squamous-cell carcinoma and melanoma. Melanoma tumors account for only 2% of skin cancer diagnoses but is the most aggressive form of skin cancer (**Figure 2**). It is almost exclusively confined to the Caucasian population and its incidence has been rising during the past decades. Melanoma incidence among US and Northern Europe white population has increased by circa 3% annually from 1982 and 2011 (Whiteman et al., 2016). The melanoma incidence rate is projected to continue rising, as long as there are no significant improvements regarding sun-seeking and tanning behavior and use of protective clothing or sunscreen (Leiter et al., 2014). It is not entirely understood whether the habit of sunbathing results from

**Figure 2. Melanoma.** Image from National Cancer Institute. https://visualsonline.cancer.gov/details.cfm?imageid=9186

an aesthetic preference or it involves physiological addiction. Epidermal keratinocytes produce POMC and the POMC-derived β-endorphin upon UV exposure (Fell et al., 2014). β-endorphin is an endogenous opioid neuropeptide that has analgesic effects and can cause tolerance and addiction (Olive et al., 2001). It has also been proposed to induce sun-seeking behavior (Fell et al., 2014).

Melanoma is the deadliest among skin cancers, and metastatic melanoma features a particularly poor prognosis. The median survival period was 6–9 months with an overall survival (OS) of 10%–15% in 2008 (Thirlwell & Nathan, 2008). However, great advances have been made in recent years in the management of metastatic melanoma. Treatment with the immune checkpoint inhibitor targeting programmed death-1 (PD-1) nivolumab increased the OS to 71% at 1 year and 41% at 3 years (Hodi et al., 2010). 95% of melanomas are cutaneous melanomas, however, ocular, mucosal, genitourinary, meningeal and gastrointestinal melanomas can occur (Markovic et al., 2007). Among cutaneous melanomas, the sites of occurrence of melanoma tumors are sex-dependent. The back area is the most common in males, whereas arms and legs are more common in females (Newell et al., 1988).

Melanoma tumor genomes are notoriously unstable and carry the highest mutational burden among all cancers (Cancer Genome Atlas, 2015). Exposure to UV can trigger the formation of photoproducts that distort the DNA helix, generating C > T and CC > TT transitions, namely UV-fingerprint mutations, which contribute to >90% of all non-synonymous single nucleotide variants (nsSNVs) in melanoma (Hodis et al., 2012). The most frequent mutation found in cutaneous melanoma is the hot-spot BRAFV600E somatic mutation in approximately 50% of tumors, that results in a hyperactive BRAF-MAPK pathway (Forbes et al., 2008). NRAS somatic mutations is the second major mutation, found in 28% of cutaneous melanoma tumors. Interestingly, hot-spot BRAF and NRAS mutations are mutually exclusive (Cancer Genome Atlas, 2015; Davies et al., 2002).

In addition to the exposure to UV radiation in susceptible populations, the most important risk for the development of cutaneous malignant melanoma is the number of melanocytic nevi. Nevi are a benign clonal proliferation of melanocytic cells with a heterogeneous genetic background (Magana-Garcia & Ackerman, 1990). 20-30% of melanomas arise from preexisting nevi (Rivers, 2004). Congenital nevi have been reported to feature a high prevalence of *BRAF* mutations (Pollock et al., 2003; Yazdi et al., 2003), while other studies have pointed to *NRAS* mutations (Bauer et al., 2007; Carr & Mackie, 1994). A

reason for this discrepancy is the study methodology. Nevus size and whether its origin is congenital or acquired after birth are factors that mark different nevi subpopulations that need to be taken into consideration for the analysis of genetic alterations. In fact, genetic characterization of large/giant congenital nevi shows that they feature NRAS and not BRAF mutations (Charbel et al., 2014). A majority of nevi are acquired after birth. However, individuals with fair skin and a propensity to sunburn are more prone to develop nevi during their lifetime. In a study, 78% of all acquired nevi studied had a *BRAF* mutation, whereas *NRAS* was mutated in only 6% of cases (Roh et al., 2015).

In the light of the high frequency of BRAF mutations in nevi, it is clear that this mutation is not sufficient to drive melanomagenesis. Nevi carrying mutated BRAF eventually undergo oncogene-induced senescence, involving increased expression of the p16 cell cycle inhibitor of kinase 4A ($p16^{INK4A}$) (Michaloglou et al., 2005). $p16^{INK4A}$ and p14 alternate reading frame protein ($p14^{ARF}$) are tumor suppressor proteins encoded by the cyclin-dependent kinase inhibitor 2A (*CDK2A)* gene, crucial at controlling cell-cycle arrest. $p16^{INK4A}$ has been found to be frequently silenced epigenetically in BRAF-mutated melanomas, however, it was not sufficient to drive melanoma transformation *in vitro*, suggesting that other genes are involved in bypassing BRAF-induced senescence (Dhomen et al., 2009). Mutations occurring in other tumor suppressors, such as the phosphatase and tensin homolog (PTEN) and tumor protein 53 (TP53) have been found in advanced invasive primary melanomas (Shain et al., 2015).

Another gene that has been associated to increased risk of developing melanoma is *MC1R*, which is highly polymorphic in the Caucasian population (Valverde et al., 1995). Several *MC1R* loss-of-function germline variant alleles have been associated to red hair, fair skin and freckling, which fail to stimulate cAMP production in response to α-MSH signaling to induce melanin production (Frandberg et al., 1998; Schioth et al., 1999). Furthermore, an increased risk of skin melanoma has been found for carriers of some of these variants, such as Val60Leu, Arg151Cys, and Arg160Trp (Palmer et al., 2000).

### 1.2.2 Stages in cutaneous melanocytic tumors progression

Due to their easy visualization, melanocytic lesions are well characterized and classified. The Clark scale comprises six steps of progression from a benign nevus to a fully transformed malignant melanoma (Clark et al., 1969): (1) the common acquired melanocytic nevus (CMN); (2) lentiginous melanocytic nevus (LMN); (3) dysplastic melanocytic nevus (DMN); (4) primary malignant melanoma with radial growth phase (RGP), which may be in situ or invasive

but is non-tumorigenic; (5) primary malignant melanoma with vertical growth phase (VGP), invasive and tumorigenic; and (6) metastatic melanoma. CMN are fully benign local proliferations of melanocytes. DMN are intermediate lesions that progressively acquire genetic mutations and present signs of atypia such as abnormal morphology, aberrant differentiation and nuclear atypia. Most DMN remain stable or regress but a fraction can progress to malignant melanoma. A RGP melanoma is generally non-invasive (*in situ*) and expands along the surface of the epidermis showing increased signs of pigmentation variegation, atypia and irregular margins. RGP lesions can progress to the more advanced VGP stage, associated with higher metastasis risk. VGP lesions are nodular in morphology and can invade the dermis and continue proliferating, forming a dermal mass larger than the original mass located in the epidermis. VGP lesions undergo additional genomic progression to metastatic melanoma, which is responsible for the lethality of cutaneous malignant melanoma (Elder, 2016).

### 1.2.3 MAPK/ERK pathway and melanoma

The Ras-Raf-MEK-ERK pathway, is one of the most studied intracellular signaling cascades. It consists of a series of proteins that communicates an extracellular stimulus from a cell surface receptor to the nucleus of the cell. Small peptides, namely mitogens, bind to receptors in the cell membrane triggering phosphorylation of the cytoplasmic domain of the receptor. This allows the GDP-bound Ras protein to exchange its GDP by GTP. Subsequently, GTP-bound Ras can modify the conformation of Raf protein, which leads to activation of Raf. Raf is a family of serine/threonine kinases, found to be mutated in many types of human cancers. Ras-induced activated Raf forms homo- or heterodimers with other proteins like kinase suppressor of Ras (KSR) (Ritt et al., 2006), and then recruits downstream mitogen-activated protein kinase kinase (MAPKK), which is phosphorylated and, in turn, phosphorylates MAPK/ERK. Phosphorylated extracellular-signal regulated kinase (ERK) is active and modulates the activity of transcription factors that are involved in cell cycle regulation or the translation of mRNA to proteins. MAPK activation phosphorylates 40S ribosomal protein S6 kinase (RSK), which in turn phosphorylates ribosomal protein S6 (RPS6) (Pende et al., 2004). RPS6 induces the translation of proteins involved in the regulation of glucose homeostasis, cell growth and proliferation (Magnuson et al., 2012). RSK can also directly regulate transcription factors such as c-MYC through phosphorylation (Zhu et al., 2008).

The Raf protein features a catalytic domain with kinase activity and an N-terminal regulatory domain that contains the Ras-binding activating domain and a cysteine-rich domain responsible for autoinhibition of the catalytic domain (Chong & Guan, 2003; Cutler et al., 1998). The basis of this self-regulatory mechanism is common to the three different members of the Raf family, A-Raf, B-Raf and C-Raf (Maurer et al., 2011; Tran & Frost, 2003). However, these proteins are differentially regulated at the level of post-translational modifications, which has an impact on their autoinhibitory activity (Tran et al., 2005). Whereas B-Raf is constitutively phosphorylated at serine 445 (Marais et al., 1997) and is more readily activated by Ras (Wellbrock et al., 2004), A-Raf and C-Raf need supplementary phosphorylations of activating residues and dephosphorylation of inhibitory residues in order to display full catalytic activity,

Approximately 50% of metastatic melanomas harbor hyperactivating *BRAF* mutations. Over 90% of the BRAF mutations are at codon 600, and over 90% of these are the single nucleotide mutation BRAFV600E. The second most frequent mutation is BRAFV600K in about 5% of cases (Forbes et al., 2008). Hyperactive BRAF is able to continue the signaling cascade independently of RAS activation and is functional as a monomer (Wan et al., 2004). The homologous mutations of the ARAF or CRAF genes are rare events in human cancer, since these proteins do not share the constitutively phosphorylated residues occurring in B-Raf. The BRAFV600E mutation causes a higher basal kinase activity of this protein and makes it a key player in tumorigenesis (Emuss et al., 2005).

To this date, there is no effective cure for metastatic melanoma, although great advances have been made with the development of immunotherapy (Syn et al., 2017) and targeted therapies using BRAF-MAPK inhibitors such as vemurafenib (Bollag et al., 2010). However, a broad interpatient heterogeneity and a variety of initiating events in the onset of melanoma lead to drug resistance and therapy failure in a majority of cases. Until recently, dacarbazine, a chemotherapeutic agent has been the most widely used treatment for metastatic melanoma, with unsatisfactory results (Gogas et al., 2007). The knowledge of the melanoma signature BRAFV600E mutation (Davies et al., 2002) propelled the development of targeted therapies using BRAF pathway inhibitors, such as vemurafenib (Bollag et al., 2010) and dabrafenib (Gibney & Zager, 2013). BRAF inhibitors provided striking anti-tumor responses and have been a breakthrough in the treatment of metastatic melanoma. However, the response to the treatment is short (average 7

months) and the tumors progress as resistance develops (Chapman et al., 2011; Flaherty et al., 2010; Hauschild et al., 2012; Sosman et al., 2012).

A study addressing the evolution of tumors under BRAF inhibition therapy identified several subsets of genes, such as G-protein coupled signaling, cAMP and PKA signaling and leukocyte extravasation, as the most significantly altered pathways in cells that have undergone BRAF inhibition treatment, compared to the parental untreated cell line (Kansler et al., 2017).

Another study found that among MAPK-reactivating mechanisms, *NRAS* mutations were detected in 18% of progressive tumors, *KRAS* mutations in 7%, *BRAF* amplification in 19% and mutant BRAF alternative splice variants in 13% of progressive tumors (Shi et al., 2014). A subset of melanoma cells resistant to BRAF inhibition with vemurafenib, expressed a 61 KDa variant of the BRAFV600E protein. p61BRAFV600E lacks exons 4-8, which include the Ras-binding domain, and is able to dimerize in a Ras-independent manner (Poulikakos et al., 2011). A MEK1 activating mutation and *CDKN2A* loss were also detected at a lower proportion. Therefore, among all the disease progressive samples a reactivation of the MAPK pathway as a mechanism of resistance to BRAF inhibition was found at a 70% frequency. Moreover, the study identified that PI3K-PTEN-AKT pathway mutations, constituted a second core acquired resistance pathway at a 22% frequency that overlapped with the MAPK core pathway. This study also showed that the mutational signature of the progressive tumors has a reduction in C > T transitions as well as an attenuated dipyrimidine motif, indicating non-UV related DNA damage (Shi et al., 2014).

## 1.3 MITF, the master regulator of melanocytes

The microphthalmia-associated transcription factor (MITF) was first discovered due to coat color mutations in mice (Hertwig, 1942). MITF belongs to the basic helix-loop-helix leucine zipper (bHLHZip) family of transcription factors. Mice that are deprived of MITF cannot produce melanocytes (Steingrimsson et al., 2004). Mutations at the mouse *Mitf* locus result in pigmentation defects of the coat, small eyes and deafness. Moreover, mast cell defects have also been recognized for certain *Mitf* alleles (Dubreuil et al., 1991). Therefore, it is regarded as the master regulator of the melanocytic lineage as it is required for the development, growth and survival of melanocytes, where it regulates the expression of various differentiation and cell-cycle progression genes (Steingrimsson et al., 2004). MITF is an evolutionarily conserved transcription factor subject to differential splicing, thus, being expressed as multiple

isoforms that differ in their first exon and promoter usage (Hodgkinson et al., 1993) (**Figure 3**). In most isoforms, the initial variable exon is spliced onto the exon 1B1b and then continues with exons 2–9 that include all the functionally important motifs necessary for protein dimerization and transactivation ability (Hershey & Fisher, 2005). The shortest isoform, termed MITF-M, which is the predominant isoform in melanocytes, contains a short exon 1M directly spliced onto exons 2–9 (Steingrimsson et al., 1994).

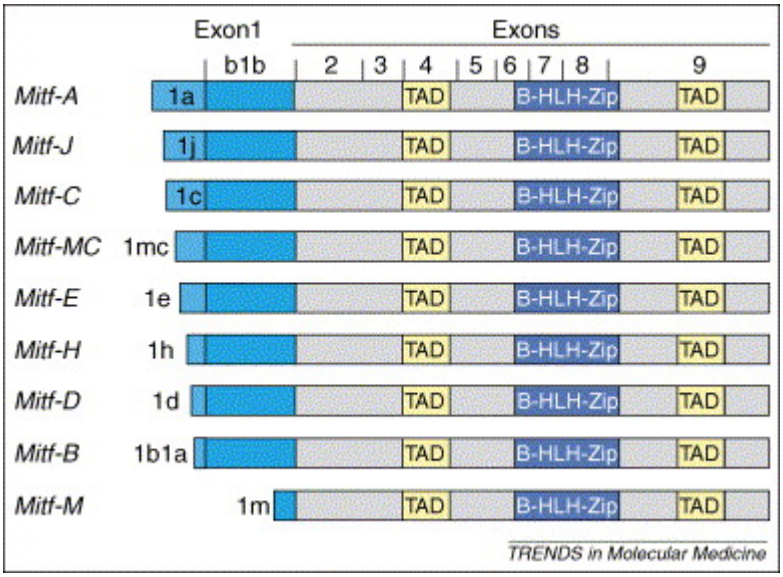


**Figure 3. The nine different isoforms of MITF described in humans.** Each MITF isoform features a variable exon 1 containing an isoform-specific promoter. Exons 2-9, which include the bHLHZIP and transactivation domain (TAD) are common to all isoforms. Figure obtained with permission from Elsevier according to permit number 4432560184009 (Levy et al., 2006).

The other isoforms of MITF have been described in a variety of cell types, including osteoclasts, natural killer cells, macrophages, mast cells, B cells, and cardiac muscle cells. MITF-MC is expressed in bone marrow-derived mast cells (Takemoto et al., 2002). MITF-D is mostly expressed in the human retinal pigment epithelium (RPE) (Takeda et al., 2002), while MITF-A, MITF-B, MITF-E and MITF-H are more ubiquitous (Hershey & Fisher, 2005). In the RPE, A, D, H and M isoforms of MITF have been detected at comparable levels

(Maruotti et al., 2012), in contrast with other studies that reported that MITF-M is not expressed in RPE cell lines (Shibahara et al., 2001). Whether these different isoforms have tissue-restricted functions is not well known. MITF-MC has been shown to selectively activate the promoter of the gene encoding the mouse mast cell protease 6 (*Mmcp6*) and to fail to activate the pigmentation related gene tyrosinase (*TYR*), known to be a target of MITF in melanocytes, as shown by gene transactivation assays (Takemoto et al., 2002). MITF-H has been shown to have a greater transactivation potential than MITF-M in cardiac cells, suggesting that the activity of MITF in the heart is isoform-specific (Tshori et al., 2007). Moreover, two isoforms of MITF called (+) and (-) exist, differing in exon 6a. The (+) isoform of MITF encodes six additional amino acids between Leu185 and Thr186, upstream of the DNA-binding basic domain (Hodgkinson et al., 1993). Both the MITF-M and MITF-H isoforms have been found to be expressed as (-) and (+) versions, although it is possible that this could be the case for all the MITF isoforms (Hallsson et al., 2000). Interestingly, the (+) isoform that includes the extra exon 6a exhibits a strong inhibitory effect on DNA synthesis (Bismuth et al., 2005). Furthermore, isoform quantification across melanoma samples revealed that differential expression is dependent on MEK1-ERK2 activation and that MITF(-) expression is enriched in a subset of metastatic melanomas (Primot et al., 2010).

### 1.3.1 MITF mutations in humans

In humans, mutations of *MITF* that lead to reduced transcription activation potential of MITF (Grill et al., 2013) have been linked to the relatively rare pigmentation disorders Waardenburg Syndrome type 2A (WS2A) (A. E. Hughes et al., 1994) and Tietz's Syndrome (TS) (Read & Newton, 1997; Smith et al., 2000). The WS2A subtype of the Waardenburg Syndrome, originated by mutations in *MITF* is the most common subtype and is characterized by permanent hearing loss caused by abnormalities of the inner ear and heterochromia of the irises. TS is a more severe syndrome displaying complete deafness and a more generalized hypopigmentation. A biallelic mutation of MITF has been associated to COMMAD syndrome, an extremely rare disease, characterized by coloboma, osteopetrosis, microphthalmia, macrocephaly, albinism, and deafness. The severity of this phenotype indicates that MITF plays an important role in ocular morphogenesis and bone homeostasis in humans (George et al., 2016).

Sporadic somatic mutations have been found in a 16% of a cohort of 50 melanoma metastases (Cronin et al., 2009). A germline mutation *MITFE318K* has been linked to familial or sporadic melanoma (Yokoyama et al., 2011)

(Bertolotto et al., 2011). This mutation affects a small ubiquitin-like modifier (SUMO)-ylation site that negatively modulates the transcriptional activity of MITF, therefore leading to an increase in function of the MITF protein (Bertolotto et al., 2011; Murakami & Arnheiter, 2005). In addition, a more recent publication shows that the MITFE318K mutation can delay BRAFV600E-induced senescence in human melanocytes, concomitant with decreased expression of $p16^{INK4A}$. This role of MITFE318K in bypassing BRAF-induced senescence may be the underlying mechanism that favor melanomagenesis (Ballotti & Bertolotto, 2017).

### 1.3.2 Transcriptional regulation of MITF

MITF is subject to diverse mechanisms of transcriptional control. The CREB-mediated regulation of the MITF-M promoter is central to the melanogenesis process. This is mediated by α-MSH activation of the MC1R receptor at the melanocyte membrane triggering cAMP signaling (Bertolotto et al., 1998; Price, Horstmann, et al., 1998). Despite cAMP signaling being ubiquitous, it specifically regulates the MITF-M promoter due to the cooperation of CREB with SOX10, a transcription factor exclusive to neural crest-derived cell types (Huber et al., 2003). Depletion of the transcriptional activator of MITF PAX3 induces apoptosis in melanoma cells (Kubic et al., 2012). Hypoxia-inducible factor 1 (HIF-1) can repress MITF through the recruitment of the differentially expressed in chondrocytes protein 1 (DEC1) to the MITF promoter (Son et al., 2014). Interferon γ (IFN-γ) inhibits CREB binding to the MITF promoter by promoting the association of CREB binding protein (CBP) with signal transducer and activator of transcription 1 (STAT1) (Feige et al., 2011), thus inhibiting the transcription of MITF. N-Oct-3 (BRN2) is a neuronal-specific factor expressed in melanoblasts which is lost as they undergo differentiation to melanocytes (Cook et al., 2003). Oncogenic BRAF induces BRN2 which, in turn, binds to the MITF promoter and increases MITF transcription. However, in non-transformed melanocytes, BRN2 is not expressed and wild-type BRAF cannot upregulate MITF through BRN2 (Wellbrock et al., 2008).

β-catenin is another transcriptional activator of MITF. It can dimerize with the lymphoid enhancer-binding factor 1 (LEF1) and transactivate the MITF-M promoter (Yasumoto et al., 2002). It can also bind directly to the MITF protein (Schepsky et al., 2006). Interestingly, LEF-1 and MITF physically interact and synergistically enhance transactivation of the MITF-M promoter (Saito et al., 2002). When the β-catenin-binding domain of LEF-1 is mutated, LEF-1 and MITF cannot enhance transactivation of the MITF-M promoter. Thus, MITF's self-activation of the M promoter requires interaction with LEF1 and β-catenin

and might be an important mechanism for preserving sustained levels of expression of MITF during melanocyte development (Saito et al., 2003).

### 1.3.3 Post-translational modifications of MITF

A number of post-translational modifications, including phosphorylation, ubiquitination, SUMOylation and acetylation, are important for the regulation of MITF stability and function as a transcription factor. Steel factor (Sl), also known as stem cell factor (SCF), is a c-Kit receptor ligand essential for melanocyte development. It activates the BRAF-MAPK pathway, triggering the phosphorylation of at least two serine residues (Ser73 and Ser409) in MITF (Phung et al., 2011; Wu et al., 2000). Phosphorylation of Ser73 in MITF by extracellular-signal regulated kinase 2 (ERK2) (Hemesath et al., 1998) induces the association of histone acetyl transferase p300/CBP with the transactivation domain of MITF (Price, Ding, et al., 1998), whereas Ser409 of MITF is phosphorylated by p90 ribosomal s6 kinase (p90RSK) (Wu et al., 2000). The phosphorylation of MITF on these two residues enhances its transactivation ability. At the same time, phosphorylated Ser73 is required for human ubiquitin carrier protein 9 (hUBC9)-mediated ubiquitination of Lys201 and leads to subsequent proteasome-induced degradation of MITF (Price, Ding, et al., 1998; Wu et al., 2000; Xu et al., 2000). The phosphorylation event at Ser409 has been shown to be a priming site for further phosphorylation of three nearby residues at the C-terminus by glycogen synthase kinase-3β (GSK3β), a kinase that is known to target proteins for ubiquitination and degradation (Ploper et al., 2015). In this context, Wnt signaling might be able to both drive MITF transcriptional regulation and stabilize the protein by inhibiting GSK3β kinase activity and MITF degradation. In addition, GSK3β has been shown to phosphorylate Ser298 of MITF. The mutation of this phosphorylatable residue, which has been found in WS2A, impairs the transcriptional activity of MITF *in vitro* (Takeda, Takemoto, et al., 2000). In contrast, another study shows that mutations of Ser298 to alanine or proline did not affect the DNA-binding or transactivation ability of MITF (Grill et al., 2013).

SUMOylation has been shown to affect MITF, rendering it less active transcriptionally. The receptor activator of NF-kappa B ligand (RANKL)/p38 pathway phosphorylates MITF at Ser307 in osteoclasts, which allows a SUMO protease to deSUMOylate Lys316 of MITF (Bronisz et al., 2014). This enables MITF to recruit cofactors FUS (fused in sarcoma protein) and Brahma-related gene 1 (BRG1) to form a complex that stimulates transcription in these cells (Bronisz et al., 2014; Mansky et al., 2002). This finding was especially relevant since the MITF germline variant E318K that predisposes to familial melanoma

and renal carcinoma, was found to abrogate SUMOylation of K316 (Bertolotto et al., 2011; Yokoyama et al., 2011). PIAS3, protein inhibitor of the activated signal transducer and activator of transcription 3 (STAT3), is a SUMO-protein ligase that can covalently attach a SUMO peptide to its substrates, modulating their function. It was originally discovered by its ability to inhibit the transcriptional ability of STAT3 (Chung et al., 1997). Although PIAS3 has been found to modulate MITF through SUMOylation (Miller et al., 2005), PIAS3 can bind directly to MITF and prevent it from binding to osteoclast-specific gene promoters in a SUMOylation-independent manner that could be dependent on cell lineage context (Hikata et al., 2009; Murakami & Arnheiter, 2005). Phosphorylation of MITF Ser409 and STAT3 recruiting of PIAS3 dissociates it from MITF, enhancing MITF transcription of target genes in mast cells and melanocytes (Levy et al., 2003; Sonnenblick et al., 2004).

Apart from SUMOylation, lysine residues in MITF, such as K206 and K243, have been shown to be acetylated, possibly regulating the activation of MITF's target genes (Cheli et al., 2011).

### 1.3.4 MITF and melanoma

MITF functions as an oncogene and a focal amplification of MITF has been described in 20% of metastatic melanomas (Garraway et al., 2005), and has been found in a post-relapse tumor sample (Van Allen et al., 2014). As previously described, the MITF germline mutation E318K is linked to familial or sporadic melanoma. MITF cooperates with hyperactive mutant BRAFV600E in transforming human melanocytes in vitro (Garraway et al., 2005). However, the role of MITF in melanoma appears to be more complex and needs further investigation. MITF is a tightly regulated transcription factor that has been suggested to exert its function as a rheostat, in which different levels of expression of MITF dictate phenotype outcome in melanoma (Hoek & Goding, 2010) (**Figure 4**). This model says that the level of MITF activity determines cellular function. Long-term depletion of MITF drives senescence in melanoma cells (Giuliano et al., 2010), impairing DNA replication, mitosis and genomic stability (Strub et al., 2011). Low expression has been associated with an invasive phenotype whereas intermediate levels promote proliferation and high expression of MITF activates a differentiation-associated cell cycle arrest via increase in cyclin-dependent kinase inhibitors, leading to a non-proliferating phenotype with elevated differentiation (Carreira et al., 2005; Strub et al., 2011).

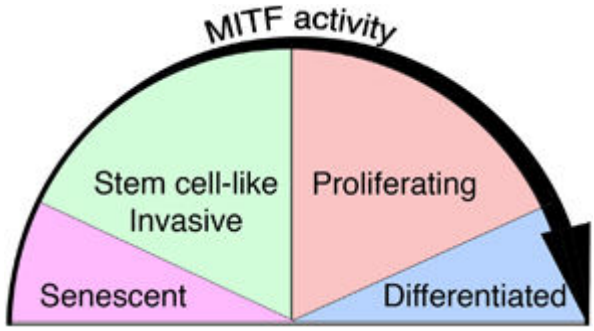


**Figure 4. MITF rheostat model**. MITF has been hypothesized to control the phenotypic switch of melanocytes and melanoma cells according to its expression level. Figure obtained with permission from Springer Nature according to permit number 4403750847962 (Goding, 2011).

High expression of MITF has been shown to display anti-proliferative effects. On the other hand, $MITF^{high}$ melanomas display greater resistance to BRAF/MEK-inhibition targeted therapy by overcoming the cytotoxic effects of the inhibitors (Wellbrock & Arozarena, 2015). Overexpression of MITF *in vitro* increases the expression of anti-apoptotic and pro-survival genes when compared to control cells (Van Allen et al., 2014), whereas hyperactive BRAF lowers the expression of MITF to basal levels, that might be required for the survival of melanoma cells (Wellbrock & Marais, 2005). Even though these two studies may seem to be contrasting, it could be hypothesized that a genomic amplification of MITF counteracts the BRAF-induced reduction of MITF which is required for sustaining melanoma survival, without impairing proliferation and clonal expansion. Overexpression of MITF halts the proliferative phenotype, indicating that MITF-positive melanoma cells present a finely-tuned control of the expression of MITF.

Another study shows that BRN2 represses MITF expression, marking two distinct subpopulations of melanoma cells, those with MITF or BRN2 expression (Goodall et al., 2008), which highlights melanoma tumors heterogeneity and their possible different phenotypes regarding their invasiveness or migratory ability during melanoma progression. As the master regulator of the melanocytic lineage and an oncogene important for melanoma survival, motility, oxidative stress and DNA repair (Liu et al., 2009); modulating MITF is likely to be crucial in controlling tumor proliferation and a relevant target of future research in melanomagenesis.

## 1.4 The MiT-TFE subfamily of transcription factors

MITF belongs to the basic helix-loop-helix leucine zipper (bHLHZip) family of transcription factors, a large family first described by Murre et al. (Murre et al., 1989). It includes other members such as C-MYC, a well-known oncogene in several types of tumors (Baudino & Cleveland, 2001; Dang, 2012). The members of this family are characterized by evolutionarily conserved domains, including a basic region at the N-terminus required for binding of the transcription factor to DNA. The DNA binding domain generally interacts with the consensus sequence CANNTG, called E-box (Ephrussi boxes), or to variations thereof by one or two nucleotides (Aksan & Goding, 1998). Following the basic domain, other two structural domains of the protein mediate dimerization with other proteins, forming homo- or hetero-dimeric complexes. These are the helix-loop-helix domain (HLH) that presents two α-helices connected by a loop, and a leucine-zipper domain (Zip) which forms a helix that is contiguous to the second helix of the bHLH domain. The leucine zipper consists of heptad repeats of leucine in a pattern of hydrophobic residues followed by polar residues with an amphipathic nature (Jones, 2004). In addition to MITF, TFEB (transcription factor EB), TFE3 (transcription factor 3), and TFEC (transcription factor EC) (Hodgkinson et al., 1993; M. J. Hughes et al., 1993) are bHLHZip factors that constitute a subfamily within the larger family of bHLHZip proteins, namely microphthalmia subfamily of bHLHZip transcription factors (MiT-TFE) (Hemesath et al., 1994).

### 1.4.1 Dimerization properties of the MiT-TFE transcription factors

The members of the bHLHZip family of transcription factors need to form dimers in order to be transcriptionally active. C-Myc participates in the formation of heterodimers with other members of the family, such as Max, Mad and Mnt, and depending on which dimer is formed, these factors will positively or negatively function to regulate cell growth, proliferation, differentiation, and apoptosis (Amati & Land, 1994). An example of this kind of transcription molecular switch is that c-Myc/MAX heterodimers operate as a transcriptional activator to promote cell differentiation, whereas MAD/MAX heterodimers bound to the same DNA regulatory element are transcriptional repressors (Luscher, 2012). Modulating the dimerization properties of these transcription factors is an attractive approach that could provide the basis for new cancer cures (Dang, 2012). Transcription factors of the MiT-TFE family need to form dimers in order to bind DNA and exert their function. They have been shown to form homo- or hetero-dimers through their bHLHZip motif with members within the subfamily. These proteins display nearly identical basic regions and

very similar HLH and Zip domains (Hodgkinson et al., 1993). However, they fail to dimerize with other related bHLHZip proteins such as c-Myc, MAX or USF (Hemesath et al., 1994). Upon dimerization, the MiT-TFE factors are able to bind DNA regulatory elements of their target genes, such as the E-box (CACGTG) and M-box (CATGTG) through their basic domain (**Figure 5A**). They regulate the transcription of genes involved in a wide range of different cellular processes, ranging from cellular homeostasis (Settembre & Ballabio, 2014) and pluripotency (Betschinger et al., 2013), to lineage-specific differentiation, reviewed in (Steingrimsson et al., 2004).

Recently, a three-dimensional structure of MITF in the absence of DNA revealed that the homodimeric assembly of MITF is asymmetric. One of the

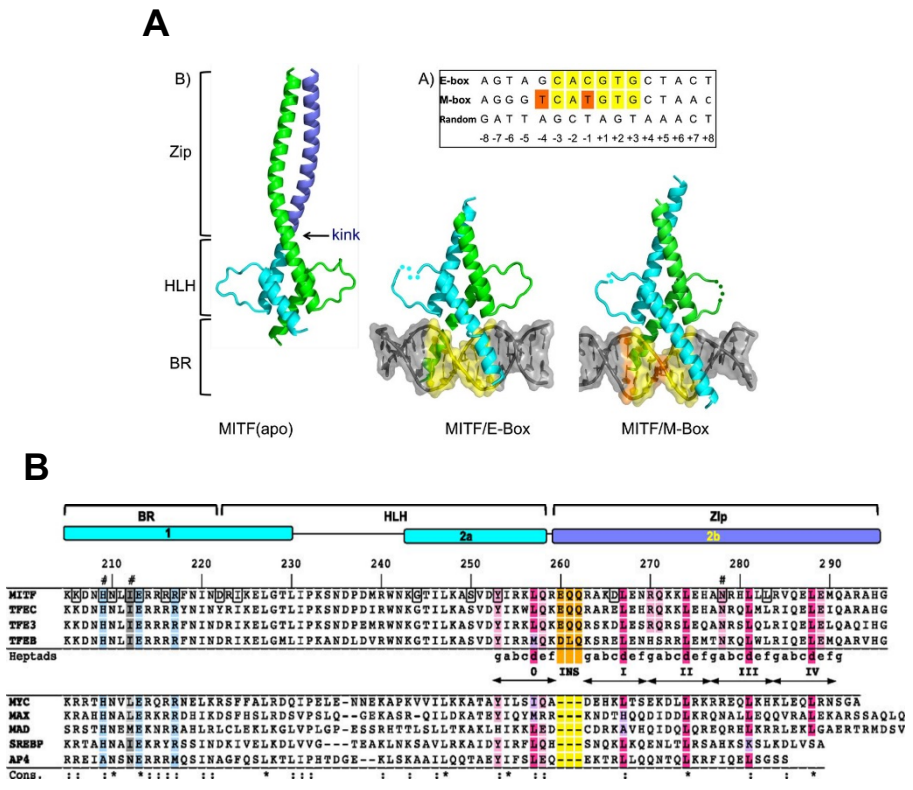


**Figure 5. Dimerization and DNA binding properties of MITF.** (A) Structural characterization of the MITF DNA-binding and assembly region. (B) Multiple sequence alignment of the MiT-TFE transcription factors (top) and canonical bHLHZip transcription factors (bottom) (Pogenberg et al., 2012).

two alpha-helices of the leucine zipper forms a kink due to an interruption of the coiled coil register consisting of an insertion of three residues at the junction of the two first heptad repeats (Pogenberg et al., 2012) (**Figure 5B**). This particular break in the heptad pattern is termed stammer. Skip, stammer and stutter motifs, corresponding to the insertion of one, three or four residues, respectively, introduce some structural flexibility into long coiled coils, with the coiled-coil heptad continuity (J. H. Brown et al., 1996; Lupas & Gruber, 2005). Stammers within leucine zippers are uncommon and possibly driven by the protein's functional requirements. All the MiT-TFE transcription factor family members contain the same three-residue insert in the N-terminal part of the leucine zipper, forming an essential structural element for the proper recognition of the homotypic dimerization partner in the MITF/TFE subfamily of bHLHZip transcription factors and the key determinant for heterodimerization selectivity (Pogenberg et al., 2012).

### 1.4.2 TFEB

TFEB has been described as the master regulator of cellular clearance pathways by transcriptionally upregulating genes involved in lysosome and autophagosome biogenesis and function, lysosomal exocytosis and lipid metabolism (Palmieri et al., 2011; Settembre et al., 2013; Settembre et al., 2011). It acts as a link between nutrient and signal-sensing mammalian target of rapamycin complex 1 (mTORC1) and the transcriptional regulation of the machinery that responds to nutritional stress (Roczniak-Ferguson et al., 2012; Settembre et al., 2012). TFEB activates the transcription of target genes through direct binding to the Coordinated Lysosomal Expression and Regulation (CLEAR) consensus sequences (TCACGTGA), which are enriched in a great number of loci nearby transcription start sites (TSS) of promoters associated to lysosomal genes (Martina, Diab, Lishu, et al., 2014; Palmieri et al., 2011).

TFEB controls lipid catabolism in the liver, regulating the peroxisome proliferator-activated receptor-γ coactivator 1α (Pgc1α) (J. Lin et al., 2005), a transcriptional coactivator involved in energy metabolism and master regulator of mitochondrial biogenesis (Valero, 2014). However, increasing focus on TFEB has revealed diverse tissue-specific functions. Loss of TFEB results in defective development of the endoderm (Young et al., 2016), and TFEB-deficient mice showed abnormal vascularization of the placenta with lethality effects during embryonic development (Steingrimsson et al., 1998).

Furthermore, TFEB regulates post-ischemic angiogenesis, inducing adenosine monophosphate (AMP)-kinase (AMPK) and autophagy (Fan et al.,

2018). TFEB-induced lysosomal activity is also essential for bone resorption by osteoclasts (Ferron et al., 2013) and, interestingly, it has been reported to be activated, together with TFE3, in macrophages exposed to pathogens, triggering the increased expression of cytokines and chemokines (Pastore et al., 2016). Presentation of intracellular antigens such as viral antigens is generally achieved by degradation of cytosolic proteins by the proteasome followed by transport into the endoplasmic reticulum where the processed antigen is loaded onto the major histocompatibility complex (MHC) class I. Presentation of exogenous antigens at macrophages and other antigen-presenting cells involves a certain degree of lysosomal degradation of the antigens that is controlled by TFEB through regulation of lysosomal activity (Samie & Cresswell, 2015).

More recent studies point to an increasing interest on TFEB's role in neurodegeneration and lysosomal storage disorders. TFEB has been shown to enhance neurotrophy and prevent loss of dopaminergic neurons through activation of the MAPK and AKT pathways, inducing phosphorylation of the eukaryotic translation initiation factor 4E-binding protein 1 (4E-BP1) and ribosomal protein S6 kinase beta-1 (S6K1), which leads to an increase in protein synthesis (Torra et al., 2018). Therefore, TFEB as a therapeutic target transcends beyond lysosomal regulation.

### 1.4.3 TFE3

Similar to TFEB, Transcription Factor E3 (TFE3) participates in the biogenesis of lysosomes and autophagosomes and the clearance of cellular debris upon starvation or lysosomal stress, through the activation of the CLEAR network of target genes (Martina, Diab, Li, et al., 2014; Martina, Diab, Lishu, et al., 2014). Depletion of TFE3 abolishes the increase in starvation-induced lysosomal function. This is regulated, by the mTOR complex and the nutritional status that dictates subcellular localization of TFE3. TFE3 is a key regulator of cell metabolism; it activates the insulin signaling cascade in hepatocytes, stimulates glycogen synthesis in skeletal muscle and liver through the activation of GSK3β, and its absence may induce the onset of insulin resistance (Iwasaki et al., 2012; Nakagawa et al., 2006). Moreover, recent evidence points to a role of TFE3 in thermogenesis and lipid metabolism in adipose tissue (Fujimoto et al., 2013).

Other functions of TFE3 have been described that are linked to lysosomal biogenesis, suggesting that the relevance of this cellular process spans over many different tissues, such as the regulation of thymus-dependent humoral immunity together with TFEB (Huan et al., 2006), and bone resorption in

osteoclasts (Hershey & Fisher, 2004; Steingrimsson et al., 2002). Interestingly, TFE3 has a role in the maintenance of cellular pluripotency, where embryonic stem cells (ESC) require cytoplasmic localization of TFE3 in order to start differentiation by exiting their naïve pluripotent state (Betschinger et al., 2013).

### 1.4.4 TFEC

TFEC is the least studied among the members of this family of transcription factors. In mice and rats it is not ubiquitously expressed and it lacks the acidic transcriptional activating domain, but is able to form heterodimers with TFE3 that inhibit TFE3-dependent transactivation (Zhao et al., 1993). However, the human homolog of TFEC contains this acidic domain and can activate or inhibit CANNTG motifs associated to *TYR* or the heme oxygenase-1 gene promoter (Yasumoto & Shibahara, 1997). In contrast to MITF and TFE3 mutant mice, mutations in TFEC do not induce abnormalities in osteoclast development (Steingrimsson et al., 2002).

### 1.4.5 The MiT-TFE factors and cancer

In addition to the prominent role of MITF in melanoma survival and progression, *MITFE318K* has been linked to renal clear cell carcinoma (Bertolotto et al., 2011). Interestingly, the related TFEB and TFE3 proteins have also been reported to be dysregulated in pediatric renal cell carcinomas (Kuiper et al., 2003) (Ramphal et al., 2006),

MITF, TFEB and TFE3 have been identified as regulators of metabolic reprogramming in pancreatic ductal adenocarcinoma (PDA) cells. These factors appear to escape cytoplasmic retention under normal fully-fed conditions in PDA cells in contrast with non-transformed human pancreatic ductal epithelial cells. In PDA cells, they localize to the nucleus and maintain high levels of autophagy and amino acid supply required for stimulation of anabolic pathways and proliferation. In this context, the MiT-TFE factors constitute a marker of pancreatic adenocarcinoma aggressiveness (Perera et al., 2015).

Many carcinogenesis events originate from aberrant transcription factor activity or can indirectly modulate transcription factor activity (Konstantinopoulos & Papavassiliou, 2011). The MiT-TFE family members are no exception and have been reported to be dysregulated in many forms of cancer (Haq & Fisher, 2011). Ongoing efforts on targeting oncogenic transcription factors may lead to selective death of tumor cells that depend on these pathways, in contrast to normal cells that can find redundancies in normal signaling pathways (Yeh et al., 2013).

## 1.5 The mTORC1/2 complexes

The mammalian target of rapamycin complex, also known as mechanistic target of rapamycin complex, consists of the mTOR phosphatidylinositol 3-kinase-related kinase (PIKK) forming the core of two distinct complexes, mTORC1 and mTORC2 (Heitman et al., 1991), that associate with different proteins and localize to different subcellular compartments. Dishevelled, Egl-10 and Pleckstrin (DEP) domain-containing mTOR-interacting protein (DEPTOR) is a negative regulator of the mTOR catalytic activity, common to both complexes (Peterson et al., 2009). Specific to the mTORC1 are the regulatory-associated protein of mTOR (RAPTOR) (Hara et al., 2002) and the 40-kDa proline-rich Akt substrate (PRAS40) (Sancak et al., 2007). In turn, rapamycin-insensitive companion of mTOR, (RICTOR) and the mammalian stress-activated MAP kinase-interacting protein 1 (mSIN1) form part of the mTORC2 (Zoncu et al., 2011). The mTORC1/2 complexes control protein synthesis necessary for cell growth and proliferation. This complex is capable of sensing various signaling pathways, growth factors, hormones, redox status and certain amino acids and derivatives, ensuring the availability of the adequate resources for protein synthesis (Bartolome & Guillen, 2014; Hay & Sonenberg, 2004).

The FK506-binding protein 12 (FKBP12) binds to the macrolide rapamycin forming a complex that directly inhibits the mTORC1 (E. J. Brown et al., 1994). On the other hand, the mTORC2 is insensitive to rapamycin (Jacinto et al., 2004). Active mTORC2 can induce phosphorylation of AKT at Ser473, a step needed for full activation of AKT (Sarbassov et al., 2005).

### 1.5.1 The mTORC1 pathway

Active mTORC1 phosphorylates S6K1 and 4E-BP1 facilitating mRNA translation. The tuberous sclerosis complex (TSC) is the main upstream regulator of mTORC1. It stimulates the GTPase activity of the Rheb protein that hydrolyzes Rheb-GTP to Rheb-GDP. TSC can be inhibited by AKT, MAPK and Wnt pathways, but it is also controlled by the cellular energy status through an activating phosphorylation by AMPK, a kinase that is active when the ATP to AMP ratio is low. Another feature of this complex that connects the cell environmental status to cellular metabolism is that amino acid deprivation can inhibit mTORC1 activity. Of note, the particular circulating amino acids responsible for the activation of the complex remain elusive. Arginine and leucine have been shown to be required for mTORC1 activation, however they were not sufficient (Hara et al., 1998). More recent studies support a two-step mechanism for the activation of mTORC1 by two distinct groups of amino

acids, namely priming and activating amino acids (Dyachok et al., 2016). Additionally, mTORC1 plays a pivotal role in the regulation of autophagy in a transcription-independent manner. Under sufficient supply of nutrients, growth factors and cellular signaling stimuli, mTORC1 is activated at the lysosomal surface and, through phosphorylation, inhibits proteins that are important for autophagy and lysosomogenesis. These include TFEB (Martina et al., 2012; Roczniak-Ferguson et al., 2012) and TFE3 (Martina, Diab, Lishu, et al., 2014), two important transcriptional regulators of these cellular processes, and ULK1 and ATG13 (Hosokawa et al., 2009), proteins that are directly involved in the formation of autophagosomes.

When amino acids are abundant, this induces a conformational change in Rag-GTPase heterodimers. These heterodimers interact with the regulatory-associated protein of mTOR (Raptor), a member of the mTORC1 complex, which in turn localizes the complex to the surface of late endosomes and lysosomes where it is activated by Rheb-GTP (Sancak et al., 2008) (Martina & Puertollano, 2013). This highlights the notion of the endosome-lysosomal network being a central hub for intracellular signaling and not just mere degradation stations (Perera & Zoncu, 2016).

TFEB, contains a number of amino acids that are likely to be modified by a panel of different kinases by means of phosphorylation. Serine 142 of TFEB has been shown to be phosphorylated by ERK and mTORC1, which also targets serine 211 of TFEB. This takes place at the outer lysosomal membrane and affects the subcellular localization of the protein. Phosphorylated TFEB at the lysosomal membrane is bound by 14-3-3 proteins that mask a nuclear localization signal (NLS) in the vicinity, thereby retaining TFEB in the cytoplasm (Pena-Llopis et al., 2011; Settembre et al., 2012). Similarly, mTORC1 phosphorylates TFE3 and MITF, and regulates their activity through the same mechanism of cytoplasmic retention (Martina, Diab, Lishu, et al., 2014; Martina & Puertollano, 2013). Inactivation of the complex due to the lack of nutrients or mitogens switches off the mTORC1 and MAPK/ERK pathways, leading to nuclear translocation of these factors and upregulation of target genes. Unphosphorylated TFEB and TFE3 shuttle to the nucleus, where they bind to CLEAR consensus sequences (further described in **Page 120**), whereas nuclear MITF has been shown to activate genes involved in melanogenesis in MNT-1 melanoma cells (Bentley et al., 1994; Hah et al., 2012). mTORC1-induced shuttling of the MiT/TFE proteins to the nucleus establishes a negative feedback loop, turning on the expression of genes required for mTORC1 activity such as FNIP2, RagC/D, and vATPase and promoting lysosomogenesis and autophagy that increase amino acid pools

(Palmieri et al., 2011; Zhang et al., 2015). Interestingly, mTORC1 can be positively regulated through the MAPK/ERK axis by two different routes, pointing to a crosstalk between these two distinct pathways in the regulation of the CLEAR network. First, ERK can phosphorylate and inhibit the TSC, and this, in turn, activates mTORC1 (Xue et al., 2017). Second, MAPK signaling leads to phosphorylation of raptor on proline sites prior to raptor-mediated scaffolding and recruitment to the lysosomes of active mTORC1 (Carriere et al., 2011).

### 1.5.2 mTORC1 and melanoma

The mTORC1 protein complex can sense the cellular nutritional status and regulate the synthesis of mRNA, controlling cellular growth and proliferation. Hyperactive BRAF-MAPK signaling is known to be a hallmark of melanoma tumors. ERK1/2 downstream of the BRAF/MAPK pathway can phosphorylate RSK which, in turn, activates mTORC1 in melanoma cells and its downstream targets, promoting increased protein translation, growth and proliferation (Romeo et al., 2013). A role of mTORC1/2 in bypassing oncogene-induced senescence has been described (Dankort et al., 2009). In another study, BRAFV600E mutation and CDKN2A loss were not sufficient to drive melanomagenesis in a mouse model, as this leads to repression of the PI3K-AKT axis, oncogene-induced senescence (OIS) and growth arrest. However, the melanocytes that underwent transformation exhibited increased mTORC1 and AKT-mTORC2 signaling, suggesting that mTORC1/2 activation is a mechanism used by tumor cells to bypass BRAF-induced senescence and trigger progression (Damsky et al., 2015). Dysregulation of mTORC1 has an impact on the signaling mechanisms affecting tumor progression, which defines the complex as an oncogene that may be relevant in several types of cancer.

## 1.6 Subcellular localization of the MiT-TFE transcription factors

As previously described, MITF is expressed as different tissue-specific isoforms that differ in their N-termini. Furthermore, the subcellular localization of MITF has been reported to vary across tissues or cell lines examined. The MITF-M isoform which is predominantly expressed in melanocytes, is constitutively nuclear (Takebayashi et al., 1996). This is in contrast with TFEB, TFE3, and other MITF isoforms, which have been shown to be located in the cytoplasm under normal conditions. In monocytes, MITF-A is cytoplasmic and shuttles to the nucleus upon RANKL signaling and, interestingly, deletion of

the 1B1b N-terminal region of MITF-A that is absent in melanocyte-specific MITF-M, promotes constitutively nuclear localization of the protein and may contribute to increased transcriptional activity (Lu et al., 2010). Independently, nuclear localization signals (NLS) spanning amino acids 197-206 and 214-217 within the DNA-binding region of MITF-M have been described, which are required for shuttling of the protein into the nucleus. Disruption of this NLS results in cytoplasmic retention of MITF (Fock et al., 2018; M. Sato et al., 1999; Takebayashi et al., 1996). A third NLS between residues 255 and 265 has been identified. This in line with another study showing that two C-terminal truncations found in WS2A and TS, R214X and R259X cause the mutated MITF protein to have increased presence in the cytoplasm (Grill et al., 2013).

Additionally, a hydrophobic nuclear export signal (NES) has been described between amino acids 75 and 80 of MITF-M. Stimulation of ERK activity with 12-O-Tetradecanoylphorbol-13-acetate (TPA) treatment in melanoma cells, triggered phosphorylation of Ser73 which primed subsequent phosphorylation of Ser69 by GSK3β, leading to activation of the NES and cytoplasmic accumulation of MITF-M (Ngeow et al., 2018).

The predominant nuclear localization of MITF-M under normal fully-fed conditions has been explained by the absence of an N-terminal domain important for cytoplasmic retention (Martina & Puertollano, 2013; Roczniak-Ferguson et al., 2012). This N-terminal region of 30 amino acids present in some isoforms of MITF such as MITF-A, is conserved in the N-terminus of TFEB and between amino acids 110-140 of TFE3 (Martina, Diab, Lishu, et al., 2014; Martina & Puertollano, 2013) (**Figure 6**). It contains a Rag-binding domain that allows the interaction of these factors with active Rag-GTPase heterodimers, which is required for the localization of these factors to the lysosome and subsequent phosphorylation by different kinases that regulate their subcellular localization. Phosphorylation of TFEB and TFE3 by mTORC1 allows the interaction with 14-3-3 proteins that retain them in the cytoplasm (Roczniak-Ferguson et al., 2012; Settembre et al., 2012) (**Figure 6**). In a similar mechanism, ERK2 phosphorylates TFEB and promotes its cytoplasmic retention (Settembre et al., 2011). Moreover, AKT inhibition has been shown to block AKT-mediated phosphorylation of TFEB at Ser467. Unphosphorylated TFEB at this residue resulted in translocation of TFEB to the nucleus and subsequent enhancement of its transcriptional activity leading to induction of autophagy and clearance of intralysosomal aggregates in a model of neurological Batten disease (Palmieri et al., 2017).

These studies suggest that kinases regulate the subcellular localization of the MiT-TFE transcription factors, and that this has a profound effect on expression of their target genes, which are involved in several crucial cellular processes, from metabolism, to the regulation of growth and proliferation. However, it is important to note that when assaying the phosphorylation status of these proteins, ectopically overexpressed factors present in non-physiologic concentrations could saturate the ability of the relevant kinases to phosphorylate them, and therefore escape the normal regulation of its cytoplasmic retention. As an example, when overexpressing TFEB, a significant fraction can be found in the nucleus of normally fed cells (Puertollano et al., 2018).

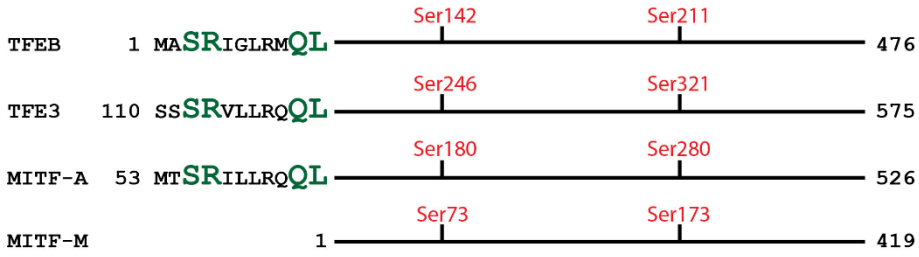


**Figure 6. Multisequence alignment of the Rag-binding domain and mTOR phosphorylation sites in TFEB, TFE3, MITF-A and MITF-M.** The residues marked in green have previously been identified as required for the interaction between Rag proteins and TFEB (Martina & Puertollano, 2013). MITF-M lacks this Rag-binding domain. Serine residues marked in red are the mTOR phosphorylation sites in TFEB which are conserved in TFE3 and MITF.

## 1.7 The endosomal system

Endosomes are membrane-bound compartments contained within eukaryotic cells. These vesicles originate from the *trans* Golgi and can be categorized as early endosomes, recycling endosomes, late endosomes and fully mature lysosomes. Endosomes store and sort intracellular material that will be recycled back to the plasma membrane or to the Golgi system, whereas acidified late endosomes mature to lysosomes. Fully mature acidic lysosomes are capable of fusing with autophagosomes, targeting their content for protein degradation in a process known as autophagy, which is vital for intracellular recycling and clearance of unwanted debris.

The endosomal and lysosomal network has traditionally been considered as a mere mechanism of intracellular sorting and delivery, degradation and recycling. However, recent studies point to a very complex role as a major signaling hub that links environmental cues such as sensing amino acid availability through the mTORC1 pathway to gene regulation involved in cellular metabolism (Dibble & Manning, 2013). For example, lysosome-mediated degradation of epidermal growth factor receptor (EGFR) and other receptor tyrosine kinases (RTKs) which downregulate mitogenic signals (Burke et al., 2001), and processing of 5' adenosine monophosphate-activated protein kinase (AMPK) signaling that leads to upregulation of mitophagy (Laker et al., 2017).

### 1.7.1 The melanosome

Melanosomes are rather large organelles (~500 nm in diameter) closely related to lysosomes. They are thought to originate from the ER or the *trans* Golgi as stage I premelanosomes. The notion that endosomes originate from the *trans* Golgi network is supported by the accumulation of mature premelanome protein (PMEL) in endosomal vesicles before the formation of non-pigmented stage I premelanosomes (Raposo et al., 2001). It is suggested that the endosomes destined to form melanosomes favor the accumulation of melanosome-related proteins while they discard proteins directed to the cellular membrane or to the formation of lysosomes (Raposo & Marks, 2002). Stage II melanosomes develop characteristic internal striations formed by proteolitically cleaved PMEL. In the next steps of development, stage III melanosomes become elongated and progressively acquire melanosome-specific enzymes like TYR and tyrosinase-related protein-1 (TYRP1). These melanogenic enzymes have been shown to be transported through the Golgi system to the nascent melanosome, indicating an overlap with lysosomal biogenesis (Kushimoto et al., 2003). Stage III melanosomes begin to synthesize melanin and to deposit it onto the luminal fibrillar matrix until they become fully melanized mature stage IV melanosomes.

### 1.7.2 The lysosome

The lysosome is a type of endosomal vesicle with the characteristic of a highly acidic lumen that contains about 60 different hydrolases, among them nucleases, proteases, glycosidases, lipases, phosphatases, sulfatases and phospholipases, which require an optimum pH of 4.5-5.0. Lysosomal acidification is carried out by a highly conserved multimeric enzyme complex, the vacuolar-type (V-type) ATPases located at the lysosomal membrane. Their function is to utilize energy from ATP to pump protons into the lysosomal

lumen. Besides vATPases, the lysosomal membrane contains a wide array of different proteins. These include highly conserved ion and channel transporters, which regulate the content of the lysosomes and the export of degradation products. An example of a channel protein crucial for lysosomal function is the transient receptor potential cation channel mucolipin (TRPML), which regulates the release of Ca2+ from the lysosome via calmodulin-mediated lysosomal fission and recovery (Peters & Mayer, 1998). In addition, lysosome-associated membrane proteins (LAMPs) are highly-glycosylated proteins that protect the lysosomal membrane against digestion by lysosomal hydrolases. SNARE (soluble NSF (N-ethylmaleimide-sensitive factor) attachment protein receptor) proteins mediate the fusion of lysosomes with their target intracellular compartments (Pu et al., 2016). Mature lysosomes can fuse with vesicles that engulf extracellular material that has been taken up through the process of endocytosis for further digestion. Lysosomes can also fuse with autophagosomes that contain misfolded aggregates, oxidized lipids, pathogens and damaged or unneeded intracellular components, in a process called autophagy. The products from endocytic vesicles or autophagic degradation are used to meet the nutritional needs of the cell for energy production or availability of building blocks for the biosynthesis of new cellular components.

A small fraction of all the cellular lysosomes are secretory lysosomes, also called lysosome-related organelles. Secretory lysosomes localize closer to the plasma membrane. The process of exocytosis is calcium-dependent and regulated by TFEB, which controls the transcription of genes involved in translocation to the plasma membrane and unloading of cellular metabolites (Medina et al., 2011). Lysosomal exocytosis is very active in some cell lineages. Melanocytes secrete melanosomes with the pigment melanin (Raposo & Marks, 2002). Osteoclasts resorb bone material by endocytosis and transport the vesicles through the cytoplasm to the opposite pole at the basal plasma membrane, releasing their content into the extracellular space (Salo et al., 1997). Spermatozoa secrete hydrolases during fertilization (Tulsiani et al., 1998). Lysosomal exocytosis is important for the immune function through the secretion of antigen-loaded MHC-II complex by dendritic cells, and cytotoxic T cells secretory degranulation (Pu et al., 2016). In addition, lysosomes migrate to the plasma membrane to promote repair, a process dysregulated in muscular dystrophy (Han et al., 2007).

## 1.8 Autophagy

Autophagy, or “self-eating”, is a catabolic pathway involving the delivery of

intracellular material to acidic lysosomes that mediate degradation and recycling. Autophagy can be divided into three different subtypes. Microautophagy directly delivers cytosolic components to the lysosome through small invaginations in the lysosomal membrane. During chaperone-mediated autophagy (CMA), a substrate is targeted for degradation by forming a complex with heat shock cognate 71 kDa (hsc70) proteins, which are recognized by chaperones. The complex is transported to the lysosomal membrane where it binds a CMA receptor for internalization. Finally,

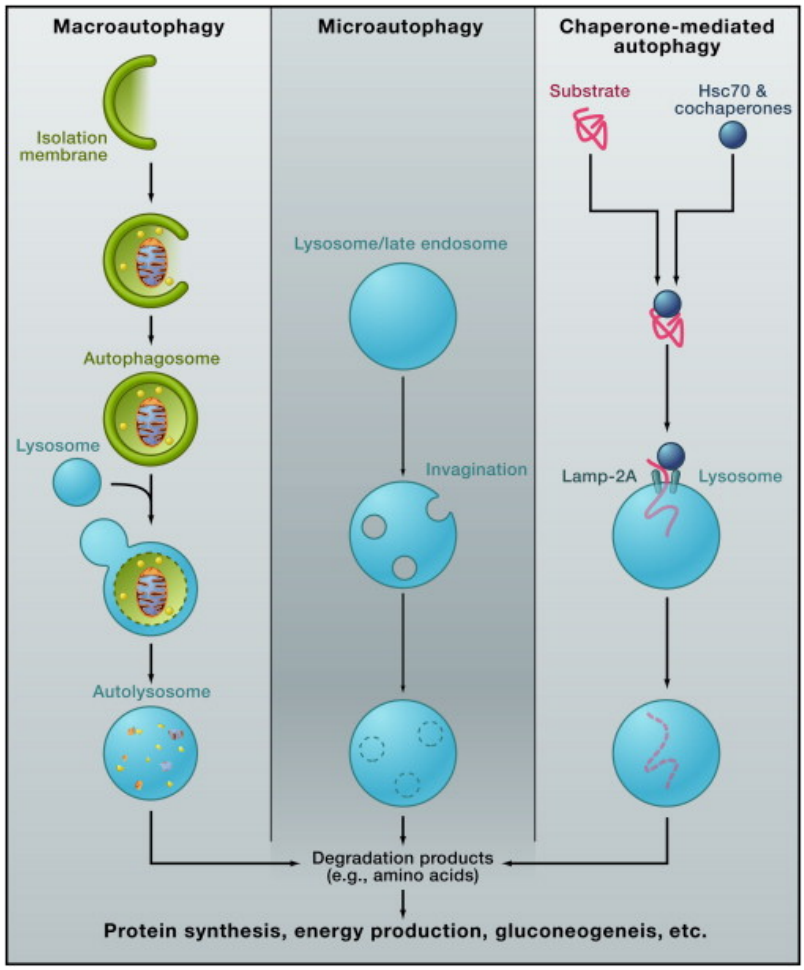


**Figure 7. Three major types of the autophagy process.** Figure obtained with permission from Elsevier according to permit number 4375950128309 (Mizushima & Komatsu, 2011).

macroautophagy, which is the most studied type, involves the fusion of the autophagosome, an endosomal membrane-bound organelle that engulfs intracellular material, with an acidic lysosome, forming an autolysosome (**Figure 7**). In turn, macroautophagy can be divided into bulk autophagy or selective autophagy, the latter referring to the degradation of specific subcellular structures, such as mitophagy of mitochondria, lipophagy of lipid droplets, or chlorophagy of chloroplasts. There are 35 autophagy-related genes (ATGs) identified so far, with a subset (the “core” ATGs) being conserved across eukaryotic organisms from yeast to mammals (Bento et al., 2016; Mizushima & Komatsu, 2011), governing autophagosome induction and formation, expansion, closure and fusion with lysosomes.

### 1.8.1 Initiation of autophagy

Autophagy initiation is controlled by mTORC1 and is triggered by starvation and other stresses that release mTORC1 from the lysosome. Inactive mTORC1 impairs the phosphorylation of autophagy-initiating UNC51-like kinase 1 (ULK1) and TFEB. Unphosphorylated TFEB shuttles to the nucleus and activates the transcription of genes involved in the regulation of downstream autophagy (Palmieri et al., 2011; Sardiello et al., 2009; Settembre et al., 2011). Unphosphorylated ULK1 is active and, promotes phosphorylation and activation of beclin-1 (BECN1), and thus initiates phagophore formation, the autophagosome precursor, nearby the endoplasmic reticulum (ER) (Itakura & Mizushima, 2010; Russell et al., 2013). It remains unclear whether the ER membrane forms part of a newly synthesized phagophore, and whether other structures of the endomembrane system (Golgi, mitochondria) also contribute to the complex process of autophagosome biogenesis (Bento et al., 2016; Hailey et al., 2010; Mizushima et al., 2011). Next, the ATG14-containing class III phosphatidylinositol 3-kinase (PI3K) complex is recruited to the nascent autophagosome where it interacts with BECN1.

### 1.8.2 Expansion of the autophagosome

In both yeast and mammals, ubiquitin-like proteins contribute to the expansion of the lysosome. The mammalian ATG5, ATG12 and ATG16L protein complex associates with the phagophore until dissociation following vesicle maturation (Mizushima et al., 2003; Mizushima et al., 2001), a process regulated by the Golgi protein RAB33A which binds and inhibits ATG16L1 (Itoh et al., 2008).

A second mechanism involving ubiquitin-like proteins that promote autophagosomal expansion, includes the protein ATG8, also known as microtubule-associated protein light chain 3 (LC3). The cysteine protease

ATG4, with four isoforms in mammals, exposes a glycine in the C-terminus of LC3 (Kirisako et al., 2000), which is then named LC3-I, and subsequently is covalently conjugated to phosphatidylethanolamine (PE) to constitute the lipidated form LC3-II (Geng & Klionsky, 2008), a process that determines autophagosomal size (Z. Xie et al., 2008). Nutrient starvation and stress can induce lipidation of LC3 (Kabeya et al., 2000). Eventually LC3-II will undergo deconjugation. Deficiencies in the deconjugation step have been associated to impaired macroautophagy, although the mechanism is not entirely understood (Nair et al., 2012). LC3 constitutes one of the most prominent markers in experimental research for the assessment of the autophagy function in mammals.

### 1.8.3 Autophagosome completion and fusion

The last step in autophagosome formation involves its maturation and fusion with a lysosome or late endosome in order to conform a fully mature autolysosome that can undergo degradation of the cargo. Microtubules play an important role in phagosome trafficking (Monastyrska et al., 2009). UV radiation resistance-associated gene protein (UVRAG) can interact with the PI3K complex at the autophagosome and activate Rab7, a GTPase that promotes fusion with lysosomes (C. Y. Liang et al., 2008), in collaboration with other proteins from the SNARE family (Pu et al., 2016). The soluble hydrolases in the lysosome are active in the lysosomal low pH and can degrade the substrates provided by the autophagosome in the final step of the autophagy process.

### 1.8.4 Autophagy in human disease

Defective lysosomal function is the cause of a group of more than 50 rare inherited metabolic disorders denominated lysosomal storage diseases (LSDs). These disorders are characterized by mutations that usually result in deficiency of a single enzyme required for the metabolism of substrates, leading to enlarged lysosomal vacuoles filled with undegraded material, often localized adjacent to the nucleus. They are further classified, depending on the substrate that accumulates, into lipid storage disorders, mucopolysaccharidoses, or glycoprotein storage disorders. Pompe disease is another LSD characterized by an accumulation of glycogen in the lysosomes of muscle cells, nervous system and liver. To this date there is no cure for LSDs, and treatment is mostly symptomatic.

Recently, increasing attention has been drawn to a link between abnormal lysosomal function and neurodegeneration, and the induction of autophagy as

a potential therapeutic target for conditions such as Huntington's, Parkinson's and Alzheimer disease (AD), where pathogenic protein aggregation is a hallmark. These conditions involve changes in mTORC1, dynein and Rab7 activity (Caviston et al., 2011; Erie et al., 2015; Wen et al., 2017), preventing degradation of protein deposits by the autolysosomal pathway, through a mechanism not yet fully elucidated. Accumulation of lysosomes that disturb the normal morphology of neuronal axons, due to blockade of lysosomal proteolysis and vesicle transport, has been described in AD (Lee et al., 2011).

Understanding the role of the autophagy response in cancer biology is crucial in the search for novel effective therapies. Many anticancer agents activate autophagy, as it can serve as a mean for promoting survival through efficient use of available nutrients, handling of oxidative stress and limiting DNA damage. Activated autophagy can be detected at the most hypoxic regions of the tumor where there is considerable metabolic stress, conferring a survival advantage.

Autophagy inhibition improves the performance of anticancer drugs, including the response to chemotherapy, in several tumor samples and preclinical models. It has been shown to enhance the cytotoxic activity of effector T lymphocytes and natural killer (NK) cells against tumoral cells (Amaravadi et al., 2011). Human pancreatic tumors and pancreatic cancer cell lines are dependent on elevated basal levels of autophagy compared to normal pancreatic cells (Yang et al., 2011). Consistent with that, autophagy inhibition was shown to induce apoptosis and to halt tumor growth (Marchand et al., 2015). During oncogenic transformation, lysosomes undergo changes in pH, subcellular localization or composition. Reduction of RAB7 expression promotes lysosomal relocation to the cell periphery, which has been documented in prostate cancer and is associated with increased tumor invasiveness (Steffan et al., 2014). It has been proposed that the mechanism behind this involves the unloading of proteolytic enzymes into the extracellular space that then digest extracellular matrix (Steffan et al., 2014). In addition, the endosomal network can incorporate proteins such as the transmembrane type 1 matrix metalloproteinase into the plasma membrane invadopodia, facilitating tumor migration, invasion and metastasis (Macpherson et al., 2014; Monteiro et al., 2013). Peripheral lysosomal relocation has also been associated with increased expression of integrins in the plasma membrane, enhancing migration and cell adhesion necessary for the establishment of new tumor populations (Dozynkiewicz et al., 2012). Importantly, tumor cells that undergo the process of autophagy cease cell division and motility and enter a dormant state, while maintaining the capacity to regenerate and resume

proliferation when proper growth conditions are restored. Tumor regeneration and re-emergence form latency is a key issue in cancer management (White & DiPaola, 2009).

Paradoxically, a tumor-suppressive role of autophagy in line with its basic role at clearing damaged organelles and cellular components has been documented. This role is particularly prominent in hepatocellular carcinoma. Mice carrying deletions of *Atg5* or *Atg7* display inactivated autophagy and pile-up cellular waste. Defective autophagy leads to increased DNA-damaging ROS production, genomic instability and generalized inflammation, which may promote tumor initiation (Komatsu et al., 2007; Takamura et al., 2011). Monoallelic loss of *Beclin 1*, a gene required for autophagy induction, has been reported in ovarian and breast cancer (X. H. Liang et al., 1999). *Beclin 1* deletions induce chromosome instability and tumor initiation (Mathew et al., 2007). A very common mutagenesis event in a wide fraction of human cancers involve mutations that lead to abnormal activity of the PI3K and mTOR pathways. Hyperactive PI3K inhibits autophagy and simultaneously stimulates uncontrolled cell growth and proliferation, regardless of nutrient and growth signals availability, which eventually leads to extreme metabolic stress and cell death (S. Jin et al., 2007), perhaps in a delicate balance that is still advantageous to the tumor. Therefore, autophagy has been referred to as a double-edged sword regarding whether it contributes to the suppression or promotion of tumorigenesis (White & DiPaola, 2009). Current efforts are directed to understand how pharmacological modulation of autophagy in cancer could lead to the development of novel, effective therapies, depending on the particular autophagy context, whether it is activated or suppressed.

On another note, current research on therapies that aim to prolong lifespan show that the autophagy pathway is one of those implicated in the aging process. Age-related impaired autophagy has been reported in rat liver and studies with *Saccharomyces cerevisiae*, *Caenorhabditis elegans* and *Drosophila melanogaster* revealed that specimens deficient in key autophagy genes *Atgs* showed a reduced lifespan (Martinez-Lopez et al., 2015). The effects of pharmacological approaches directed to promote longevity like caloric restriction, sirtuin-1 activation, mTOR or insulin growth factor inhibition require autophagy activation (Rubinsztein et al., 2011). However, there are other documented effects that are autophagy-independent. Thus, autophagy is one of the players to be considered before the challenge of understanding the complex biological process of aging, with the goal of boosting cellular rejuvenation and lifespan extension.

### 1.8.5 Autophagy and melanoma

A number of autophagy-related genes have been found to be overexpressed across melanoma tumors compared to other cancer types. Specifically, expression of Rab7 is increased from early stages of melanoma, resulting in enhanced lysosomal trafficking. Rab7-induced autophagy promotes tumor fitness, proliferation and remodeling of extracellular matrix, migration and invasion (Alonso-Curbelo et al., 2015). A genetically engineered mouse model tested depletion of *Atg7* in a *Braf*$^{V600E}$ and *Pten*-deficient context, showed that *Atg7*-impaired melanomas have growth defects, increased senescence and oxidative stress. Moreover, the antiproliferative effects induced by BRAF inhibition were more pronounced in the *Atg7*-deficient tumors (X. Xie et al., 2015). Partial loss of *ATG5*, has been identified as the only autophagy-related marker of advanced stage and poor prognosis in melanoma tumors. This was confirmed in mice carrying a melanocyte-specific heterozygous deletion of *ATG5* that presented melanoma tumors with increased metastatic potential and resistance to BRAF inhibition with dabrafenib (Garcia-Fernandez et al., 2016). BRAF inhibition therapy in metastatic melanoma has been shown to increase cytoprotective autophagy triggered by the ER-stress response through binding of BRAF to the chaperone GRP78 that induces ER expansion (Ma et al., 2014). In contrast, *ATG5* depletion in melanoma cell lines reduced their proliferation rate, invasion and metastatic potential, pointing to the requirement of a basal level of autophagy for melanoma tumors to endure acidic conditions and metabolic stress (Marino et al., 2012). It further highlights the importance of taking into account whether therapies designed to treat metastatic melanoma partially or completely abolish the autophagy function, as this may worsen patient survival.

Malignant melanomas often present areas significantly more melanized than adjacent healthy skin. Microscopy analysis of those hyperpigmented regions shows the presence of “coarse melanin”, characterized by a large number of melanosome-engulfing autophagosomes (Lazova & Pawelek, 2009). Despite the fact that autophagy degradation of defective melanosomes prevents leakage of melanogenesis by-products that are toxic for the cell, increased autophagy and coarse melanin in melanoma tumors are defined as markers of poor prognosis (Lazova et al., 2010).

# Aims

MITF is a bHLHZip transcription factor that regulates differentiation, growth and survival of melanocytes and is found to be amplified in a fraction of melanoma tumors. The close relatives of MITF, TFEB and TFE3, have recently been shown to be key regulators of lysosome and autophagosome biogenesis. Both have been shown to be regulated in a similar fashion by post-translational modifications resulting in effects on their subcellular localization and activity. This work focuses on characterizing the interactions and functional interplay between MITF and its relatives TFEB and TFE3 in melanoma. Three major aims have been addressed:

- **Aim 1**: Determining the expression of the MiT-TFE transcription factors in melanoma and analyzing the effects of signaling pathways on their subcellular localization.

- **Aim 2**: Assessing the interactions among the MiT-TFE transcription factors with regard to dimerization properties and transcriptional cross-regulation.

- **Aim 3**: Characterizing the overlap in target gene selection of the MiT-TFE transcription factors in melanoma cells and the biological processes involved.

# 2 Materials and methods

## 2.1 Plasmid constructs

Site-directed mutagenesis (Braman et al., 1996) was used to generate FLAG-tagged mouse MITF-M constructs carrying the Ser73Ala and Ser409Ala mutations, GFP-tagged human MITF-A constructs carrying the Ser180Ala and Ser504/508/512Ala mutations and the pEGF-N1-MITF-M (+) construct, the FLAG-tagged and GFP-tagged MITF(Δ259-261), MITF(Δ259-261)_N269_R270insEQQ and N269_R270insEQQ constructs. MLANA-intron-2, TFEB-intron-1 and MITF-enhancer luciferase reporter constructs were generated by amplifying human genomic DNA from Skmel28 cells and restriction digestion and ligation in the appropriate luciferase reporter constructs. Site-directed mutagenesis was also used to mutate the regulatory element in both the TFEB-intron-1 and the MITF-enhancer luciferase reporter constructs to scrambled versions. Gibson assembly cloning method (Gibson et al., 2009) was used to generate the FLAG-HA-tagged human TFE3 construct and the FLAG-tagged human MAX construct. All the constructs used for the generation of the stable inducible cell lines were generated by restriction enzyme digestion followed by ligation to a pBac recipient plasmid. Further details on the generation of each of these constructs are explained below in separate sections.

### 2.1.1 Site-directed mutagenesis and cloning

I performed in vitro site-directed mutagenesis PCR (Braman et al., 1996) in order to mutate the plasmid constructs used in these experiments and to amplify genomic DNA for the generation of the luciferase reporter constructs used in transcription activation assays. I used 0.02 units/µl Q5® Hot Start High-Fidelity DNA polymerase (#M0493S, NEB), 1X Q5® reaction buffer, 0.5 µM of primers, 200 µM dNTPs, and 1 ng of template plasmid in a total volume of 20 µl adjusted with DEPC water. The plasmid mutagenesis PCR reaction was carried out at the conditions shown in **Table 1**. PCR conditions for amplification of genomic DNA are shown in **Table 2**. A quarter of the PCR product (5 µl) was loaded on an agarose gel to confirm that the PCR was successful and the amplified fragment showed the correct size. Subsequently, 20 units of DpnI (#R0176S, NEB) were added to the PCR product and incubated at 37°C for one hour in order to digest the parental plasmid template. 1 µl of the DpnI-treated PCR product was mixed with 5 units of T4 polynucleotide kinase (PNK) (#M0201S, NEB) and 0.5 µL of 10x T4 DNA ligase buffer in a total volume of

5 µl, and incubated at 37°C for 30 minutes in order to phosphorylate the 5'-ends of the amplified DNA fragments. Next, the phosphorylated mutated DNA fragments were recircularized by DNA ligation using 400 units of T4 DNA ligase (#M0202S, NEB). For transformation, 2.5 µl of the ligation product were added to 25 µl of NEB® 5-alpha Competent E. coli cells (High Efficiency) (#C2987, NEB), which were incubated for 30 min on ice, then heat-shocked at 42°C for 30 seconds and re-incubated on ice for 5 minutes. Transformed bacteria were allowed to grow in 475 µl of SOC outgrowth medium (#B9020S, NEB) for one hour at 37°C prior to plating onto LB agar plates containing the appropriate antibiotic matching the resistance gene contained in the plasmid. Plates were incubated at 37°C overnight and then a number of colonies was isolated and inoculated overnight at 37°C in LB medium liquid cultures with the appropriate selection antibiotic. Plasmid DNA was isolated using Monarch® Plasmid Miniprep Kit (#T1010S, NEB) and sent out to GENEWIZ Beckman Coulter genomics for Sanger sequencing using universal primers aligning to the plasmid backbone.

**Table 1. PCR cycling conditions for mutagenesis PCR of plasmid constructs**

| | Temperature (°C) | Time (sec) | Number of cycles |
|---|---|---|---|
| Initial denaturation | 98 | 30 | 1 |
| Denaturation | 98 | 10 | 35 |
| Annealing | 50-72* | 20 | |
| Extension | 72 | 20 sec/kb | |
| Final extension | 72 | 120 | 1 |

* According to primer pair melting temperature

**Table 2. PCR cycling conditions for genomic DNA amplification**

| | Temperature (°C) | Time (sec) | Number of cycles |
|---|---|---|---|
| Initial denaturation | 98 | 30 | 1 |
| Denaturation | 98 | 10 | 35 |
| Annealing | 50-72* | 20 | |
| Extension | 72 | 20 sec/kb | |
| Final extension | 72 | 120 | 1 |

* According to primer pair melting temperature

### 2.1.2 MITF constructs

FLAG-tagged MITF-M constructs carrying the Ser73Ala and Ser409Ala mutations were generated from a p3XFLAG-CMV$^{TM}$-14 construct expressing a FLAG-tagged version of mouse MITF-M (MITF-M-FLAG), kindly provided by Colin Goding. The GFP-tagged MITF-A plasmid (Addgene plasmid #38132) was provided by Shawn Ferguson (Roczniak-Ferguson et al., 2012) and was used to generate by site-directed mutagenesis a GFP-tagged version of human MITF-A carrying the Ser180Ala and Ser504/508/512Ala mutations. The pEGFP-N1-MITF-M (+) construct was generated by *in vitro* mutagenesis from the pEGFP-N1-MITF-M (-) (Addgene plasmid # 38131) kindly provided by Shawn Ferguson (Roczniak-Ferguson et al., 2012). The primers used for the in vitro mutagenesis are listed in **Table 3**.

A FLAG-tagged deletion construct MITF(Δ259-261) construct was generated from the MITF-M-FLAG construct described above. A GFP-tagged MITF(Δ259-261) was generated from a wild type mouse MITF-M construct (pEGFP-N1-MITF-M), kindly provided by Valerie Fock (Fock et al., 2018). A FLAG-tagged MITF(Δ259-261)_N269_R270insEQQ MITF construct was generated from the FLAG-tagged MITF(Δ259-261) construct by site-directed mutagenesis, whereas GFP-tagged MITF(Δ259-261)_N269_R270insEQQ was generated from the GFP-tagged MITF(Δ259-261) construct. FLAG-tagged N269_R270insEQQ construct was generated from MITF-M-FLAG and GFP-tagged N269_R270insEQQ was mutated from pEGFP-N1-MITF-M by site-directed mutagenesis. All the primers used for the *in vitro* mutagenesis are listed in **Table 3**.

### 2.1.3 TFEB and TFE3 constructs

The human GFP-tagged pEGFP-N1-TFEB (Addgene plasmid # 38119), and pEGFP-N1-TFE3 (Addgene plasmid # 38120) were kindly provided by Shawn Ferguson (Roczniak-Ferguson et al., 2012).

A TFE3-FLAG-HA construct was generated by amplifying TFE3 from the pEGFP-N1-TFE3 vector and cloning into a pBac FLAG-HA vector downstream of a tetracycline response element (TRE), using Gibson assembly (Gibson et al., 2009). 50 ng of amplified FLAG-HA backbone were mixed with 3-fold molar excess of amplified TFE3 PCR product, together with 15 µl of DEPC water for a total volume of 25 µl. 25 µl of 2X Gibson Assembly Master Mix (E2611S, NEB) were added to the mix and incubated 15 minutes at 50°C. Subsequently, high-competent E. coli were transformed with the ligation mixture. Cloning primers are listed in **Table 3**.

### 2.1.4 MAX-FLAG construct

A construct expressing a MAX-FLAG fusion protein was generated by digesting the pVZ1-MAX vector (kindly provided by R. N. Eisenman (Ayer et al., 1993), containing the human MAX gene, by digesting it with the BamHI and NotI restriction enzymes followed by ligation into a pcDNA3.1(+) vector. Subsequently, FLAG was amplified from the MITF-M-FLAG construct with the primers listed in **Table 3**, and cloned into the pcDNA3.1(+)-MAX construct with Gibson assembly. 50 ng of the pcDNA3.1(+)-MAX fragment amplified with the primers listed in **Table 3** were mixed with 3-fold molar excess of the PCR product containing FLAG**.** 15 µl of DEPC water for a total volume of 25 µl were added in addition to 25 µl of 2X Gibson Assembly Master Mix (E2611S, NEB). The ligation mix was incubated 15 minutes at 50°C. Subsequently, high-competent E. coli were transformed with the ligation mixture.

### 2.1.5 Constructs for transcription activation assays

The TYR promoter reporter construct contains a 380 bp region at the promoter of the human *TYR* gene between bases -382 and -3 upstream of the TSS at location +1. This sequence was then cloned into a pGL3-Basic vector upstream of the luciferase reporter gene and verified by Sanger sequencing. The regions within MLANA intron 2 enhancer (MLANA-intron-2), TFEB intron 1 enhancer (TFEB-int1) and MITF intron 1 enhancer (MITF-enh) containing putative regulatory elements were amplified from human genomic DNA (see **Site-directed mutagenesis and cloning, Table 2**). The 731 bp PCR product of MLANA-intron-2 was digested using NheI and XhoI and ligated into the NheI and XhoI sites at the multiple cloning site upstream of the 5´ end of the luciferase gene in a pGL3-Basic vector. To generate the TFEB-int1 reporter vector, an 853 bp fragment containing a CAGCTGA regulatory element within intron 1 of the TFEB gene was blunt-ligated into the NheI site of the pGL3-Promoter vector. The scrambled TFEB intron 1 (TFEB-int1-scrbl) was generated by mutating the TFEB-int1 luciferase reporter plasmid by changing the CAGCTGA regulatory element to CCCTTTA. To generate the MITF-enh reporter vector, a 670 bp fragment containing a CACGTG regulatory element within intron 1 of the MITF gene was blunt-ligated into the NheI site of the Pgl3-Promoter vector. The scrambled MITF intron 1 enhancer (MITF-enh-scrbl) was generated by mutating the MITF-enh reporter plasmid by changing the CACGTG regulatory element to CCCTTTA. All the constructs were confirmed by sequencing (Genewiz, Essex, UK). Primers used for cloning are listed in **Table 3**.

The pGL3-Basic vector (#E1751, Promega) was used as a control for tyrosinase (pTYR) transactivation, whereas pGL3-Promoter vector (#E1761, Promega) was used as a control for MLANA intron 2 enhancer (MLANA-intron-2), TFEB intron 1 enhancer (TFEB-intron-1) and TFEB intron 1 scrambled (TFEB-int1-scrbl) promoter constructs.

**Table 3. Primers used for cloning and mutagenesis of plasmid constructs**

| Construct name | Primer sequence |
|---|---|
| pBac-pEGFP | FW 5'-TAATTAACGCGTTGAACCGTCAGATCCGCTAG-3' |
| | REV 5'-GGCTGATTATGATCTAGAGTCG-3' |
| MITF-M-FLAG-S73A | FW 5'-CGCACCCAACGCCCCTATGGCTA-3' |
| | REV 5'-CTGCTCCCCGGCACTGGT-3' |
| MITF-M-FLAG-S409A | FW 5'-CCGGAGGAGCGCTATGAGCGCAG-3' |
| | REV 5'-CTGCTTGTTTTTGAAGCTC-3' |
| pEGFP-N1-MITF-A-S180A | FW 5'-CGCACCCAACGCCCCCATGGCTATGCTTACG-3' |
| | REV 5'-CTGCTCCCCGGCACCGGT-3' |
| pEGFP-N1-MITF-A | FW 5'-CAAAACAAGCGCCCGGAGGAGCAGTATGAGC-3' |
| S504/508/512A | REV 5'-GCAGCTCCGGGGGCCACTGAGGAAAGGAGTGG-3' |
| pEGFP-N1-MITF-M (+) | FW 5'-TTTCCCACAGAGTCTGAAGCAAGAGCAC-3' |
| | REV 5'-AATACACGCTGTGAGCTCCCTTTTTATG -3' |
| pBac-FLAG-HA | FW 5'-GACTACAAAGACCATGACGG-3' |
| | REV 5'-CTCAAACAGTGTATATCATTG-3' |
| pBac-TFE3-FLAG-HA | FW 5'-TGATATACACTGTTTGAGATGTCTCATGCGGCCGAAC-3' |
| | REV 5'-TCATGGTCTTTGTAGTCGGACTCCTCTTCCATGCTG-3' |
| MITF-(Δ259-261) | FW 5'-CAACGAGCTAAGGACCTTG-3' |
| | REV 5'-TTGCAACTTCCGGATGTAG-3' |
| MAX-FLAG | FW 5'-AGCTCCGGATGGAGGCCAGCGACTACAAAGACCATG-3' |
| | REV 5'-GGCTGATCAGCGGGTTTAAACTACTTGTCATCGTC-3' |
| pcDNA3.1(+)-MAX | FW 5'-GCTGGCCTCCATCCG-3' |
| | REV 5'-AAACCCGCTGATCAGCCT-3' |
| MITF-EQQins | FW 5'-GCAACGACAGAAGAAGCTGGAG-3' |
| | REV 5'-TGTTCGTTTTCAAGGTCCTTAGC-3' |
| MLANA-intron-2 | FW 5'-TCTAGGCTAGCAGCAGTTCTCACAGTTGGGT-3' |
| | REV 5'-TCTAGCTCGAGCACCAATTTGTGCCAGGC-3' |
| TFEB-intron-1 | FW 5'-ACTGTTTGAGGACCCACAG-3' |
| | REV 5'-AGTGCTTGGCCTAGTCAG-3' |
| TFEB-intron-1-scrambled | FW 5'-TTATGTCCTCATGACCTTCCCC-3' |
| | REV 5'-AGGGCCTGTCTGGAGAGCCCCT-3' |

## 2.2 Cell culture

Four human melanoma cell lines were used in this study, namely 501Mel cells (generously donated by Ruth Halaban (Halaban et al., 2002)), SkMel28 cells (#HTB-72) obtained from the ATCC, SkMel31 cells (#HTB-73) obtained from

the ATCC and A375P cells (#CRL-3224) also obtained from the ATCC. HEK293T human embryonic kidney cells (#CRL-3216, ATCC) were used for luciferase assays since they do not express the MiT/TFE transcription factors endogenously. All the cells were grown in Dulbecco's Modified Eagle (DMEM) medium (#10569-010, GIBCO) supplemented with 10% fetal bovine serum (FBS #10270-106, GIBCO). The cells were grown at 37°C in 5% CO2 and split with fresh medium two to three times per week.

## 2.3 Inducible cell lines

### 2.3.1 GFP-tagged MITF, TFEB and TFE3

In order to be able to induce expression of the different transcription factors at will, I used an inducible piggybac (pBac) system. We generated inducible 501mel cells by transfecting the cells with three piggybac (pBac) vectors, one generating either GFP-tagged human MITF (pBac-pEGFP-N1-MITF), TFEB (pBac-pEGFP-N1-TFEB), TFE3 proteins (pBac-pEGFP-N1-TFE3) or GFP alone (pBac-pEGFP-N1), one containing a reverse-tetracyclin transcription activator, and one containing transposase. The pBac vectors were a gift from Dr. Kazuhiro Murakami (Hokkaido University) (Magnusdottir et al., 2013). The GFP-tagged MITF-M, TFEB and TFE3 cDNAs were amplified from the plasmids pEGFP-N1-MITF-M (Addgene plasmid # 38131), pEGFP-N1-TFEB (Addgene plasmid # 38119), and pEGFP-N1-TFE3 (Addgene plasmid # 38120), kindly provided by Shawn Ferguson (Roczniak-Ferguson et al., 2012), using the primers listed in **Table 3** (pBac-pEGFP), and then introduced into the pBac vector by digestion of the PCR product and the pBac recipient vector using the MluI and NotI restriction sites. DNA ligation was performed at the 3:1 insert to backbone ratio using Instant Sticky-end Ligase Master Mix (M0370S, NEB). The ligation products were transformed into high-competent cells. Bacterial plasmid DNA was isolated from individual colonies and sequenced as described above in **Site-directed mutagenesis and cloning**. Cells transfected with the pBac plasmids were cultured in DMEM medium supplemented with 10% FBS and kept under G418 selection (#10131-035, GIBCO) for 8 days to obtain stable cell lines. Expression of the constructs was induced by addition of 0.2 µg/mL doxycycline to the culture medium.

### 2.3.2 MITF knockdown cell lines

In order to be able to induce knockdowns of MITF at will, we generated two piggybac constructs containing miRNAs under the regulation of an inducible promoter. 501 Mel MITF inducible knockdown cell lines were generated using a piggybac transposable vector pPBhCMV_1-miR(BsgI)-pA-3 obtained from

Dr. Kazuhiro Murakami (Hokkaido University) (Magnusdottir et al., 2013). MicroRNAs target sequences were selected using the BLOCK-iT RNAi Designer, targeting both MITF-M exon 2 (miR(MITF-X2) and 8 (miR(MITF-X8). A non-targeting control (miR(NTC) was used as a negative control. The BLOCK-iT RNAi Designer was also used to design primers for inserting the pre-miRNA (including a mature miRNAi sequence, terminal loop and incomplete sense targeting sequence required for the formation of the stem-loop structure) RNAi into the murine miR-155 cassette in the piggybac vector pPBhCMV_1-miR(BsgI)-pA-3 containing the reverse tetracycline transcription activator. Sequences of the mature miRNAs and the primers used for the generation of the pre-miRNAs are listed in **Table 4**. Primers were annealed by initial denaturation at 95°C followed by slow cooling in water bath forming a short double stranded DNA with overhangs matching a BsgI overhang. The backbone vector was digested with BsgI (#R05559S, NEB) and the vector DNA purified after running the DNA on an agarose gel. The backbone vector and the annealed primers were ligated at 15:1 insert to backbone molar ratio using Instant Sticky-end Ligase Master Mix (M0370S, NEB). The ligation products were transformed into high-competent cells and the plasmid DNA isolated from the individual clones were screened as described above in Mutagenesis and cloning. For generation of miR-MITF cell lines, 501Mel cells were transfected with the transposase-containing plasmid pA-CAG-pBase, the plasmids pPBhCMV_1-miR(MITF_X2)-pA and pPBhCMV_1-miR(MITF_X8)-pA encoding miRNA targeting two different exons of MITF and the plasmid pPB-CAG-rtTA-IRES-Neo (10:5:5:1) that confers resistance to neomycin. For miR-Ctrl cell lines, 501Mel cells were transfected with pA-CAG-pBase, pPBhCMV_1-miR(NTC)-pA encoding a non-targeting miRNA and pPB-CAG-

**Table 4. miRNA sequences and primers used for the MITF knockdown cell lines**

| | |
|---|---|
| **miR-NTC** | |
| **Mature miRNA** | **AAATGTACTGCGCGTGGAGAC** |
| FW | 5'-GAAATGTACTGCGCGTGGAGACGTTTTGGCCACTGACTGACGTCTCCACGCAGTACATTTCA-3' |
| REV | 5'-AAATGTACTGCGTGGAGACGTCAGTCAGTGGCCAAAACGTCTCCACGCGCAGTACATTTCAG-3' |
| **miR-MITF-X2** | |
| **Mature miRNA** | **AAAGGTACTGCTTTACCTGCT** |
| FW | 5'-GAAAGGTACTGCTTTACCTGCTGTTTTGGCCACTGACTGACAGCAGGTAGCAGTACCTTTCA-3' |
| REV | 5'-AAAGGTACTGCTACCTGCTGTCAGTCAGTGGCCAAAACAGCAGGTAAAGCAGTACCTTTCAG-3' |
| **miR-MITF-X8** | |
| **Mature miRNA** | **TAAGATGGTTCCCTTGTTCCA** |
| FW | 5'-GTAAGATGGTTCCCTTGTTCCAGTTTTGGCCACTGACTGACTGGAACAAGAACCATCTTACA-3' |
| REV | 5'-TAAGATGGTTCTTGTTCCAGTCAGTCAGTGGCCAAAACTGGAACAAGGGAACCATCTTACAG-3' |

rtTA-IRES-Neo (10:10:1). After 48 hours of transfection, miR-MITF, miR-empty vector and non-transfected cells were selected with 0.5mg/ml G418 (#10131-035, GIBCO) for 2 weeks and 1ug/ml of doxycycline was used for induction.

## 2.4 Transfection of plasmids

Cells were cultured in 6 or 12-well plates one day prior to transfection. Then they were transfected with 2 µg of plasmid DNA using 6 µl FuGENE HD transfection reagent (#E2311, Promega) and diluted up to a 100 µL of serum-free medium per mL of cell culture medium. The cell culture medium containing the transfection complexes was removed after 24 hours and replaced with fresh culture medium. The cells were harvested 48 hours after transfection cells for RNA or protein extraction. Expression of the constructs was verified by Western blotting.

## 2.5 RNAi treatment

Cells were cultured in 6 or 12-wells plates one day prior to transfection. Cells were transfected with 10 µM of the respective siRNA and 1 µL Lipofectamine™ RNAiMAX transfection reagent (#13778075, Invitrogen) in 100 µL of Optimem Pro (#31985-062, GIBCO) transfection medium per mL of cell culture medium. Cells were harvested for RNA or protein extraction 2 days after transfection. The siRNAs used for the procedure were the following: siRNA for human MITF (#4390824, Ambion), siRNA for human TFEB (#M-009798-02, Dharmacon), siRNA for human TFE3 (#M-009363-03, Dharmacon) and a control siRNA (#4390843, Ambion).

## 2.6 Gene expression analysis from melanoma and melanocyte cell lines

The expression of MITF, TFEB, TFE3 and TFEC mRNA transcripts was obtained from 23 different melanoma cell lines and a human melanocyte cell line using microarray analysis performed in the laboratory of Dr. Lionel Larue (Institut Curie. Paris, France) (Rambow et al., 2015) and kindly shared with the Steingrimsson laboratory.

## 2.7 Immunostaining and confocal imaging

501mel and Skmel28 cells ($3x10^4$ per well) were cultured for 48 hours in 8-well chamber slides (#354108 from Falcon). In order to induce MITF expression in the inducible 501mel cell lines, 0.2 µg/mL of doxycycline were added to the cell culture medium. At day 2, cells were fixed for 2 min with 2% paraformaldehyde (PFA) (#P6148, Sigma Aldrich) in cell culture medium and then for 15 min with

4% PFA in PBS (**Appendix I**). For imaging of the overexpressed GFP-tagged factors, cells were washed 3 times with PBS, followed by DAPI staining (#D-1306, Life Technologies) and two additional washes with PBS. The chambers were then removed and the samples allowed to dry prior to adding a drop of Fluoromount-G™ (#00-4958-02, Invitrogen) onto each well and then topping with a cover slide. For immunostaining of the endogenous MiT/TFE factors, following the treatment with Torin1 (#4247, Tocris) or PLX4032 (#S1267, Selleck Chemicals) inhibitors, cells were washed once with PBS after fixation, then permeabilized for 8 min with 0.1% Triton X-100 in PBS, followed by 3 washes with PBS. They were then blocked with blocking buffer (5% normal goat serum, 0.05% Triton X-100 and 0.25% BSA in PBS) for 1 hour at room temperature, and stained overnight at 4°C with 0.25% BSA in PBS antibody buffer containing the primary antibodies: MITF (MS771-PABX, Thermo Scientific), TFEB (#4240, CST) (#2775, CST), and TFE3 (#14779, CST) (**Table 5**). Cells were then washed 3 times with PBT (0.1% Tween-20 in PBS) and stained for 1 hour at room temperature with the Alexa Fluor 546 goat anti-mouse IgG(H+L) (#A11003, Invitrogen) or the Alexa Fluor 488 goat anti-rabbit IgG(H+L) (#A11070, Invitrogen) (**Table 6**) fluorescent secondary antibodies diluted in PBT. Subsequently, the cells were washed twice with PBT and once with PBS and finally stained with DAPI and prepared for imaging as previously described. Imaging was performed using a FluoView FV1200 laser scanning confocal microscope (Olympus) equipped with a PlanApo N 60X/1.40 ∞/0.17 Oil Microscope Objective. The environmental temperature was set to 17°C. Images were digitally zoomed (1.5X) using FluoView 4.2 acquisition software.

**Table 5. Primary antibodies used for Western Blotting and immunostaining**

| Primary antibodies | | | | |
|---|---|---|---|---|
| **Name** | **Clonality** | **Product #** | **Company** | **Dilution used** |
| MITF | Mouse monoclonal | MS771-PABX | Thermo Scientific | 1:2000 |
| TFEB | Rabbit polyclonal | 4240 | CST | 1:2000 |
| TFE3 | Rabbit polyclonal | 2775 | CST | 1:2000 |
| GFP | Rabbit polyclonal | ab290 | Abcam | 1:5000 |
| FLAG | Mouse monoclonal | F3165 | Sigma Aldrich | 1:5000 |
| Actin | Mouse monoclonal | MAB1501 | Millipore | 1:10000 |
| Actin | Rabbit monoclonal | 4970 | CST | 1:4000 |

**Table 6. Secondary antibodies used for immunostaining**

| Secondary antibodies | | | | | |
|---|---|---|---|---|---|
| **Name** | **Channel** | **Isotype** | **Product #** | **Company** | **Dilution used** |
| Alexa Fluor goat anti-mouse | 546 | IgG(H+L) | A11003 | Invitrogen | 1:1000 |
| Alexa Fluor goat anti-rabbit | 488 | IgG(H+L) | A11070 | Invitrogen | 1:1000 |

## 2.8 Western blotting

### 2.8.1 Protein extraction from cell cultures

For total protein extraction, cells were cultured in 6 or 12-wells plates. The day of harvest, cells were washed with PBS, lysed in a variable amount (depending on culture plate size and concentration of the protein to be analyzed) of 1x Laemmli sample buffer containing 63 mM Tris-HCl (pH 6.8) (#RES3098T-B7, Sigma Aldrich), 0.1% 2-Mercaptoethanol (#M3148, Sigma Aldrich), 0.0005% Bromophenol blue (#114391, Sigma Aldrich), 10% glycerol (#G5516, Sigma Aldrich) and 2% SDS (#L3771, Sigma Aldrich), boiled at 95°C for 5 minutes and the samples were stored at -20°C until further use.

### 2.8.2 Gel electrophoresis, transfer and western blot

Samples were then run on 8% or 10% gels. To make 8% resolving gels, 2.1 mL of 40% acrylamide (#1610140, Bio-Rad), 2.5 mL of resolving gel (lower) Tris Buffer (**Appendix I**), 100 µl of 10% ammonium persulfate (APS) (#A3678, Sigma Aldrich), 10 µl of N,N,N′,N′-Tetramethylethylenediamine (TEMED) (#T9281, Sigma Aldrich) and 530 mL of distilled water were mixed and poured between two glass plates, topped with 100% isopropanol to avoid contact of the gel with air which prevents polymerization. Upon polymerization of the resolving gel, a 5% stacking gel was prepared by mixing 375 µl of 40% acrylamide, 750 µl of stacking gel (upper) Tris Buffer (**Appendix I**), 30 µl of 10% APS, 3 µl of TEMED and 2.17 mL of distilled water. The stacking gel solution was added on top of the resolving gel between the glass plates after removal of the isopropanol, and a comb was inserted for loading well formation. Enough incubation time was allowed for the gel to harden and use. The gel was placed in electrophoresis cassettes and covered with 1x running buffer (**Appendix I**). One lane of the gel was loaded with 5 µl of PageRuler™ Prestained Protein Ladder (#26616, Thermo Scientific), and different amounts

of protein samples extracted from cell cultures were loaded in the remaining wells, ranging from 15 µl to 40 µl of protein sample. Samples were run at 100V for 20 min and subsequently at 130V until the front dye would diffuse out of the gel. Gels were removed from the glass plates and washed in 1X transfer buffer (**Appendix I**). A 0.2 µm PVDF membrane (#88520, Thermo Scientific) was activated for 10 seconds in methanol and then washed in 1x transfer buffer. Gel and membrane were assembled in a wet transfer cassette covered in 1x transfer buffer and the gel proteins were blotted onto the PVDF membrane at 90V for 100 min at 4°C. The membranes were blocked with 5% BSA in TBS-T (0.1% Tween 20 in TBS (**Appendix I**) for 1 hour at room temperature, and stained overnight at 4°C with 3% BSA in TBS-T and one of the appropriate primary antibody (**Table 5**) in 5% BSA TBS-T blocking buffer. Membranes were washed 3x with TBS-T and stained for 1 hour at room temperature with the anti-mouse IgG(H+L) DyLight 800 conjugate (#5257, CST) or the anti-rabbit IgG(H+L) DyLight 680 conjugate (#5366, CST) (**Table 7**) fluorescent secondary antibodies. The membranes were again washed 3x with TBS-T and visualized using CLx Imager (LI-COR Biosciences).

**Table 7. Secondary antibodies used for Western blotting**

| Secondary antibodies | | | | | |
|---|---|---|---|---|---|
| **Name** | **Channel** | **Isotype** | **Product #** | **Company** | **Dilution used** |
| Anti-mouse | 800 nm | IgG(H+L) | 5257P | CST | 1:10000 |
| Anti-rabbit | 680 nm | IgG(H+L) | 5366S | CST | 1:10000 |

### 2.8.3 Quantification

Images obtained from scanning of Western blotting membranes with the CLx Imager (LI-COR Biosciences) were quantified using ImageJ software. The intensity of the bands of each immunoblotted protein was normalized with the actin loading control. An example of the quantification protocol can be found online (https://di.uq.edu.au/community-and-alumni/sparq-ed/sparq-ed-services/using-imagej-quantify-blots).

## 2.9 Co-immunoprecipitation

For coimmunoprecipitation experiments, cells were cultured in 6-well plates or in individual 10-cm plates and then lysed with a lysis buffer containing 50mM

TrisHCL pH 7.4, 150 mM NaCl, 1 mM EDTA, 1% Triton X-100 and supplemented with 1:100 protease inhibitor cocktail (#P8340, Thermo Scientific) and 1:100 PMSF (100 mM) for 15 min on a shaker at 4°C. The lysates were scraped and collected in microcentrifuge tubes, homogenized by pipetting several times and then allowed to rotate in a rotating platform at 4°C for 10 min. The lysates were centrifuged in order to remove cell debris at 14000 g for 10 min at 4°C. 10% of the supernatant was collected as the input fraction and the rest of the supernatant was used for immunoprecipitation. For the immunoprecipitation of GFP-tagged proteins, samples were rotated for 2 hours with 1 µl per million cells of antibodies against GFP (#ab290, Abcam). Subsequently, immunocomplexes were formed by adding 20 µl of protein A/G plus-agarose beads (#sc-2003, Santa Cruz Biotechnology) for 1 hour at 4 °C on a rotating platform. Samples were centrifuged (2,500 rpm for 5 min) to collect the beads and then washed with TBS buffer and centrifuged 3 times. The samples were eluted with 25µl of 2x Laemmli buffer. For the immunoprecipitation of FLAG-tagged proteins, samples were rotated for 3 hours with the ANTI-FLAG M2 Affinity Gel (#A2220, Sigma-Aldrich) as described by the manufacturer's instructions, followed by centrifugation of the immunocomplexes at 8200 g for 30 seconds at 4°C, and 3 cycles of washes and centrifugations with TBS. The immunoprecipitated FLAG-tagged proteins and coimmunoprecipitated proteins were eluted by competition with 150 ng/µl 3X FLAG peptide in TBS shaking at 4°C for 30 min, followed by centrifugation at 8200 g for 30 seconds at 4°C. Eluted immunoprecipitated samples and previously collected supernatant were boiled with 2x Laemmli buffer for 5 min.

## 2.10 Transcription activation assays

HEK293T cells ($1.5x10^4$ per well) were seeded in white 96-well plates (#781965, BRAND) and cultured for 24h prior to transfection (FuGENE, Promega) with 33 ng of a construct carrying the relevant regulatory region (TYR, MLANA, TFEB-int1 or TFEB-Int1-scrb) coupled to the luciferase gene, 33 ng of an MITF-M construct and 33 ng of a pRL Renilla control reporter vector. Cells were assayed 24 hours after transfection using the Luciferase DualGlo kit (E2940, Promega) as described by the manufacturer. The luminescence activity was measured in a multimode microplate reader (GloMax, Promega) with a 300-millisecond reading per well. The luciferase signal of each sample was normalized to the renilla signal for transfection efficiency and cell viability. The pGL3-Basic (#E1751, Promega) or pGL3-Promoter (#E1761, Promega) vectors were used in order to calculate the fold induction of each regulatory element activity, respectively. Three technical

replicates per sample were included in each assay and the assays were repeated for at least three biological replicates. Error bars indicate standard error of the mean (SEM) and statistical significance was assessed with student's t-tests.

## 2.11 Quantitative PCR for gene expression analysis

**Table 8. Gene-specific primers used for RT-qPCR**

| Gene target | Primer sequence |
|---|---|
| β-Actin | FW 5'-AGGCACCAGGGCGTGAT-3' |
| | REV 5'-GCCCACATAGGAATCCTTCTGAC-3' |
| RPLP0 | FW 5'-CACCATTGAAATCCTGAGTGATGT-3' |
| | REV 5'-TGACCAGCCCAAAGGAGAAG -3' |
| MITF (+/-) | FW 5'-CGACAGAAGAAACTGGAGCAC-3' |
| | REV 5'-AAATCTGGAGAGCAGAGACCC-3' |
| MITF (+) | FW 5'-ATGGAAACCAAGGTCTGCCC-3' |
| | REV 5'-GGGAAAAATACACGCTGTGAGC-3' |
| MITF 3'UTR | FW 5'-GGGATCCAAACTGGAAGACA-3' |
| | REV 5'-AGGAAGCAGTTTGTGCGAAT-3' |
| TFEB | FW 5'-AAGGAGCGGCAGAAGAAAGA-3' |
| | REV 5'-CCAACTCCTTGATGCGGTCA-3' |
| LC3B | FW 5'-CCGCACCTTCGAACAAAGAG-3' |
| | REV 5'-AAGCTGCTTCTCACCCTTGT-3' |
| LAMP1 | FW 5'-CACCATCCAGGCGTACCTTT-3' |
| | REV 5'-TGTTCACAGCGTGTCTCTCC-3' |
| ATP6V0D2 | FW 5'-TTCTTGAGTTTGAGGCCGACA-3' |
| | REV 5'-TGGATAGAGGGTCTCTCGGT-3' |
| ATP6V1C1 | FW 5'-TTGCATGCGGCAACTTCAAA-3' |
| | REV 5'-CGTGCCAACCTTTAAGTCAGG-3' |
| CTSD | FW 5'-TCAGGGCGAGTACATGATCC-3' |
| | REV 5'-GGGGACAGCTTGTAGCCTTT-3' |
| CTSZ | FW 5'-GCTATGGCGGATCGGATCAA-3' |
| | REV 5'-TACCGCAGTCGATGACGTTC-3' |
| GNS | FW 5'-TTGCCCATTTTGAGAGGTGC-3' |
| | REV 5'-CAGTGACGTTACGGCCTTCT-3' |

TRIzol reagent (#15596-026, Ambion) was used for total RNA extraction, followed by isopropanol precipitation of the RNA. The cDNA was generated according to the manufacturer's instructions with High-Capacity cDNA Reverse Transcription Kit (#4368814, Applied Biosystems). Exon-spanning human gene-specific primers for q-PCR were designed using NCBI Primer BLAST (**Table 8**), and qPCR performed with the SensiFAST SYBR Lo-ROX Kit (#BIO-94020, Bioline) using a CFX384 Touch Real-Time PCR Detection System (Bio-Rad). The qRT-PCR reactions were performed in technical triplicates, using 1 ng/µl cDNA, 0.3 µM of primer mix and 2.5 µl of SensiFAST SYBR Lo-ROX per reaction, adjusted to 5 µl with DEPC treated water. Cycling conditions are described in **Table 9**. The fold change in gene expression was calculated with the 2^(-Delta Delta C(T)) method (Livak & Schmittgen, 2001), normalized to the geometrical mean of β-Actin and human ribosomal protein lateral stalk subunit P0 (RPLP0) expression. Standard curves for primer efficiency were calculated using the formula E=10^(-1/slope) for each primer pair.

**Table 9. PCR cycling conditions for RT-qPCR**

| | Temperature ($^{o}$C) | Time (sec) | Number of cycles |
|---|---|---|---|
| Initial denaturation | 95 | 120 | 1 |
| Denaturation | 95 | 5 | 40 |
| Annealing | 60 | 10 | |
| Extension | 72 | 10 | |

## 2.12 Proliferation assay

1x10$^5$ cells were seeded per well onto a 12-wells plate. After 24 hours, cells were transfected for the overexpression of GFP-tagged TFEB (pEGFP-N1-TFEB), TFE3 (pEGFP-N1-TFE3) or GFP alone (pEGFP-N1). On day three, cells were trypsinized and seeded onto 96-well plates at a density of 2x10$^3$ cells per well in triplicates. Images were recorded with Incucyte Zoom system (Essen BioScience) every 2 hours for at least 7 days. Collected images were then analyzed using Incucyte software by measuring cell confluency to graph the growth curves. The doubling time was calculated with the formula: Duration x log(2)/log(FinalConfluency)-log(InitialConfluency).

## 2.13 Bioinformatics and data visualization of ChIP-seq analysis

ChIP-sequencing data were obtained and analyzed by Ramile Dilshat (unpublished data), who performed ChIP-seq experiments using a transfected TFEB-GFP construct in 501Mel cells. She then generated WIG files (.wig), text files that define the ChIP-seq data tracks. Data tracks were loaded onto the IGV genome browser (Robinson et al., 2011) (Thorvaldsdottir et al., 2013) in order to analyze the location of binding sites provided by these datasets across the genome. Gene Ontology (GO) analyses were performed with the web tool DAVID (Huang da et al., 2009a, 2009b) using default parameters. Motif discovery and motif enrichment analyses (AME) (McLeay & Bailey, 2010) were performed using the MEME suite web tool (Bailey et al., 2009) using default parameters. Venn diagrams were generated using JVenn web plug-in (Bardou et al., 2014) or manually using Graphpad Prism 7.

## 2.14 Statistical analysis

Results are represented as grouped analysis of the mean from three or more independent experiments with standard error of the mean (SEM). Graphpad Prism 7 was used for all the statistical analysis. Analysis of qRT-PCR and Western blot quantification of the regulatory loop, were performed using multiple t-tests, comparing each cell mean to the control cell mean and multiple comparison correction by Holm-Sidak method with statistical significance set as *P<0.05. All the remaining statistical analysis of qRT-PCR, including analysis of autophagy genes and the effects of mTOR inhibition were performed using two-way analyses of variance (ANOVA). Statistical analysis of the doubling time calculated from the proliferation assay and the luciferase reporter assays, were performed using one-way ANOVA. ANOVA analysis were performed comparing each cell mean to the control cell mean and multiple comparison correction by Sidak method with statistical significance set as *P<0.05.

# 3 Results

## 3.1 MiT-TFE transcription factors are expressed in melanoma

Previous analysis performed in the lab using RNA sequencing data from 368 metastatic melanoma tumors from The Cancer Genome Atlas (TCGA) Research Network: (Cancer Genome Atlas, 2015; "http://cancergenome.nih.gov/,") showed that the expression of TFEB, TFE3 and TFEC was 14-fold, 4-fold and 40-fold lower, respectively, than that of MITF (**Figure 8A**) (Möller et al., submitted). In addition, analysis of TCGA showed that MITF, TFEB, TFE3 and TFEC mRNAs are expressed across melanoma tumors and are subject to a number of somatic genetic alterations in a subset of 363 melanoma specimens. 131 (36%) of all the samples in the dataset harbor at least one somatic genetic alteration associated with MITF, TFEB, TFE3 or TFEC, including in-frame, missense or truncating mutations, genetic fusions, genomic amplifications and mRNA overexpression (**Figure 8B**). A majority of the alterations detected in these tumors that affected MITF are copy number amplifications and mRNA upregulations. I could not detect any recurrent MITF mutation across the tumors. Most mutations affecting TFEB and TFE3 were missense mutations with a single occurrence. Interestingly, four samples featured a missense G103E mutation in TFEC. The significance of this mutation is unknown and only 1 out of the 4 mutated samples was

**A**

| | MITF | TFEB | TFE3 | TFEC | Fold MITF/TFEB | Fold MITF/TFE3 |
|---|---|---|---|---|---|---|
| Metastatic melanoma | 5947 | 437 | 1442 | 144 | 13.6 | 4.1 |

**B**

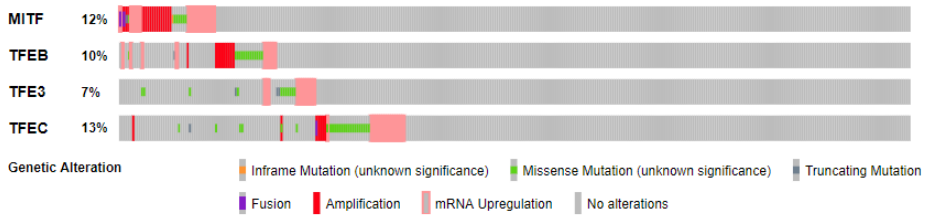

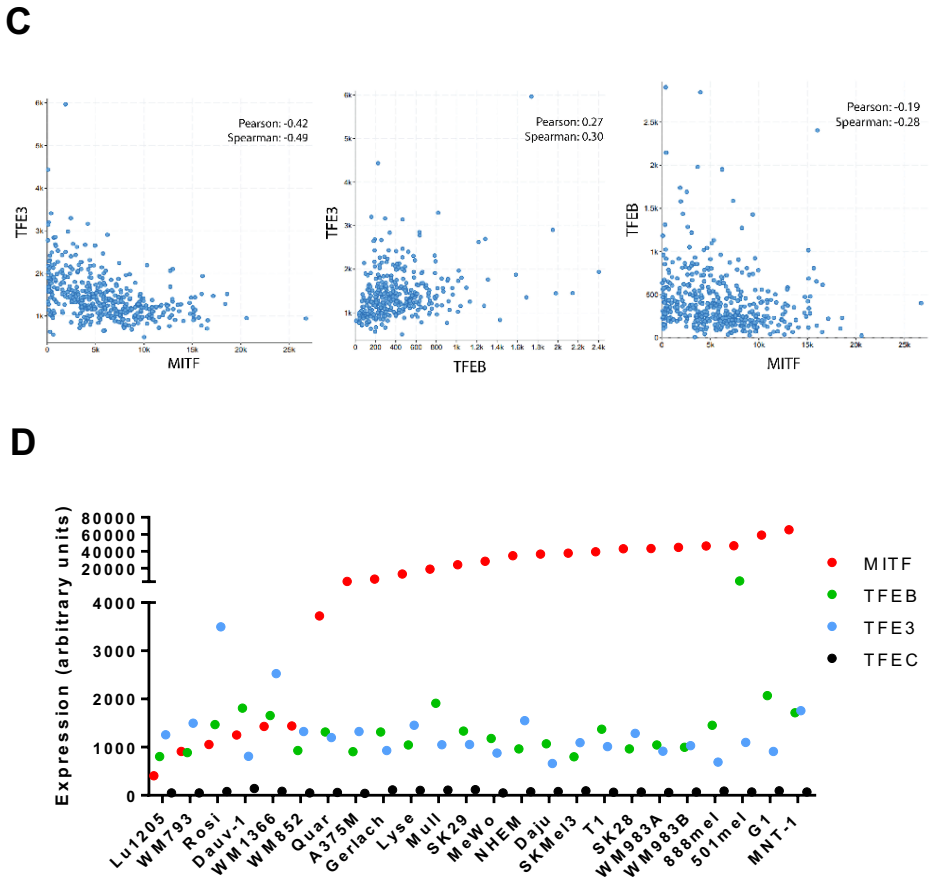


**Figure 8. MITF, TFEB, TFE3 and TFEC mutations and expression across melanoma tumors and cell lines.** (A) Mean expression of MITF, TFEB, TFE3 and TFEC in TCGA tumor samples (368 metastatic melanomas). (B) Oncoprint chart showing genetic alterations in the MITF, TFE3, TFEB and TFEC genes found in 363 melanoma biopsies. (C) Co-expression analysis of MITF, TFEB and TFE3 in the same subset of melanoma samples. Spearman's rank correlation coefficient (rho) is -0.49 for TFE3 and MITF, 0.30 for TFE3 and TFEB and -0.28 for TFEB and MITF. (D) Cell lines were sorted by MITF expression. No correlation was observed in expression between MITF and TFEB ($r^2$=0.07365), MITF and TFE3 ($r^2$=0.1223), or TFEB and TFE3 ($r^2$= 0.00047).

associated with a change in copy number of TFEC. Furthermore, I investigated the gene expression data generated by the TCGA across 363 melanoma biopsies for analysis of the correlation in gene expression between MITF, TFEB and TFE3. TFE3 and MITF negatively correlate in expression (rho=-

0.49), whereas a weak positive correlation in expression between TFE3 and TFEB was observed (rho=0.3). TFEB and MITF appeared to have a weak negative correlation (rho=-0.28) (**Figure 8C**).

Next, we obtained gene expression profiles for 23 melanoma cell lines as well as in the normal human epidermal melanocytes (NHEM) generated using a microarray platform (Rambow et al., 2015). I analyzed the expression of MITF, TFEB, TFE3 and TFEC and found that MITF is highly expressed in most of the lines (**Figure 8D**). Whereas TFEB and TFE3 are detected in most of these cell lines, TFEC is either not expressed, or is expressed at very low levels in the cells lines. Moreover, the expression of TFEC across metastatic tumors is 41-fold lower than that of MITF (**Figure 8A**). This suggests that TFEC is not important in the melanocyte lineage. I therefore focused on MITF, TFEB and TFE3 in the remaining analysis. I sorted the melanoma cell lines by MITF expression and determined correlation to TFEB and TFE3 expression. No correlation was found between the expression of MITF and TFEB ($r^2$=0.07365), MITF and TFE3 ($r^2$=0.1223), or TFEB and TFE3 ($r^2$= 0.00047) in these cell lines (**Figure 8D**).

## 3.2 Subcellular localization of MITF, TFEB and TFE3 is affected by signaling pathways

Recently, it has been shown that the subcellular localization of TFEB and TFE3 is regulated by the mTOR pathway (Martina et al., 2012; Martina, Diab, Lishu, et al., 2014). In order to determine if this pathway also affects the localization of these transcription factors in the melanocyte lineage, I analyzed the endogenous expression of these transcription factors in human melanoma cell lines by immunostaining and confocal microscopy and determined whether their subcellular localization responds to signaling cues. All three transcription factors, MITF, TFEB and TFE3, were detected in the human melanoma cell line 501Mel using immunocytochemistry. Antibodies specific for each factor are listed in **Table 5**. Whereas TFEB and TFE3 were located mostly in the cytoplasm of 501Mel cells but also in the nucleus, MITF showed a predominant nuclear presence (**Figure 9A**). The major isoform of MITF in melanocytes and melanoma cells is MITF-M which is primarily located in the nucleus (Fock et al., 2018). The cytoplasmic retention of TFEB and TFE3 is mediated by a domain of 30 amino acids that is responsible for binding to Rag GTPases at the lysosome surface (Roczniak-Ferguson et al., 2012). The Rag-binding domain is N-terminal in TFEB, whereas in TFE3 it is located between amino acids 110-140 (Martina, Diab, Lishu, et al., 2014). Interestingly, MITF-M lacks this N-terminal region resulting in a constitutive nuclear presence of the

protein, in contrast with other MITF isoforms such as MITF-A (Martina & Puertollano, 2013). Western blot analysis showed that the MITF, TFEB and TFE3 proteins are expressed in 501Mel melanoma cells (**Figure 9B**). The western analysis also showed that whereas TFE3 and MITF are both expressed in the SKmel28 cells, TFEB is not expressed in those cells (**Figure**

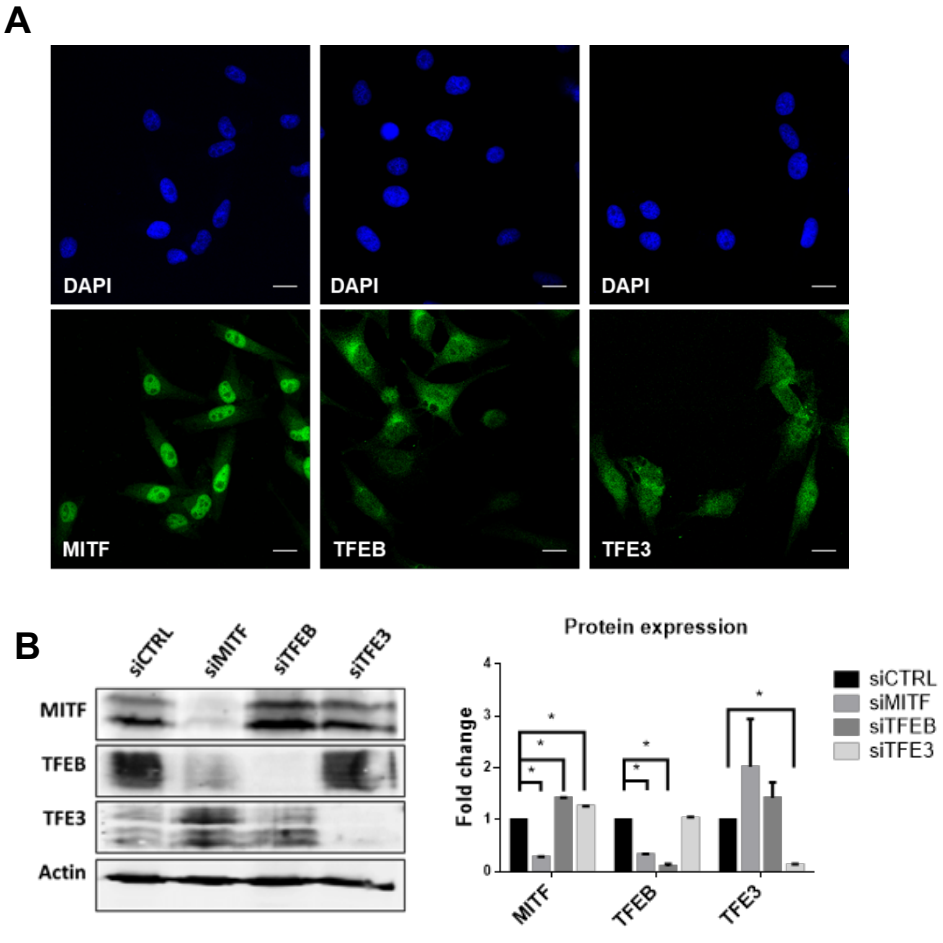


**Figure 9. MITF, TFEB and TFE3 are expressed in 501 Mel cells.** (A) Immunofluorescence images showing the expression of endogenous MITF, TFEB and TFE3 in 501 Mel melanoma cells. Blue indicates DAPI staining whereas green indicates staining of each of the three transcription factors. (B) Western blot analysis of MITF, TFEB and TFE3 proteins after MITF, TFEB and TFE3 siRNA knockdown in 501 Mel cells. Shown is a representative figure and quantification of three independent experiments, bars represent SEM. * indicates significance at $p<0.05$.

**10**). Short-term knockdown with siRNA against each factor resulted in severe reduction or absence of each specific protein, confirming the specificity of the antibodies used (**Figure 9B, 10**).

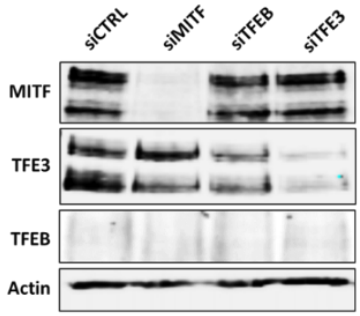


**Figure 10. MITF and TFE3, but not TFEB are expressed in Skmel28 cells.** Western blot analysis of MITF, TFEB and TFE3 protein levels after MITF, TFEB and TFE3 siRNA knockdown in Skmel28 cells, TFEB protein expression was below detection levels. Shown is a representative figure for three independent experiments.

Phosphorylation of TFEB at Ser142 by mTORC1 and MAPK promotes its cytoplasmic localization (Settembre et al., 2011). Therefore, I investigated if inhibiting the mTORC1 and BRAF-MAPK pathways would affect the subcellular localization of the MiT-TFE subfamily of transcription factors in melanoma cells. Using the mTORC1/2 inhibitor Torin1, and the BRAFV600E

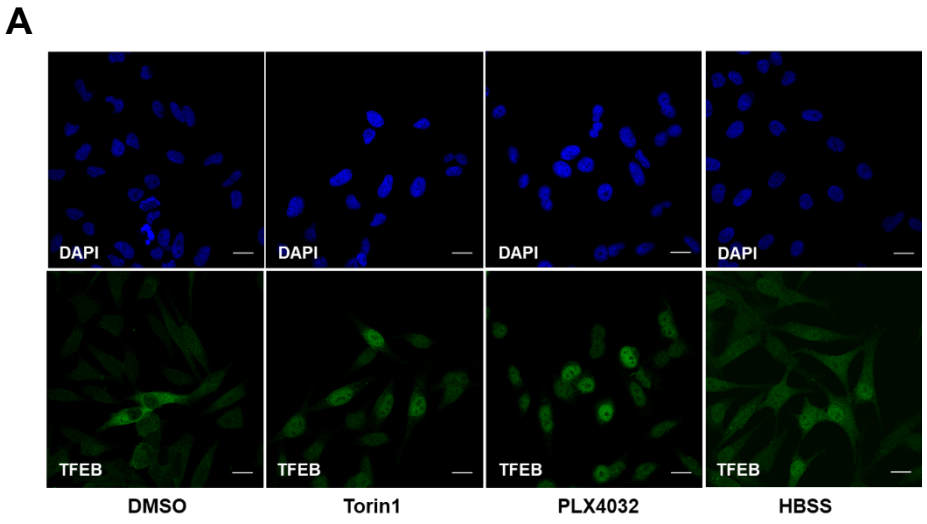

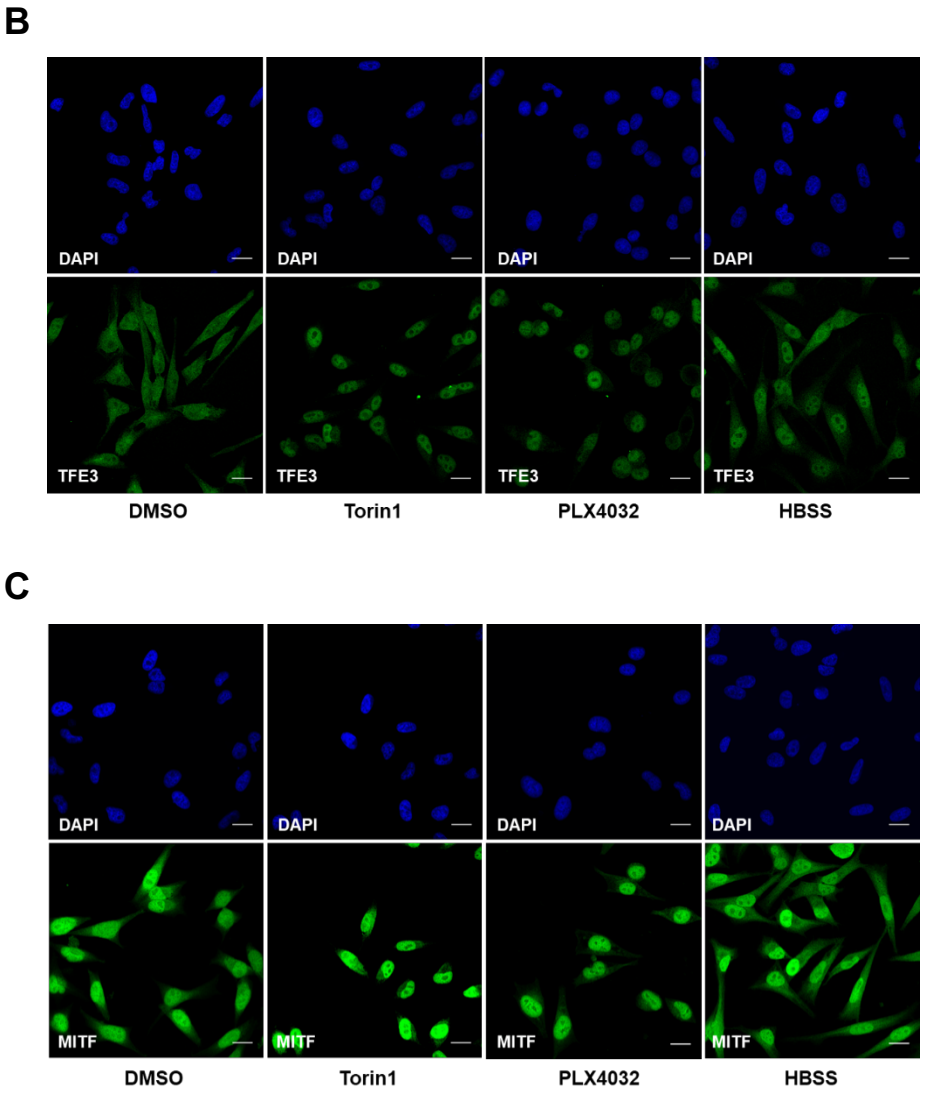


**Figure 11. Signaling affects cytoplasmic location of the MITF-TFE family in 501Mel cells.** Immunofluorescence images of human 501Mel cells after treatment with vechicle (DMSO), an mTOR inhibitor (Torin1, 1 μM), BRAFV600E selective inhibitor (PLX4032, 2 μM) or starved with HBSS minimum medium for three hours, showing endogenous TFEB (A), TFE3 (B) and MITF (C) in green. Blue indicates DAPI staining.

selective inhibitor vemurafenib (PLX4032) in human 501Mel cells, resulted in an increased nuclear localization of endogenous TFEB and TFE3 proteins, suggesting that mTORC and/or BRAF mediate signals that modulate the

subcellular localization of TFEB and TFE3 in melanoma cells (**Figure 11A, B**). Furthermore, both inhibitors resulted in reduced cytoplasmic presence of MITF (**Figure 11C**). The same results were observed when constructs containing GFP-fusions of the MITF-M, TFEB and TFE3 proteins were overexpressed in 501Mel cells using a doxycycline-inducible piggybac (pBac) system, and subsequent treatment with Torin1 (**Figure 12**). Torin1 treatment led to nuclear localization of all three proteins and a reduction in their presence in the cytoplasm. This suggests that overexpression does not affect the nucleocytoplasmic distribution of these factors (**Figure 12**). In Skmel28 melanoma cells, TFEB is not expressed (**Figure 10, 13A**). Similar to 501Mel cells, TFE3 shows a cytoplasmic distribution and translocation to the nucleus upon mTORC and BRAF inhibition (**Figure 13B**). MITF is mostly nuclear in this cell line, with reduced cytoplasmic presence after treatment with the kinase inhibitors (**Figure 13C**).

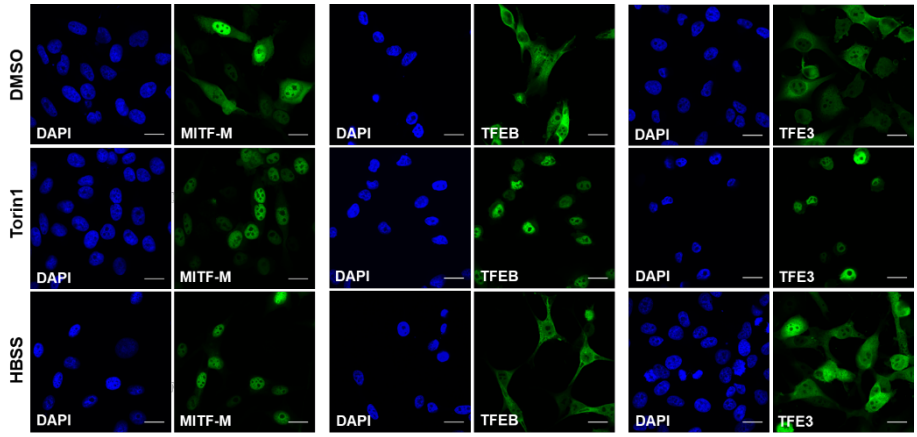


**Figure 12. MITF, TFEB and TFE3 subcellular localization in 501Mel cells is affected upon mTORC inhibition but not starvation.** Human 501Mel cells expressing doxycycline-inducible MITF-M, TFEB or TFE3 were treated with an mTORC1 inhibitor or HBSS-starved for three hours, then fixed for GFP imaging.

Both 501Mel and Skmel28 are human melanoma cell lines that carry the mutation BRAFV600E, which makes BRAF constitutively active and a driver in tumorigenesis (Davies et al., 2002). Therefore, I analyzed the subcellular localization of the MiT-TFE factors and whether it is affected by the mTOR and BRAF signaling pathways in a wild type BRAF context, using the Skmel31 human melanoma cell line. MITF and TFE3, but not TFEB are expressed in these cells (**Figure 14A**). In contrast to my observations in the 501Mel and

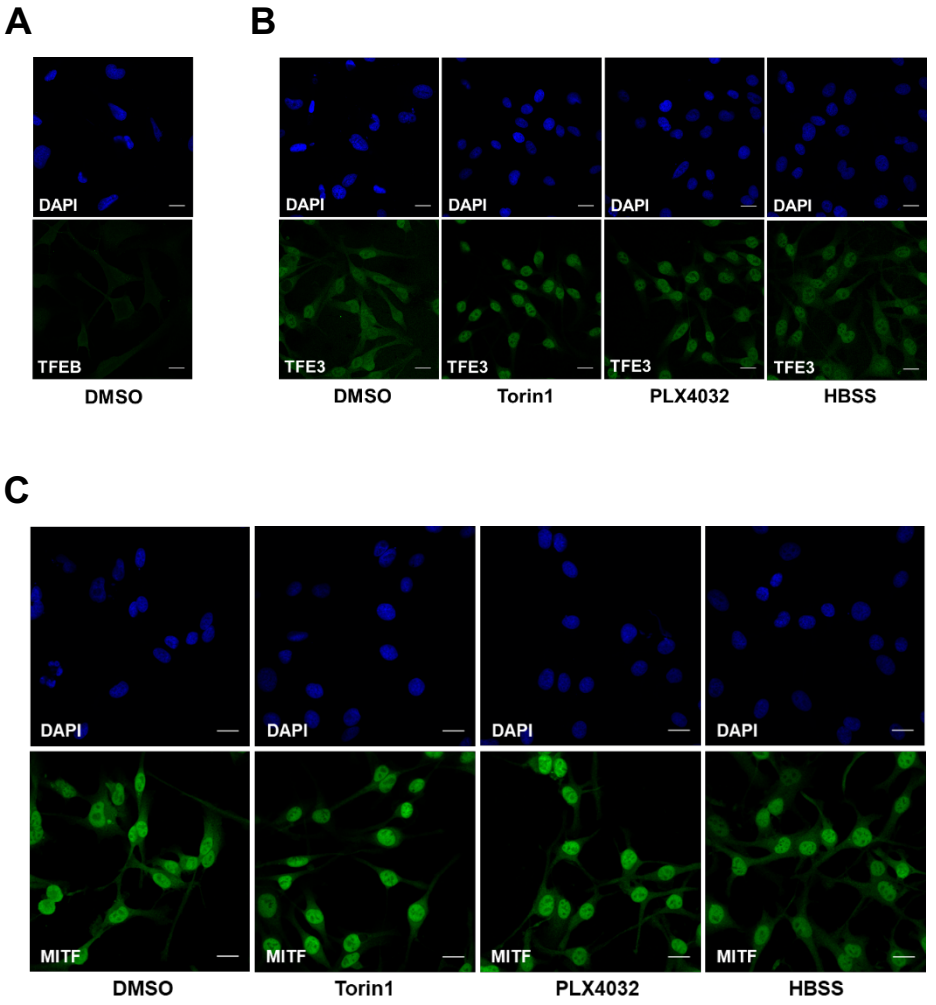


**Figure 13. Signaling affects cytoplasmic location of the MITF-TFE family in Skmel28 cells.** Immunofluorescence images of human Skmel28 cells after treatment with vechicle (DMSO), an mTOR inhibitor (Torin1), BRAF inhibitor (PLX4032) or starved with HBSS minimum medium for three hours, showing endogenous TFEB (A), TFE3 (B) and MITF (C) in green. Blue indicates DAPI staining.

Skmel28 cell lines, TFE3 has a substantial nuclear pattern in the Skmel31 cell line, and inhibition of mTORC or BRAF does not affect the localization of the protein significantly (**Figure 14B**). Interestingly, a considerable fraction of MITF was found to be expressed in the cytoplasm of these cells, and it did not respond significantly to mTORC or BRAF inhibition (**Figure 13C**).

In addition to direct drug-mediated inhibition of mTORC1, amino acid deprivation has been shown to inhibit mTORC1 and trigger nuclear localization of the MiT/TFE transcription factors in HeLa and HEK293T cells (Martina & Puertollano, 2013; Settembre et al., 2012). In order to determine if this was also the case in melanoma cells, the cells were treated for three hours with Hank's balanced saline solution (HBSS) medium lacking glucose and amino acids. This only partially enriched the nuclear localization of TFEB and TFE3

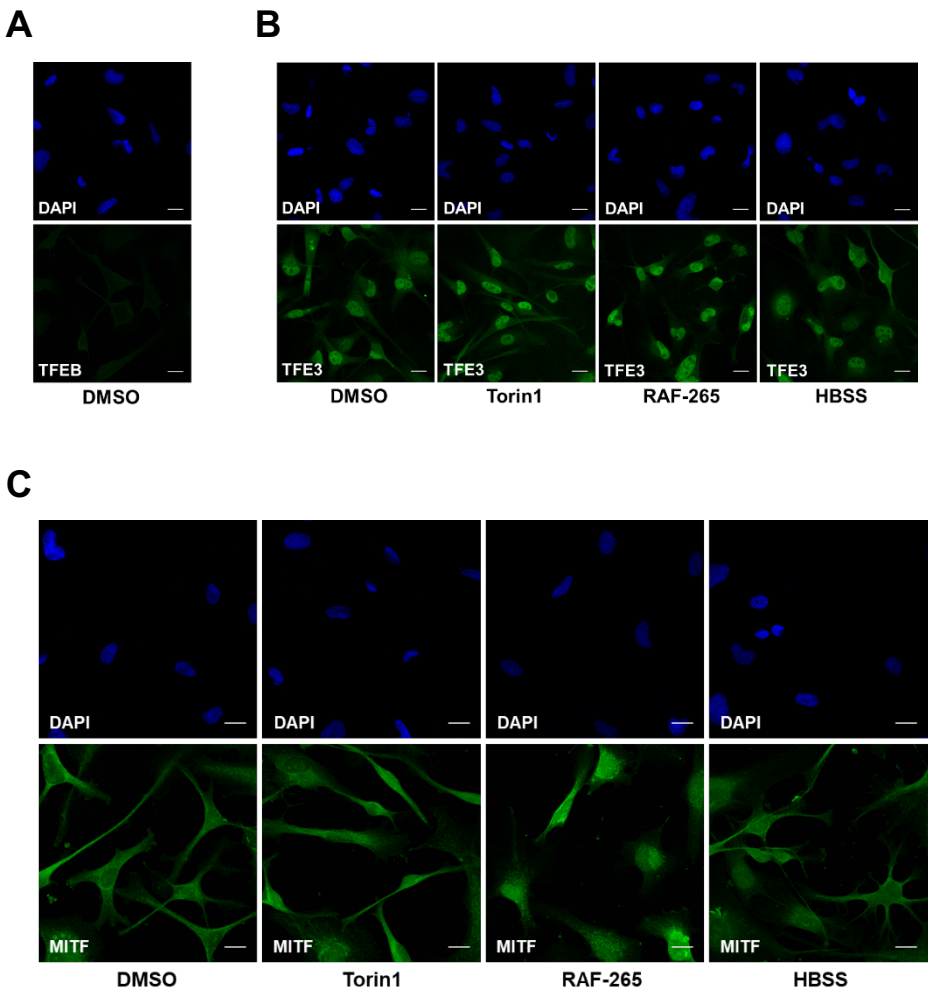


**Figure 14. Signaling affects cytoplasmic location of the MITF-TFE family in Skmel31 cells.** Immunofluorescence images of human Skmel31 cells after treatment with vechicle (DMSO), an mTOR inhibitor (Torin1, 1 μM), BRAF inhibitor (RAF-265, 5 μM) or starved with HBSS minimum medium for three hours, showing endogenous TFEB (A), TFE3 (B) and MITF (C) in green. Blue indicates DAPI staining.

(**Figure 11A, B, 12, 13A, B**). The majority of the proteins remained cytoplasmic, suggesting that mTORC1 was still active upon starvation in these cells (**Figure 11, 12, 13, 14**). Taken together, these data confirm that the MiT-TFE subfamily of transcription factors are expressed in a subset of melanoma cell lines and their subcellular localization is regulated by the mTORC1 and BRAF-MAPK axis but not starvation. It is plausible that mTORC1 might be unresponsive to amino acid depletion in melanoma cells and that starvation-induced autophagy undergoes a different regulation in these cells.

### 3.2.1 Phosphorylation of MITF affects its subcellular localization

I have shown that mTORC inhibition induces the nuclear translocation of TFEB and TFE3 but also reduces the cytoplasmic fraction of MITF-M in melanoma cells. Interestingly, Ser73 of MITF is located in a conserved domain that corresponds to Ser142 of TFEB (**Figure 6**). In MITF this residue has been shown to be phosphorylated by the MAPK pathway in melanoma cells. Thus, in order to investigate whether mTOR can phosphorylate Ser73 of MITF, I performed immunoblotting in melanoma cells overexpressing either wild type MITF-M or a mutated version carrying a Ser73 to alanine (S73A) mutation of MITF-M, a non-phosphorylatable version of MITF. The cells were treated with Torin1 or vehicle. In accordance with previous studies showing that phosphorylation at Ser73 generates a mobility shift observable by Western blotting, in which the upper band corresponds to phosphorylated Ser73 (Hemesath et al., 1998), overexpressed S73A mutant resolved as a single band. Pharmacological inhibition of BRAF and mTORC decreased the intensity of the upper band of the wild type protein, especially when both treatments were performed in combination, suggesting that both signaling pathways can phosphorylate Ser73 of MITF-M in melanoma cells (**Figure 15**). Mutation of Ser409 to alanine also triggered a mobility shift of the MITF protein, as observed by a lower molecular weight of the MITF doublet in western blot. The upper band did not disappear upon mutation of Ser409Ala, suggesting that phosphorylation of Ser73 can still take place (**Figure 15**).

Next, I analyzed if the phosphorylation status of Ser73 affects the nucleocytoplasmic distribution of MITF. For this, I overexpressed the MITF-A isoform in 501Mel cells. The reason for choosing this isoform is that since MITF-M is primarily located in the nucleus, the fraction that shuttles between the cytoplasm and the nucleus is a minor component of the total protein (**Figure 11**). However, MITF-A is mostly cytoplasmic in 501Mel cells and therefore this isoform is more appropriate for this analysis. When the mTOR pathway was blocked with Torin1, MITF-A translocated to the nucleus (**Figure 16**). This same effect was achieved when mutating Ser180 of MITF-A to

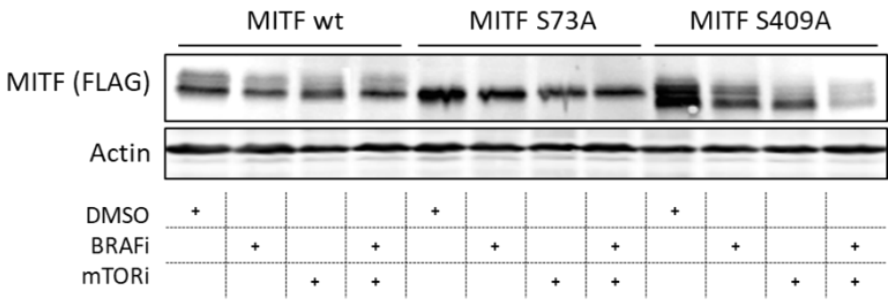


**Figure 15. BRAF and mTORC kinase inhibition affect the phosphorylation of Ser73 of MITF.** Overexpression of FLAG-tagged wt MITF, S73A MITF and S409A MITF in 501 Mel cells. Cells were treated with DMSO (vehicle), BRAF inhibitor (RAF-265, 5 μM) and mTOR inhibitor (Torin1, 1 μM) for three hours prior to protein extraction.

alanine, the serine residue that corresponds to Ser73 of MITF-M. This mutant version of the MITF-A isoform is exclusively nuclear (**Figure 16).** Taken together, these data suggest that mTORC is able to phosphorylate Ser73 of MITF-M and Ser180 of MITF-A, promoting the cytoplasmic retention of the MITF protein. This is more pronounced in the longer MITF-A isoform, due to

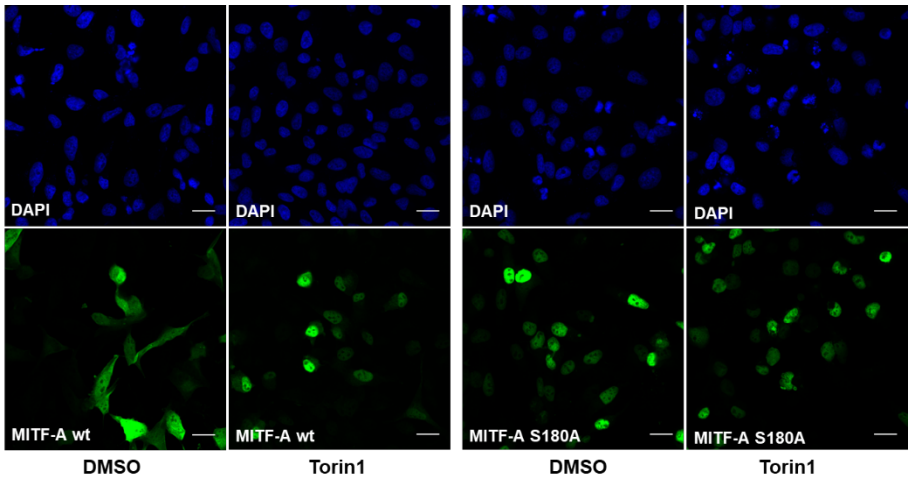


**Figure 16. MITF-A subcellular localization is dependent upon phosphorylation of Ser180 by mTORC.** Human 501Mel cells overexpressing wild type (wt) or S180A MITF-A were treated with DMSO (vehicle) or an mTORC inhibitor (Torin1, 1 μM) for three hours, then fixed for GFP imaging.

its more prominent cytoplasmic distribution under normal conditions. These data indicate that the phosphorylation of MITF takes place through Ser73 of MITF-M and its homologous Ser180 in MITF-A. We cannot exclude the possibility that a different site that depends upon phosphorylation of that specific residue is also involved.

The RANKL-dependent signaling pathway has been shown to activate TFEB and induce lysosomal biogenesis in osteoclasts through the phosphorylation of Ser462/463/467/469 at the C-terminus of TFEB by protein kinase C β (PKCβ) (Ferron et al., 2013). This domain is serine-rich and is conserved in MITF (**Figure 17A**). Other serine residues within this domain, Ser397/401/405 in MITF-M, have been identified as a phosphodegron domain that targets the protein for degradation (Ploper et al., 2015). This serine-rich C-terminal domain is conserved in TFEB, TFE3 and TFEC (**Figure 17A**). I analyzed whether GSK3β-mediated phosphorylation of Ser504/508/512 in MITF-A, the residues corresponding to Ser397/401/405 in MITF-M, are involved in the regulation of the subcellular localization of MITF. For this, I overexpressed GFP-tagged wild type or Ser504/508/512Ala versions of MITF-A in 501Mel cells, and treated the cells with a GSK3β inhibitor or vehicle. MITF-A is located in both the nucleus and the cytoplasm of these cells. The Ser504/508/512Ala MITF-A mutant displayed a more pronounced cytoplasmic presence than wild type MITF-A (**Figure 17B**), indicating that phosphorylation of these sites affects the nuclear localization of the protein. Next, the inhibitor CHIR99021, a potent selective inhibitor of GSK3β, was employed in order to assess changes in the subcellular localization of MITF-A upon inactivation of the pathway. The selective GSK3β inhibitor increased the nuclear presence of wild type MITF-A (**Figure 17B**). Interestingly, treating cells overexpressing S504/508/512A MITF-A with the GSK3β inhibitor resulted in a predominant nuclear localization of the protein (**Figure 17B**), similar to the effect of the inhibitor on wild type MITF-A. This indicates that blockade of the GSK3β signaling pathway induces nuclear localization of MITF-A regardless of the phosphorylation status of Ser504/508/512, amino acids that were previously reported to be phosphorylation targets of GSK3β (Ploper et al., 2015). Mutation of this serine-rich domain is not sufficient to prevent nuclear localization of MITF upon GSK3β inhibition.

These data indicate that, similarly to the mTOR pathway, GSK3β can promote the cytoplasmic retention of MITF in melanoma cells, possibly through the phosphorylation of a region that has yet not been identified, different from the one described by Ploper and colleagues. Moreover, mutating the three serines Ser504/508/512Ala to non-phosphorylatable alanine at the C-terminal

region of MITF, slightly increased the cytoplasmic presence of the protein. This suggests that Ser504/508/512Ala are not the residues mediating the GSK3β-induced cytoplasmic retention of MITF. In summary, GSK3β can phosphorylate a number of different residues of MITF and affect its subcellular localization and activity.

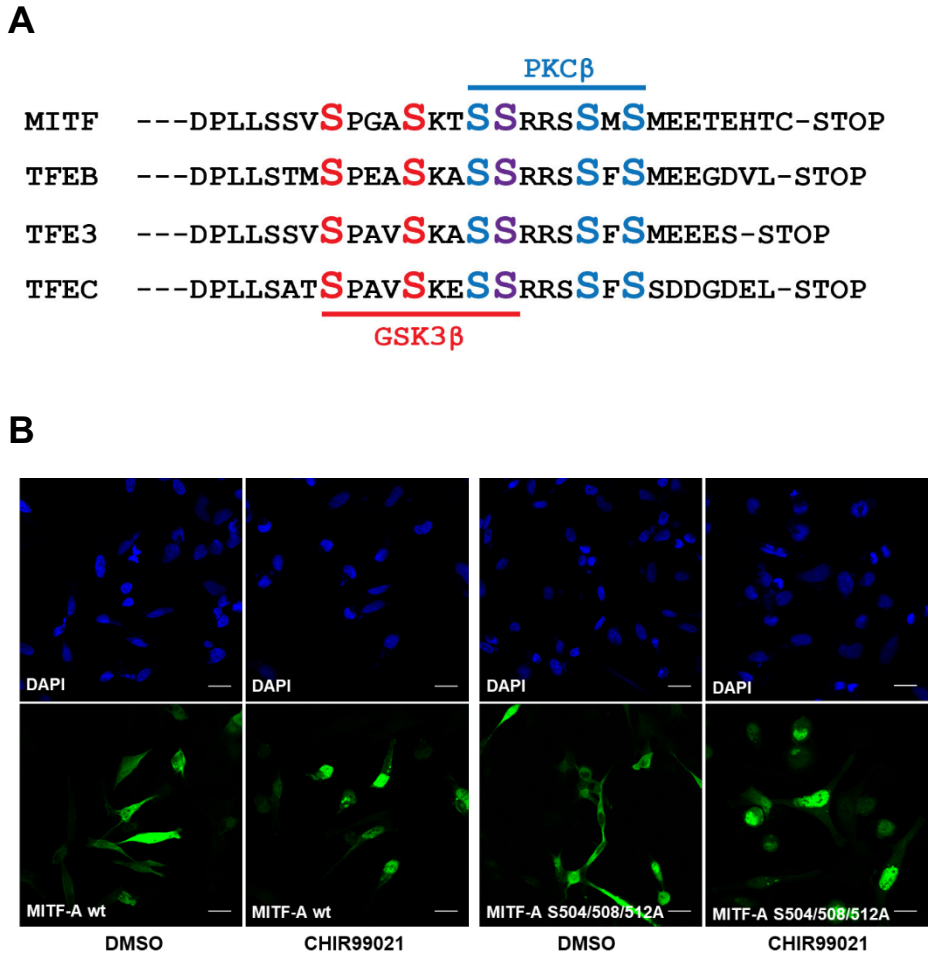


**Figure 17. MITF-A subcellular localization is dependent upon phosphorylation by GSK3β.** (A) The MiT-TFE factors feature a serine-rich C-terminal domain. Four serines wiithin this domain are putative PKCβ phosphorylation sites, marked in blue and purple (Ferron et al., 2013). Putative C-terminal GSK3 phosphorylation sites, marked in red and purple (Ploper et al., 2015). (B) Human 501Mel cells overexpressing wild type (wt) or S504/508/512A MITF-A were treated with an GSK3β inhibitor (CHIR-99021, 1 μM) for three hours, then fixed for GFP imaging.

## 3.3 MITF, TFEB and TFE3 interact in melanoma cells

The bHLHZip transcription factors require the formation of homo- or heterodimers in order to bind DNA and activate target genes. The different members of the bHLHZip family, such as MYC, MAX, MAD and MNT form heterodimers that modulate cell growth, proliferation, differentiation, apoptosis (Amati & Land, 1994) and oncogenesis (Baudino & Cleveland, 2001; Dang, 2012). As previously mentioned in the introduction, selection of dimerization partners of these factors has an impact on the transcription of their target genes. c-Myc/MAX heterodimers promote the transcription of genes involved in cell proliferation, whereas MAD/MAX heterodimers bound to the same DNA regulatory element are transcriptional repressors (Luscher, 2012). *In vitro* translated MITF has been shown to form stable DNA-binding heterodimers with TFEB, TFE3, and TFEC (Hemesath et al., 1994).

In order to determine if MITF, TFEB and TFE3 are able to interact in melanoma cells, 501mel cells expressing piggybac vectors containing doxycycline-inducible GFP-tagged TFEB, TFE3, or empty vector, (EV) were co-transfected with FLAG-tagged MITF or TFE3. The GFP-tagged protein was immunoprecipitated with GFP antibodies. Sodium dodecyl sulfate–polyacrylamide gel electrophoresis (SDS-PAGE) was performed using whole lysate and the immunoprecipitated fraction of each sample. Subsequently, immunoblotting was performed using antibodies against GFP, FLAG and actin as a loading control. FLAG-tagged MITF was detected when GFP-tagged TFEB and TFE3 were pulled down suggesting that MITF can form heterodimers with both TFEB and TFE3 (**Figure 18A**). Likewise, FLAG-tagged

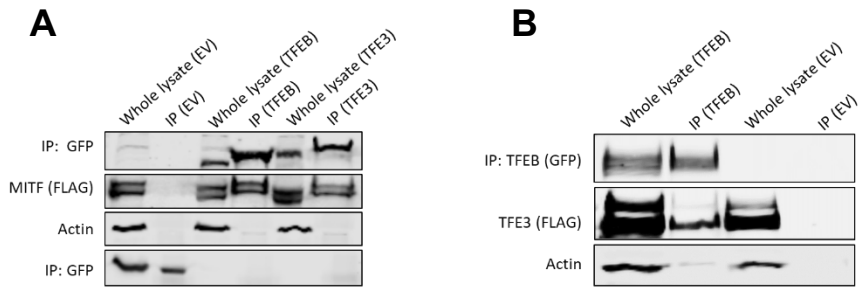


**Figure 18. MITF, TFEB and TFE3 interact.** Western blots showing the results of the following co-immunoprecipitation experiments: An MITF FLAG-tagged construct was co-transfected with GFP-tagged EV, TFEB or TFE3 (A). A FLAG-HA-tagged TFE3 construct was co-transfected with GFP-tagged TFEB (B). IP=immunoprecipitated. EV=empty vector.

TFE3 was detected in the TFEB pull-down fraction (**Figure 18B**), showing that TFE3 and TFEB can interact in melanoma cells. Neither TFE3 nor TFEB were detected when the GFP empty vector was immunoprecipitated, showing that the interaction is specific (**Figure 18A, B**). I conclude that MITF, TFEB and TFE3 are able to interact in melanoma cells, possibly forming functional heterodimers that cooperate at transcribing their target genes.

### 3.3.1 The role of a three-residue insertion in the leucine zipper of the MiT-TFE transcription factors

The crystal structure of MITF revealed how the MITF-TFE family of proteins form specific hetero- or homodimers and avoid dimerizing with other bHLHzip proteins (Pogenberg et al., 2012). This is due to an asymmetric homodimeric assembly because of the insertion of a three-residues stammer at the junction of the two first heptad repeats of the leucine zipper (**Figure 5**). This sequence is present in all the MiT-TFE transcription factors family members (Pogenberg et al., 2012) and the structural feature is probably also conserved. To characterize whether the three-residue region within the N-terminal region of MITF's leucine zipper has an impact on its transcription ability and its role in determining the interaction partners in a cellular context, an MITF construct termed MITF(Δ259-261) lacking this region was generated. HEK293T cells transfected with MITF(Δ259-261) showed that, similar to wild type MITF, this protein is nuclear (**Figure 19A**) (Sigvaldadóttir, 2016) (Pogenberg et al., **manuscript II**, in preparation).

In order to determine if this deletion mutation affects transcription activation potential of MITF, I performed transactivation assays in HEK293T cells using different variations of the binding elements present in the tyrosinase promoter. The wild type tyrosinase promoter has two E-box-like CATGTG regulatory elements that have been mutated to the canonical E-box CACGTG and M-box TCATGTGA elements (**Figure 19B**). Luciferase transactivation assays upon co-transfection of the cells with wild type or MITF(Δ259-261) versions of MITF, together with the E-box or M-box tyrosinase promoter, showed that the MITF(Δ259-261) mutant is able to transactivate these DNA regulatory elements as efficiently as wild type MITF (**Figure 19C**) (Sigvaldadóttir, 2016) (Pogenberg et al., **manuscript II**, in preparation).

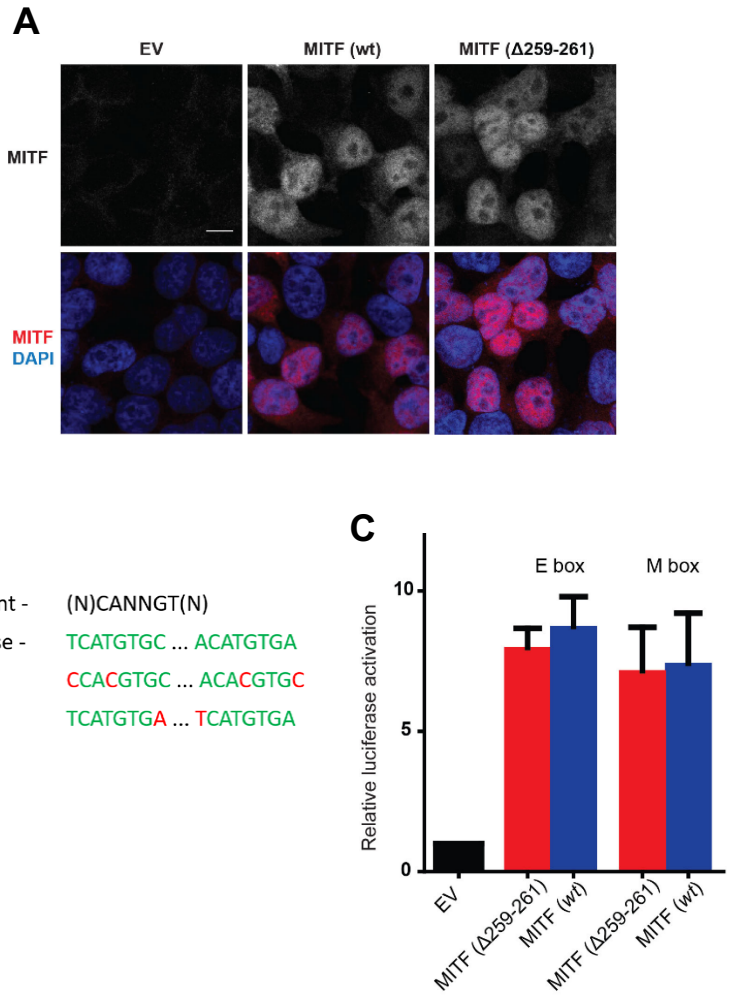


**Figure 19. MITF(Δ259-261) maintains its major nuclear localization and transcriptional ability.** (A) Immunofluorescence images showing the expression of overexpressed MITF(Δ259-261) in HEK293T cells. Blue indicates DAPI staining whereas red indicates staining of wt MITF or MITF(Δ259-261). (B) Transactivation assays in HEK293T cells in which MITF(Δ259-261) or wt MITF were co-transfected with TYR promoters containing either M- or E-boxes or an empty vector (EV) control.

Next, I used co-immunoprecipitation studies to analyze the ability of MITF(Δ259-261) to form homo- or heterodimers with wild type MITF, TFEB or TFE3. I ectopically co-expressed GFP-tagged wild type or MITF(Δ259-261) proteins with a FLAG-tagged wild type MITF construct and immunoprecipitated

the GFP-tagged proteins. Western blot analysis of the immunoprecipitated fraction indicated that GFP-tagged MITF(Δ259-261) can form homodimers with FLAG-tagged MITF(Δ259-261) but does not interact with FLAG-tagged wild type MITF (**Figure 20A**). When co-expressing GFP-tagged TFEB and TFE3 with FLAG-tagged wild type MITF or MITF(Δ259-261), wild type MITF was detected in the TFEB and TFE3 immunoprecipitated fractions (**Figure 20B**). However, MITF(Δ259-261) was not detected, which suggests that the MITF(Δ259-261) fails to dimerize with wild type TFEB or TFE3 (**Figure 20B**). As a negative control, an empty vector expressing GFP was co-expressed with either FLAG-tagged wild type MITF or MITF(Δ259-261). The FLAG-tagged MITF was detected in the whole lysate but not in the sample fraction containing immunoprecipitated GFP alone (**Figure 20C**). This indicates that the FLAG and GFP tags used in this experiment are not able to interact with each other

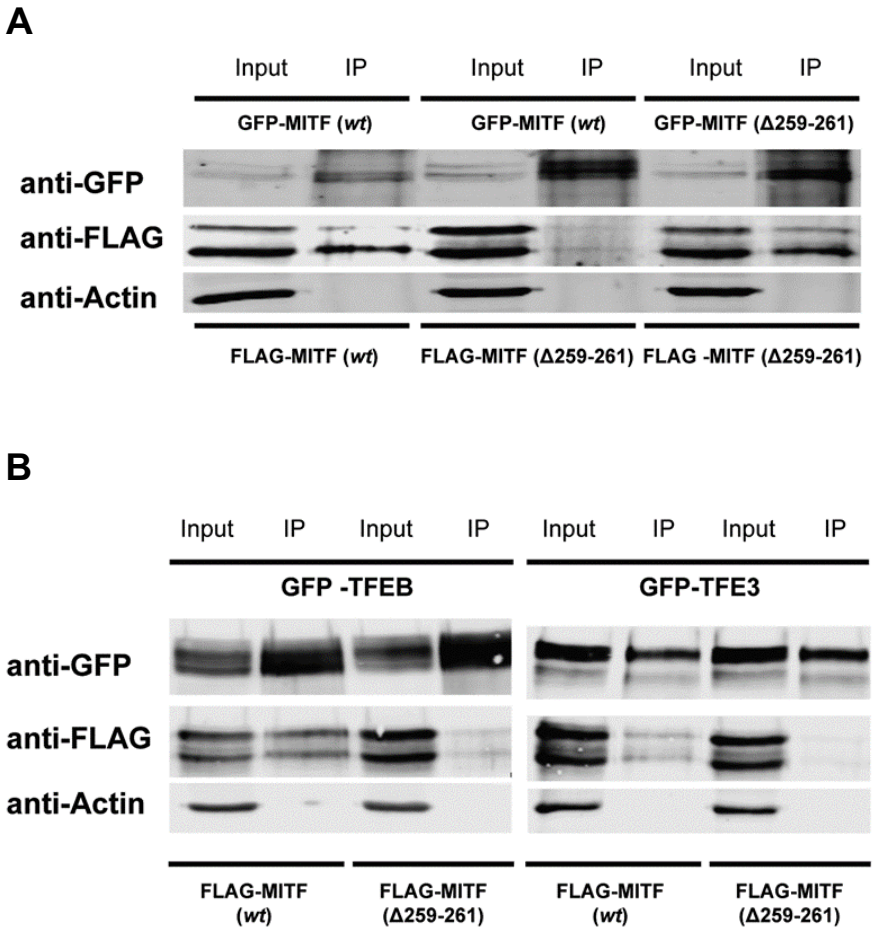

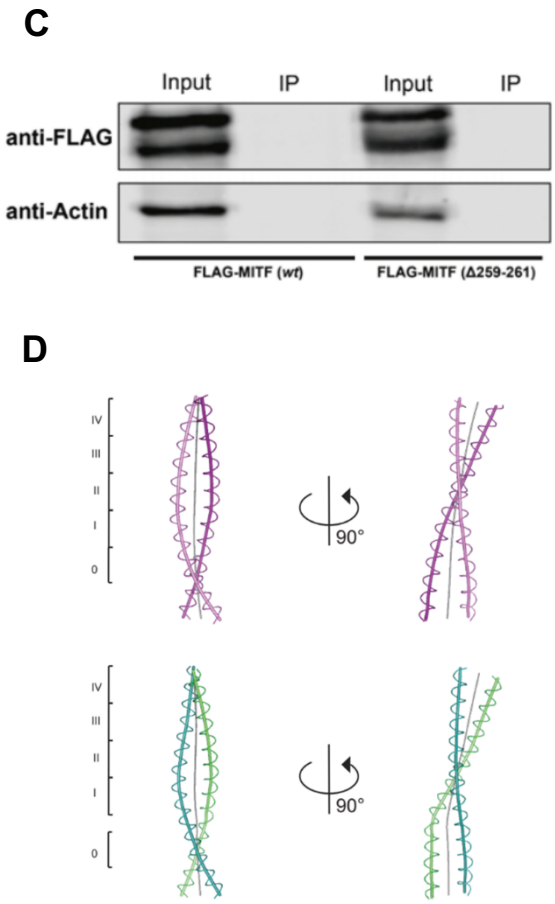


**Figure 20. Dimerization properties of MITF (Δ259-261).** FLAG-tagged wt and MITF (Δ259-261) mutants were expressed together with either GFP-tagged wt or MITF (Δ259-261) (A), GFP-tagged TFEB or TFE3 (B) or an empty vector expressing GFP alone as a negative control (C) in 501mel cells. Protein interactions were analyzed by coIP by Western blot detection of either anti-FLAG or anti-GFP antibodies. (D) Removal of the 3 amino acid insert in the MITF(Δ259-261) structure leads to a regular symmetrical coiled-coil arrangement (upper panel) as opposed to the asymmetry found in wild type MITF (lower panel).

or with the MITF, TFEB and TFE3 proteins and that the protein-protein interactions observed are specific. Therefore, these observations allowed us to confirm that the three-residue insert results in an asymmetric assembly that restricts the ability of MITF to dimerize exclusively with the TFE family of transcription factors (**Figure 20D**).

Next, we hypothesized that removal of the three-residue insertion would allow novel interactions with other bHLHZip transcription factors such as MAX, a canonical bHLHZip transcription factor that does not present such a break in the leucine zipper. I tested this by co-expressing either GFP-tagged versions of wild type or MITF(Δ259-261) proteins together with a FLAG-tagged MAX construct and immunoprecipitated the GFP-tagged proteins. Interestingly, MITF(Δ259-261) was able to interact with MAX whereas wild type MITF was not (**Figure 21**). This indicates that the absence of the three amino acid region alters the selection of interaction partners of the MiT-TFE factors and may allow the formation of new interactions with other bHLHZip transcription factors, such as the c-Myc/MAX/MAD family.

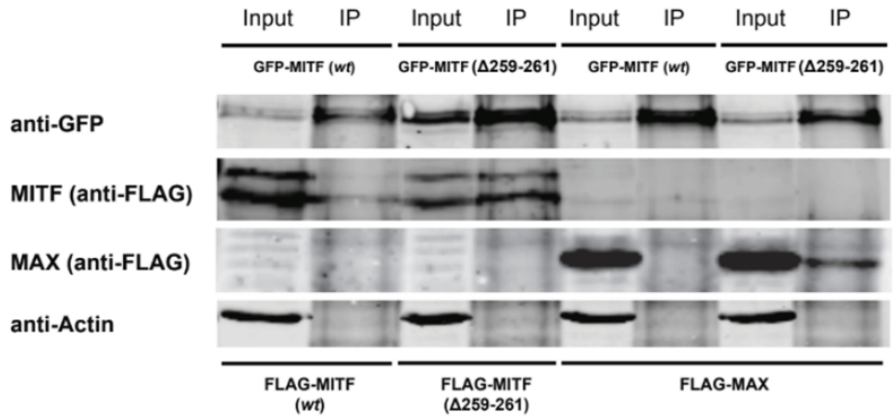


**Figure 21. Change in heterodimerization specificity of MITF(Δ259-261).** A FLAG-tagged wt MITF, MITF(Δ259-261) and MAX mutants were expressed together with either GFP-tagged wt MITF or MITF(Δ259-261) in 501 Mel cells. Protein interactions were analyzed by coIP by Western blot detection of either anti-FLAG or anti-GFP antibodies.

Modification of the heptad structure within the leucine zipper with the aim of modulating the dimerization ability of MITF, might lead to the generation of an MITF protein that will only be able to homodimerize. This would potentially be a useful tool in order to dissect the unique function of MITF homodimers as opposed to the multiple homo- and heterodimeric combinations that occur in nature. I have shown that although MITF(Δ259-261) failed to heterodimerize with wild type MITF, TFEB or TFE3, it can dimerize with MAX and possibly

other bHLHZip transcription factors and may therefore lead to a potential gain of function of the resulting novel heterodimers. Therefore, I generated two new MITF constructs with the aim of developing an MITF mutant that would only be able to form homodimers. First I generated a mutant lacking the three residues insert (Δ259-261) in the first heptad of the leucine zipper, although containing amino acids 260-262 (EQQ) now placed in the second heptad of MITF (MITF(Δ259-261)_N269_R270insEQQ MITF). This mutant was termed

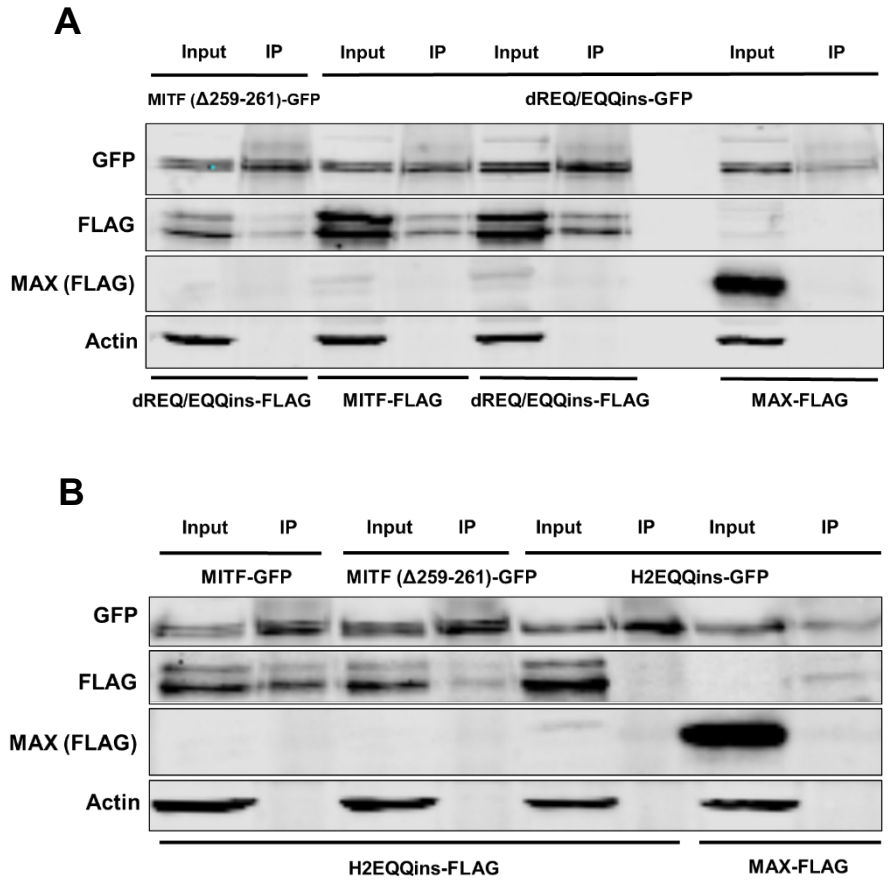


**Figure 22. Change in heterodimerization specificity of MITF stammer-mutants.** Protein interactions were analyzed by coIP by Western blot detection of either anti-FLAG or anti-GFP antibodies in 501Mel cells. (A) FLAG-tagged wt MITF, dREQ/EQQins and MAX mutants were expressed together with either GFP-tagged MITF (Δ259-261) dREQ/EQQins in 501Mel cells. (B) FLAG-tagged H2EQQins and MAX mutants were expressed together with either GFP-tagged wt MITF, MITF (Δ259-261) or H2EQQins in 501Mel cells.

dREQ/EQQins. The second mutant carried the N269_R270insEQQ insertion in the wild type MITF, termed H2EQQins. We hypothesized that this construct would contain two kinks in the leucine zipper. I used co-immunoprecipitation studies to analyze the ability of these two MITF mutants to homo- or heterodimerize with wild type MITF or with MITF(Δ259-261). FLAG-tagged dREQ/EQQins formed homodimers with GFP-tagged dREQ/EQQins (**Figure 22A**). It also dimerized with wild type MITF (**Figure 22A**). However, the dimerization ability of dREQ/EQQins with MITF(Δ259-261) was reduced and it did not interact with MAX (**Figure 22A**). Interestingly, H2EQQins was not able to homodimerize and its interaction with MITF(Δ259-261) was weak. It did not dimerize with MAX but dimerized with wild type MITF (**Figure 22B**).

To summarize, we have successfully identified a three-residue insertion located at the first heptad of the leucine zipper of the MiT-TFE transcription factors that is responsible for the selective dimerization ability of these factors. In addition, removal of these three amino acids in MITF resulted in a protein that could form functional homodimers with ability to localize to the nucleus and transactivate target DNA regulatory elements. This mutant, termed MITF(Δ259-261), failed to heterodimerize with wild type MiT-TFE factors but gained the ability to form *de novo* interactions with other bHLHZip transcription factors such as MAX, that does not present the three-residue insertion and the asymmetric assembly associated to this break in the first leucine zipper heptad. My attempts to generate an MITF mutant that is only able to homodimerize, by translocating the three-residue insertion to the second heptad or by introducing a second three-residues insertion in the second heptad, did not succeed. However, I observed that these mutants displayed different dimerization properties. We emphasize that modulating the dimerization properties of the MiT-TFE transcription factors by means of modifying the structure of their leucine zipper region, might prove useful to understand how the multiple combinations of dimers in which these factors participate affect the regulation of their target genes.

## 3.4 MITF, TFEB and TFE3 regulatory loop

Chromatin immunoprecipitation-sequencing (ChIP-seq) is a technique broadly used in molecular biology to identify binding sites of proteins that associate with DNA such as transcription factors (Farnham, 2009; Park, 2009). It combines immunoprecipitation of the chromatin fragments bound to the protein of interest using an antibody against that particular protein and subsequent DNA sequencing of the chromatin fragments obtained. ChIP-seq data is publicly available for MITF in 501mel cells (Laurette et al., 2015) and in

Colo829 human melanoma cells (Webster, 2014). In addition, Ramile Dilshat in the Steingrimsson lab has generated ChIP-seq data for TFEB in 501mel cells (Ramile Dilshat, unpublished). This data was analyzed in order to determine if MITF and TFEB are involved in regulating the expression of each other, and of TFE3. This analysis showed that MITF and TFEB bind to a region within intron 1 of TFEB (**Figure 23A**). In addition, they both bind to an intronic region downstream of the promoter specific for MITF-A (**Figure 23B**). In contrast, neither MITF nor TFEB were found to bind to the TFE3 promoter or any intronic region within the TFE3 gene (**Figure 23C**). This data suggests that

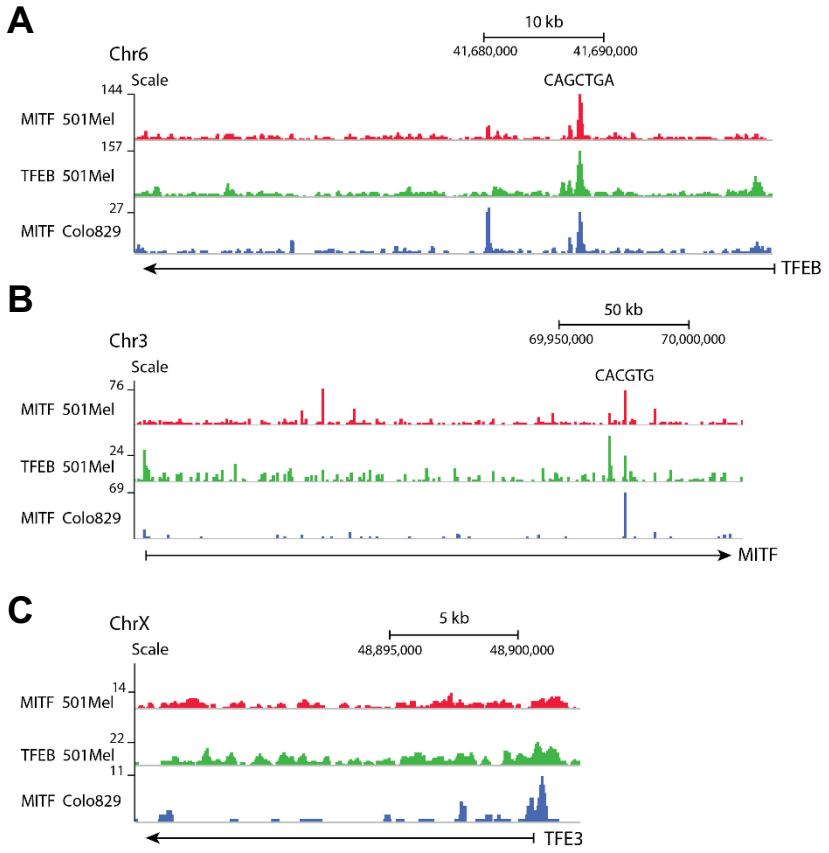


**Figure 23. MITF and TFEB bind to the MITF and TFEB genes.** MITF chIP-seq data in 501Mel and Colo829 melanoma cells, and TFEB chIP-seq data in 501Mel cells, show that MITF and TFEB bind to the intron 1 of TFEB (A) and that MITF and TFEB bind to different intronic regions of MITF (B). No binding sites in the TFE3 gene have been observed (C).

MITF and TFEB can potentially regulate the transcription of both MITF and TFEB through binding to DNA regulatory elements, whereas they cannot directly transactivate any putative DNA regulatory elements in TFE3.

Since MITF and TFEB bind to each other's regulatory regions, it was important to determine if they affect each other's expression. In order to determine whether MITF, TFEB and TFE3 are able to influence each other's expression I assayed the effects of transient doxycycline-inducible overexpression and short-term knockdown of each individual factor on the expression of the other factors in 501 Mel and Skmel28 human melanoma cell lines. I analyzed the mRNA expression by RT-qPCR of human 501mel melanoma cell lines overexpressing pBac-MITF, pBac-TFEB, and pBac-TFE3. The overexpressed MITF protein is the (-) isoform lacking exon 6a that encodes the alternative six amino acids just in front of the basic domain. I used primers specific for MITF (+) to measure the expression of the endogenous MITF mRNA (**Appendix II, Figure 38**) and universal MITF (+/-) primers to detect expression of total MITF mRNA; TFEB and TFE3 were assayed using gene-specific primers (**Table 8**). Overexpressing MITF (-) significantly increased TFEB mRNA expression whereas TFE3 levels remained unchanged (Figure 21A). In addition, MITF (-) overexpression significantly reduced the expression of endogenous MITF as detected using primers specific to the MITF (+) isoform (**Figure 24A**). Overexpression of TFEB in the 501Mel cell line resulted in reduced MITF expression whereas TFE3 mRNA levels were unaffected (**Figure 24B**). Finally, overexpressing TFE3 resulted in decreased MITF expression whereas TFEB mRNA levels were not significantly changed

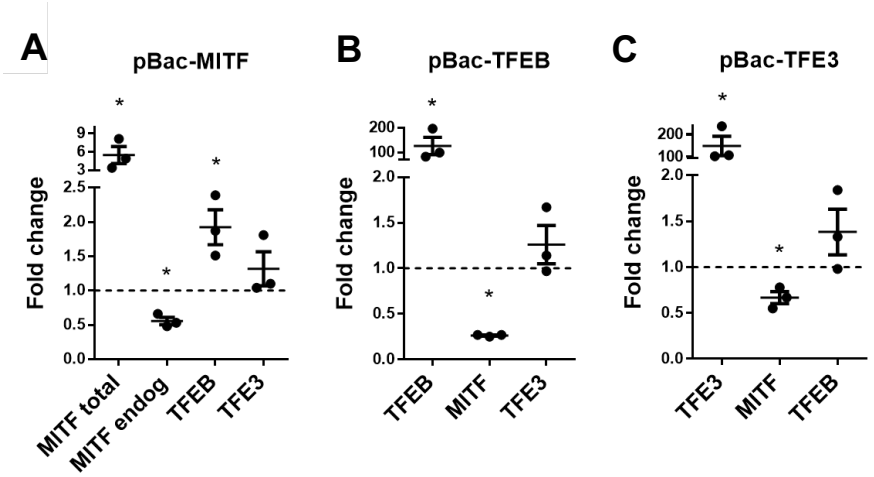

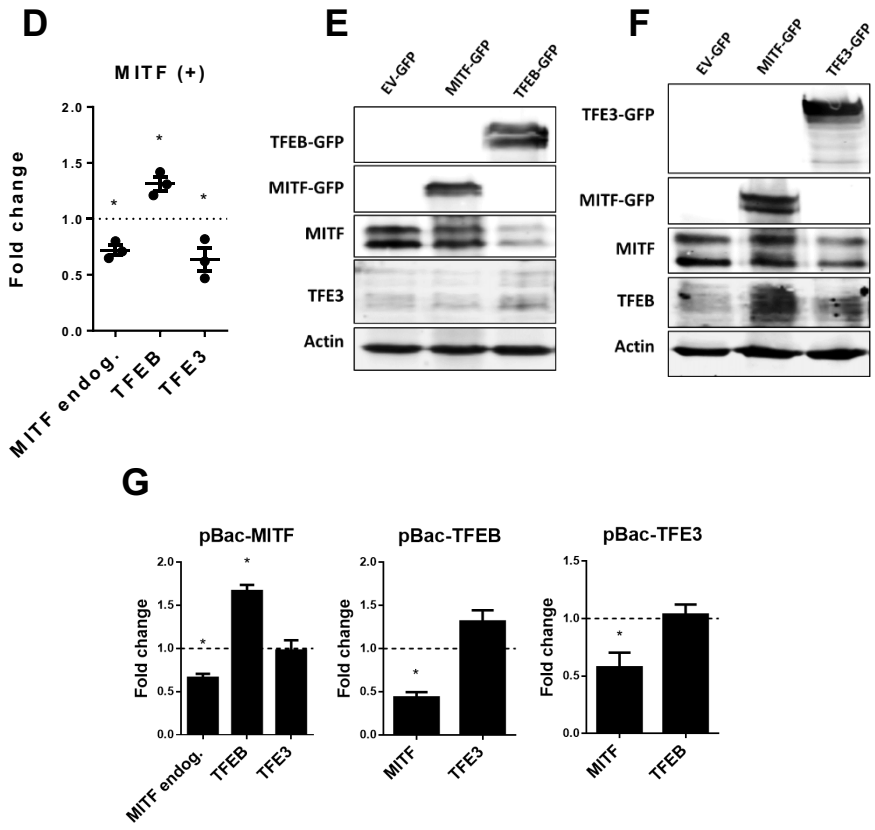


**Figure 24. MITF, TFEB and TFE3 regulate each other's expression in 501Mel cells.** The expression of MITF, TFEB and TFE3 as determined by RT-qPCR after overexpression of MITF (-) (A), TFEB (B), TFE3 (C) and MITF (+) (D) in 501mel cells compared to empty vector. Bars represent SEM. * indicates significance at $p<0.05$. Western blot analysis of MITF, TFEB and TFE3 protein levels after overexpression of MITF (E, F), TFEB (E) and TFE3 (F) in 501mel cells. Shown is a representative figure for at least three independent experiments and overall quantification (G). Bars represent SEM. * indicates significance at $p<0.05$.

(**Figure 24C**). I also analyzed the effects of overexpressing MITF (+) on the mRNA levels of its family members and found that the effects were comparable to those observed after the overexpression of the (-) isoform, suggesting that the presence or absence of those six amino acids does not have additional effects (**Figure 24D**).

These observations were also detected at the protein level, assayed by western blotting. Ectopic expression of MITF increased TFEB protein

expression and decreased levels of endogenous MITF (**Figure 24E, F, G**). Overexpression of TFEB or TFE3 resulted in reduced MITF expression whereas overexpression of TFE3 did not significantly affect the expression of the MITF protein (**Figure 24E, F, G**).

In order to validate the effects of the overexpression, I also used siRNA to knock down MITF, TFEB and TFE3 in 501mel melanoma cells and then performed qPCR and western blot analysis to determine effects on expression of the other factors. MITF knockdown dramatically reduced TFEB mRNA (**Figure 25A)** and protein levels (**Figure 9B**) to a degree comparable to that

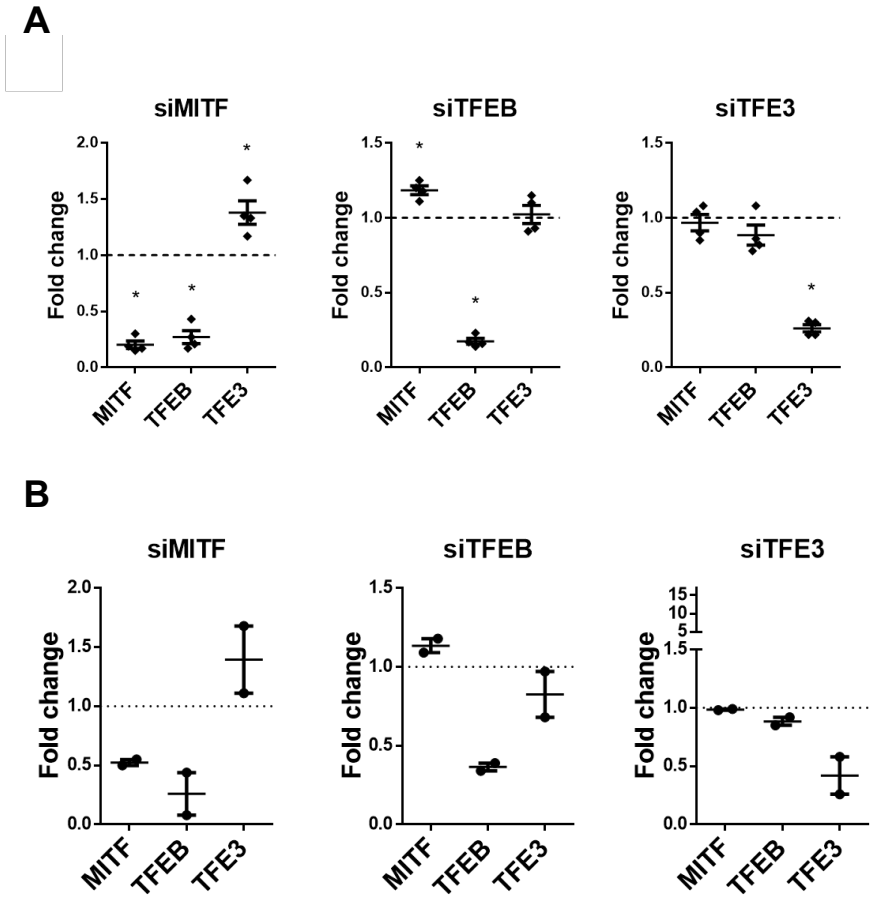


**Figure 25. Knockdown of MITF, TFEB and TFE3 affect each other's expression.** The expression of MITF, TFEB and TFE3 as determined by RT-qPCR after siRNA knockdown of each factor compared to control siRNA in 501Mel (A) and Skmel28 (B). For the 501Mel knockdown, shown is the average of four independent experiments. Bars represent SEM. * indicates significance at $p<0.05$.

observed upon TFEB knockdown. MITF siRNA also resulted in increased TFE3 mRNA (**Figure 25A**) and protein levels (**Figure 9B**). On the other hand, TFEB knockdown increased the mRNA (**Figure 25A**) and protein levels (**Figure 9B**) of MITF to some extent but did not affect the expression of TFE3. Lastly, TFE3 knockdown did not affect the mRNA levels of MITF or TFEB (**Figure 25A**) whereas expression of the MITF protein was increased (**Figure 9B**). The replication of the knock-down experiments of each individual factor in Skmel28 showed similar effects on the mRNA (**Figure 25B**) and protein expression (**Figure 10**). Likewise, the overexpression experiments in Skmel28 cells confirmed the results observed in 501Mel cells (**Figure 26**).

In conclusion, these data indicate that MITF, TFEB and TFE3 are able to regulate each other's mRNA expression in melanoma cells, possibly through direct binding to genomic regulatory elements and thus direct transcriptional regulation. In addition, MITF can repress the expression of TFE3 and, in turn, overexpression of TFE3 has an inhibitory effect on the expression of MITF. The absence of binding sites for MITF within the TFE3 gene suggests that indirect effects that need further elucidation may be involved in the cross-regulatory relationship between MITF and TFE3.

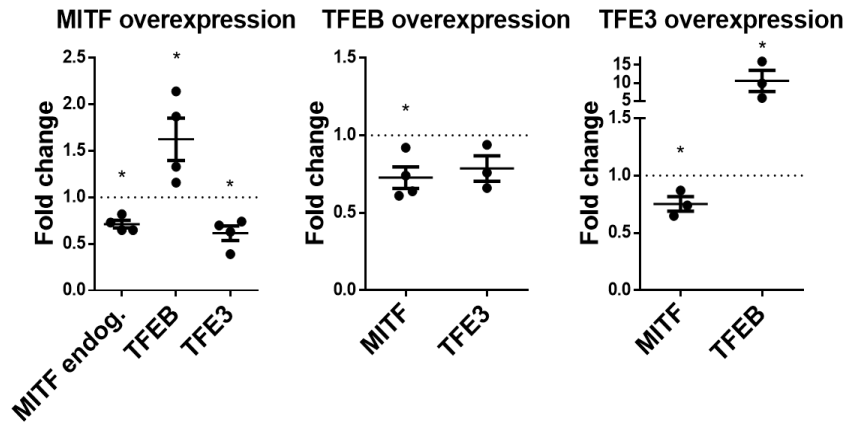


**Figure 26. MITF, TFEB and TFE3 regulate each other's expression in SkMel28 cells.** RNA expression of MITF, TFEB and TFE3 after overexpression of GFP-tagged MITF (+), TFEB and TFE3 in Skmel28 cells compared to control empty vector. Shown is the average of at least three independent experiments, bars represent SEM

### 3.4.1 MITF directly regulates the expression of TFEB

I have shown that MITF affects expression of TFEB and binds to an element in intron 1 of TFEB. In addition, ectopic expression of MITF can affect the expression of endogenous MITF and it binds to potential DNA regulatory elements in the *MITF* gene. Therefore, I investigated whether the effects of MITF on the transcription of TFEB and MITF are due to its direct interaction with the respective DNA regulatory elements. Analysis of the MITF ChIP-seq data revealed a CAGCTGA element at the binding site located in intron 1 of *TFEB* (**Figure 27A**) and a CACGTG motif in the binding site located within the *MITF* gene. In order to determine if these regulatory elements mediate a direct MITF-dependent regulation, I cloned an 853-base pair sequence of intron 1 of TFEB containing the region between bases -29,373 and -28,521 upstream of the exon 2 of TFEB. This sequence carries the CAGCTGA binding site in a central location. In addition, I mutated the potential MITF-binding motif to CCCTTTA. Likewise, the aforementioned DNA sequence located between bases -10,366 and -9,697 upstream of the TSS of MITF-M was isolated. This sequence contains the potential MITF binding site CACGTG centrally located. Another version of this construct was generated where this element was mutated to CCCTTTA (**Figure 27B**). The four constructs were subcloned into the pGL3-Promoter luciferase reporter plasmid (**Figure 27A, B**). The resulting reporter constructs were transfected into HEK293T cells, which express the MITF and TFE proteins at very low levels, together with a construct expressing the wild type MITF-M protein. The tyrosinase (TYR) promoter was used as a positive control. The results showed transactivation of the tyrosinase (TYR) promoter by MITF, suggesting that the assay worked as intended (**Figure 27C**). The expression of the reporter gene downstream of the TFEB intron 1 element was significantly increased upon expression of FLAG-tagged MITF-M. This enhanced transactivation was abrogated when the 7-base pair sequence was scrambled (**Figure 26C**). In contrast, overexpression of MITF-M did not alter the luciferase signal of the putative regulatory region at MITF relative to empty pGL3-promoter construct or when the CACGTG element was scrambled, indicating that this region is not responsible for the MITF transcriptional self-repression observed in the overexpression or siRNA studies. Surprisingly, the MITF binding site in intron 1 of TFEB is a CAGCTG element and not a canonical CACGTG E-box. MITF has not previously been shown to bind to this sequence, therefore, I analyzed whether there are more occurrences of the CAGCTG element in the set of sequences reported to be bound by MITF in the ChIP-seq data published by Laurette et al. (2015). Analysis of motif enrichment (AME) (McLeay & Bailey, 2010) of the MITF ChIP-

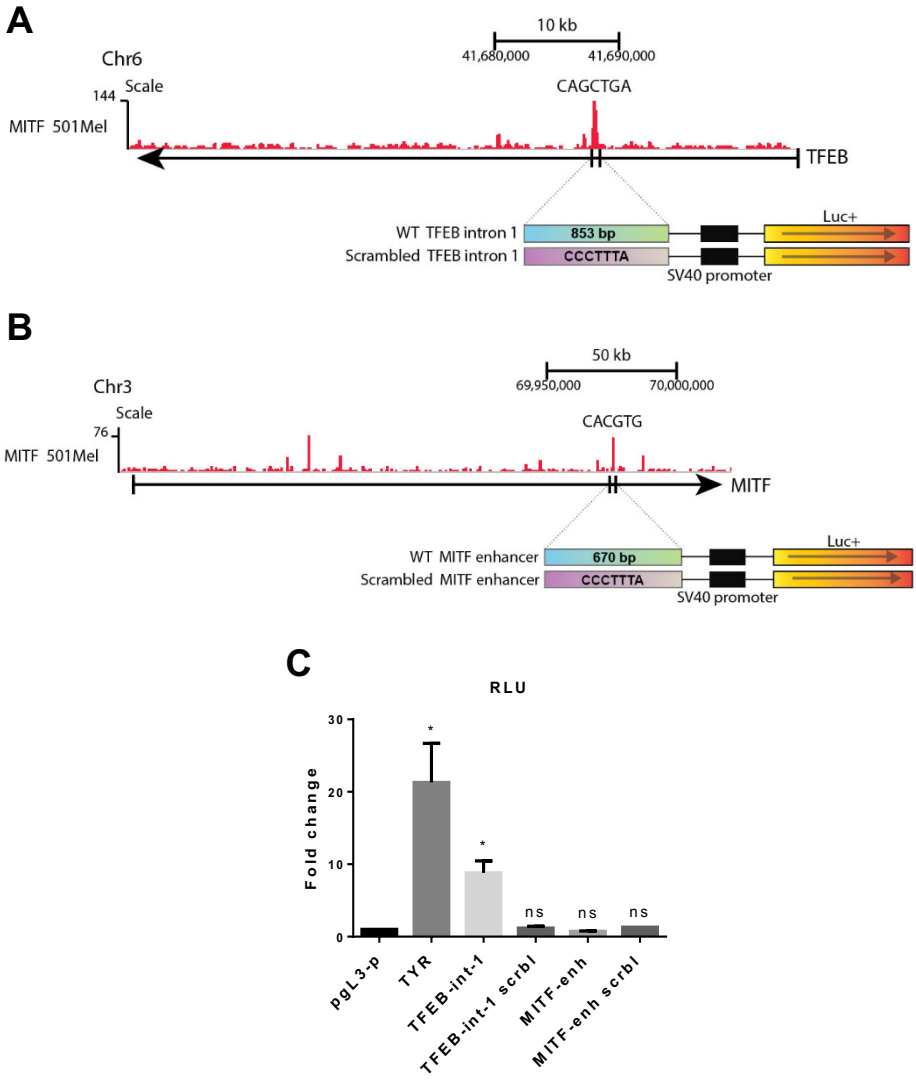


**Figure 27. MITF upregulates TFEB through transactivation of a CAGCTGA motif at intron 1.** (A) ChIP-seq data revealed that MITF binds to a CAGCTGA element with an intronic region of TFEB. (B) Putative binding sites of MITF at a regions upstream of the TSS of MITF-M. (C) HEK293T cells were transiently co-transfected with a p3XFLAG-CMV-14 construct with MITF-M or without (empty vector, EV) and luciferase constructs and assayed after 24h for luciferase activity. Luminiscence signal is expressed as fold change over an empty luciferase reporter (for tyrosinase) or a luciferase reporter containing a minimal SV40 promoter (for TFEB intron 1, TFEB intron 1 scrambled, MITF enhancer and MITF enhancer scrambled). Error bars represent the SEM of three experiments.* indicates significance at $p<0.05$.

seq dataset revealed that the CACGTGA motif was found in 36% of the sequences that were reported to be bound by MITF, CACGTG in 41%, CAGCTG in 32% and CAGCTGA (the motif found to be bound by MITF in the TFEB promoter) in 16%. The CCCTTTA motif used as a scramble control occurred in 6.8% of the sequences. Therefore, the canonical E-box is 6-fold enriched and the CAGCTG motif is enriched 4.6-fold compared to the scramble control (**Table 10, upper panel**). AME analysis of the TFEB ChIP-seq dataset found the CACGTGA motif in 20.48% of the sequences, CAGCTGA in 27.84%, CACGTG in 34.17% and CAGCTG in 51.01%. The scrambled CCCTTTA motif was found in 11.21% of the sequences. Thus, the canonical E-box motif was enriched approximately 1.8-fold in the TFEB ChIP-seq dataset and the CAGCTGA motif 2.5-fold (**Table 10, bottom panel**).

**Table 10. Analysis of motif enrichment (AME) across MITF and TFEB binding sites.** E-value: estimate of the expected number of motifs with the given log likelihood ratio (or higher), and with the same width and site count, that one would find in a similarly sized set of control random sequences TP: number of loci correctly identified as motifs in the sequence. FP: number of loci incorrectly identified as motifs in the sequence.

| MITF binding sites | | | | | |
|---|---|---|---|---|---|
| Motif | E-value | TP | %TP | FP | %FP |
| CACGTGA | 1.93e-630 | 2547 | 36.27 | 189 | 2.69 |
| CAGCTGA | 2.95E-165 | 1107 | 15.76 | 195 | 2.78 |
| CACGTG | 6.53e-561 | 2876 | 40.95 | 429 | 6.11 |
| CAGCTG | 7.27e-358 | 2216 | 31.55 | 408 | 5.81 |
| CCCTTTA | 3.63E-20 | 477 | 6.79 | 219 | 3.12 |

| TFEB binding sites | | | | | |
|---|---|---|---|---|---|
| Motif | E-value | TP | %TP | FP | %FP |
| CACGTGA | 2.78E-126 | 1158 | 20.48 | 312 | 5.52 |
| CAGCTGA | 1.18E-242 | 1574 | 27.84 | 298 | 5.27 |
| CACGTG | 1.59E-129 | 1932 | 34.17 | 821 | 14.52 |
| CAGCTG | 1.32e-464 | 2884 | 51.01 | 661 | 11.69 |
| CCCTTTA | 3.81E-28 | 634 | 11.21 | 293 | 5.18 |

These results indicate that MITF directly regulates its target genes through the direct binding to CANNTG motifs, including the enhancement of the transcriptional regulation of TFEB by MITF through a CAGCTG motif located in TFEB's intron 1.

### 3.4.2 mTOR and expression of MITF, TFEB and TFE3

Since inhibiting mTOR signaling results in increased nuclear localization of TFEB, TFE3 and MITF in melanoma cells, it is reasonable to assume that this will lead to increased transcription activation of their target genes. Moreover, I have shown in the previous chapter that MITF, TFEB and TFE3 to a certain extent, regulate each other's expression. Therefore, I investigated whether mTOR signaling affects the expression of the MiT-TFE factors at the mRNA or protein levels. 501mel cells were treated with the mTORC1/2 inhibitor Torin1 and subsequently, I analyzed their mRNA expression by RT-qPCR. Interestingly, treatment with Torin1 significantly increased the mRNA expression of MITF, but did not affect the expression of TFEB or TFE3 (**Figure 28A**). I have shown that ectopic overexpression of MITF, TFEB and TFE3 negatively affects the expression of endogenous MITF in two melanoma cell lines (**Figure 24, 26**). Therefore, I investigated whether blockade of the mTOR pathway would enhance these negative regulatory effects, due to an increased nuclear localization of these factors upon mTORC inhibition in 501Mel cells (**Figure 11, 12**). RT-qPCR was used to analyze the mRNA expression of human 501mel melanoma cell lines expressing pBac-MITF, pBac-TFEB, and pBac-TFE3 after treating the cells with Torin1 or vehicle (DMSO) prior to RNA extraction. I confirmed that overexpression of the three factors can inhibit the mRNA expression of endogenous MITF in melanoma cells (**Figure 28B**). An increase in the endogenous MITF mRNA levels after treatment with Torin1 was observed (**Figure 28A, B**). However, this increase was not seen when MITF or TFEB were overexpressed (**Figure 28B**). Indeed, the reduction in MITF mRNA levels upon TFE3 or TFEB overexpression compared to empty vector was significantly more pronounced when the cells were treated with Torin1 compared to vehicle. This indicates that the increase in mRNA expression of MITF upon mTORC inhibition does not take place when an increase in TFEB or TFE3 expression severely reduce transcription of MITF.

Subsequently, I analyzed the protein levels of MITF upon mTORC inhibition and overexpression of GFP-tagged TFEB, TFE3 or EV as a control. As expected, in 501 Mel cells overexpressing TFEB, the expression of MITF protein is significantly reduced, indicating a strong suppression mediated by TFEB (**Figure 28C, D**). Overexpression of TFE3 also strongly reduced the

MITF protein levels, although the effect was not as pronounced as with TFEB overexpression (**Figure 28C, D**). Phosphorylation at Ser73 generates a mobility shift, in which the upper band corresponds to phosphorylated Ser73, as observed by Western blotting (Hemesath et al., 1998). Inhibiting the mTORC1/2 complex can affect the ratio of the upper band of MITF so that the lower band becomes more prominent. This indicates that mTORC can phosphorylate MITF, as previously shown in Figure 16 (**Figure 28C, E**).

Next, I investigated whether the phosphorylation status of MITF would affect the stability of the protein. For this, the cells were treated with cycloheximide in order to block de novo protein translation. Interestingly, blockade of protein translation upon three hours' treatment with cycloheximide led to an increase in the ratio of MITF's upper to lower band. This finding might suggest that cycloheximide triggers phosphorylation of MITF at Ser73 and that the lower band of MITF, corresponding to unphosphorylated Ser73, is readily degraded and short-lived if there is no sustained translation of MITF in these cells (**Figure 28C, E**). In the light of this observation, the proteasome inhibitor MG132 was used in order to analyze whether the lower band is effectively being degraded by the proteasome pathway. Interestingly, the sharp decrease of intensity of the lower band of MITF upon cycloheximide treatment was abrogated when the proteasome was inhibited (**Figure 28F**). In addition, the overall abundance of MITF protein increased by 50% when compared to cycloheximide treatment alone (**Figure 28G**). In conclusion, these data indicate that mTORC signaling increases transcription of MITF. On the other hand, mTORC inhibition increases the nuclear localization of TFE3 and its activity as a transcriptional repressor of MITF. Interestingly, this increased transcription of MITF does not correlate with increased protein expression. I hypothesize that inhibition of mTORC triggers dephosphorylation of MITF, which induces proteasome-mediated degradation of MITF. This in turn, might stimulate a higher turnover rate observed as rapid degradation of dephosphorylated MITF coupled with increased transcription through an unknown mechanism.

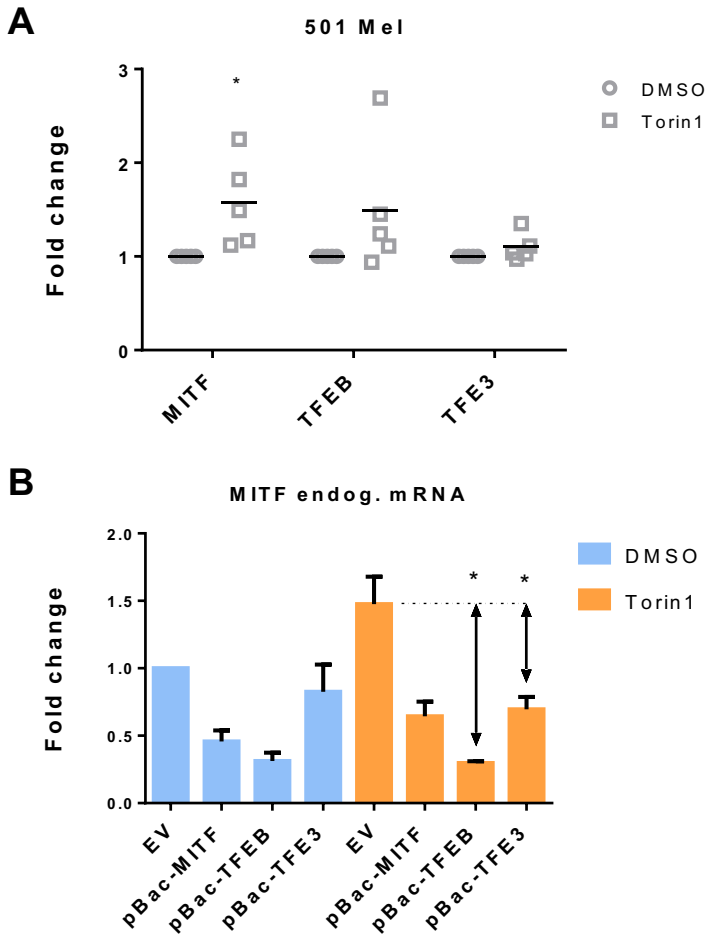
A
501 Mel
Fold change
3
2
1
0
*
DMSO
Torin1
MITF
TFEB
TFE3
B
MITF endog. mRNA
Fold change
2.0
1.5
1.0
0.5
0.0
*
*
DMSO
Torin1
EV
pBac-MITF
pBac-TFEB
pBac-TFE3
EV
pBac-MITF
pBac-TFEB
pBac-TFE3
C
EV
TFEB
TFE3
GFP
MITF (C5)
Actin
DMSO
CHX
mTORi

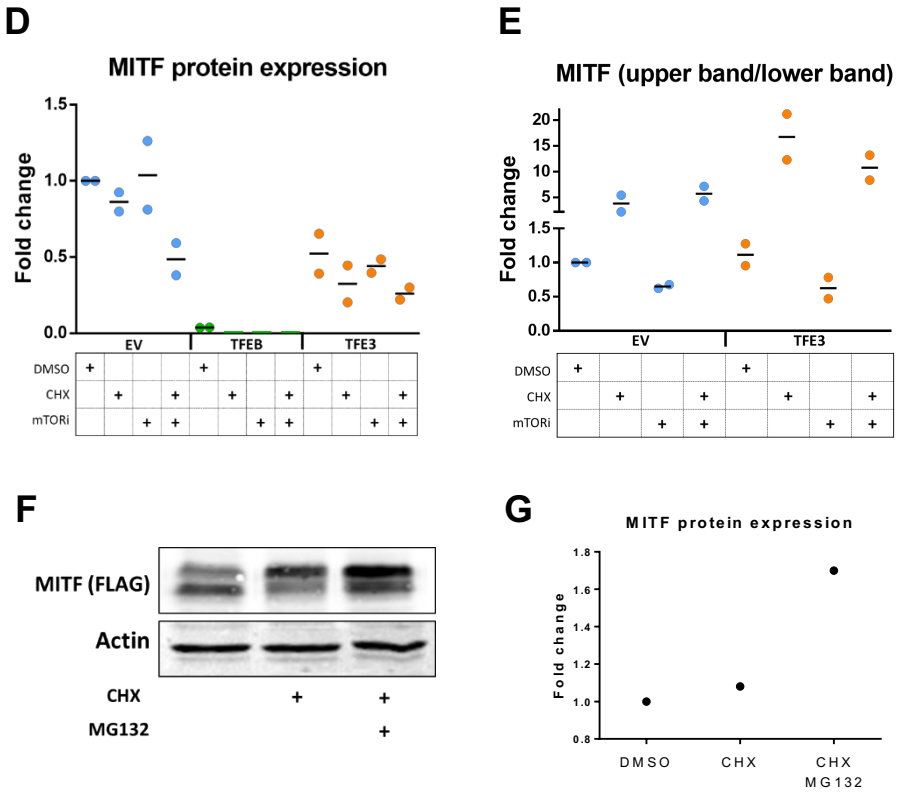


**Figure 28. mTOR inhibition induces the expression of MITF and increases protein turnover due to increased dephosphorylation and degradation.** (A) The expression of MITF, TFEB and TFE3 as determined by RT-qPCR after treatment with an mTOR inhibitor for three hours (Torin1, 1 μM) compared to vehicle (DMSO). (B) The expression of MITF as determined by RT-qPCR upon overexpression of MITF (-), TFEB and TFE3 with or without mTOR inhibition for three hours (Torin1, 1 μM). Error bars represent SEM. * indicates significance at $p<0.05$. (C) MITF protein immunoblotting upon overexpression of empty vector (EV), TFEB and TFE3, with or without mTOR inhibition (Torin1, 1 μM) or cycloheximide treatment (70 μM) for three hours. Shown is a representative figure for at least two independent experiments and quantification of MITF expression relative to actin (D) or the ratio of upper band to lower band of MITF (E), represented as fold change relative to EV vehicle control. (F) MITF protein immunoblotting upon cycloheximide treatment (70 μM) or cycloheximide and MG132 (10 μM) treatment for three hours. (G) Quantification of MITF expression normalized to actin represented as fold change relative to vehicle control. Only one individual experiments is shown.

### 3.4.3 TFE3 overexpression impairs proliferation of 501Mel cells

Previous studies have shown that $BRAF^{V600E}$ is beneficial for the proliferation of melanoma cells (Hingorani et al., 2003). Moreover, it has been shown that MITF is required for the BRAF-mediated stimulation of proliferation, and that MITF depletion blocks DNA synthesis in $BRAF^{V600E}$ melanoma cells (Wellbrock et al., 2008). BRAF effects on cell growth and proliferation through MITF are due to induction of CDK4, CDK2 and p21, which are transcriptional targets of MITF that mediate cell cycle progression. CDK2 and p21 were previously identified as MITF target genes in melanoma cells (Carreira et al., 2005; Du et al., 2003; Wellbrock et al., 2008).

Using a 501mel cell line expressing a doxycycline-inducible miRNA targeting MITF, I investigated whether MITF knockdown would affect the ability of these cells to proliferate, and also whether the overexpression of TFEB or TFE3 in these cells with or without knockdown of MITF would have any impact on their proliferation rate. When MITF was knocked down using the inducible miRNA pBac system I observed a decreased proliferation rate in these cells (**Figure 29A**) and an increase in doubling time from 29 hours to approximately 38 hours (**Figure 29B**). Overexpressing TFEB had no effect on the proliferation rate of the 501 Mel cells expressing a miRNA control (**Figure 29B, C**). However, TFE3 overexpression markedly slowed down the proliferation of these cells (**Figure 29C**) and the doubling time increased to approximately 37 hours, similar to that of cells with a miRNA targeting MITF (**Figure 29B**). Next, I analyzed the proliferation rate of the 501Mel cells expressing an miRNA to knock down MITF or an miRNA control and simultaneously overexpressing TFEB or TFE3. The MITF knockdown cells proliferated slower than the control cells. However, overexpression of TFEB or TFE3 in the knockdown cells did not affect the proliferation rate significantly, compared to the EV control, since the variability among the samples was remarkably high (**Figure 29D**).

To summarize, TFE3 negatively affects the proliferation of 501Mel cells, possibly through the repression of the transcription of MITF, which has been shown to be required for survival and cell cycle regulation of human melanoma cells. In addition, neither TFEB nor TFE3 can rescue the proliferation of melanoma cells lacking MITF.

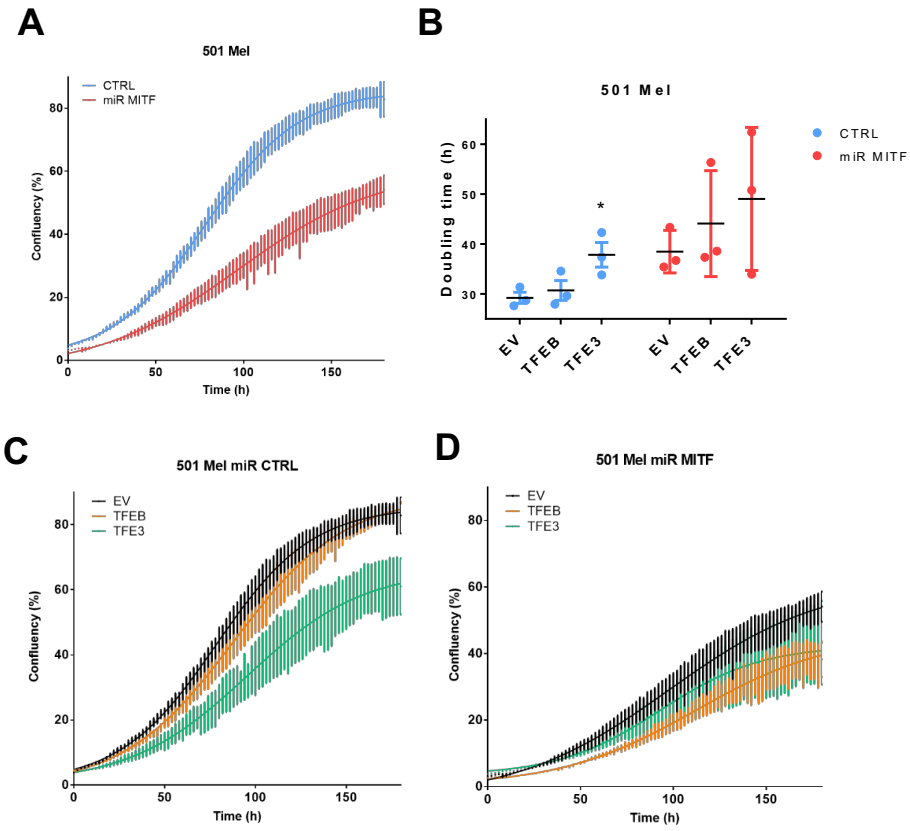


**Figure 29. MITF knockdown reduces the proliferation of 501mel cells.** (A) Growth curve after measuring confluency of 501mel cells expressing an miRNA against MITF or miRNA control. (B) Graph showing doubling time calculated with the formula: Duration x log(2)/log(FinalConfluency)-log(InitialConfluency) of 501mel cells expressing miRNA against MITF or miRNA control and overexpressing empty vector (EV), TFEB or TFE3. Error bars represent SEM. * indicates significance at $p<0.05$. (C, D) Growth curve after measuring confluency of 501 Mel cells expressing a miRNA control (C) or against MITF (D) and overexpressing empty vector (EV), TFEB or TFE3.

## 3.5 MITF, TFEB and TFE3 activate similar DNA motifs that determine a subset of shared target genes

TFEB is known to directly bind to a 10-base pair palindromic sequence GTCACGTGAC, a type of E-box that is enriched in the proximal promoters of

many lysosomal genes. This sequence has been named Coordinated Lysosomal Expression and Regulation (CLEAR) element (Sardiello et al., 2009). TFE3 is able to regulate genes that are involved in the autophagy process and lysosomal biogenesis through the binding to the E-box consensus sequence CACGTG, which is contained within the CLEAR regulatory element (Aksan & Goding, 1998). Moreover, it has been shown that mutating a series of CLEAR elements present in the promoter of the lysosomal gene encoding the Ca2+ release channel mucolipin-1 (MCOLN1) abrogated its transcriptional activation by TFEB and TFE3 (Martina, Diab, Lishu, et al., 2014). TYR and MLANA are two well-known pigmentation genes that are downstream effectors of MITF. Both genes contain E/M-box elements known to be bound by MITF and required for transcriptional activation (Aksan & Goding, 1998; Verastegui et al., 2000). Moreover, oligonucleotides encompassing E-box and M-box motifs were used to determine the crystal structure of MITF when bound to DNA (Pogenberg et al., 2012).

Previous studies in the lab suggest that MITF, TFEB and TFE3 are all able to activate the transcription of tyrosinase through the two E-box elements within its promoter (Arnþórsson, 2016). The transcription factors bind to the same DNA element, the E-box (CANNTG), and specifically recognize two subsets of the E-box, the CLEAR box (GTCACGTGAC), in the promoter regions of lysosomal and autophagy genes, and the M-box (GGTCATGTGCT), previously thought to be a pigment-cell-specific regulatory element of transcription (Jackson et al., 1991). Analysis of ChIP-seq datasets shows a strong binding site for MITF and TFEB in intron 2 of the pigmentation-gene MLANA (**Figure 30A**). In order to assess whether MITF, TFEB and TFE3 can all transactivate from this MLANA regulatory element, I performed transcription activation assays using a luciferase reporter plasmid containing a 692-base pair sequence containing the CACGTGA binding site for MITF and TFEB within intron 2 of the *MLANA* gene. GFP-tagged versions of MITF, TFEB or TFE3 were overexpressed in HEK293T cells co-transfected with this reporter (**Figure 30A**). Overexpression of the three transcription factors increased the luciferase signal from the reporter plasmid containing the putative transcriptional regulatory element of MLANA 5-fold when compared to the control pGL3-promoter luciferase reporter plasmid (**Figure 30B**). Importantly, the expression of the TFE3 construct was 6-fold higher than that of MITF, whereas the expression of TFEB was 4-fold higher than that of MITF (**Figure 30C**) in HEK293T cells used for this assay. This suggests that the three factors, MITF, TFEB and TFE3 are capable of activating common regulatory elements that contain sequences related to the canonical palindromic E-box and thus, overlap in the regulation of the transcription of target genes, including those involved in pigmentation (Verastegui et al., 2000). However, since there is a

lot more TFE3 and TFEB proteins expressed in these assays than MITF, we cannot exclude the possibility that MITF is a more potent transcriptional activator of MLANA than either TFEB or TFE3.

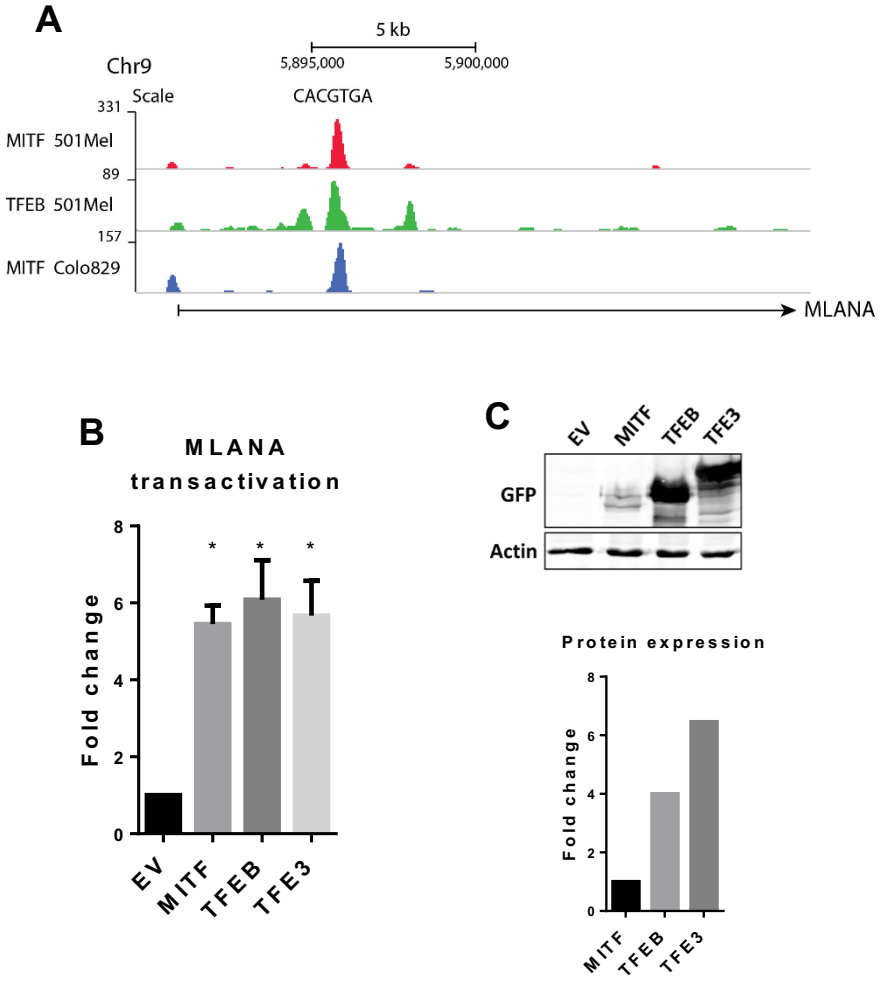


**Figure 30. MITF, TFEB and TFE3 transactivate a regulatory element in an intronic region of MLANA.** (A) ChIP-seq data revealed that MITFand TFEB bind to a CACGTGA motif within an intronic region of MLANA. (B) HEK293T cells were transiently co-transfected with a pEGFP-N1 constructs with MITF-M, TFEB, TFE3 or without (empty vector, EV) and luciferase constructs and assayed after 24h for luciferase activity. Luminiscence signal is expressed as fold change over an empty luciferase reporter. Error bars represent the SEM of three experiments. * indicates significance at $p<0.05$. (C) Western blot analysis and quantification of the protein expression of MITF, TFEB and TFE3 proteins after transfection of the respective plasmid constructs in HEK293T cells. Shown is a representative figure.

### 3.5.1 MITF and TFEB bind to unique and shared target genes in melanoma cells

Ramile Dilshat, a PhD student in the Steingrimsson laboratory, has recently performed ChIP-seq experiments in 501mel cells using a GFP-tagged TFEB construct (Ramile Dilshat, unpublished). Details on this ChIP-seq experiment are to be published in her PhD thesis but in order to gain insights into the overlapping function of MITF and TFEB, we compared this data to the published MITF ChIP-seq data in 501Mel cells of Laurette and colleagues (Laurette et al., 2015). We identified the annotated genes corresponding to the binding sites detected across the genome in the MITF and TFEB ChIP-seq datasets. We found 682 genes that are bound by the two factors and might be shared target genes in this human melanoma cell line (**Figure 31A**). The representation factor of the subset of overlapping target genes was 3.3, indicating that the number of genes found to be present in both ChIP-seq databases is 3-fold higher than the overlap expected purely by chance.

Subsequently, I performed gene ontology (GO) analysis of the 682 target genes in order to look for over-represented classes of genes and to identify their relevant biological role. The analysis of "biological processes" terms showed significant enrichment of genes involved in intracellular and phagosomal pH reduction, transferrin transport, and lysosomal organization

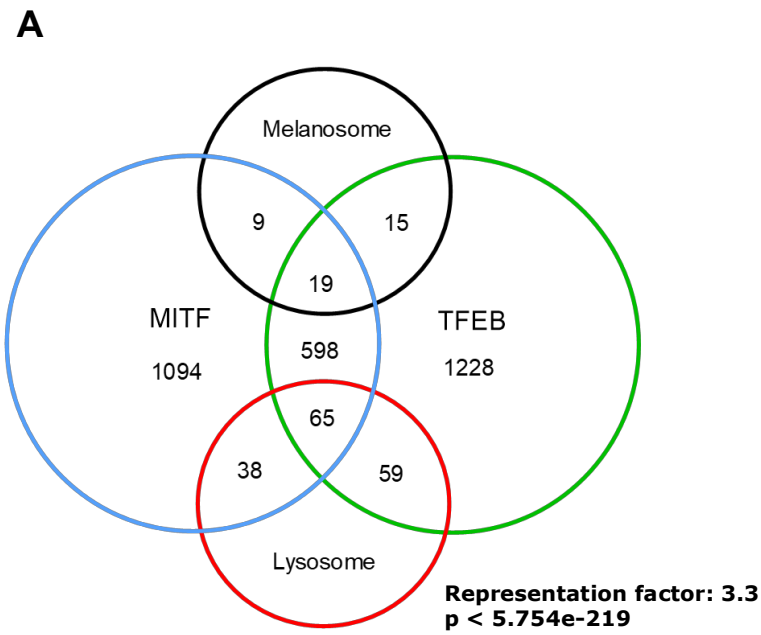

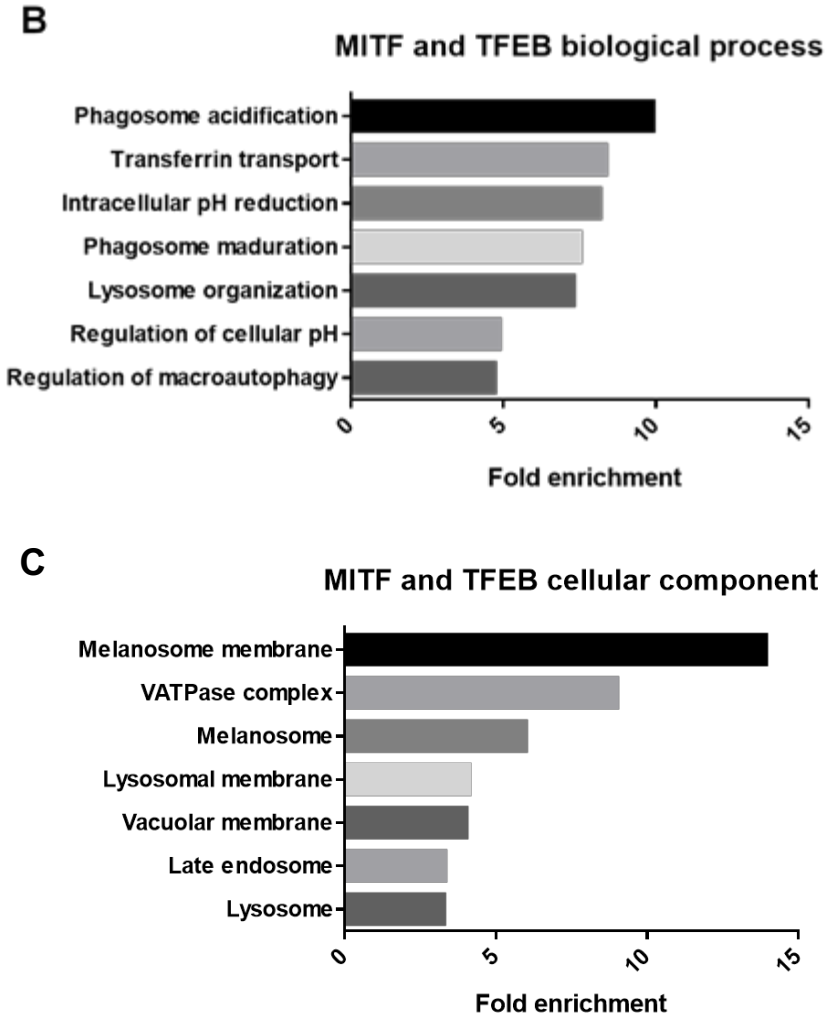


**Figure 31. MITF and TFEB bind to a subset of shared target genes, including melanosomal and lysosomal genes.** (A) Venn diagram showing the overlapping target genes of MITF and TFEB and whether they associate with melanomes or lysosomes. (B) GO analysis of the overlapping target genes. Terms from „biological process“ and (C) „cellular compartment“. The X-axis represents the fold enrichment corresponding to each term.

and regulation of macroautophagy. This confirms previous observations that both MITF and TFEB are able to regulate the endosomal pathways (**Figure 31B, Table 11**). The analysis of “cellular component” terms displayed a higher

over-representation of genes located at the melanosomal and endosomal-lysosomal membranes, together with the vATPase complex. Approximately 10% of the 682 genes were lysosomal genes and 3% melanosomal genes (**Figure 31A, C, Table 11**). However, 598 genes, a major fraction of the 682 genes found to be common targets of MITF and TFEB, do not fall under these categories and are not over-represented in any specific biological pathway or cellular compartment **(Figure 31A**).

**Table 11. GO analysis of the overlapping target genes of MITF and TFEB.** Terms from „biological process" (upper panel) and cellular compartment (lower pannel). Only terms with a fold enrichment score over 2.5 are shown.

| Overlapping gene targets of MITF and TFEB | | | |
|---|---|---|---|
| **Biological process** | **# genes** | **Fold e.** | **p-value** |
| Phagosome acidification | 8 | 9.91 | 1.83E-02 |
| Transferrin transport | 9 | 8.36 | 1.69E-02 |
| Intracellular pH reduction | 11 | 8.17 | 1.55E-03 |
| Phagosome maduration | 9 | 7.52 | 3.92E-02 |
| Lysosome organization | 12 | 7.3 | 1.44E-03 |
| Regulation of cellular pH | 14 | 4.88 | 1.63E-02 |
| Regulation of macroautophagy | 23 | 4.72 | 1.64E-05 |
| Organic acid transmembrane transport | 15 | 4.44 | 2.19E-02 |
| Regulation of autophagy | 30 | 3.36 | 1.46E-04 |
| Response to insulin | 21 | 3.3 | 2.64E-02 |
| Vesicle organization | 30 | 3.14 | 6.26E-04 |
| Response to peptide hormone | 29 | 2.6 | 4.06E-02 |
| **Cellular compartment** | **# genes** | **Fold e.** | **P value** |
| Melanosome membrane | 5 | 13.93 | 4.88E-02 |
| Proton-transporting VATPase complex | 7 | 9 | 2.27E-02 |
| Melanosome | 19 | 5.99 | 1.50E-06 |
| Lysosomal membrane | 43 | 4.12 | 2.28E-11 |
| Vacuolar membrane | 48 | 4.02 | 1.57E-12 |
| Late endosome | 23 | 3.32 | 1.28E-03 |
| Lysosome | 65 | 3.28 | 2.18E-13 |
| Vacuole | 72 | 3.16 | 2.99E-14 |
| Endocytic vesicle | 24 | 2.87 | 8.68E-03 |

Next, we analyzed the MITF and TFEB ChIP-seq datasets in order to identify the specific binding sites across the entire genome in 501Mel cells that are bound by MITF and TFEB. We found 553 sites that are bound by both transcription factors (**Figure 32A**). Next, motif analysis to investigate whether any motifs are enriched in the overlapping binding sites was performed. Using the MEME Suite (Bailey et al., 2009) a GTCACGTGA motif was found, which corresponds to a CLEAR box, to be significantly enriched across the overlapping sequences bound by MITF and TFEB, with an E-value of 1.6e-015 (**Figure 32B**). The zinc finger protein 263 (ZNF263) binding motif was also found (**Figure 32C**). The E-value is an estimate of the expected number of motifs with the given log likelihood ratio (or higher), and with the same width and site count, that one would find in a similarly sized set of control random sequences (Bailey et al., 2009). This finding further supports the notion that MITF and TFEB can both regulate a set of genes involved in endosomal biogenesis and autophagy.

I also analyzed whether MITF and TFEB bind to regions in the vicinity of genes corresponding to the gene ontology category for pigmentation (GO:0043473) (**Appendix III, Table 15**) and a published list of lysosomal/autophagy genes (Perera et al., 2015) (**Appendix III, Table 16**). I found that out of 96 pigmentation genes, 25 are bound by both MITF and TFEB, whereas only 2 are bound by MITF alone and 1 gene by TFEB alone (**Figure 32D, Table 12**). Analysis of the lysosomal and autophagy-related genes shows that of the 139 genes, 87 are bound by both factors, 9 are bound by MITF alone and 1 gene is bound exclusively by TFEB (**Figure 32E, Table 12**). This indicates an extensive overlap in the genes regulated by both MITF and TFEB. However, it also suggests that some genes are regulated only by one of the factors and not by the other. *SPNS2* is the only pigmentation gene to be bound by TFEB and not MITF, in addition, it correlates with TFEB in the melanoma samples analyzed (**Table 12**). In contrast, the pigmentation genes *NF1* and *SOX10* are bound by MITF only and *SOX10* correlates with MITF in expression in the melanoma samples (**Table 12**). *ATP6V1E2* is the only lysosomal gene that is exclusively bound by TFEB, whereas *ATP6V0D2*, *ATP6V0A2*, *BECN1*, *GALC*, *GLB1L*, *MAP1LC3B2*, *SLC17A5*, *SNCA*, *ULK2* are bound by MITF alone (**Table 13**). Out of the 9 target genes that are bound by MITF but not by TFEB; only *MAP1LC3B2*, *ULK2* and *SNCA* correlate in expression with *MITF* (**Table 13**). Furthermore, *ATP6V1E2* is the only gene exclusively bound by TFEB that correlates in expression with *TFEB* across melanoma samples (**Table 13**).

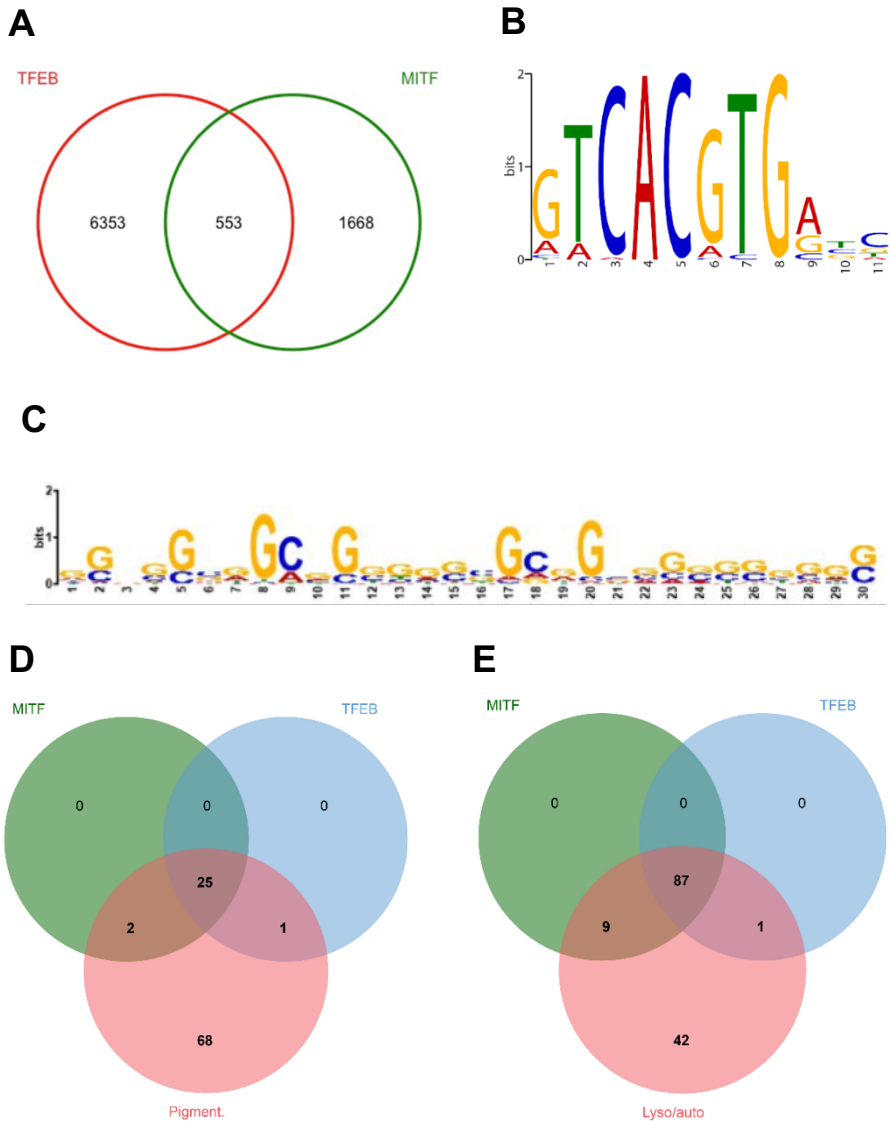


**Figure 32. MITF and TFEB bind to a subset of ovelapping binding sites.** (A) Venn diagram showing the overlapping binding sites across the genome of 501Mel cells. (B, C) Motif discovery analysis of the overlapping binding sites of MITF and TFEB, showing the CLEAR box (B) and the ZNF263 binding motif (C). (D, E) MITF and TFEB have common binding sites in a significant fraction of pigmentation genes (D) and lysosomal genes (E).

**Table 12. List of the pigmentation genes found to be exclusively bound by MITF or TFEB in 501Mel cells and whether they correlate in gene expression with MITF or TFEB across 363 melanoma samples in TCGA.**

| Gene | Bound only by | Correlation? |
|---|---|---|
| SPNS2 | TFEB | TFEB |
| NF1 | MITF | No |
| SOX10 | MITF | MITF |

**Table 13. List of the lysosomal genes found to be exclusively bound by MITF or TFEB in 501Mel cells and whether they correlate in gene expression with MITF or TFEB across 363 melanoma samples in TCGA.**

| Gene | Bound only by | Correlation? |
|---|---|---|
| ATP6V1E2 | TFEB | No |
| ATP6V0D2 | MITF | No |
| ATP6V0A2 | MITF | No |
| BECN1 | MITF | No |
| GALC | MITF | No |
| GLB1L | MITF | No |
| MAP1LC3B2 | MITF | MITF |
| SLC17A5 | MITF | No |
| SNCA | MITF | MITF |
| ULK2 | MITF | MITF |

### 3.5.2 MITF, TFEB and TFE3 differentially regulate the transcription of autophagy-related genes

Previous analyses in the lab (Möller at al., submitted) have shown that in a subset of 368 metastatic melanomas categorized in The Cancer Genome Atlas (TCGA) Research Network: ("http://cancergenome.nih.gov/,"), a number of lysosomal/autophagy-related genes (**Appendix III, Table 16**) are found among the top 2000 genes, whose expression correlates with that of MITF. In addition, a different subset of lysosomal genes has been found to correlate in expression with TFEB or TFE3 across metastatic melanomas. Of the 139 lysosomal and

autophagy-related genes, 37 correlated with MITF and 30 genes with TFEB and/or TFE3, suggesting that each of these factors may differentially regulate specific subsets of lysosomal genes (**Table 14**). MITF, TFEB and TFE3 may be modulating different aspects of this complex biological process (Möller at al., submitted). The manuscript by Möller et al. describes a correlation between MITF and genes required for vesicle trafficking and endosomal transporters, consistent with the previously reported role of MITF as a master regulator of the v-ATPase complex (Zhang et al., 2015), whereas TFEB and TFE3 correlate with genes that code for enzymes involved in proteolytic cleavage, as determined by gene ontology analysis.

**Table 14. Correlation of lysosomal/autophagy genes with MITF, TFEB or TFE3 in melanoma samples.**

| Lysosomal/autophagy genes correlating with MITF | |
|---|---|
| HPS4 | ATP6V0A1 |
| SNCA | VPS18 |
| ASAH1 | ATG2A |
| ATP6V1C1 | CTSF |
| CLCN7 | CD63 |
| ATP6V1H | VPS33A |
| ATP6V0A4 | ATP6V1E1 |
| SLC11A2 | ARL8B |
| ATP6V1G1 | VPS8 |
| CLCN5 | LAPTM4B |
| ATG14 | NEU1 |
| ATP6V1B2 | HPS1 |
| ATP6V1A | CTSL1 |
| ATP6V1D | MAP1LC3B2 |
| TMEM55A | CLCN6 |
| WIPI1 | HEXA |
| LAMP2 | GBA |
| CTSL2 | ULK2 |
| CTNS | |

| Lysosomal/autophagy genes correlating with TFEB/TFE3 | |
|---|---|
| DNASE2 | FUCA1 |
| SLC12A4 | SQSTM1 |
| SLC29A3 | CTSA |
| ANPEP | GABARAPL1 |
| SMPD1 | CTSS |
| IDS | CTSC |
| ATG7 | ARSA |
| SLC44A2 | PSAP |
| CTSW | TPP1 |
| ATP6V0E1 | CTSZ |
| GAA | DPP4 |
| ATG13 | CTSH |
| CTSB | PIK3CG |
| CTSD | NPC2 |
| MAP1LC3A | NAGA |

Therefore, I proceeded to analyze whether *in vitro* modulation of the expression of MITF, TFEB and TFE3 would affect the mRNA expression of several autophagy-related genes. A375P human melanoma cells were used, a cell line that expresses low levels of the three transcription factors (**Appendix**

**IV, Table 17**), in order to minimize the effects mediated by a predominant endogenous factor that might dilute these experimental observations. I analyzed the mRNA expression of several target genes upon overexpression of MITF, TFEB or TFE3 and siRNA-mediated knockdown of MITF or TFE3. The mRNA expression of TFEB in A375P cells was very low (**Appendix IV, Table 17**) and the protein was undetectable by Western blotting, thus no siRNA-mediated silencing of TFEB was performed in this experiment. The lysosomal genes that were analyzed in this assay included LC3 and LAMP1, which are involved in the formation of autophagosomes; the vATPase subunits ATP6V0D2 and ATP6V1C1, which participate in the acidification of the lysosome; the cathepsin proteases CTSD and CTSZ, and the polysaccharide-degrading sulfatase GNS. The three last genes encode proteins that are important for proteolytic cleavage of substrates in the lysosomes. In the light of the ChIP-seq datasets used throughout this study, all seven genes feature binding sites for both MITF and TFEB and therefore, are classified as overlapping target genes. The results showed that transcription of ATP6V0D2, ATP6V1C1 and CTSD was increased upon MITF and TFEB overexpression, whereas only the expression of ATP6V0D2 increased upon TFE3 overexpression (**Figure 33A**). Interestingly, the TFEB-induced increase in ATP6V1C1 expression was abrogated when MITF was knocked down using siRNA, suggesting that activation of the transcription of this vATPase subunit by TFEB is dependent on MITF (**Figure 33B**). On the other hand, TFEB-induced increase in CTSD expression remained unaffected upon silencing MITF (**Figure 33B**). The expression of CTSZ and GNS was slightly reduced when TFEB was overexpressed, regardless of whether MITF was knocked down or not (**Figure 33B**). Knockdown of MITF significantly inhibited the transcription of ATP6V0D2 (**Figure 33C**), whereas silencing of TFE3 significantly increased the mRNA expression of ATP6V1C1 (**Figure 33C**). Knockdown of MITF did not repress the expression of ATP6V1C1, which remained at basal values. However, when TFE3 was overexpressed in these cells with partially depleted MITF, ATP6V1C1 expression was significantly decreased (**Figure 33D**), indicating that whereas MITF positively regulates ATP6V1C1, TFE3 might play a role in the negative regulation of this vATPase subunit.

As shown before, MITF positively regulates ATP6V1C1, whereas TFE3 is a negative regulator of this gene. Moreover, TFEB can increase the expression of ATP6V1C1 only when MITF is being expressed (**Figure 33**). In contrast, the expression of CTSD increases when either MITF or TFEB are overexpressed. Therefore, I tested whether these two genes correlate in expression with *MITF*, *TFEB* and *TFE3* across the 363 melanoma samples in the TCGA. Additionally, I included alpha-synuclein (SNCA) in this analysis. *SNCA* is a lysosome-related gene that I found to be exclusively bound by MITF and to positively

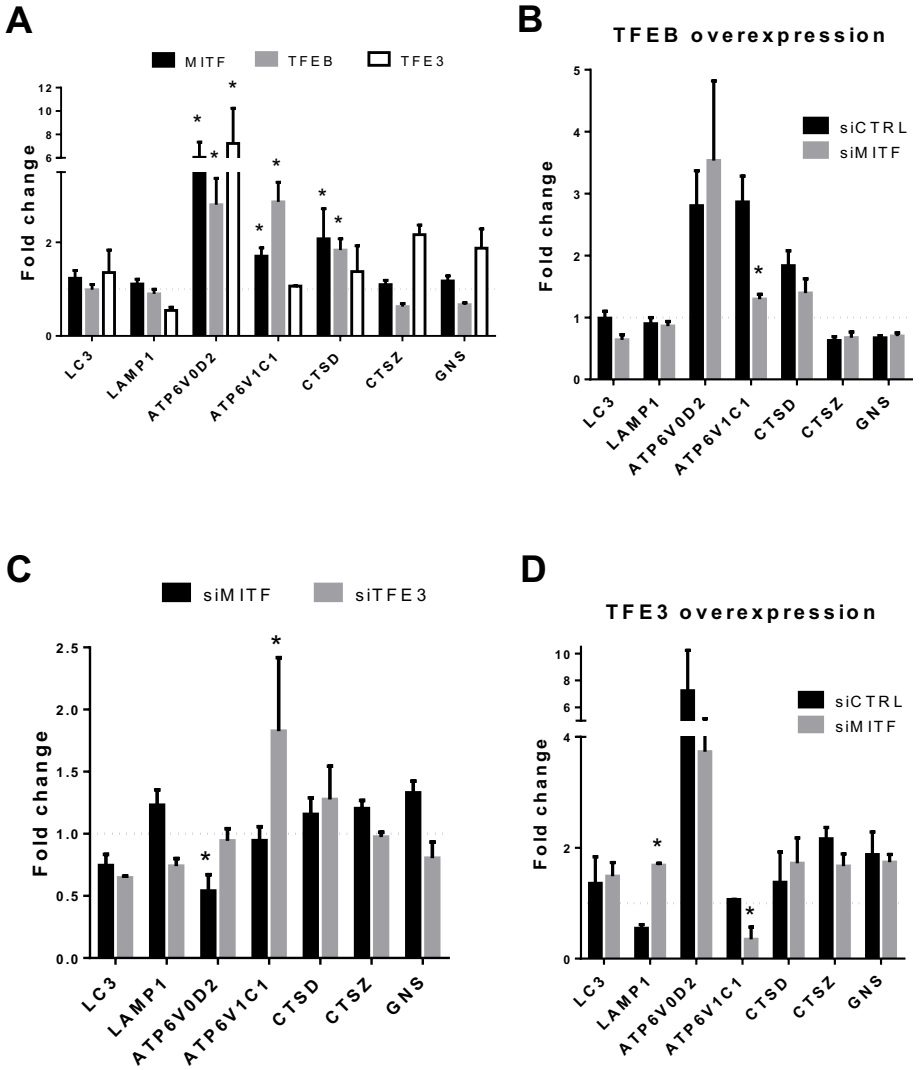


**Figure 33. MITF, TFEB and TFE3 differentially regulate a selection of autophagy-related genes.** The expression of a subset of autophagy genes as determined by RT-qPCR after overexpression of MITF, TFEB and TFE3 (A), siMITF treatment versus siCTRL in cells overexpressing TFEB (B), knockdown of MITF or TFE3 (C) and siMITF treatment versus siCTRL in cells overexpressing TFE3 (D). Shown is the average of at least three independent experiments. Bars represent SEM. * indicates significance at $p<0.05$.

correlate with *MITF* in the TCGA database of melanoma samples. *ATP6V1C1* correlates positively with *MITF* (**Figure 34A**) whereas it negatively correlates with *TFE3* (**Figure 34B**), supporting the previous observations that MITF activates the expression of this vATPase subunit whereas TFE3 has an inhibitory role at the transcriptional level (**Figure 33A, C, D**). On the other hand, *CTSD* does not correlate with *MITF* (**Figure 34C**) but it positively correlates with TFEB (**Figure 34D**), suggesting that although both MITF and TFEB can bind to *CTSD*, their effects on its regulation might differ. I found that the expression of *SNCA* strongly correlates with *MITF* expression (**Figure 34E**) and moderately anti-correlates with *TFE3* (**Figure 34F**). *SNCA* is a gene believed to have a role in the formation of synaptic vesicles at the presynaptic terminals. Following the findings indicating that MITF and TFE3 may differentially regulate specific autophagy-related genes such as ATP6V1C1, further efforts could be directed at determining whether they play opposite roles at the transcriptional regulation of *SNCA* and other genes involved in the endosomal pathways.

In this study I have shown that MITF and TFEB bind to similar motifs across the genome and therefore regulate a subset of common target genes that includes both pigmentation and lysosomal genes. I have reported a subtype of the E-box motif, namely the CLEAR box, to be enriched within a set of overlapping sequences that are bound by both MITF and TFEB. The CLEAR motif has been associated with the transcriptional control of a large number of genes that are involved in the regulation of endosomal pathways, lysosomal function and autophagy (Palmieri et al., 2011), indicating that both factors are involved in the transcriptional control of these pathways in melanoma cells. Real time quantitative PCR analysis on a selection of autophagy-related genes revealed that MITF, TFEB and TFE3 can activate the transcription of a number of lysosomal genes. However, some of these genes show an exclusive correlation with only one of the factors and appear to be differentially regulated, indicating that the roles of MITF, TFEB and TFE3 do not overlap entirely in regulating the autophagy pathway.

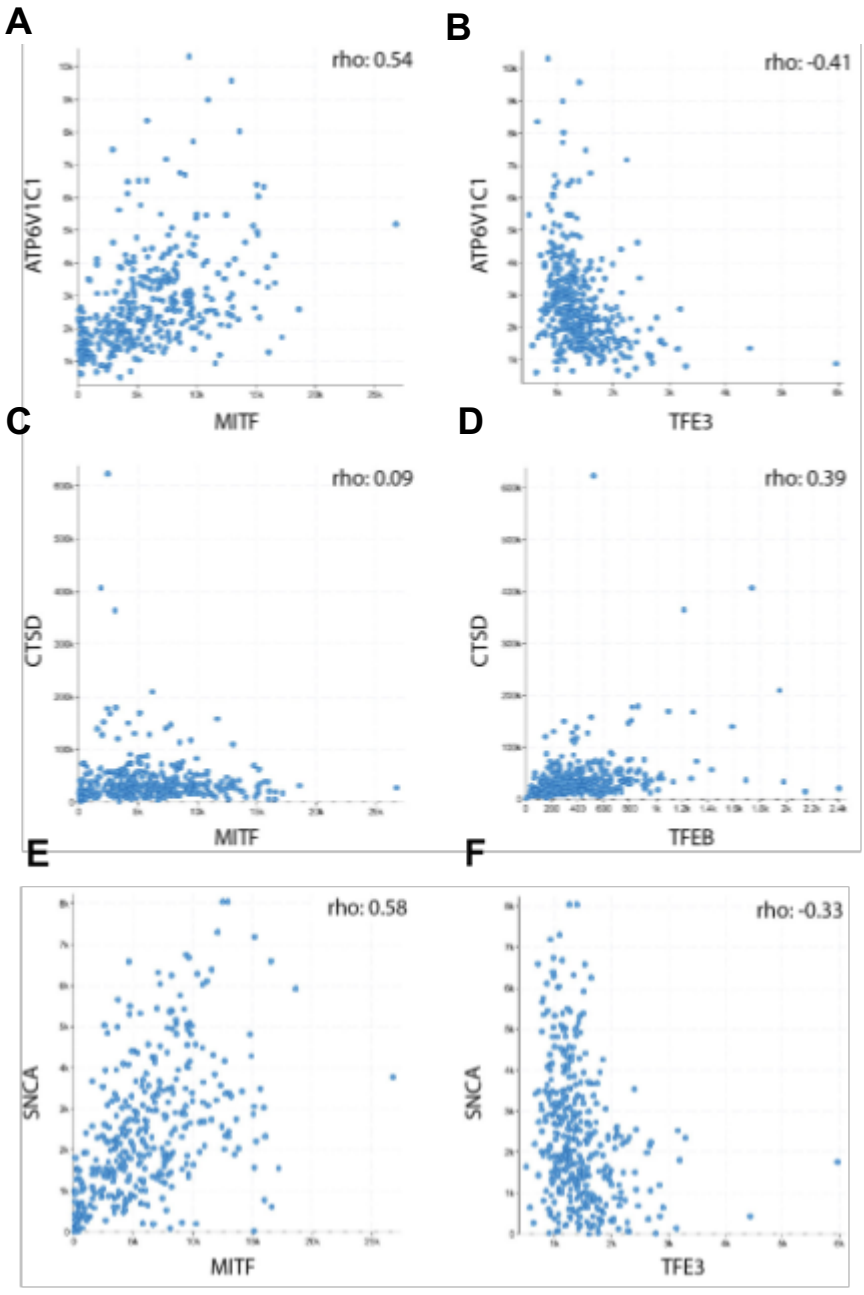


**Figure 34. Analysis of the correlation in gene expression between MITF, TFEB or TFE3 and selected lysosomal genes across 363 metastatic melanoma samples.** Correlation between ATP6V1C1 and MITF (A) or TFE3 (B). Correlation between CTSD and MITF (C) or TFEB (D). Correlation between SNCA and MITF (F) or TFE3 (G).

# 4 Discussion

## 4.1 Summary

The aim of this thesis was to determine the expression of the MIT-TFE factors and their interactions in melanoma tumors and cell lines. These factors constitute a subfamily featuring high structural homology, they share a conserved bHLHZip domain, which is more similar than in the larger family of basic helix-loop-helix leucine zipper family of transcription factors.

Previous studies have shown that MITF, TFEB, TFE3 and TFEC can form DNA-binding heterodimers, but not with other bHLHZip transcription factors such as Myc and Max, defining the discrete MiT-TFE subfamily of transcription factors within the bHLHZip transcription factors (Hemesath et al., 1994). However, the dimerization properties of these factors have not been thoroughly described in melanoma cells. Furthermore, the role of TFEB and TFE3 in melanoma is poorly understood. Here, I performed co-immunoprecipitation studies in 501Mel cells and observed that MITF, TFEB and TFE3 can interact with each other. Moreover, I characterized a three-residue insertion responsible for selection of dimerization partners by introducing a break within the first heptad of the leucine zipper of these factors.

Using melanoma cell lines available in our lab, I analyzed the subcellular localization of these transcription factors and how it is affected by the mTORC and the BRAF-MAPK signaling pathways, two signaling cascades that are known to trigger phosphorylation of TFEB, TFE3 and some isoforms of MITF to modulate their subcellular distribution. Blockade of these signaling pathways using drug inhibitors resulted in nuclear translocation of MITF, TFEB and TFE3 in the melanoma cell lines analyzed, potentially affecting their stability, the activity of these proteins as transcription factors and the regulation of downstream biological processes.

Analysis of MITF and TFEB binding sites by ChIP-seq in melanoma cells reveals the existence of binding sites for MITF and TFEB in the regulatory regions of both *MITF* and *TFEB* genes, but not in *TFE3*. I overexpressed and knocked down MITF, TFEB or TFE3 in human melanoma cells and showed that the MITF, TFEB and TFE3 proteins affect each other's expression in melanoma cells, thus forming a regulatory loop. Moreover, the alteration in

expression of these proteins may induce phenotypic changes, including proliferation.

The ChIP-seq datasets for MITF and TFEB showed a significant overlap of binding sites and target genes. This overlap of target genes includes a number of lysosomal and autophagy-related genes, indicating that these two factors may collaborate in regulating endosomal biogenesis and the autophagy process. Subsequently, I characterized the expression of a number of autophagy-related genes upon overexpression or knockdown of MITF, TFEB and TFE3 and also their co-expression across a publicly available database of melanoma specimens. I found that the expression of a subset of autophagy-related genes is induced by MITF, TFEB and TFE3 indiscriminately. However, my analysis also shows that their role in autophagy regulation does not entirely overlap and that each factor may be required for a particular stage within the autophagy process.

## 4.2 MITF, TFEB and TFE3 are expressed in melanoma

Basic helix–loop–helix leucine zipper (bHLHZip) transcription factors are known to participate in development by controlling cell proliferation and differentiation. Many of them are also known to be dysregulated in several types of cancer. MITF is a bHLHZip factor that was first discovered due to coat color mutations in mice (Hodgkinson et al., 1993). In humans, mutations in MITF have been linked to the pigmentation disorder Waardenburg Syndrome Type 2A (WS2A) (A. E. Hughes et al., 1994) and Tietz's syndrome (TS) (Smith et al., 2000). MITF has been described as a key regulator of melanocyte development. TFEB and TFE3 are important in the regulation of lysosomal biogenesis and autophagy (Martina, Diab, Lishu, et al., 2014; Sardiello et al., 2009). MITF, TFEB and TFE3 have been found to be dysregulated in pancreatic ductal adenocarcinoma (Kuiper et al., 2003; Perera et al., 2015) and renal clear cell carcinoma. In this study, the co-expression of the MiT-TFE family was analyzed across several melanoma cell lines and melanoma tumor samples. MITF, TFEB and TFE3 are expressed to some extent across a majority of these cell lines, whereas TFEC is not. The expression of TFEB and TFE3 is roughly 50-fold lower than MITF across cell lines (**Figure 8**). This is in line with previous studies from our lab showing that across 368 metastatic melanoma specimens, MITF is 14-fold and 4-fold more highly expressed than TFEB and TFE3, respectively (Möller at al., submitted). Although significant expression of TFEC was not detected across cell lines or melanoma samples, 13% of melanoma specimens among the 448 included in The Cancer Genome Atlas (TCGA) Research Network: ("http://cancergenome.nih.gov/,") feature

genetic alterations in the *TFEC* locus. A majority of those are mRNA upregulation events, hence, this could suggest that TFEC is silenced in the melanocyte lineage and that increased mRNA expression of TFEC might have role in melanoma development.

## 4.3 TFE3, TFEB and MITF show increased nuclear localization upon inhibition of mTOR or BRAF

By immunostaining of cell preparations and confocal imaging I found that TFEB and TFE3 are present in both the cytoplasm and the nucleus in melanoma cells, whereas MITF is mostly nuclear. This is in accordance with previous studies showing that MITF-M is the main isoform expressed in melanocytes and melanoma cells. MITF-M lacks an N-terminal domain responsible for the interaction with Rag proteins that promote the cytoplasmic retention of TFEB and TFE3 (Martina, Diab, Lishu, et al., 2014; Martina & Puertollano, 2013; Takebayashi et al., 1996). However, I observed that a fraction of MITF-M localizes to the cytoplasm of 501Mel, Skmel28 and Skmel31 human melanoma cells (**Figure 9A, 11C, 13C, 14C**). Ectopically overexpressed GFP-tagged MITF-M in 501Mel cells was also partly localized to the cytoplasm (**Figure 12**), therefore ruling out the possibility that other MITF isoforms that contain the N-terminal Rag-binding domain, such as MITF-A, were responsible for the cytoplasmic signal.

Several studies have shown that a panel of kinases participating in different signaling cascades are able to phosphorylate MITF, TFEB and TFE3 (Hemesath et al., 1998; Hong et al., 2010; Martina et al., 2012; Puertollano et al., 2018; Settembre et al., 2011). The mTOR and BRAF-MAPK signaling pathways are the two most studied in this regard, showing that they can phosphorylate Ser142 and Ser211 of TFEB (**Figure 6**) (Settembre et al., 2012). Interestingly, both domains are conserved in the MITF protein and correspond to Ser73 and Ser173 of MITF-M and Ser180 and Ser280 of MITF-A (**Figure 6**). Phosphorylation of Ser73 of MITF-M by ERK has been shown to enhance the activity of MITF by increasing its association with the transcriptional coactivator histone acetyl transferase p300/CBP (Price, Ding, et al., 1998; S. Sato et al., 1997). Phosphorylation of Ser409 of MITF by p90 ribosomal s6 kinase (p90RSK) prevents the recruitment of PIAS3, a corepressor of MITF (Levy et al., 2003). Phosphorylation of MITF on Ser73 and Ser409 has been shown to enhance its transcriptional potential and, at the same time, trigger ubiquitination and degradation of the MITF protein by the proteasome (Price, Ding, et al., 1998; Wu et al., 2000; Xu et al., 2000).

mTORC phosphorylates TFEB at the lysosomal membrane. Phosphorylated TFEB is recruited by scaffolding 14-3-3 proteins that mask a nuclear localization signal (NLS) in the protein, thus promoting cytoplasmic retention of TFEB (Martina & Puertollano, 2013; Pena-Llopis et al., 2011; Settembre et al., 2012). Therefore, I assessed whether drug inhibition of mTORC and BRAF would alter the subcellular distribution of MITF-M observed under normal conditions. In this thesis I showed that inhibiting mTORC or BRAF promoted nuclear translocation of TFEB and TFE3, and reduced the fraction of MITF located in the cytoplasm, when compared to vehicle treatment in 501Mel and Skmel28 cells (**Figure 11, 12, 13**). These two cell lines harbor the hyperactivating mutation BRAFV600E, a mutagenesis event that has been reported in approximately 50% of melanoma tumors. In order to assess the nuclear localization of these factors in wild type BRAF context I utilized the Skmel31 cell line that is BRAF wild type. This cell line did not express TFEB at detectable levels as determined by immunostaining (**Figure 14A**). TFE3 showed a major nuclear presence in this cell line and inhibition of mTOR had no effect on its localization, whereas inhibiting BRAF slightly decreased the cytoplasmic localization of TFE3 (**Figure 14B**). More cytoplasmic MITF was detected in Skmel31 cells than in the other cell lines analyzed. However, its subcellular localization did not respond significantly to inhibition of mTORC or BRAF, suggesting that the regulation of the subcellular localization of the MiT-TFE factors in melanoma cells might be BRAF status-dependent.

A publication of Martina and colleagues (Martina & Puertollano, 2013) shows that a Rag-binding domain is required for mTORC-mediated cytoplasmic retention of TFEB. This Rag-binding domain protein is also shared by MITF-A but not MITF-M. It consists of 30 N-terminal aminoacids located at the exon 1B1b of MITF-A, an exon that is present in all the MITF isoforms except for MITF-M due to alternative splicing (Hodgkinson et al., 1993). Martina and colleagues showed that a fraction of MITF-M is observable in the cytoplasm of the human ARPE-19 retinal epithelium cells used in their study, although it did not co-localize with active Rag proteins. This could suggest that interaction with Rag proteins may not be the only mechanism behind mTORC-mediated cytoplasmic retention of MITF-M. Indeed, a nuclear localization signal (NLS) that mediates nuclear translocation of MITF-M has been reported between amino acids 210 and 221. MITF-M lacking the NLS is retained in the cytoplasm (Fock et al., 2018). Thus, I conclude that although MITF-M lacks a major signal that mediates the cytoplasmic retention upon mTORC signaling, there may be other domains in MITF that play a role in regulating its subcellular localization that remain to be elucidated. Furthermore, phosphorylation events

mediated by the mTOR and BRAF-MAPK pathways may regulate the subcellular localization of MITF-M in a Rag-independent manner.

Another unexpected observation I made was that starvation of the cell cultures with HBSS medium, a minimum cell culture medium that lacks glucose and amino acids, did not induce nuclear translocation of MITF, TFEB or TFE3. Starvation induces inactivation of mTOR and calcium-dependent dephosphorylation of TFEB via the phosphatase calcineurin (Medina et al., 2015). Dephosphorylation of TFEB and TFE3 triggering an increase in the cellular clearance pathways has been reported in several publications (Martina, Diab, Li, et al., 2014; Settembre et al., 2013; Settembre et al., 2012). The absence of effects on the subcellular localization of any of the three factors upon starvation, suggests that nutritional stress in these melanoma cell lines is not sufficient to promote nuclear localization of the transcription factors. Leucine has been proposed as the key molecular switch in starvation-driven mTORC1 inactivation (Fox et al., 1998; Wolfson et al., 2016). Interestingly, in melanoma cells with hyperactive MAPK signaling, leucine deprivation failed to inactivate the mTORC1 pathway and trigger the autophagy response (Sheen et al., 2011). Perera and colleagues have shown that MITF, TFEB and TFE3 can escape cytoplasmic retention mediated by mTOR regulation under fully-fed conditions in pancreatic ductal adenocarcinoma (PDA), in contrast to non-transformed human pancreatic ductal epithelial cells. The constitutive localization of the three factors in PDA can induce autophagy activity, thereby maintaining a high supply of amino acids, which is advantageous for tumor development (Perera et al., 2015). Moreover, a subset of genes involved in endolysosomal trafficking and autophagy have been found to be overexpressed in melanoma (Alonso-Curbelo et al., 2015). It is tempting to speculate that, in cells of the melanocytic lineage and melanoma, the expression of an MITF-M isoform is able to circumvent Rag-dependent mechanisms for cytoplasmic retention as an evolutionary advantage of these cell types. Melanoma cells express a constitutively active isoform of MITF that supports strong proliferation and cell growth and allows a highly-developed endosomal network that enhances survival under the stressful conditions of the tumor microenvironment.

## 4.4 mTOR regulates the distribution of MITF, its protein turnover and stability

### 4.4.1 mTOR phosphorylates MITF at a site dependent on Ser73

Previous studies have shown that a number of different kinases take part in

the phosphorylation of several serine-residues in MITF, TFEB and TFE3. Ser122, Ser142, and Ser211 of TFEB (Martina et al., 2012; Roczniak-Ferguson et al., 2012; Settembre et al., 2011; Vega-Rubin-de-Celis et al., 2017) and Ser321 of TFE3 (Martina, Diab, Lishu, et al., 2014) are phosphorylated by mTORC1, promoting their cytoplasmic localization (**Figure 6**). Consistent with that, mutations of Ser142 or Ser211 of TFEB or mTORC inhibition result in nuclear translocation of the TFEB protein. ERK-mediated phosphorylation of Ser73 of MITF, homologous to Ser142 of TFEB, has been shown to enhance transcriptional activity of MITF (Hemesath et al., 1998). In addition, Wu and colleagues showed that a double Ser73/409Ala mutant of MITF resulted in increased half-life. They reported that the mutant was transcriptionally incompetent and resistant to ubiquitin-mediated proteolysis (Wu et al., 2000). However, these two studies have not shown any effects of the phosphorylation status of MITF on the subcellular localization of MITF.

In this thesis, I analyzed the effects of the blockade of mTORC kinase activity on the phosphorylation status of MITF and whether this has an impact on the subcellular localization of the protein. For this purpose, the use of specific antibodies against specific phosphorylated amino acids of the MITF protein would have proven useful. Unfortunately, the phospho-specific antibodies against Ser73 available at the time the experiments were performed did not work successfully. Therefore, I was limited to analyze the mobility shift of an MITF doublet as shown by Western blotting in order to infer the phosphorylation status of Ser73 upon mTOR inhibition. Importantly, previous studies describe that the upper band of the MITF doublet corresponds to phosphorylated Ser73 (Hemesath et al., 1998; Wu et al., 2000) and that MAPK-ERK signaling increases the phosphorylation of Ser73 and therefore the intensity of the upper band. As shown in **Figure 15**, the Ser73Ala mutant of MITF-M resolves as a single band in Western blot. This corresponds to the lower band of the MITF doublet. The addition of a phosphate group would theoretically add roughly ∼90 Da to the molecular weight of the protein whereas the mobility shift I observe is around 5 KDa, suggesting that additional post-translational modifications are primed by the phosphorylation of Ser73 of MITF. Another possibility is that phosphorylation of Ser73 of MITF induces a conformational change that affects its mobility through the SDS-PAGE gel. A three-hour inhibition of both mTORC and BRAF using specific inhibitors resulted in reduced intensity of the upper band of wild type MITF and Ser409Ala MITF after three hours, although the upper band did not disappear completely (**Figure 15**). No alterations in protein levels of the single band observed for the Ser73Ala MITF were observed. This indicates that, in addition

to the BRAF signaling pathway, mTOR can phosphorylate MITF in a site that is either Ser73 itself or dependent on Ser73 phosphorylation, and that other kinases may be involved in this phosphorylation event.

### 4.4.2 Dephosphorylation of Ser73 promotes nuclear localization and degradation of MITF

The MITF-A isoform shows a predominantly cytoplasmic distribution in melanoma cells as opposed to MITF-M which is primarily nuclear. Thus, the effects of a drug-mediated increase in nuclear localization of the MITF protein would be easier to observe on MITF-A than on MITF-M. Inhibition of mTOR triggered nuclear translocation of MITF-A (**Figure 16**), suggesting that MITF-A shares the mechanism of regulation of its subcellular localization with TFEB and TFE3 (**Figure 11A, B, 12, 13B, 14B**). Following the observation that mTOR inhibition reduces the intensity of the upper band of MITF-M to a certain degree, which is dependent on Ser73 phosphorylation, I transfected these cells with a version of MITF-A where Ser180, the serine residue that corresponds to Ser73 of MITF-M is mutated to alanine. Ser180Ala MITF-A was almost exclusively nuclear, suggesting that the phosphorylation event at Ser180 of MITF-A is crucial for cytoplasmic localization of the protein (**Figure 16**).

In order to determine if mTOR inhibition affected the expression of the MiT-TFE factors I analyzed their mRNA expression by RT-qPCR. In **Figure 28**, real time qPCR analysis of MITF showed increased mRNA levels in 501Mel cells upon three-hour treatment with mTOR inhibitor (**Figure 28A**). Thus, with the purpose of analyzing whether the mTOR-mediated increase in MITF transcription would translate to the protein level, I analyzed the endogenous levels of MITF by Western blot upon mTORC inhibition. I did not observe an increase in protein levels (**Figure 28C, D**). Thus, I analyzed any potential effects of mTOR on protein stability and degradation of MITF. To this end, the cells were treated with cycloheximide, a potent inhibitor of protein translation. Unexpectedly, cycloheximide treatment increased the upper to lower band ratio of MITF, coupled with a markedly reduced presence of the lower band (**Figure 28C, E**). mTOR inhibition significantly decreased the upper to lower band ratio, suggesting dephosphorylation of MITF, as previously discussed (**Figure 15**). However, treatment with the mTOR inhibitor and cycloheximide severely reduced the presence of the lower band, similar to treatment of cycloheximide alone (**Figure 28C, E**). These results suggest that dephosphorylation of Ser73 or a different site primed by dephosphorylation of Ser73 triggers degradation of the MITF protein. Subsequently, the proteasome inhibitor MG132 was used with the aim of assessing whether the degradation

of dephosphorylated MITF is mediated by the proteasome complex. As shown in **Figure 28F**, inhibition of the proteasome increased the intensity of the lower band despite blockade of protein translation with cycloheximide treatment. In addition, total protein levels of MITF increased when compared to cycloheximide treatment or vehicle control (**Figure 28F, G**). This suggests that degradation of MITF is through the proteasome pathway. Another interesting observation from this experiment was that, as seen by Western blotting (**Figure 28C, F**), there is not only an increased ratio of MITF's upper band to lower band upon cycloheximide treatment compared to vehicle control, but the presence of the upper band is increased in absolute terms, with or without Torin1 treatment, compared to vehicle control. It is possible that this is due to cycloheximide-mediated blockade of protein translation, which may prevent *de novo* synthesis of proteins that are required for dephosphorylation of MITF. It has been shown that protein and mRNA levels of protein phosphatase 1 alpha (PP1α) decline over time after cycloheximide treatment, suggesting that this treatment also affects transcription (Price, Horstmann, et al., 1998). Cycloheximide-induced blockade of protein translation can reduce the expression of transcription factors and ribosomal proteins and thus, affect downstream transcriptional machinery (Gokal et al., 1986). Moreover, the cells undergoing mTORC inhibition in this assay still have an active BRAF-MAPK pathway, which I have shown to trigger phosphorylation of MITF at the same site/s (**Figure 15**). Cycloheximide treatment has been reported to inhibit MAPK phosphatase-1, which in turn induces phosphorylation of ERK (W. W. Lin & Hsu, 2000). This effect of cycloheximide could explain the observed increase in phosphorylation of MITF.

Wu and colleagues showed 18 years ago that MAPK-ERK signaling phosphorylates MITF at Ser73 and Ser409, targeting MITF simultaneously for increased activity and degradation (Wu et al., 2000). However, this study is considerably different to the statements discussed in this thesis. Wu et al. used Steel factor (Sl) to stimulate the MAPK-ERK pathway and showed a sharp decrease in MITF protein levels after blockade of protein translation. Interestingly, in the work by Wu and colleagues, they show that the Ser73Ala MITF mutant underwent degradation similar to the wild type protein upon MAPK-ERK stimulation, suggesting that the phosphorylation of other sites different to Ser73 are involved in this MAPK-mediated degradation of MITF. In addition, they reported that a double mutant Ser73/409Ala is more stable when compared to wild type or Ser73Ala MITF. It is important to notice that the Ser73/409Ala mutant reported by Wu et al. ran at a significantly lower molecular weight to what was expected (see Figure 6A in Wu et al.). This has

not been observed in our lab (data not shown) suggesting that the particular construct used might not be full-length MITF.

In this thesis, I have shown that mTORC can phosphorylate MITF on a residue or combination of residues dependent on the phosphorylation of Ser73. A recent publication showed that inhibition of the BRAF-MAPK pathway with vemurafenib did not affect the stability of wild type MITF upon cycloheximide treatment. Furthermore, Ser73Ala MITF was not found to have a shorter half-life than the wild type protein (Fock et al., 2018). This study also shows an increase in phosphorylation of ERK upon cycloheximide treatment, which could result in increased phosphorylation of MITF. Therefore, in the light of these results, I cannot conclude whether the observed relative increase of the upper band of MITF upon blockade of *de novo* protein translation with cycloheximide treatment is a result of increased degradation of the fraction of MITF that is unphosphorylated or a mobility shift due to an increase of phosphorylated MITF at Ser73. Nevertheless, in **Figure 28C, D**, I show that the levels of total MITF protein decrease upon cycloheximide treatment and that inhibition of proteasomal activity abrogates the degradation triggered by cycloheximide treatment (**Figure 28F, G**). The lower band of MITF rapidly disappears when protein translation is inhibited, which may suggest that MITF is continuously expressed and that phosphorylation is important in order to stabilize MITF. The fact that I observed an increase in mRNA levels of MITF upon mTOR inhibition could point to a downstream effect of the increased degradation of MITF that triggers an increase in *MITF* transcription. In this line, I observed that transient siRNA-mediated knockdown of MITF resulted in increased transcription of the *MITF* gene (**Figure 25**). This clearly indicates that MITF suppresses its own expression and is involved in its own regulation. I will discuss this further in the **section 5.7** describing the regulatory loop between MITF, TFEB and TFE3. These data imply an mTORC-dependent effect on MITF turnover: MITF is degraded faster when mTORC is inactive and there is increased *de novo* expression aimed to compensate for the loss of MITF protein (**Figure 35**). Finally, I conclude that the mechanisms behind transcriptional and post-transcriptional regulation of MITF by the mTORC pathway are complex and require further elucidation.

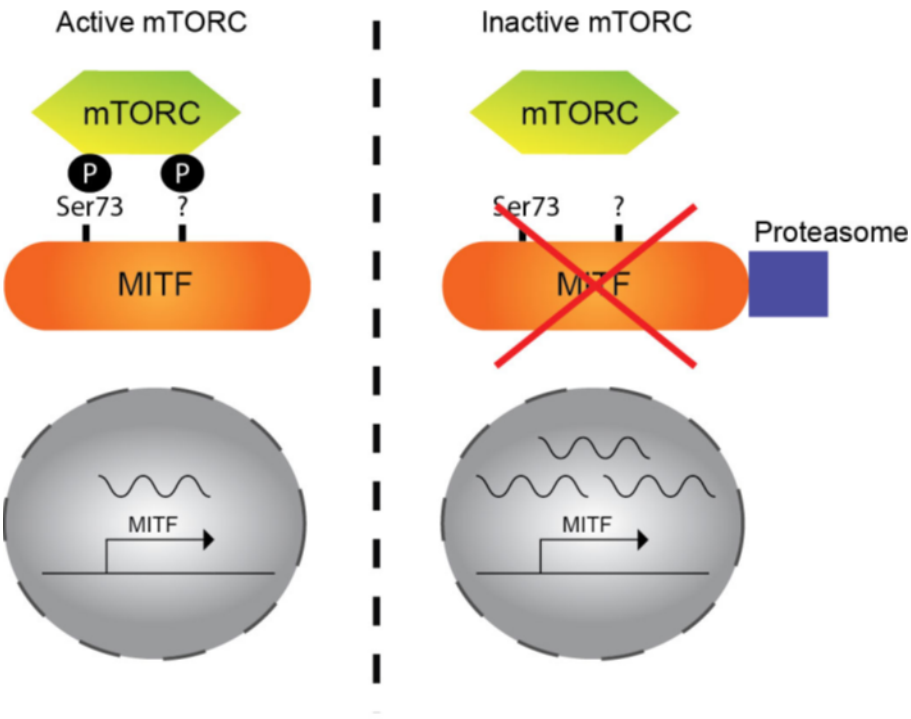


**Figure 35. Proposed model for the effects of mTOR inhibition on MITF.** Pharmacological or stress-induced inactivation of mTOR promotes dephosphorylation of MITF at Ser73 and additional Ser73-dependent residue/s, which triggers degradation of MITF by the proteasome and a compensatory increase in MITF transcript expression.

## 4.5 GSK3β signaling pathway affects the subcellular localization of MITF

Ploper and colleagues have characterized a C-terminal domain of MITF which contains several serine residues (**Figure 17A**). They linked three of these residues, corresponding to Ser504/508/512 in MITF-A, to GSK3β-mediated phosphorylation and proteasomal degradation. Active Wnt signaling induced endosomal sequestration and inactivation of the GSK3β complex which led to increased stability of the protein and enhanced endosomal biogenesis in a positive feedback loop (Ploper et al., 2015). In their work they do not report whether the mutation of these three C-terminal serines of MITF-M affects its subcellular localization. When I overexpressed the Ser504/508/512Ala MITF-A mutant, the protein was significantly more cytoplasmic than wild type MITF in 501Mel cells (**Figure 17B**). Blockade of the GSK3β pathway with the

selective inhibitor CHIR99021, induced nuclear localization of MITF-A, as opposed to the more ubiquitous presence of the protein observed in the vehicle control (**Figure 17B**). This is similar to the increase in nuclear localization of MITF observed upon inhibition of mTOR discussed in the previous chapter. Interestingly, the Ser504/508/512Ala mutant of MITF-A localized to the nucleus upon GSK3β inhibition (**Figure 17B**). This suggests that the GSK3β pathway regulates the subcellular localization of MITF-A in a manner independent of the three C-terminally located serines characterized by Ploper et al. (2015). Another study highlighted GSK3β as a negative modulator of the autophagy response showing that this kinase can phosphorylate TFEB and promote cytoplasmic retention of the protein. The use of the GSK3β inhibitor CHIR99021 affected the electrophoretic mobility of TFEB, suggesting a dephosphorylation event, coupled with an increase in its nuclear localization. Moreover, GSK3β inhibition elicited the autophagy response in human pancreatic cancer cells through TFEB (Marchand et al., 2015).

I conclude that, in addition to inducing phosphorylation of the C-terminus of MITF leading to proteasome-mediated degradation of the MITF protein, GSK3β affects the subcellular localization of MITF, possibly through the phosphorylation of alternative sites in MITF. Elucidating which residues are targets of phosphorylation by GSK3β in MITF and whether they are conserved in TFEB, would prove useful to understand how this signaling pathway affects the subcellular localization and activity of transcription factors, such as MITF and TFEB, that are crucial for the regulation of autophagy in cancer cells, including melanoma.

## 4.6 Dimerization of MITF, TFEB and TFE3 in melanoma cells

In this thesis, I show that the three factors, MITF, TFEB and TFE3, interact in 501Mel cells (**Figure 18**), possibly forming functional heterodimers. This is in line with previous studies showing that these factors are capable of forming stable DNA-binding heterodimers when translated *in vitro* in a cell-free system (Hemesath et al., 1994) and that TFE3 can heterodimerize with MITF in osteoclasts (Weilbaecher et al., 1998). Moreover, TFE3 has been suggested to preferentially heterodimerize, as opposed to MITF's preference to form homodimers (Hemesath et al., 1994). This is in contrast with a study that claims that TFE3 does not form heterodimers with MITF in mouse B16 melanoma cells, and that TFE3 homodimers cannot bind M-box elements (Verastegui et al., 2000). Previous studies in the lab have shown that TFE3 was able to transactivate a luciferase reporter construct containing the wild type tyrosinase

promoter. The tyrosinase promoter features two DNA regulatory motifs, which are a variation of an M-box with a 5' flanking thymine in only one of the DNA strands. The presence of 5' flanking thymines in both strands is sometimes considered as part of the M-box motif (Aksan & Goding, 1998). Thus, these two motifs were mutated to the canonical M-box in order to test whether TFE3 could activate the M-box element. TFE3 was able to activate the modified tyrosinase promoter with two M-boxes (Arnþórsson, 2016). This was performed in HEK293T cells that do not express any of the MiT-TFE transcription factors, suggesting that TFE3 alone can bind to M-box elements and activate gene transcription, in contrast to the study by Verastegui and colleagues.

Verastegui et al. (2000) immunoprecipitated nuclear extracts of B16 mouse melanoma cells, which endogenously express MITF and TFE3, and reported that virtually no TFE3 was pulled down by the anti-MITF antibody. In this thesis, I have used whole 501Mel cell lysates in order to co-immunoprecipitate overexpressed MITF and TFE3. One possible explanation for this discrepancy is that MITF is expressed at a much higher level in B16 cells than TFE3, therefore favoring the detection of MITF homodimers over MITF-TFE3 heterodimers. Another possible explanation is that perhaps only the cytoplasmic fraction of MITF interacts with TFE3, which is present in both the cytoplasm and nuclei of these cells. However, I show that immunoprecipitation of TFE3, pulled down abundant MITF (**Figure 18**), suggesting that these interactions take place in the nucleus as well. In addition, overexpression of MITF or TFE3 did not result in a different subcellular localization of the protein, when compared to their endogenous localization in 501Mel cells (**Figure 11, 12**). Perhaps overexpression of TFE3 enables MITF-TFE3 heterodimers to take place. Further investigations on this matter should include cell fractionation preparations in order to determine in which subcellular compartment these interactions occur.

### 4.6.1 A three-residue insert mediates the selection of dimerization partners of the MiT-TFE factors

In this thesis I successfully characterized a three-residue domain, the stammer, which disrupts the continuity of the coiled-coil leucine zipper domain of the MiT-TFE transcription factors, as responsible for their dimerization properties. I have generated an MITF mutant where the motif has been excised, MITF (Δ259-261), and demonstrated that the lack of the stammer motif does not affect the mutant's subcellular localization or functionality as a transcription factor (Pogenberg, Ballesteros Alvarez et al., **Manuscript II**, in

preparation). Generation of a crystal structure of MITF(Δ259-261) showed that the dimeric arrangement is unperturbed whereas the stability of the protein is enhanced. The presence of the stammer in the MiT-TFE transcription factors interrupts the leucine zipper heptad pattern present in other bHLHZip factors such as c-Myc, MAD and MAX. This restricts the ability of MITF, TFEB, TFE3 and TFEC to selectively dimerize with each other and avoid the other family members. Removal of the stammer, as shown by co-immunoprecipitation studies using the MITF(Δ259-261) mutant alters the selection of homotypic interactions in which the mutant can participate. MITF(Δ259-261) severely reduces its ability to interact with TFEB and TFE3, although its ability to homodimerize remains intact (**Figure 20**). Interestingly, as observed in the co-immunoprecipitation studies, MITF(Δ259-261) gains interaction abilities with MAX (**Figure 21**), indicating that the removal of the stammer allows for *de novo* homotypic interactions with other bHLHZip factors that do not have the three-residue insertion in the leucine zipper. These data have implications for future perspectives in research aiming to manipulate the specificity of the interactions and dimerization ability of transcription factors containing a leucine zipper.

We were interested in taking this further by developing an MITF mutant that would only homodimerize and not dimerize with any other MiT-TFE transcription factor, in order to study the specific role of MITF homodimers in melanoma. The MITF(Δ259-261) mutant was able to interact with MAX and possibly other bHLHZip transcription factors and, therefore, may act in a dominant negative fashion. Therefore, I cannot rule out newly acquired functions of the heterodimers containing this mutation that do not occur *in vivo*. I therefore generated two new MITF mutants: one in which the stammer was moved from the junction between heptads 0-I to the one between heptads I and II (**Figure 5B**), and a second mutant containing the wild type stammer and a second stammer introduced at the junction between heptads I-II. Co-immunoprecipitation studies showed that both mutants were able to dimerize with wild type MITF and displayed a severely reduced interaction ability with MITF(Δ259-261) (**Figure 22**). Interestingly, the mutant containing two stammer insertions failed to homodimerize (**Figure 22B**). These results indicate that the presence of the three-residue insert is critical for the interaction with the other MiT-TFE family members. When the insertion was placed at the junction between heptads I-II of the leucine zipper in the dREQ/EQQins mutant (MITF(Δ259-261)_N269_R270insEQQ), the protein displayed the same dimerization properties as the wild type MITF protein, suggesting that this change in localization of the insertion did not have an impact on the dimerization properties of the protein.

The selection of dimerization partners has been shown to be a mechanism that modulates transcription factor activity (Amoutzias et al., 2008). A good example of this concept in bHLHZip transcription factors is the c-Myc/MAX/MAD network, with c-Myc and MAX forming dimers that promote cell differentiation in contrast with MAX/MAD heterodimers that have a repressive function (Amati & Land, 1994; Luscher, 2012). This highlights that the fine-tuned balance of the relative concentrations of these factors can profoundly impact cell biology and cell fate. The development of a hypothetical novel mutation in MITF that would only allow the protein to form heterodimers, coupled with genetic editing techniques like CRISPR could prove valuable to investigate the function of MiT-TFE homodimers versus heterodimers and to gain insights into the underlying mechanisms of target gene selection.

## 4.7 MITF, TFEB and TFE3 regulatory loop in melanoma

Another major finding of this thesis was that the MiT-TFE transcription factors affect each other's expression and form a regulatory loop that involves both direct and indirect effects. This constitutes yet another layer of regulation of the expression and function of the factors. In this study, I demonstrate that MITF, TFEB and TFE3 are expressed to some extent across a majority of melanoma samples and cell lines and they display a complex cross-regulatory relationship, affecting each other's expression through a combination of direct transcriptional activity and indirect effects that need further investigation (**Figure 36**). Ectopic overexpression of MITF reduced the endogenous transcription of MITF in a self-limiting regulatory loop. MITF and TFE3 participate in a negative regulatory loop in melanoma and I found that TFE3-mediated reduction in MITF expression affects the proliferation of a human melanoma cell line. I suggest that an indirect regulatory mechanism is involved in the effects of MITF on TFE3 since there are no binding sites for MITF located in the *TFE3* gene. This finding is further strengthened by the observation that the expression levels of MITF and TFE3 anti-correlate across a well-established database of melanoma specimens accessible at TCGA ("http://cancergenome.nih.gov/,") (**Figure 8C**).

On the other hand, I show that MITF can induce the expression of TFEB through direct binding and transcriptional activation. In turn, TFEB inhibits the expression of MITF. A limitation of this study was the fact that I only had access to MITF and TFEB ChIP-seq data in melanoma cells. Therefore, I cannot conclude whether the TFE3-mediated reduction in MITF expression involves direct repression of transcription. More efforts are needed to reveal the mechanism underneath the homeostatic self-regulation of MITF expression

and whether the inhibitory effects of TFEB and TFE3 on MITF are direct transcriptional effects or indirect effects.

TFEB has been shown to control cellular lipid metabolism through a starvation-induced auto-regulatory loop that involves nuclear translocation of TFEB and increased transcription of *TFEB* (Settembre et al., 2013). In this study, I have not assessed whether TFEB overexpression or depletion affects expression of the endogenous mRNA or protein levels of TFEB. Since intron 1 of *TFEB* features a binding site for both MITF and TFEB, as shown by ChIP-seq data (**Figure 23A**), further investigations on whether TFEB stimulates its own expression through this particular motif would prove useful.

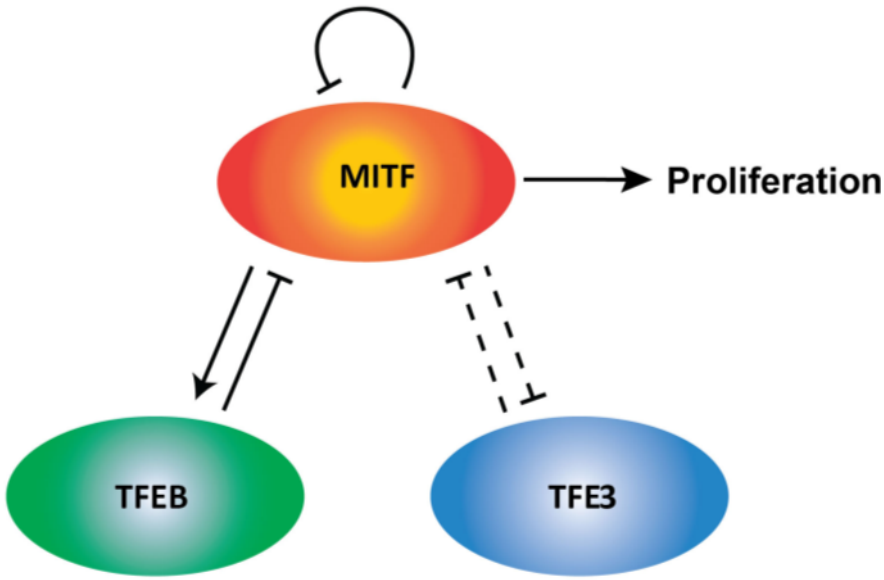


**Figure 36. Model of the cross-regulatory relationship between MITF, TFEB and TFE3 in melanoma.**

### 4.7.1 MITF, TFEB and TFE3 inhibit the expression of MITF

It is known that the transcriptional regulation of MITF throughout development, during proliferation and differentiation of the melanocytic lineage and melanoma progression is complex and involves several different mechanisms.

Transcription factors, such as PAX3, SOX10 and LEF-1 have been shown to positively regulate MITF-M expression, leading to differentiation of melanocytes during neural crest development (Potterf et al., 2000; Stolt et al., 2008; Takeda, Yasumoto, et al., 2000; Tassabehji et al., 1992). In this study I show that ectopic overexpression of MITF-M represses the endogenous expression of MITF in melanoma cells at both the mRNA and protein levels in two different melanoma cell lines (**Figure 24, 26**). In addition, the transient siRNA-mediated knockdown of MITF resulted in increased transcription of the *MITF* gene (**Figure 25**). This clearly indicates that MITF suppresses its own expression and is involved in its own regulation. Publicly available ChIP-seq data show that there are MITF-peaks upstream of the first common exon 2 (in the first intron of the M-isoform) containing potential binding sites with CACGTG motifs (**Figure 23B**). Luciferase reporter assays were employed in order to analyze whether a particular E-box motif in this region was responsible for the self-repression of MITF. I therefore generated a reporter construct containing a 670 bp sequence within the first intron of MITF-M with the CACGTG element that is a binding site for MITF (**Figure 27B**). I also generated another construct where this element was mutated to CCCTTTA as a scrambled control (**Figure 27B**). Overexpression of MITF did not repress transactivation of any of these two reporter constructs when compared to the empty reporter construct (**Figure 27C**). We therefore plan to further characterize how MITF inhibits its own expression by analyzing whether MITF transrepresses a reporter gene under an alternative DNA regulatory element that is located upstream in the *MITF* gene, which presumably is a binding site for MITF (**Figure 23B**).

The observations that MITF can repress its own expression in a self-regulatory loop contradict previous studies showing that MITF itself induces the transactivation of its own promoter. MITF-M was reported to activate its own expression when it was co-expressed with lymphoid-enhancing factor 1 (LEF-1). However, expression under the MITF-M promoter was enhanced by the expression of MITF only when the domain in LEF-1 that mediates binding and formation of transcriptional complexes with β-catenin was intact (Saito et al., 2003; Yasumoto et al., 2002). Previous studies have shown that β-catenin alone, a transcription factor downstream of the Wnt signaling pathway, activates the transcription of MITF and melanocyte differentiation (Larue et al., 2003). In this case MITF-M may merely act as a co-factor that enhances the activity of β-catenin, without having any affinity to that particular regulatory region within the MITF-M promoter. In another study, Northern blot analysis showed that α-MSH treatment resulted in increased mRNA expression of

MITF, peaking at two hours and entering a declining phase beyond this time point, indicating a homeostatic regulatory mechanism that was coupled with a decrease in protein expression beginning at 4 hours (Price, Horstmann, et al., 1998). Interestingly, when protein translation was inhibited with cycloheximide, there was no decline observed in MITF mRNA expression, suggesting that increased MITF protein is required for the observed reduction of MITF's transcription. I hypothesize that an increase in MITF protein expression may inhibit the transcription of MITF in a self-repressing regulatory loop through direct binding to regulatory elements within the *MITF* gene.

TFEB and TFE3 overexpression can repress the expression of both MITF mRNA and protein (**Figure 24, 26**). In turn, knockdown of TFEB increases the expression of MITF whereas knockdown of TFE3 does not (**Figure 25**). I assessed by RT-qPCR the mRNA expression of MITF upon TFEB or TFE3 overexpression on MITF mRNA expression in the presence of an mTORC inhibitor. mTORC inhibition increases nuclear localization of TFEB and TFE3 and might hypothetically enhance the inhibitory effect of TFEB and TFE3 on MITF expression. Inhibition of mTORC further enhanced the decrease in MITF transcripts upon TFEB and TFE3 overexpression; the TFE3-mediated reduction in MITF's mRNA expression was more profound when mTORC was inhibited (**Figure 28B**). In contrast, mTORC inhibition did not further enhance the reduction of MITF protein levels (**Figure 28C, D**) (**Figure 35**).

#### *4.7.1.1 MITF knockdown reduces the proliferation rate of a MITF$^{high}$ melanoma cell line*

In this thesis, I have shown that a 501Mel cell line expressing doxycycline-inducible miRNA against MITF shows a reduced proliferation rate and extended doubling time when compared to control cells (**Figure 29A, B**). Overexpression of TFE3 in cells expressing control miRNA recapitulated the lower proliferation rate of the miR-MITF cells, suggesting that TFE3-mediated modulation of the expression of MITF may have an impact in the proliferation ability of certain melanoma cell lines and tumors (**Figure 29B, C**). I hypothesize that TFE3 can negatively affect the proliferation rate of 501Mel cells through the transcriptional repression of MITF, as discussed in the previous chapter. Slow-proliferating miR-MITF cells did not increase their doubling time upon TFE3 overexpression (**Figure 29B, D**), which suggests that the effects of TFE3 on the proliferation of 501Mel cells are MITF-dependent. Surprisingly, TFEB overexpression did not affect the proliferation of the cells expressing a control miRNA (**Figure 29**) despite the severe effects on MITF transcription upon TFEB overexpression observed in other experiments performed in this cell line

(**Figure 24, 28**). I have observed that transient transfection of TFEB in these cells induced high mortality. I did not observe an increase in cell mortality with the transfection of empty vector or TFE3. I transfected the cells with either TFEB, TFE3 or empty vector (EV) control at the same time as the miRNA expression was induced, and after 24 hours, cells were trypsinized and transferred to a new plate for analysis of confluency. Therefore, a high mortality due to transfection with TFEB could have led to the selection of non-transfected cells which would virtually be the same as those overexpressing empty vector. One way to get past this problem would be to use stable cell lines expressing both the doxycycline-inducible miR-MITF construct and TFEB or TFE3 constructs, together with their respective controls. This way I would likely avoid the high cell mortality rates sometimes observed upon lipofectamine transfections.

It is not surprising to observe that MITF is required to maintain the proliferation rate of some melanoma cell lines. Previous studies in the lab have shown that transient or stable knockdown of MITF impairs proliferation of Skmel28 cells. Skmel28 cells carrying a CRISPR Cas9-mediated knockout of MITF also show significantly reduced growth and migration ability (Ramile Dilshat, manuscript in preparation). Hence, I hypothesize that in melanoma cell lines expressing MITF, a higher expression of TFE3 can significantly reduce the transcription and protein expression of MITF (**Figure 24, 28**), which in turn impairs the proliferation ability of these cells (**Figure 29B, C**).

MITF has a very well established role in maintaining melanocyte lineage identity and in conferring anti-apoptotic effects in melanoma (Garraway et al., 2005). However, to this date there is not a broad consensus on whether MITF is crucial for sustaining proliferation and growth in melanoma. A study has shown that the effects of doxycycline-inducible titration of MITF with an shRNA against MITF in melanoma cells were not as profound as expected, and that single-cell heterogeneity was a major factor in the variability of the response to MITF depletion, even within a fairly homogeneous cell line (Vlckova et al., 2018). Using the microRNA miR-101 to reduce MITF expression in melanoma cell lines established from 29 patients with stage IV metastatic melanomas, resulted in suppressed cell proliferation, invasion and migration (Luo et al., 2013).

MITF regulates genes involved in DNA replication and repair and depletion of MITF triggers the DNA damage response and entry into a senescence state (Strub et al., 2011). It was proposed that cells depleted of MITF do not survive or become undifferentiated non-melanoma tumor cells (Vachtenheim &

Ondrusova, 2015), raising doubts of whether we can consider MITF-negative cell lines to be melanomas. Different levels of MITF expression in melanoma modulate the cellular function. In response to environmental triggers, melanoma cells can shuttle between an invasive low-proliferating phenotype characterized by low expression of MITF and a more differentiated, proliferative and less invasive phenotype with higher expression of MITF (Hoek & Goding, 2010). Relapsed melanoma tumors following adoptive cell transfer therapy targeting premelanosome protein (PMEL) showed reduced expression of pigmentation genes and inflammation-dirven dedifferentiation (Landsberg et al., 2012). Inflammatory cues inhibit the translation initiation factor eIF2B and induce the expression of activating transcription factor 4 (ATF4) which, in turn, represses MITF and activates tyrosine-protein kinase receptor UFO (AXL) (Falletta et al., 2017). MITF expression levels have been found to anticorrelate with AXL and a low MITF/AXL ratio is a marker of resistance to several targeted therapies in melanoma tumors, including BRAF inhibition (Muller et al., 2014).

Interestingly, ectopic expression of MITF in a well-established MITF-negative cell line, RPMI-7951, did not result in activation of lineage-specific differentiation markers nor downstream targets of MITF (Vachtenheim et al., 2001). This is in line with another study showing that MITF activation of melanocyte-specific promoters is dependent on the activation of chromatin remodelers BRG1 and SMARCA2 (de la Serna et al., 2006). However, the transcription of genes involved in cell-cycle arrest and induction of the differentiation did not require the expression of the chromatin remodelers mentioned above, highlighting the role of MITF in regulating melanoma survival and identity. Thus, it is important to take into consideration that the cellular context associated to different MITF expression levels across tumors and cell lines may be caused by profound changes of the chromatin architecture and transcriptional landscape and therefore may not be possible to recapitulate through transient modulation of MITF expression.

### 4.7.2 MITF directly induces the expression of TFEB through an E-box-like motif

I show that MITF increases the expression of TFEB mRNA and protein (**Figure 24, 26**). Analysis of MITF ChIP-seq data revealed a binding site in intron 1 of TFEB (**Figure 23**). Using luciferase reporter gene assays on HEK293T cells I demonstrate that the increase in TFEB expression mediated by MITF is through direct binding to a CAGCTGA motif located at the binding site reported by the ChIP-seq data (**Figure 27**). Therefore, I analyzed whether the CAGCTG(A) sequence, where the two central bases are swapped with respect

to the canonical E-box CACGTG motif, represents a common motif in the MITF ChIP-seq dataset published by Laurette and colleagues and the TFEB ChIP-seq dataset from our lab (Ramile Dilshat, unpublished). Analysis of motif enrichment (AME) of the MITF binding sites across the ChIP-seq dataset from 501Mel cells (Laurette et al., 2015) showed that the CAGCTGA motif is present in 16% of the MITF-bound sequences, compared to 36% of the sequences presenting a CACGTGA element and 7% that contain a CCCTTTA motif, used as scramble control in the transactivation assay (**Table 10**). These data suggest that MITF can bind to CAGCTGA motifs and activate the transcription of downstream genes. Analysis of the MITF structure bound to the CACGTG and CATGTG sequences showed that Arg217 of MITF forms specific bonds with the two central bases of the E-box (CACGTG) motif, whereas it does not form base-specific bonds with the two central bases of the CATGTG M-box motif (Pogenberg et al., 2013). Instead, specific bonds are formed with the two bases flanking the 6 bp motif, -4 and +4, and with -3, -2 and +3, counting from the center of the motif (**Figure 37**). These bases are all conserved in the GCAGCTGA motif at the MITF binding site in *TFEB* used in this experiment.

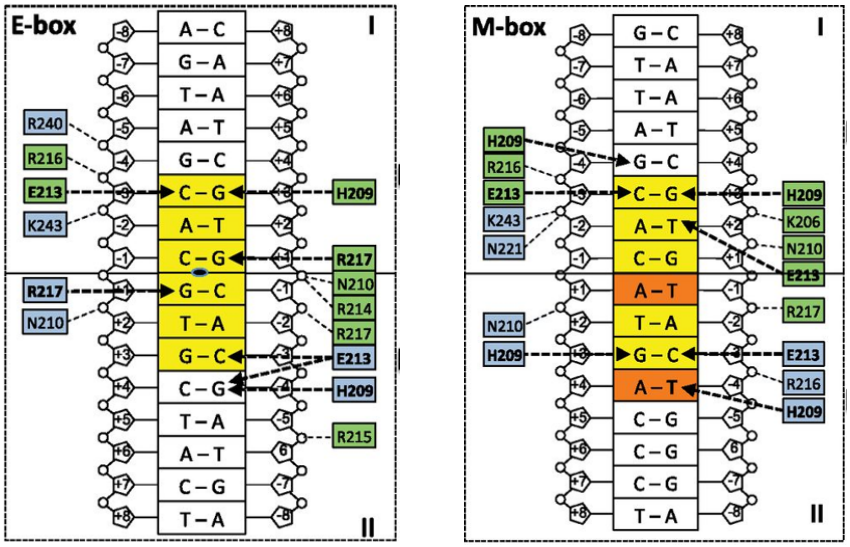


**Figure 37. MITF/DNA interactions with the E-box (left) and M-box (right).** Base-specific interactions are highlighted in bold. Hydrogen bonds are represented in regular characters and dashed lines.. Adaptation from (Pogenberg et al., 2012)

### 4.7.3 MITF negatively affects the transcription of TFE3

Verastegui et al. (2000) reported that stimulation of cAMP signaling with forskolin induced the expression of MITF protein while it decreases the expression of TFE3 (Verastegui et al., 2000). In this thesis, I have shown that transient MITF overexpression resulted in reduced expression of TFE3 in Skmel28 cells and in 501Mel cells. However, no reduction in mRNA or protein expression of TFE3 was detected in the doxycycline-inducible pBac-MITF 501Mel cell line (**Figure 24, 26**). It is important to point out that both Skmel28 and 501Mel cell lines exhibit high endogenous levels of MITF whereas the expression of TFE3 is much lower. Therefore, overexpressing MITF might have weak repercussions on TFE3's overall expression. Knocking down MITF, on the other hand, led to increased transcription of TFE3 in both cell lines (**Figure 25**), although at the protein level the effect was not significant due to high variability (**Figure 9B**). Verastegui and colleagues have explained their observations such that TFE3 and MITF are differentially regulated by cAMP signaling. I have shown that MITF inhibits the expression of TFE3. Therefore, an increase in MITF expression upon stimulation of cAMP signaling with forskolin inhibits TFE3 expression. I did not find any binding sites for MITF or TFEB in the *TFE3* gene upon analysis of both ChIP-seq datasets (**Figure 23C**). It is likely that the regulation of TFE3 does not involve direct transcriptional regulation by MITF or TFEB. Other mechanisms are likely to be involved and need further characterization.

## 4.8 MITF and TFEB display a common repertoire of target genes

Many efforts have been directed at elucidating how MITF, TFEB and TFE3 direct the selection of transcriptional targets while they bind to similar DNA regulatory elements. These factors are able to regulate a similar repertoire of target genes but each one seems to regulate a specific set of genes. Previous results in the lab and by other researchers, have shown that MITF, TFEB and TFE3 overlap in their ability to activate E-box motifs present in the vicinity of their target genes (Aksan & Goding, 1998). Here, I report that an E-box located in intron 2 of MLANA, a gene involved in the pigment process and established as a marker of melanocytic differentiation and melanoma diagnosis, is bound by both MITF and TFEB. Moreover, MITF, TFEB and TFE3 are able to transactivate a MLANA regulatory element, as shown using a luciferase reporter assay (**Figure 30**). Interestingly, previous studies in the lab using a CRISPR MITF knock-out Skmel28 cell line showed that the expression of MLANA transcripts was severely affected by the lack of MITF and that TFEB

or TFE3 overexpression in this knockout cell line was not able to drive the expression of this gene (Katrín Möller, unpublished data). The mechanism by which MITF, and not TFEB nor TFE3, is required for the transcription of MLANA in these cells is unknown but may be dependent on the context of chromatin architecture.

Analysis of MITF and TFEB ChIP-seq datasets in 501Mel human melanoma cells has shown that 682 genes, approximately 30% of the genes in each of the datasets, are bound by both MITF and TFEB. Interestingly, over 85% of the overlapping genes are not melanosomal or lysosomal genes, but no other GO terms were found to be significantly enriched in this analysis. Analysis of the overall specific binding sites of MITF and TFEB showed that 25% (553) of the binding sites reported for MITF are shared with TFEB (**Figure 32A**) and motif discovery analysis on these 553 overlapping binding sites revealed the CLEAR box as the most frequent DNA regulatory element among these genes (**Figure 32B**), together with the zinc finger protein 263 (ZNF263) binding motif. A limitation of this study is that for the analysis of MITF binding sites, we overlapped the ChIP-seq dataset in 501Mel cells with a dataset obtained in Colo829 cells (Webster et al., 2014). It is possible that superimposing these two datasets has filtered out a large number of genes that are bound by MITF in 501Mel cells, considering the broad heterogeneity in genetic and epigenetic profile between cell lines. We confirmed that many lysosomal and pigmentation genes are bound by both MITF and TFEB, thus likely representing shared targets (**Figure 32C, D**); a striking majority of a well-established list of lysosomal and autophagy-related genes, which can be found in **Appendix III, Table 16**; featured binding sites for both transcription factors.

These finding are in agreement with other studies demonstrating that MITF, in addition to its role in controlling the transcription of a great number of pigmentation and melanosomal genes, correlates with the expression of a large number of lysosomal genes in melanoma cell lines. Ectopic overexpression of MITF has been reported to enhance the biogenesis of endosomal vesicles and expression of associated markers (Ploper et al., 2015). TFEB, has been depicted as the master regulator of autophagy and lysosomogenesis, through the direct binding and transcriptional modulation of CLEAR regulatory elements, located in the vicinity of promoters that regulate the trancription of several lysosome and autophagy-related genes (Palmieri et al., 2011). Moreover, our lab in collaboration with Vivian Pogenberg at the EMBL in Hamburg has succesfully generated a crystal structure of MITF bound to the CLEAR box, indicating that the regulation of lysosomal and autophagy-

related genes by MITF is through direct binding to these particular motifs (Möller et al, submitted).

## 4.9 The complex regulation of autophagy

Previous analysis performed in the lab (Möller, 2016) have shown that the regulation of a significant fraction of lysosomal and autophagy-related genes is mediated by the MiT/TFE transcription factors. In their work, gene ontology analysis showed that MITF mainly correlates with a subset of genes required for phagosome acidification and transmembrane transport, whereas the subset of genes correlated with TFEB/TFE3 is involved in proteolysis and degradation of the autophagy cargo. These data indicate that the three factors are important for the control of two distinct aspects within the complex autophagy process. Indeed, work performed by Ploper and colleagues (2015), showed that overexpression of MITF in C32 melanoma cells induced the expression of several lysosomal genes and increased the presence of intracellular vesicles that were positive for LAMP1 and Rab7, indicating an expansion of the late endosomal network. Interestingly, MITF overexpression did not increase autophagy function. Considering that a number of autophagy genes remained unaffected upon MITF overexpression, they concluded that MITF can elicit an increase in endosomal biogenesis but other transcriptional events are required in order to obtain fully functional lysosomes (Ploper et al., 2015).

We have thoroughly analyzed the ChIP-seq data of MITF and TFEB (**Figure 32, 34E**), the correlation of lysosomal genes with MITF, TFEB and TFE3 in melanoma samples (**Appendix III, Table 16; Figure 34**) and performed qPCR measurements of the expression of lysosomal genes in a melanoma cell line (**Figure 33**). The data compiled in this thesis indicate that MITF, TFEB and TFE3 are able to increase the mRNA expression of autophagy-related genes. However, some autophagy-related genes are exclusive targets of one of these factors, whereas other genes involved in the process, such as ATP6V0D2, are shared targets of MITF, TFEB and TFE3. In more detail, MITF and TFEB can increase the expression of *ATP6V0D2*, *ATP6V1C1* and *CTSD*, genes involved in autophagy vesicle acidification and substrate proteolysis (**Figure 33A**). However, MITF is important for the regulation of *ATP6V1C1* but is not required for the transcription of *CTSD*, which is also upregulated by TFEB. *TFEB* correlates in expression with *CTSD* in melanoma tumors and is important for the regulation of *CTSD* in the melanoma cell line analyzed. TFEB can induce the transcription of the ATPase subunit *ATP6V1C1*, but is not essential, as it cannot induce the transcription of *ATP6V1C1* when MITF is silenced (**Figure 33B**). In addition, I found that TFE3

is a negative modulator of ATP6V1C1, it is not required for the transcription of CTSD and might be required for the expression of CTSZ and GNS (**Figure 33C, D**).

Taken together, these data indicate that MITF, TFEB and TFE3 bind to a repertoire of target genes that are involved in lysosomal biogenesis and autophagy. However, the regulation of their autophagy-related transcriptional targets does not entirely overlap and seems to have different outcomes. This suggests that each factor may regulate a specific subset of target genes and that the regulation of autophagy requires the interplay of the three factors. Alternatively, heterodimers involving different combinations of the three factors may be important for some of the genes.

## 4.10 Final remarks and future directions

Genetic and genomic alterations that affect the levels of expression and/or functionality of bHLHZip transcription factors have been long known to play a role in human disease. The *MYC* oncogene has been found to be dysregulated in >50% of human cancers making this factor and its network partners forefront targets for the development of novel therapies. However, targeting transcription factors is notoriously difficult due to the lack of active sites for small molecules and their natural nuclear localization (Dang, 2012), which leads to the search for indirect approaches.

MITF displays a prominent role in melanoma survival and progression, with the mutant MITFE318K linked to familial and sporadic melanoma (Yokoyama et al., 2011), but also renal clear cell carcinoma (Bertolotto et al., 2011). Increased MITF expression, associated with chromosome 3p amplification, has been found in a subset of malignant melanomas (Garraway et al., 2005). Interestingly, the related TFEB protein is expressed at high levels in pediatric renal cell carcinomas (Kuiper et al., 2003) and TFE3 has also been reported to be translocated in up to 30–50% of renal cancer cases (Ramphal et al., 2006). In healthy human kidney, the four MiT-TFE subfamily members are expressed at comparable levels. In contrast, a subset of renal cell carcinoma tumors displayed a fusion of *TFEB*, located in chromosome 6, with the *Alpha* gene in chromosome 11. *AlphaTFEB* fusion gene links *TFEB* with the regulatory regions upstream of the *Alpha* gene, leading to promoter substitution and a 60-fold increase in expression (Kuiper et al., 2003). TFE3 depletion in TFE3-translocated renal cell carcinoma inhibited tumor proliferation, and ectopic overexpression of MITF rescued proliferation (Davis et al., 2006). Likewise, TFE3 restored cell proliferation of an MITF-driven renal

clear carcinoma when MITF was knocked down (Davis et al., 2006), indicating that MITF and TFE3 may have redundant roles at regulating proliferation and survival of specific tissues.

Dimerization is an important layer of regulation of transcription factors and it is crucial for bHLHZip factors to be functional in their role at transcribing downstream target genes. In this thesis, we have described the structural feature within the leucine zipper of the MiT-TFE transcription factors that restricts their dimerization ability within the subfamily and demonstrated that they can form heterodimers in melanoma cells. Dysregulation in the expression of MITF, TFEB and TFE3 could most likely affect the proportion of dimers formed and alter the regulation of target genes. Another network of bHLHZip transcription factors that has been widely studied is the Myc-Max-Mad network. Max is a ubiquitous protein that by forming heterodimers with Myc, can recruit nucleosome remodelers such as histone acetyl transferases (HATs) that would expose binding sites in target promoters and allow transcription by the relevant factors. Mad-Max heterodimers silence their target genes by recruiting histone deacetylases (HDACs), which have the opposite effect to the recruitment of HATs (Amoutzias et al., 2008). Chromatin remodelers such as BRG1 and HDAC7 have been reported to modify the configuration of chromatin at genomic loci that are bound by MITF for activation of the transcription of target genes in melanoma and osteoclasts, respectively (Laurette et al., 2015; Stemig et al., 2015). Interestingly, it has been shown that HDAC7 features an MITF-interacting domain, and that its ability to repress transcription was largely independent on its catalytic domain, suggesting that recruitment of MITF is a mechanism of transcriptional repression independent of the deacetylase activity of HDAC7 (Pham et al., 2011), which is reminiscing of the role of Mad-Max heterodimers at silencing downstream promoters.

I have shown that phosphorylation events downstream of signaling pathways such as BRAF-MAPK and mTORC are crucial at regulating the subcellular localization and activity of MITF, TFEB and TFE3. Moreover, blockade of the mTORC pathway triggers a partial dephosphorylation event on MITF that has an impact on protein stability, inducing proteasome-mediated degradation of MITF and an increase in transcription through a mechanism that remains to be elucidated.

The effects of mTORC on MITF expression further link the master regulator of melanocytes and melanoma to the endosomal pathways and autophagy, a new role of MITF that is receiving increasing attention. Here, I have shown that, in addition to TFEB and TFE3, MITF regulates the expression of genes

involved in lysosomogenesis and autophagy. This finding points to a certain degree of redundancy or cooperation between these factors at regulating their target genes. However, it is also apparent that they activate different subsets of genes that do not overlap entirely, and that the expression of one factor alone is not sufficient to drive lysosomogenesis and the autophagy process. I have also observed that MITF and TFE3 have antagonistic roles in regulating a subset of lysosomal genes. One of them, alpha-synuclein (SNCA) has been shown to be a direct target of MITF in the melanocytic lineage (Hoek et al., 2008). Alpha-synuclein is a protein involved in vesicle trafficking that is expressed predominantly in the brain. Interestingly it is also expressed in melanoma lesions, and it has been proposed as a marker in melanoma and an important player in a reported association between Parkinson's disease diagnosis and first-degree family history of melanoma (Gao et al., 2009; Welinder et al., 2014). MITF is expressed in the central nervous system. Specifically, in the mouse brain, MITF is detected in the cortex, hippocampus, cerebellum and olfactory bulb. Several isoforms have been detected across the different brain tissues but, interestingly, MITF-M is predominant in the olfactory bulb where it has been associated to the maintenance of homeostatic neuroplasticity (Atacho et al., submitted). Taken together, these studies indicate that the multi-layered interactions existing within the network of MiT-TFE transcription factors may have implications that go beyond melanoma biology.

BRAF inhibition, and specifically the vemurafenib agent that I used in this study for the inhibition of mutant BRAFV600E in 501Mel and Skmel28 cells, has been the most promising therapeutic approach for the treatment of metastatic melanoma in recent years (Bollag et al., 2010). Several upstream regulators and downstream targets of the mTOR pathway have been found to be dysregulated in several types of cancer. Two well characterized mTOR downstream effectors, p70S6K and 4EBP1 have been reported to contribute to the process of tumorigenesis (Law, 2005). It is important to take into consideration that pharmacological modulation of BRAF and/or mTOR activity can exert direct effects on a wide array of cellular processes, including cell cycle regulation, cell metabolism and autophagy, but also indirect effects through the regulation of the subcellular localization of MITF, TFEB and TFE3, their activity and stability. Unwanted effects that could lead to an upregulation of the autophagy response have been linked to increased vesicle trafficking and chemoresistance in melanoma (Huang et al., 2012)

In light of the evidence indicating that the roles of MiT-TFE factors do not overlap completely despite being able to activate similar DNA regulatory

elements, more efforts are needed to clarify how the selection of their particular target genes is mediated. Perhaps these factors require the interaction with different cofactors that attract them to secondary motifs or that modify nuclear architecture. My findings demonstrate that the MiT-TFE transcription factors are able to regulate each other's expression, and that MITF is the predominant family member across several melanoma cell lines and tumors, leading to a higher presence of MITF homodimers compared to other possible combinations of dimers. Considering the crucial role of the MiT-TFE transcription factors in several types of cancer and disease, understanding the imbalance in expression of these factors and how this may impact the phenotype and biology in diseased versus normal tissue, could prove valuable for uncovering novel druggable vulnerabilities in tumors and autophagy-related pathologies.

# References


Adameyko, I., Lallemend, F., Aquino, J. B., Pereira, J. A., Topilko, P., Muller, T., . . . Ernfors, P. (2009). Schwann cell precursors from nerve innervation are a cellular origin of melanocytes in skin. *Cell, 139*(2), 366-379. doi:10.1016/j.cell.2009.07.049

Adameyko, I., Lallemend, F., Furlan, A., Zinin, N., Aranda, S., Kitambi, S. S., . . . Ernfors, P. (2012). Sox2 and Mitf cross-regulatory interactions consolidate progenitor and melanocyte lineages in the cranial neural crest. *Development, 139*(2), 397-410. doi:10.1242/dev.065581

Aksan, I., & Goding, C. R. (1998). Targeting the microphthalmia basic helix-loop-helix-leucine zipper transcription factor to a subset of E-box elements in vitro and in vivo. *Mol Cell Biol, 18*(12), 6930-6938.

Alonso-Curbelo, D., Osterloh, L., Canon, E., Calvo, T. G., Martinez-Herranz, R., Karras, P., . . . Soengas, M. S. (2015). RAB7 counteracts PI3K-driven macropinocytosis activated at early stages of melanoma development. *Oncotarget, 6*(14), 11848-11862. doi:10.18632/oncotarget.4055

Amaravadi, R. K., Lippincott-Schwartz, J., Yin, X. M., Weiss, W. A., Takebe, N., Timmer, W., . . . White, E. (2011). Principles and current strategies for targeting autophagy for cancer treatment. *Clin Cancer Res, 17*(4), 654-666. doi:10.1158/1078-0432.CCR-10-2634

Amati, B., & Land, H. (1994). Myc-Max-Mad: a transcription factor network controlling cell cycle progression, differentiation and death. *Curr Opin Genet Dev, 4*(1), 102-108.

Amoutzias, G. D., Robertson, D. L., Van de Peer, Y., & Oliver, S. G. (2008). Choose your partners: dimerization in eukaryotic transcription factors. *Trends Biochem Sci, 33*(5), 220-229. doi:10.1016/j.tibs.2008.02.002

Aoki, H., Motohashi, T., Yoshimura, N., Yamazaki, H., Yamane, T., Panthier, J. J., & Kunisada, T. (2005). Cooperative and indispensable roles of endothelin 3 and KIT signalings in melanocyte development. *Dev Dyn, 233*(2), 407-417. doi:10.1002/dvdy.20340

Arnþórsson, Á. Ö. (2016). *The role of MITF, TFEB and TFE3 in endolysosomal regulation in melanoma.* (MSc), University of Iceland,

Ayer, D. E., Kretzner, L., & Eisenman, R. N. (1993). Mad: a heterodimeric partner for Max that antagonizes Myc transcriptional activity. *Cell, 72*(2), 211-222.

Bailey, T. L., Boden, M., Buske, F. A., Frith, M., Grant, C. E., Clementi, L., . . . Noble, W. S. (2009). MEME SUITE: tools for motif discovery and searching. *Nucleic Acids Res, 37*(Web Server issue), W202-208. doi:10.1093/nar/gkp335

Ballotti, R., & Bertolotto, C. (2017). Deregulated MITF sumoylation: A route to melanoma. *Mol Cell Oncol, 4*(4), e1331154. doi:10.1080/23723556.2017.1331154

Bardou, P., Mariette, J., Escudie, F., Djemiel, C., & Klopp, C. (2014). jvenn: an interactive Venn diagram viewer. *BMC Bioinformatics, 15*, 293. doi:10.1186/1471-2105-15-293

Bartolome, A., & Guillen, C. (2014). Role of the mammalian target of rapamycin (mTOR) complexes in pancreatic beta-cell mass regulation. *Vitam Horm, 95*, 425-469. doi:10.1016/B978-0-12-800174-5.00017-X

Baudino, T. A., & Cleveland, J. L. (2001). The Max network gone mad. *Mol Cell Biol, 21*(3), 691-702.

Bauer, J., Curtin, J. A., Pinkel, D., & Bastian, B. C. (2007). Congenital melanocytic nevi frequently harbor NRAS mutations but no BRAF mutations. *J Invest Dermatol, 127*(1), 179-182. doi:10.1038/sj.jid.5700490

Bentley, N. J., Eisen, T., & Goding, C. R. (1994). Melanocyte-specific expression of the human tyrosinase promoter: activation by the microphthalmia gene product and role of the initiator. *Mol Cell Biol, 14*(12), 7996-8006.

Bento, C. F., Renna, M., Ghislat, G., Puri, C., Ashkenazi, A., Vicinanza, M., . . . Rubinsztein, D. C. (2016). Mammalian Autophagy: How Does It Work? *Annu Rev Biochem, 85*, 685-713. doi:10.1146/annurev-biochem-060815-014556

Bertolotto, C., Abbe, P., Hemesath, T. J., Bille, K., Fisher, D. E., Ortonne, J. P., & Ballotti, R. (1998). Microphthalmia gene product as a signal transducer in cAMP-induced differentiation of melanocytes. *J Cell Biol, 142*(3), 827-835.

Bertolotto, C., Lesueur, F., Giuliano, S., Strub, T., de Lichy, M., Bille, K., . . . Bressac-de Paillerets, B. (2011). A SUMOylation-defective MITF germline mutation predisposes to melanoma and renal carcinoma. *Nature, 480*(7375), 94-98. doi:10.1038/nature10539

Betschinger, J., Nichols, J., Dietmann, S., Corrin, P. D., Paddison, P. J., & Smith, A. (2013). Exit from pluripotency is gated by intracellular redistribution of the bHLH transcription factor Tfe3. *Cell, 153*(2), 335-347. doi:10.1016/j.cell.2013.03.012

Bismuth, K., Maric, D., & Arnheiter, H. (2005). MITF and cell proliferation: the role of alternative splice forms. *Pigment Cell Res, 18*(5), 349-359. doi:10.1111/j.1600-0749.2005.00249.x

Bollag, G., Hirth, P., Tsai, J., Zhang, J., Ibrahim, P. N., Cho, H., . . . Nolop, K. (2010). Clinical efficacy of a RAF inhibitor needs broad target blockade in BRAF-mutant melanoma. *Nature, 467*(7315), 596-599. doi:10.1038/nature09454

Borovanský, J., & Riley, P. A. (2011). *Melanins and melanosomes : biosynthesis, biogenesis, physiological, and pathological functions*. Weinheim: Wiley-Blackwell.

Braman, J., Papworth, C., & Greener, A. (1996). Site-directed mutagenesis using double-stranded plasmid DNA templates. *Methods Mol Biol, 57*, 31-44. doi:10.1385/0-89603-332-5:31

Bronisz, A., Carey, H. A., Godlewski, J., Sif, S., Ostrowski, M. C., & Sharma, S. M. (2014). The multifunctional protein fused in sarcoma (FUS) is a coactivator of microphthalmia-associated transcription factor (MITF). *J Biol Chem, 289*(1), 326-334. doi:10.1074/jbc.M113.493874

Brown, E. J., Albers, M. W., Shin, T. B., Ichikawa, K., Keith, C. T., Lane, W. S., & Schreiber, S. L. (1994). A mammalian protein targeted by G1-arresting rapamycin-receptor complex. *Nature, 369*(6483), 756-758. doi:10.1038/369756a0

Brown, J. H., Cohen, C., & Parry, D. A. (1996). Heptad breaks in alpha-helical coiled coils: stutters and stammers. *Proteins, 26*(2), 134-145. doi:10.1002/(SICI)1097-0134(199610)26:2<134::AID-PROT3>3.0.CO;2-G

Burke, P., Schooler, K., & Wiley, H. S. (2001). Regulation of epidermal growth factor receptor signaling by endocytosis and intracellular trafficking. *Mol Biol Cell, 12*(6), 1897-1910.

Cancer Genome Atlas, N. (2015). Genomic Classification of Cutaneous Melanoma. *Cell, 161*(7), 1681-1696. doi:10.1016/j.cell.2015.05.044

Carr, J., & Mackie, R. M. (1994). Point mutations in the N-ras oncogene in malignant melanoma and congenital naevi. *Br J Dermatol, 131*(1), 72-77.

Carreira, S., Goodall, J., Aksan, I., La Rocca, S. A., Galibert, M. D., Denat, L., . . . Goding, C. R. (2005). Mitf cooperates with Rb1 and activates p21Cip1 expression to regulate cell cycle progression. *Nature, 433*(7027), 764-769. doi:10.1038/nature03269

Carriere, A., Romeo, Y., Acosta-Jaquez, H. A., Moreau, J., Bonneil, E., Thibault, P., . . . Roux, P. P. (2011). ERK1/2 phosphorylate Raptor to promote Ras-dependent activation of mTOR complex 1 (mTORC1). *J Biol Chem, 286*(1), 567-577. doi:10.1074/jbc.M110.159046

Caviston, J. P., Zajac, A. L., Tokito, M., & Holzbaur, E. L. (2011). Huntingtin coordinates the dynein-mediated dynamic positioning of endosomes and lysosomes. *Mol Biol Cell, 22*(4), 478-492. doi:10.1091/mbc.E10-03-0233

Chapman, P. B., Hauschild, A., Robert, C., Haanen, J. B., Ascierto, P., Larkin, J., . . . Grp, B.-S. (2011). Improved Survival with Vemurafenib in Melanoma with BRAF V600E Mutation. *New England Journal of Medicine, 364*(26), 2507-2516. doi:10.1056/NEJMoa1103782

Charbel, C., Fontaine, R. H., Malouf, G. G., Picard, A., Kadlub, N., El-Murr, N., . . . Guegan, S. (2014). NRAS mutation is the sole recurrent somatic mutation in large congenital melanocytic nevi. *J Invest Dermatol, 134*(4), 1067-1074. doi:10.1038/jid.2013.429

Cheli, Y., Giuliano, S., Botton, T., Rocchi, S., Hofman, V., Hofman, P., . . . Ballotti, R. (2011). Mitf is the key molecular switch between mouse or human melanoma initiating cells and their differentiated progeny. *Oncogene, 30*(20), 2307-2318. doi:10.1038/onc.2010.598

Chong, H., & Guan, K. L. (2003). Regulation of Raf through phosphorylation and N terminus-C terminus interaction. *J Biol Chem, 278*(38), 36269-36276. doi:10.1074/jbc.M212803200

Chung, C. D., Liao, J., Liu, B., Rao, X., Jay, P., Berta, P., & Shuai, K. (1997). Specific inhibition of Stat3 signal transduction by PIAS3. *Science, 278*(5344), 1803-1805.

Cichorek, M., Wachulska, M., Stasiewicz, A., & Tyminska, A. (2013). Skin melanocytes: biology and development. *Postepy Dermatol Alergol, 30*(1), 30-41. doi:10.5114/pdia.2013.33376

Clark, W. H., Jr., From, L., Bernardino, E. A., & Mihm, M. C. (1969). The histogenesis and biologic behavior of primary human malignant melanomas of the skin. *Cancer Res, 29*(3), 705-727.

Cook, A. L., Donatien, P. D., Smith, A. G., Murphy, M., Jones, M. K., Herlyn, M., . . . Sturm, R. A. (2003). Human melanoblasts in culture: expression of BRN2 and synergistic regulation by fibroblast growth factor-2, stem cell factor, and endothelin-3. *J Invest Dermatol, 121*(5), 1150-1159. doi:10.1046/j.1523-1747.2003.12562.x

Cronin, J. C., Wunderlich, J., Loftus, S. K., Prickett, T. D., Wei, X., Ridd, K., . . . Samuels, Y. (2009). Frequent mutations in the MITF pathway in melanoma. *Pigment Cell Melanoma Res, 22*(4), 435-444. doi:10.1111/j.1755-148X.2009.00578.x

Cui, R., Widlund, H. R., Feige, E., Lin, J. Y., Wilensky, D. L., Igras, V. E., . . . Fisher, D. E. (2007). Central role of p53 in the suntan response and pathologic hyperpigmentation. *Cell, 128*(5), 853-864. doi:10.1016/j.cell.2006.12.045

Cutler, R. E., Jr., Stephens, R. M., Saracino, M. R., & Morrison, D. K. (1998). Autoregulation of the Raf-1 serine/threonine kinase. *Proc Natl Acad Sci U S A, 95*(16), 9214-9219.

Damsky, W., Micevic, G., Meeth, K., Muthusamy, V., Curley, D. P., Santhanakrishnan, M., . . . Bosenberg, M. (2015). mTORC1 activation blocks BrafV600E-induced growth arrest but is insufficient for melanoma formation. *Cancer Cell, 27*(1), 41-56. doi:10.1016/j.ccell.2014.11.014

Dang, C. V. (2012). MYC on the path to cancer. *Cell, 149*(1), 22-35. doi:10.1016/j.cell.2012.03.003

Dankort, D., Curley, D. P., Cartlidge, R. A., Nelson, B., Karnezis, A. N., Damsky, W. E., Jr., . . . Bosenberg, M. (2009). Braf(V600E) cooperates with Pten loss to induce metastatic melanoma. *Nat Genet, 41*(5), 544-552. doi:10.1038/ng.356

Davies, H., Bignell, G. R., Cox, C., Stephens, P., Edkins, S., Clegg, S., . . . Futreal, P. A. (2002). Mutations of the BRAF gene in human cancer. *Nature, 417*(6892), 949-954. doi:10.1038/nature00766

Davis, I. J., Kim, J. J., Ozsolak, F., Widlund, H. R., Rozenblatt-Rosen, O., Granter, S. R., . . . Fisher, D. E. (2006). Oncogenic MITF dysregulation in clear cell sarcoma: defining the MiT family of human cancers. *Cancer Cell, 9*(6), 473-484. doi:10.1016/j.ccr.2006.04.021

de la Serna, I. L., Ohkawa, Y., Higashi, C., Dutta, C., Osias, J., Kommajosyula, N., . . . Imbalzano, A. N. (2006). The microphthalmia-associated transcription factor requires SWI/SNF enzymes to activate melanocyte-specific genes. *J Biol Chem, 281*(29), 20233-20241. doi:10.1074/jbc.M512052200

Dhomen, N., Reis-Filho, J. S., da Rocha Dias, S., Hayward, R., Savage, K., Delmas, V., . . . Marais, R. (2009). Oncogenic Braf induces melanocyte senescence and melanoma in mice. *Cancer Cell, 15*(4), 294-303. doi:10.1016/j.ccr.2009.02.022

Dibble, C. C., & Manning, B. D. (2013). Signal integration by mTORC1 coordinates nutrient input with biosynthetic output. *Nat Cell Biol, 15*(6), 555-564. doi:10.1038/ncb2763

Dozynkiewicz, M. A., Jamieson, N. B., Macpherson, I., Grindlay, J., van den Berghe, P. V., von Thun, A., . . . Norman, J. C. (2012). Rab25 and CLIC3 collaborate to promote integrin recycling from late endosomes/lysosomes and drive cancer progression. *Dev Cell, 22*(1), 131-145. doi:10.1016/j.devcel.2011.11.008

Du, J., Miller, A. J., Widlund, H. R., Horstmann, M. A., Ramaswamy, S., & Fisher, D. E. (2003). MLANA/MART1 and SILV/PMEL17/GP100 are

transcriptionally regulated by MITF in melanocytes and melanoma. *Am J Pathol, 163*(1), 333-343. doi:10.1016/S0002-9440(10)63657-7

Dubreuil, P., Forrester, L., Rottapel, R., Reedijk, M., Fujita, J., & Bernstein, A. (1991). The c-fms gene complements the mitogenic defect in mast cells derived from mutant W mice but not mi (microphthalmia) mice. *Proc Natl Acad Sci U S A, 88*(6), 2341-2345.

Dunn, K. J., Brady, M., Ochsenbauer-Jambor, C., Snyder, S., Incao, A., & Pavan, W. J. (2005). WNT1 and WNT3a promote expansion of melanocytes through distinct modes of action. *Pigment Cell Res, 18*(3), 167-180. doi:10.1111/j.1600-0749.2005.00226.x

Dyachok, J., Earnest, S., Iturraran, E. N., Cobb, M. H., & Ross, E. M. (2016). Amino Acids Regulate mTORC1 by an Obligate Two-step Mechanism. *J Biol Chem, 291*(43), 22414-22426. doi:10.1074/jbc.M116.732511

Elder, D. E. (2016). Melanoma progression. *Pathology, 48*(2), 147-154. doi:10.1016/j.pathol.2015.12.002

Emuss, V., Garnett, M., Mason, C., & Marais, R. (2005). Mutations of C-RAF are rare in human cancer because C-RAF has a low basal kinase activity compared with B-RAF. *Cancer Res, 65*(21), 9719-9726. doi:10.1158/0008-5472.CAN-05-1683

Erie, C., Sacino, M., Houle, L., Lu, M. L., & Wei, J. (2015). Altered lysosomal positioning affects lysosomal functions in a cellular model of Huntington's disease. *Eur J Neurosci, 42*(3), 1941-1951. doi:10.1111/ejn.12957

Falletta, P., Sanchez-Del-Campo, L., Chauhan, J., Effern, M., Kenyon, A., Kershaw, C. J., . . . Goding, C. R. (2017). Translation reprogramming is an evolutionarily conserved driver of phenotypic plasticity and therapeutic resistance in melanoma. *Genes Dev, 31*(1), 18-33. doi:10.1101/gad.290940.116

Fan, Y., Lu, H., Liang, W., Garcia-Barrio, M. T., Guo, Y., Zhang, J., . . . Chen, Y. E. (2018). Endothelial TFEB Positively Regulates Post-Ischemic Angiogenesis. *Circ Res*. doi:10.1161/CIRCRESAHA.118.312672

Farnham, P. J. (2009). Insights from genomic profiling of transcription factors. *Nat Rev Genet, 10*(9), 605-616. doi:10.1038/nrg2636

Feige, E., Yokoyama, S., Levy, C., Khaled, M., Igras, V., Lin, R. J., . . . Fisher, D. E. (2011). Hypoxia-induced transcriptional repression of the melanoma-associated oncogene MITF. *Proc Natl Acad Sci U S A, 108*(43), E924-933. doi:10.1073/pnas.1106351108

Fell, G. L., Robinson, K. C., Mao, J., Woolf, C. J., & Fisher, D. E. (2014). Skin beta-endorphin mediates addiction to UV light. *Cell, 157*(7), 1527-1534. doi:10.1016/j.cell.2014.04.032

Ferron, M., Settembre, C., Shimazu, J., Lacombe, J., Kato, S., Rawlings, D. J., . . . Karsenty, G. (2013). A RANKL-PKCbeta-TFEB signaling cascade is necessary for lysosomal biogenesis in osteoclasts. *Genes Dev, 27*(8), 955-969. doi:10.1101/gad.213827.113

Fields, S., & Jang, S. K. (1990). Presence of a potent transcription activating sequence in the p53 protein. *Science, 249*(4972), 1046-1049.

Flaherty, K. T., Puzanov, I., Kim, K. B., Ribas, A., McArthur, G. A., Sosman, J. A., . . . Chapman, P. B. (2010). Inhibition of Mutated, Activated BRAF in Metastatic Melanoma. *New England Journal of Medicine, 363*(9), 809-819. doi:DOI 10.1056/NEJMoa1002011

Fock, V., Gudmundsson, S. R., Gunnlaugsson, H. O., Stefansson, J. A., Ionasz, V., Schepsky, A., . . . Steingrimsson, E. (2018). Subcellular localization and stability of MITF are modulated by the bHLH-Zip domain. *Pigment Cell Melanoma Res*. doi:10.1111/pcmr.12721

Forbes, S. A., Bhamra, G., Bamford, S., Dawson, E., Kok, C., Clements, J., . . . Stratton, M. R. (2008). The Catalogue of Somatic Mutations in Cancer (COSMIC). *Curr Protoc Hum Genet, Chapter 10*, Unit 10 11. doi:10.1002/0471142905.hg1011s57

Fox, H. L., Pham, P. T., Kimball, S. R., Jefferson, L. S., & Lynch, C. J. (1998). Amino acid effects on translational repressor 4E-BP1 are mediated primarily by L-leucine in isolated adipocytes. *Am J Physiol, 275*(5 Pt 1), C1232-1238.

Frandberg, P. A., Doufexis, M., Kapas, S., & Chhajlani, V. (1998). Human pigmentation phenotype: a point mutation generates nonfunctional MSH receptor. *Biochem Biophys Res Commun, 245*(2), 490-492. doi:10.1006/bbrc.1998.8459

Fujimoto, Y., Nakagawa, Y., Satoh, A., Okuda, K., Shingyouchi, A., Naka, A., . . . Shimano, H. (2013). TFE3 controls lipid metabolism in adipose tissue of male mice by suppressing lipolysis and thermogenesis. *Endocrinology, 154*(10), 3577-3588. doi:10.1210/en.2013-1203

Gao, X., Simon, K. C., Han, J., Schwarzschild, M. A., & Ascherio, A. (2009). Family history of melanoma and Parkinson disease risk. *Neurology, 73*(16), 1286-1291. doi:10.1212/WNL.0b013e3181bd13a1

Garcia-Fernandez, M., Karras, P., Checinska, A., Canon, E., Calvo, G. T., Gomez-Lopez, G., . . . Soengas, M. S. (2016). Metastatic risk and resistance to BRAF inhibitors in melanoma defined by selective allelic loss of ATG5. *Autophagy, 12*(10), 1776-1790. doi:10.1080/15548627.2016.1199301

Garraway, L. A., Widlund, H. R., Rubin, M. A., Getz, G., Berger, A. J., Ramaswamy, S., . . . Sellers, W. R. (2005). Integrative genomic analyses identify MITF as a lineage survival oncogene amplified in

malignant melanoma. *Nature, 436*(7047), 117-122. doi:10.1038/nature03664

Geng, J., & Klionsky, D. J. (2008). The Atg8 and Atg12 ubiquitin-like conjugation systems in macroautophagy. 'Protein modifications: beyond the usual suspects' review series. *EMBO Rep, 9*(9), 859-864. doi:10.1038/embor.2008.163

George, A., Zand, D. J., Hufnagel, R. B., Sharma, R., Sergeev, Y. V., Legare, J. M., . . . Brooks, B. P. (2016). Biallelic Mutations in MITF Cause Coloboma, Osteopetrosis, Microphthalmia, Macrocephaly, Albinism, and Deafness. *Am J Hum Genet, 99*(6), 1388-1394. doi:10.1016/j.ajhg.2016.11.004

Gibney, G. T., & Zager, J. S. (2013). Clinical development of dabrafenib in BRAF mutant melanoma and other malignancies. *Expert Opin Drug Metab Toxicol, 9*(7), 893-899. doi:10.1517/17425255.2013.794220

Gibson, D. G., Young, L., Chuang, R. Y., Venter, J. C., Hutchison, C. A., 3rd, & Smith, H. O. (2009). Enzymatic assembly of DNA molecules up to several hundred kilobases. *Nat Methods, 6*(5), 343-345. doi:10.1038/nmeth.1318

Giuliano, S., Cheli, Y., Ohanna, M., Bonet, C., Beuret, L., Bille, K., . . . Bertolotto, C. (2010). Microphthalmia-Associated Transcription Factor Controls the DNA Damage Response and a Lineage-Specific Senescence Program in Melanomas. *Cancer Research, 70*(9), 3813-3822. doi:10.1158/0008-5472.Can-09-2913

Goding, C. R. (2011). Commentary. A picture of Mitf in melanoma immortality. *Oncogene, 30*(20), 2304-2306. doi:10.1038/onc.2010.641

Gogas, H. J., Kirkwood, J. M., & Sondak, V. K. (2007). Chemotherapy for metastatic melanoma: time for a change? *Cancer, 109*(3), 455-464. doi:10.1002/cncr.22427

Gokal, P. K., Cavanaugh, A. H., & Thompson, E. A., Jr. (1986). The effects of cycloheximide upon transcription of rRNA, 5 S RNA, and tRNA genes. *J Biol Chem, 261*(6), 2536-2541.

Goodall, J., Carreira, S., Denat, L., Kobi, D., Davidson, I., Nuciforo, P., . . . Goding, C. R. (2008). Brn-2 represses microphthalmia-associated transcription factor expression and marks a distinct subpopulation of microphthalmia-associated transcription factor-negative melanoma cells. *Cancer Res, 68*(19), 7788-7794. doi:10.1158/0008-5472.CAN-08-1053

Grill, C., Bergsteinsdottir, K., Ogmundsdottir, M. H., Pogenberg, V., Schepsky, A., Wilmanns, M., . . . Steingrimsson, E. (2013). MITF mutations associated with pigment deficiency syndromes and melanoma have

different effects on protein function. *Hum Mol Genet, 22*(21), 4357-4367. doi:10.1093/hmg/ddt285

Hachiya, A., Sriwiriyanont, P., Kobayashi, T., Nagasawa, A., Yoshida, H., Ohuchi, A., . . . Boissy, R. E. (2009). Stem cell factor-KIT signalling plays a pivotal role in regulating pigmentation in mammalian hair. *J Pathol, 218*(1), 30-39. doi:10.1002/path.2503

Hah, Y. S., Cho, H. Y., Lim, T. Y., Park, D. H., Kim, H. M., Yoon, J., . . . Yoon, T. J. (2012). Induction of melanogenesis by rapamycin in human MNT-1 melanoma cells. *Ann Dermatol, 24*(2), 151-157. doi:10.5021/ad.2012.24.2.151

Hailey, D. W., Rambold, A. S., Satpute-Krishnan, P., Mitra, K., Sougrat, R., Kim, P. K., & Lippincott-Schwartz, J. (2010). Mitochondria supply membranes for autophagosome biogenesis during starvation. *Cell, 141*(4), 656-667. doi:10.1016/j.cell.2010.04.009

Halaban, R., Patton, R. S., Cheng, E., Svedine, S., Trombetta, E. S., Wahl, M. L., . . . Hebert, D. N. (2002). Abnormal acidification of melanoma cells induces tyrosinase retention in the early secretory pathway. *J Biol Chem, 277*(17), 14821-14828. doi:10.1074/jbc.M111497200

Hallsson, J. H., Favor, J., Hodgkinson, C., Glaser, T., Lamoreux, M. L., Magnusdottir, R., . . . Steingrimsson, E. (2000). Genomic, transcriptional and mutational analysis of the mouse microphthalmia locus. *Genetics, 155*(1), 291-300.

Han, R., Bansal, D., Miyake, K., Muniz, V. P., Weiss, R. M., McNeil, P. L., & Campbell, K. P. (2007). Dysferlin-mediated membrane repair protects the heart from stress-induced left ventricular injury. *J Clin Invest, 117*(7), 1805-1813. doi:10.1172/JCI30848

Haq, R., & Fisher, D. E. (2011). Biology and Clinical Relevance of the Micropthalmia Family of Transcription Factors in Human Cancer. *Journal of Clinical Oncology, 29*(25), 3474-3482. doi:10.1200/Jco.2010.32.6223

Hara, K., Maruki, Y., Long, X., Yoshino, K., Oshiro, N., Hidayat, S., . . . Yonezawa, K. (2002). Raptor, a binding partner of target of rapamycin (TOR), mediates TOR action. *Cell, 110*(2), 177-189.

Hara, K., Yonezawa, K., Weng, Q. P., Kozlowski, M. T., Belham, C., & Avruch, J. (1998). Amino acid sufficiency and mTOR regulate p70 S6 kinase and eIF-4E BP1 through a common effector mechanism. *J Biol Chem, 273*(23), 14484-14494.

Hauschild, A., Grob, J. J., Demidov, L. V., Jouary, T., Gutzmer, R., Millward, M., . . . Chapman, P. B. (2012). Dabrafenib in BRAF-mutated metastatic melanoma: a multicentre, open-label, phase 3 randomised

controlled trial. *Lancet, 380*(9839), 358-365. doi:10.1016/S0140-6736(12)60868-X

Hay, N., & Sonenberg, N. (2004). Upstream and downstream of mTOR. *Genes Dev, 18*(16), 1926-1945. doi:10.1101/gad.1212704

Heitman, J., Movva, N. R., & Hall, M. N. (1991). Targets for cell cycle arrest by the immunosuppressant rapamycin in yeast. *Science, 253*(5022), 905-909.

Hemesath, T. J., Price, E. R., Takemoto, C., Badalian, T., & Fisher, D. E. (1998). MAP kinase links the transcription factor Microphthalmia to c-Kit signalling in melanocytes. *Nature, 391*(6664), 298-301. doi:10.1038/34681

Hemesath, T. J., Steingrimsson, E., McGill, G., Hansen, M. J., Vaught, J., Hodgkinson, C. A., . . . Fisher, D. E. (1994). microphthalmia, a critical factor in melanocyte development, defines a discrete transcription factor family. *Genes Dev, 8*(22), 2770-2780.

Hershey, C. L., & Fisher, D. E. (2004). Mitf and Tfe3: members of a b-HLH-ZIP transcription factor family essential for osteoclast development and function. *Bone, 34*(4), 689-696. doi:10.1016/j.bone.2003.08.014

Hershey, C. L., & Fisher, D. E. (2005). Genomic analysis of the Microphthalmia locus and identification of the MITF-J/Mitf-J isoform. *Gene, 347*(1), 73-82. doi:10.1016/j.gene.2004.12.002

Hertwig, P. (1942). Neue Mutationen und Kopplungsgruppen bei der Hausmaus. *Z. Indukt. Abstammungs- u. Vererbungsl, 80*, 220–246.

Hikata, T., Takaishi, H., Takito, J., Hakozaki, A., Furukawa, M., Uchikawa, S., . . . Toyama, Y. (2009). PIAS3 negatively regulates RANKL-mediated osteoclastogenesis directly in osteoclast precursors and indirectly via osteoblasts. *Blood, 113*(10), 2202-2212. doi:10.1182/blood-2008-06-162594

Hingorani, S. R., Jacobetz, M. A., Robertson, G. P., Herlyn, M., & Tuveson, D. A. (2003). Suppression of BRAF(V599E) in human melanoma abrogates transformation. *Cancer Res, 63*(17), 5198-5202.

Hodgkinson, C. A., Moore, K. J., Nakayama, A., Steingrimsson, E., Copeland, N. G., Jenkins, N. A., & Arnheiter, H. (1993). Mutations at the mouse microphthalmia locus are associated with defects in a gene encoding a novel basic-helix-loop-helix-zipper protein. *Cell, 74*(2), 395-404.

Hodi, F. S., O'Day, S. J., McDermott, D. F., Weber, R. W., Sosman, J. A., Haanen, J. B., . . . Urba, W. J. (2010). Improved survival with ipilimumab in patients with metastatic melanoma. *N Engl J Med, 363*(8), 711-723. doi:10.1056/NEJMoa1003466

Hodis, E., Watson, I. R., Kryukov, G. V., Arold, S. T., Imielinski, M., Theurillat, J. P., . . . Chin, L. (2012). A landscape of driver mutations in melanoma. *Cell, 150*(2), 251-263. doi:10.1016/j.cell.2012.06.024

Hoek, K. S., & Goding, C. R. (2010). Cancer stem cells versus phenotype-switching in melanoma. *Pigment Cell Melanoma Res, 23*(6), 746-759. doi:10.1111/j.1755-148X.2010.00757.x

Hoek, K. S., Schlegel, N. C., Eichhoff, O. M., Widmer, D. S., Praetorius, C., Einarsson, S. O., . . . Steingrimsson, E. (2008). Novel MITF targets identified using a two-step DNA microarray strategy. *Pigment Cell Melanoma Res, 21*(6), 665-676. doi:10.1111/j.1755-148X.2008.00505.x

Hong, S. B., Oh, H., Valera, V. A., Baba, M., Schmidt, L. S., & Linehan, W. M. (2010). Inactivation of the FLCN tumor suppressor gene induces TFE3 transcriptional activity by increasing its nuclear localization. *PLoS One, 5*(12), e15793. doi:10.1371/journal.pone.0015793

Hosokawa, N., Hara, T., Kaizuka, T., Kishi, C., Takamura, A., Miura, Y., . . . Mizushima, N. (2009). Nutrient-dependent mTORC1 association with the ULK1-Atg13-FIP200 complex required for autophagy. *Mol Biol Cell, 20*(7), 1981-1991. doi:10.1091/mbc.E08-12-1248

http://cancergenome.nih.gov/.

Huan, C., Kelly, M. L., Steele, R., Shapira, I., Gottesman, S. R., & Roman, C. A. (2006). Transcription factors TFE3 and TFEB are critical for CD40 ligand expression and thymus-dependent humoral immunity. *Nat Immunol, 7*(10), 1082-1091. doi:10.1038/ni1378

Huang da, W., Sherman, B. T., & Lempicki, R. A. (2009a). Bioinformatics enrichment tools: paths toward the comprehensive functional analysis of large gene lists. *Nucleic Acids Res, 37*(1), 1-13. doi:10.1093/nar/gkn923

Huang da, W., Sherman, B. T., & Lempicki, R. A. (2009b). Systematic and integrative analysis of large gene lists using DAVID bioinformatics resources. *Nat Protoc, 4*(1), 44-57. doi:10.1038/nprot.2008.211

Huang, Z. M., Chinen, M., Chang, P. J., Xie, T., Zhong, L., Demetriou, S., . . . Wei, M. L. (2012). Targeting protein-trafficking pathways alters melanoma treatment sensitivity. *Proc Natl Acad Sci U S A, 109*(2), 553-558. doi:10.1073/pnas.1118366109

Huber, W. E., Price, E. R., Widlund, H. R., Du, J., Davis, I. J., Wegner, M., & Fisher, D. E. (2003). A tissue-restricted cAMP transcriptional response: SOX10 modulates alpha-melanocyte-stimulating hormone-triggered expression of microphthalmia-associated transcription factor in melanocytes. *J Biol Chem, 278*(46), 45224-45230. doi:10.1074/jbc.M309036200

Hughes, A. E., Newton, V. E., Liu, X. Z., & Read, A. P. (1994). A gene for Waardenburg syndrome type 2 maps close to the human homologue of the microphthalmia gene at chromosome 3p12-p14.1. *Nat Genet, 7*(4), 509-512. doi:10.1038/ng0894-509

Hughes, M. J., Lingrel, J. B., Krakowsky, J. M., & Anderson, K. P. (1993). A helix-loop-helix transcription factor-like gene is located at the mi locus. *J Biol Chem, 268*(28), 20687-20690.

Itakura, E., & Mizushima, N. (2010). Characterization of autophagosome formation site by a hierarchical analysis of mammalian Atg proteins. *Autophagy, 6*(6), 764-776.

Itoh, T., Fujita, N., Kanno, E., Yamamoto, A., Yoshimori, T., & Fukuda, M. (2008). Golgi-resident small GTPase Rab33B interacts with Atg16L and modulates autophagosome formation. *Mol Biol Cell, 19*(7), 2916-2925. doi:10.1091/mbc.E07-12-1231

Iwasaki, H., Naka, A., Iida, K. T., Nakagawa, Y., Matsuzaka, T., Ishii, K. A., . . . Shimano, H. (2012). TFE3 regulates muscle metabolic gene expression, increases glycogen stores, and enhances insulin sensitivity in mice. *Am J Physiol Endocrinol Metab, 302*(7), E896-902. doi:10.1152/ajpendo.00204.2011

Jacinto, E., Loewith, R., Schmidt, A., Lin, S., Ruegg, M. A., Hall, A., & Hall, M. N. (2004). Mammalian TOR complex 2 controls the actin cytoskeleton and is rapamycin insensitive. *Nat Cell Biol, 6*(11), 1122-1128. doi:10.1038/ncb1183

Jackson, I. J., Chambers, D. M., Budd, P. S., & Johnson, R. (1991). The Tyrosinase-Related Protein-1 Gene Has a Structure and Promoter Sequence Very Different from Tyrosinase. *Nucleic Acids Research, 19*(14), 3799-3804. doi:DOI 10.1093/nar/19.14.3799

Jin, E. J., Erickson, C. A., Takada, S., & Burrus, L. W. (2001). Wnt and BMP signaling govern lineage segregation of melanocytes in the avian embryo. *Dev Biol, 233*(1), 22-37. doi:10.1006/dbio.2001.0222

Jin, S., DiPaola, R. S., Mathew, R., & White, E. (2007). Metabolic catastrophe as a means to cancer cell death. *J Cell Sci, 120*(Pt 3), 379-383. doi:10.1242/jcs.03349

Jones, S. (2004). An overview of the basic helix-loop-helix proteins. *Genome Biol, 5*(6), 226. doi:10.1186/gb-2004-5-6-226

Kabeya, Y., Mizushima, N., Ueno, T., Yamamoto, A., Kirisako, T., Noda, T., . . . Yoshimori, T. (2000). LC3, a mammalian homologue of yeast Apg8p, is localized in autophagosome membranes after processing. *EMBO J, 19*(21), 5720-5728. doi:10.1093/emboj/19.21.5720

Kansler, E. R., Verma, A., Langdon, E. M., Simon-Vermot, T., Yin, A., Lee, W., . . . White, R. M. (2017). Melanoma genome evolution across species. *BMC Genomics, 18*(1), 136. doi:10.1186/s12864-017-3518-8

Karafiat, V., Dvorakova, M., Pajer, P., Cermak, V., & Dvorak, M. (2007). Melanocyte fate in neural crest is triggered by Myb proteins through activation of c-kit. *Cell Mol Life Sci, 64*(22), 2975-2984. doi:10.1007/s00018-007-7330-5

Kirisako, T., Ichimura, Y., Okada, H., Kabeya, Y., Mizushima, N., Yoshimori, T., . . . Ohsumi, Y. (2000). The reversible modification regulates the membrane-binding state of Apg8/Aut7 essential for autophagy and the cytoplasm to vacuole targeting pathway. *J Cell Biol, 151*(2), 263-276.

Komatsu, M., Waguri, S., Koike, M., Sou, Y., Ueno, T., Hara, T., . . . Tanaka, K. (2007). Homeostatic levels of p62 control cytoplasmic inclusion body formation in autophagy-deficient mice. *Cell, 131*(6), 1149-1163. doi:10.1016/j.cell.2007.10.035

Konstantinopoulos, P. A., & Papavassiliou, A. G. (2011). Seeing the Future of Cancer-Associated Transcription Factor Drug Targets. *Jama-Journal of the American Medical Association, 305*(22), 2349-2350. doi:10.1001/jama.2011.727

Kubic, J. D., Mascarenhas, J. B., Iizuka, T., Wolfgeher, D., & Lang, D. (2012). GSK-3 promotes cell survival, growth, and PAX3 levels in human melanoma cells. *Mol Cancer Res, 10*(8), 1065-1076. doi:10.1158/1541-7786.MCR-11-0387

Kuiper, R. P., Schepens, M., Thijssen, J., van Asseldonk, M., van den Berg, E., Bridge, J., . . . van Kessel, A. G. (2003). Upregulation of the transcription factor TFEB in t(6;11)(p21;q13)-positive renal cell carcinomas due to promoter substitution. *Hum Mol Genet, 12*(14), 1661-1669.

Kushimoto, T., Valencia, J. C., Costin, G. E., Toyofuku, K., Watabe, H., Yasumoto, K., . . . Hearing, V. J. (2003). The Seiji memorial lecture: the melanosome: an ideal model to study cellular differentiation. *Pigment Cell Res, 16*(3), 237-244.

Laker, R. C., Drake, J. C., Wilson, R. J., Lira, V. A., Lewellen, B. M., Ryall, K. A., . . . Yan, Z. (2017). Ampk phosphorylation of Ulk1 is required for targeting of mitochondria to lysosomes in exercise-induced mitophagy. *Nat Commun, 8*(1), 548. doi:10.1038/s41467-017-00520-9

Landsberg, J., Kohlmeyer, J., Renn, M., Bald, T., Rogava, M., Cron, M., . . . Tuting, T. (2012). Melanomas resist T-cell therapy through inflammation-induced reversible dedifferentiation. *Nature, 490*(7420), 412-+. doi:10.1038/nature11538

Larue, L., Kumasaka, M., & Goding, C. R. (2003). Beta-catenin in the melanocyte lineage. *Pigment Cell Res, 16*(3), 312-317.

Laurette, P., Strub, T., Koludrovic, D., Keime, C., Le Gras, S., Seberg, H., . . . Davidson, I. (2015). Transcription factor MITF and remodeller BRG1 define chromatin organisation at regulatory elements in melanoma cells. *Elife, 4*. doi:10.7554/eLife.06857

Law, B. K. (2005). Rapamycin: an anti-cancer immunosuppressant? *Crit Rev Oncol Hematol, 56*(1), 47-60. doi:10.1016/j.critrevonc.2004.09.009

Lazova, R., Klump, V., & Pawelek, J. (2010). Autophagy in cutaneous malignant melanoma. *J Cutan Pathol, 37*(2), 256-268. doi:10.1111/j.1600-0560.2009.01359.x

Lazova, R., & Pawelek, J. M. (2009). Why do melanomas get so dark? *Experimental Dermatology, 18*(11), 934-938. doi:10.1111/j.1600-0625.2009.00933.x

Lee, S., Sato, Y., & Nixon, R. A. (2011). Lysosomal proteolysis inhibition selectively disrupts axonal transport of degradative organelles and causes an Alzheimer's-like axonal dystrophy. *J Neurosci, 31*(21), 7817-7830. doi:10.1523/JNEUROSCI.6412-10.2011

Leiter, U., Eigentler, T., & Garbe, C. (2014). Epidemiology of skin cancer. *Adv Exp Med Biol, 810*, 120-140.

Levy, C., Khaled, M., & Fisher, D. E. (2006). MITF: master regulator of melanocyte development and melanoma oncogene. *Trends Mol Med, 12*(9), 406-414. doi:10.1016/j.molmed.2006.07.008

Levy, C., Sonnenblick, A., & Razin, E. (2003). Role played by microphthalmia transcription factor phosphorylation and its Zip domain in its transcriptional inhibition by PIAS3. *Mol Cell Biol, 23*(24), 9073-9080.

Liang, C. Y., Lee, J. S., Inn, K. S., Gack, M. U., Li, Q. L., Roberts, E. A., . . . Jung, J. U. (2008). Beclin1-binding UVRAG targets the class C Vps complex to coordinate autophagosome maturation and endocytic trafficking. *Nature Cell Biology, 10*(7), 776-787. doi:10.1038/ncb1740

Liang, X. H., Jackson, S., Seaman, M., Brown, K., Kempkes, B., Hibshoosh, H., & Levine, B. (1999). Induction of autophagy and inhibition of tumorigenesis by beclin 1. *Nature, 402*(6762), 672-676. doi:10.1038/45257

Lin, J., Handschin, C., & Spiegelman, B. M. (2005). Metabolic control through the PGC-1 family of transcription coactivators. *Cell Metab, 1*(6), 361-370. doi:10.1016/j.cmet.2005.05.004

Lin, W. W., & Hsu, Y. W. (2000). Cycloheximide-induced cPLA(2) activation is via the MKP-1 down-regulation and ERK activation. *Cell Signal, 12*(7), 457-461.

Liu, F., Fu, Y., & Meyskens, F. L., Jr. (2009). MiTF regulates cellular response to reactive oxygen species through transcriptional regulation of APE-1/Ref-1. *J Invest Dermatol, 129*(2), 422-431. doi:10.1038/jid.2008.255

Livak, K. J., & Schmittgen, T. D. (2001). Analysis of relative gene expression data using real-time quantitative PCR and the 2(-Delta Delta C(T)) Method. *Methods, 25*(4), 402-408. doi:10.1006/meth.2001.1262

Lu, S. Y., Wan, H. C., Li, M., & Lin, Y. L. (2010). Subcellular localization of Mitf in monocytic cells. *Histochem Cell Biol, 133*(6), 651-658. doi:10.1007/s00418-010-0703-0

Luo, C., Merz, P. R., Chen, Y., Dickes, E., Pscherer, A., Schadendorf, D., & Eichmuller, S. B. (2013). MiR-101 inhibits melanoma cell invasion and proliferation by targeting MITF and EZH2. *Cancer Lett, 341*(2), 240-247. doi:10.1016/j.canlet.2013.08.021

Lupas, A. N., & Gruber, M. (2005). The structure of alpha-helical coiled coils. *Adv Protein Chem, 70*, 37-78. doi:10.1016/S0065-3233(05)70003-6

Luscher, B. (2012). MAD1 and its life as a MYC antagonist: an update. *Eur J Cell Biol, 91*(6-7), 506-514. doi:10.1016/j.ejcb.2011.07.005

Ma, X. H., Piao, S. F., Dey, S., McAfee, Q., Karakousis, G., Villanueva, J., . . . Amaravadi, R. K. (2014). Targeting ER stress-induced autophagy overcomes BRAF inhibitor resistance in melanoma. *J Clin Invest, 124*(3), 1406-1417. doi:10.1172/JCI70454

Macpherson, I. R., Rainero, E., Mitchell, L. E., van den Berghe, P. V., Speirs, C., Dozynkiewicz, M. A., . . . Norman, J. C. (2014). CLIC3 controls recycling of late endosomal MT1-MMP and dictates invasion and metastasis in breast cancer. *J Cell Sci, 127*(Pt 18), 3893-3901. doi:10.1242/jcs.135947

Magana-Garcia, M., & Ackerman, A. B. (1990). What are nevus cells? *Am J Dermatopathol, 12*(1), 93-102.

Magnusdottir, E., Dietmann, S., Murakami, K., Gunesdogan, U., Tang, F., Bao, S., . . . Azim Surani, M. (2013). A tripartite transcription factor network regulates primordial germ cell specification in mice. *Nat Cell Biol, 15*(8), 905-915. doi:10.1038/ncb2798

Magnuson, B., Ekim, B., & Fingar, D. C. (2012). Regulation and function of ribosomal protein S6 kinase (S6K) within mTOR signalling networks. *Biochem J, 441*(1), 1-21. doi:10.1042/BJ20110892

Mansky, K. C., Sankar, U., Han, J., & Ostrowski, M. C. (2002). Microphthalmia transcription factor is a target of the p38 MAPK pathway in response to receptor activator of NF-kappa B ligand signaling. *J Biol Chem, 277*(13), 11077-11083. doi:10.1074/jbc.M111696200

Marais, R., Light, Y., Paterson, H. F., Mason, C. S., & Marshall, C. J. (1997). Differential regulation of Raf-1, A-Raf, and B-Raf by oncogenic ras and tyrosine kinases. *J Biol Chem, 272*(7), 4378-4383.

Marchand, B., Arsenault, D., Raymond-Fleury, A., Boisvert, F. M., & Boucher, M. J. (2015). Glycogen synthase kinase-3 (GSK3) inhibition induces prosurvival autophagic signals in human pancreatic cancer cells. *J Biol Chem, 290*(9), 5592-5605. doi:10.1074/jbc.M114.616714

Marino, M. L., Pellegrini, P., Di Lernia, G., Djavaheri-Mergny, M., Brnjic, S., Zhang, X., . . . De Milito, A. (2012). Autophagy is a protective mechanism for human melanoma cells under acidic stress. *J Biol Chem, 287*(36), 30664-30676. doi:10.1074/jbc.M112.339127

Markovic, S. N., Erickson, L. A., Rao, R. D., Weenig, R. H., Pockaj, B. A., Bardia, A., . . . Melanoma Study Group of the Mayo Clinic Cancer, C. (2007). Malignant melanoma in the 21st century, part 1: epidemiology, risk factors, screening, prevention, and diagnosis. *Mayo Clin Proc, 82*(3), 364-380. doi:10.4065/82.3.364

Martina, J. A., Chen, Y., Gucek, M., & Puertollano, R. (2012). MTORC1 functions as a transcriptional regulator of autophagy by preventing nuclear transport of TFEB. *Autophagy, 8*(6), 903-914. doi:10.4161/auto.19653

Martina, J. A., Diab, H. I., Li, H., & Puertollano, R. (2014). Novel roles for the MiTF/TFE family of transcription factors in organelle biogenesis, nutrient sensing, and energy homeostasis. *Cell Mol Life Sci, 71*(13), 2483-2497. doi:10.1007/s00018-014-1565-8

Martina, J. A., Diab, H. I., Lishu, L., Jeong, A. L., Patange, S., Raben, N., & Puertollano, R. (2014). The nutrient-responsive transcription factor TFE3 promotes autophagy, lysosomal biogenesis, and clearance of cellular debris. *Sci Signal, 7*(309), ra9. doi:10.1126/scisignal.2004754

Martina, J. A., & Puertollano, R. (2013). Rag GTPases mediate amino acid-dependent recruitment of TFEB and MITF to lysosomes. *J Cell Biol, 200*(4), 475-491. doi:10.1083/jcb.201209135

Martinez-Lopez, N., Athonvarangkul, D., & Singh, R. (2015). Autophagy and aging. *Adv Exp Med Biol, 847*, 73-87. doi:10.1007/978-1-4939-2404-2_3

Maruotti, J., Thein, T., Zack, D. J., & Esumi, N. (2012). MITF-M, a 'melanocyte-specific' isoform, is expressed in the adult retinal pigment epithelium. *Pigment Cell & Melanoma Research, 25*(5), 641-644. doi:10.1111/j.1755-148X.2012.01033.x

Mathew, R., Kongara, S., Beaudoin, B., Karp, C. M., Bray, K., Degenhardt, K., . . . White, E. (2007). Autophagy suppresses tumor progression by

limiting chromosomal instability. *Genes Dev, 21*(11), 1367-1381. doi:10.1101/gad.1545107

Maurer, G., Tarkowski, B., & Baccarini, M. (2011). Raf kinases in cancer-roles and therapeutic opportunities. *Oncogene, 30*(32), 3477-3488. doi:10.1038/onc.2011.160

McLeay, R. C., & Bailey, T. L. (2010). Motif Enrichment Analysis: a unified framework and an evaluation on ChIP data. *BMC Bioinformatics, 11*, 165. doi:10.1186/1471-2105-11-165

Medina, D. L., Di Paola, S., Peluso, I., Armani, A., De Stefani, D., Venditti, R., . . . Ballabio, A. (2015). Lysosomal calcium signalling regulates autophagy through calcineurin and TFEB. *Nat Cell Biol, 17*(3), 288-299. doi:10.1038/ncb3114

Medina, D. L., Fraldi, A., Bouche, V., Annunziata, F., Mansueto, G., Spampanato, C., . . . Ballabio, A. (2011). Transcriptional activation of lysosomal exocytosis promotes cellular clearance. *Dev Cell, 21*(3), 421-430. doi:10.1016/j.devcel.2011.07.016

Michaloglou, C., Vredeveld, L. C., Soengas, M. S., Denoyelle, C., Kuilman, T., van der Horst, C. M., . . . Peeper, D. S. (2005). BRAFE600-associated senescence-like cell cycle arrest of human naevi. *Nature, 436*(7051), 720-724. doi:10.1038/nature03890

Miller, A. J., Levy, C., Davis, I. J., Razin, E., & Fisher, D. E. (2005). Sumoylation of MITF and its related family members TFE3 and TFEB. *J Biol Chem, 280*(1), 146-155. doi:10.1074/jbc.M411757200

Mitra, D., Luo, X., Morgan, A., Wang, J., Hoang, M. P., Lo, J., . . . Fisher, D. E. (2012). An ultraviolet-radiation-independent pathway to melanoma carcinogenesis in the red hair/fair skin background. *Nature, 491*(7424), 449-453. doi:10.1038/nature11624

Mizushima, N., & Komatsu, M. (2011). Autophagy: renovation of cells and tissues. *Cell, 147*(4), 728-741. doi:10.1016/j.cell.2011.10.026

Mizushima, N., Kuma, A., Kobayashi, Y., Yamamoto, A., Matsubae, M., Takao, T., . . . Yoshimori, T. (2003). Mouse Apg16L, a novel WD-repeat protein, targets to the autophagic isolation membrane with the Apg12-Apg5 conjugate. *J Cell Sci, 116*(Pt 9), 1679-1688.

Mizushima, N., Yamamoto, A., Hatano, M., Kobayashi, Y., Kabeya, Y., Suzuki, K., . . . Yoshimori, T. (2001). Dissection of autophagosome formation using Apg5-deficient mouse embryonic stem cells. *J Cell Biol, 152*(4), 657-668.

Mizushima, N., Yoshimori, T., & Ohsumi, Y. (2011). The role of Atg proteins in autophagosome formation. *Annu Rev Cell Dev Biol, 27*, 107-132. doi:10.1146/annurev-cellbio-092910-154005

Möller, K. (2016). *The role of MITF in autophagy regulation in melanoma.* (MSc), University of Iceland,

Monastyrska, I., Rieter, E., Klionsky, D. J., & Reggiori, F. (2009). Multiple roles of the cytoskeleton in autophagy. *Biol Rev Camb Philos Soc, 84*(3), 431-448. doi:10.1111/j.1469-185X.2009.00082.x

Monteiro, P., Rosse, C., Castro-Castro, A., Irondelle, M., Lagoutte, E., Paul-Gilloteaux, P., . . . Chavrier, P. (2013). Endosomal WASH and exocyst complexes control exocytosis of MT1-MMP at invadopodia. *J Cell Biol, 203*(6), 1063-1079. doi:10.1083/jcb.201306162

Muller, J., Krijgsman, O., Tsoi, J., Robert, L., Hugo, W., Song, C., . . . Peeper, D. S. (2014). Low MITF/AXL ratio predicts early resistance to multiple targeted drugs in melanoma. *Nat Commun, 5*, 5712. doi:10.1038/ncomms6712

Murakami, H., & Arnheiter, H. (2005). Sumoylation modulates transcriptional activity of MITF in a promoter-specific manner. *Pigment Cell Res, 18*(4), 265-277. doi:10.1111/j.1600-0749.2005.00234.x

Murre, C., McCaw, P. S., & Baltimore, D. (1989). A new DNA binding and dimerization motif in immunoglobulin enhancer binding, daughterless, MyoD, and myc proteins. *Cell, 56*(5), 777-783.

Nair, U., Yen, W. L., Mari, M., Cao, Y., Xie, Z., Baba, M., . . . Klionsky, D. J. (2012). A role for Atg8-PE deconjugation in autophagosome biogenesis. *Autophagy, 8*(5), 780-793. doi:10.4161/auto.19385

Nakagawa, Y., Shimano, H., Yoshikawa, T., Ide, T., Tamura, M., Furusawa, M., . . . Yamada, N. (2006). TFE3 transcriptionally activates hepatic IRS-2, participates in insulin signaling and ameliorates diabetes. *Nat Med, 12*(1), 107-113. doi:10.1038/nm1334

Newell, G. R., Sider, J. G., Bergfelt, L., & Kripke, M. L. (1988). Incidence of cutaneous melanoma in the United States by histology with special reference to the face. *Cancer Res, 48*(17), 5036-5041.

Ngeow, K. C., Friedrichsen, H. J., Li, L., Zeng, Z., Andrews, S., Volpon, L., . . . Goding, C. R. (2018). BRAF/MAPK and GSK3 signaling converges to control MITF nuclear export. *Proc Natl Acad Sci U S A, 115*(37), E8668-E8677. doi:10.1073/pnas.1810498115

Olive, M. F., Koenig, H. N., Nannini, M. A., & Hodge, C. W. (2001). Stimulation of endorphin neurotransmission in the nucleus accumbens by ethanol, cocaine, and amphetamine. *J Neurosci, 21*(23), RC184.

Opdecamp, K., Nakayama, A., Nguyen, M. T., Hodgkinson, C. A., Pavan, W. J., & Arnheiter, H. (1997). Melanocyte development in vivo and in neural crest cell cultures: crucial dependence on the Mitf basic-helix-loop-helix-zipper transcription factor. *Development, 124*(12), 2377-2386.

Palmer, J. S., Duffy, D. L., Box, N. F., Aitken, J. F., O'Gorman, L. E., Green, A. C., . . . Sturm, R. A. (2000). Melanocortin-1 receptor polymorphisms and risk of melanoma: is the association explained solely by pigmentation phenotype? *Am J Hum Genet, 66*(1), 176-186. doi:10.1086/302711

Palmieri, M., Impey, S., Kang, H., di Ronza, A., Pelz, C., Sardiello, M., & Ballabio, A. (2011). Characterization of the CLEAR network reveals an integrated control of cellular clearance pathways. *Hum Mol Genet, 20*(19), 3852-3866. doi:10.1093/hmg/ddr306

Palmieri, M., Pal, R., Nelvagal, H. R., Lotfi, P., Stinnett, G. R., Seymour, M. L., . . . Sardiello, M. (2017). mTORC1-independent TFEB activation via Akt inhibition promotes cellular clearance in neurodegenerative storage diseases. *Nat Commun, 8*, 14338. doi:10.1038/ncomms14338

Park, P. J. (2009). ChIP-seq: advantages and challenges of a maturing technology. *Nat Rev Genet, 10*(10), 669-680. doi:10.1038/nrg2641

Pastore, N., Brady, O. A., Diab, H. I., Martina, J. A., Sun, L., Huynh, T., . . . Puertollano, R. (2016). TFEB and TFE3 cooperate in the regulation of the innate immune response in activated macrophages. *Autophagy, 12*(8), 1240-1258. doi:10.1080/15548627.2016.1179405

Pawelek, J., Wong, G., Sansone, M., & Morowitz, J. (1973). Molecular biology of pigment cells. Molecular controls in mammalian pigmentation. *Yale J Biol Med, 46*(5), 430-443.

Pena-Llopis, S., Vega-Rubin-de-Celis, S., Schwartz, J. C., Wolff, N. C., Tran, T. A., Zou, L., . . . Brugarolas, J. (2011). Regulation of TFEB and V-ATPases by mTORC1. *EMBO J, 30*(16), 3242-3258. doi:10.1038/emboj.2011.257

Pende, M., Um, S. H., Mieulet, V., Sticker, M., Goss, V. L., Mestan, J., . . . Thomas, G. (2004). S6K1(-/-)/S6K2(-/-) mice exhibit perinatal lethality and rapamycin-sensitive 5'-terminal oligopyrimidine mRNA translation and reveal a mitogen-activated protein kinase-dependent S6 kinase pathway. *Mol Cell Biol, 24*(8), 3112-3124.

Perera, R. M., Stoykova, S., Nicolay, B. N., Ross, K. N., Fitamant, J., Boukhali, M., . . . Bardeesy, N. (2015). Transcriptional control of autophagy-lysosome function drives pancreatic cancer metabolism. *Nature, 524*(7565), 361-365. doi:10.1038/nature14587

Perera, R. M., & Zoncu, R. (2016). The Lysosome as a Regulatory Hub. *Annu Rev Cell Dev Biol, 32*, 223-253. doi:10.1146/annurev-cellbio-111315-125125

Peters, C., & Mayer, A. (1998). Ca2+/calmodulin signals the completion of docking and triggers a late step of vacuole fusion. *Nature, 396*(6711), 575-580. doi:10.1038/25133

Peterson, T. R., Laplante, M., Thoreen, C. C., Sancak, Y., Kang, S. A., Kuehl, W. M., . . . Sabatini, D. M. (2009). DEPTOR is an mTOR inhibitor frequently overexpressed in multiple myeloma cells and required for their survival. *Cell, 137*(5), 873-886. doi:10.1016/j.cell.2009.03.046

Pham, L., Kaiser, B., Romsa, A., Schwarz, T., Gopalakrishnan, R., Jensen, E. D., & Mansky, K. C. (2011). HDAC3 and HDAC7 have opposite effects on osteoclast differentiation. *J Biol Chem, 286*(14), 12056-12065. doi:10.1074/jbc.M110.216853

Phung, B., Sun, J., Schepsky, A., Steingrimsson, E., & Ronnstrand, L. (2011). C-KIT signaling depends on microphthalmia-associated transcription factor for effects on cell proliferation. *PLoS One, 6*(8), e24064. doi:10.1371/journal.pone.0024064

Ploper, D., Taelman, V. F., Robert, L., Perez, B. S., Titz, B., Chen, H. W., . . . De Robertis, E. M. (2015). MITF drives endolysosomal biogenesis and potentiates Wnt signaling in melanoma cells. *Proc Natl Acad Sci U S A, 112*(5), E420-429. doi:10.1073/pnas.1424576112

Pogenberg, V., Ogmundsdottir, M. H., Bergsteinsdottir, K., Schepsky, A., Phung, B., Deineko, V., . . . Wilmanns, M. (2012). Restricted leucine zipper dimerization and specificity of DNA recognition of the melanocyte master regulator MITF. *Genes Dev, 26*(23), 2647-2658. doi:10.1101/gad.198192.112

Pollock, P. M., Harper, U. L., Hansen, K. S., Yudt, L. M., Stark, M., Robbins, C. M., . . . Meltzer, P. S. (2003). High frequency of BRAF mutations in nevi. *Nat Genet, 33*(1), 19-20. doi:10.1038/ng1054

Potterf, S. B., Furumura, M., Dunn, K. J., Arnheiter, H., & Pavan, W. J. (2000). Transcription factor hierarchy in Waardenburg syndrome: regulation of MITF expression by SOX10 and PAX3. *Hum Genet, 107*(1), 1-6.

Poulikakos, P. I., Persaud, Y., Janakiraman, M., Kong, X., Ng, C., Moriceau, G., . . . Solit, D. B. (2011). RAF inhibitor resistance is mediated by dimerization of aberrantly spliced BRAF(V600E). *Nature, 480*(7377), 387-390. doi:10.1038/nature10662

Price, E. R., Ding, H. F., Badalian, T., Bhattacharya, S., Takemoto, C., Yao, T. P., . . . Fisher, D. E. (1998). Lineage-specific signaling in melanocytes. C-kit stimulation recruits p300/CBP to microphthalmia. *J Biol Chem, 273*(29), 17983-17986.

Price, E. R., Horstmann, M. A., Wells, A. G., Weilbaecher, K. N., Takemoto, C. M., Landis, M. W., & Fisher, D. E. (1998). alpha-Melanocyte-stimulating hormone signaling regulates expression of microphthalmia, a gene deficient in Waardenburg syndrome. *J Biol Chem, 273*(49), 33042-33047.

Primot, A., Mogha, A., Corre, S., Roberts, K., Debbache, J., Adamski, H., . . . Galibert, M. D. (2010). ERK-regulated differential expression of the Mitf 6a/b splicing isoforms in melanoma. *Pigment Cell Melanoma Res, 23*(1), 93-102. doi:10.1111/j.1755-148X.2009.00652.x

Pu, J., Guardia, C. M., Keren-Kaplan, T., & Bonifacino, J. S. (2016). Mechanisms and functions of lysosome positioning. *J Cell Sci, 129*(23), 4329-4339. doi:10.1242/jcs.196287

Puertollano, R., Ferguson, S. M., Brugarolas, J., & Ballabio, A. (2018). The complex relationship between TFEB transcription factor phosphorylation and subcellular localization. *EMBO J, 37*(11). doi:10.15252/embj.201798804

Rambow, F., Job, B., Petit, V., Gesbert, F., Delmas, V., Seberg, H., . . . Larue, L. (2015). New Functional Signatures for Understanding Melanoma Biology from Tumor Cell Lineage-Specific Analysis. *Cell Rep, 13*(4), 840-853. doi:10.1016/j.celrep.2015.09.037

Ramphal, R., Pappo, A., Zielenska, M., Grant, R., & Ngan, B. Y. (2006). Pediatric renal cell carcinoma: clinical, pathologic, and molecular abnormalities associated with the members of the mit transcription factor family. *Am J Clin Pathol, 126*(3), 349-364. doi:10.1309/98YE9E442AR7LX2X

Raposo, G., & Marks, M. S. (2002). The dark side of lysosome-related organelles: specialization of the endocytic pathway for melanosome biogenesis. *Traffic, 3*(4), 237-248.

Raposo, G., & Marks, M. S. (2007). Melanosomes--dark organelles enlighten endosomal membrane transport. *Nat Rev Mol Cell Biol, 8*(10), 786-797. doi:10.1038/nrm2258

Raposo, G., Tenza, D., Murphy, D. M., Berson, J. F., & Marks, M. S. (2001). Distinct protein sorting and localization to premelanosomes, melanosomes, and lysosomes in pigmented melanocytic cells. *J Cell Biol, 152*(4), 809-824.

Read, A. P., & Newton, V. E. (1997). Waardenburg syndrome. *Journal of Medical Genetics, 34*(8), 656-665. doi:DOI 10.1136/jmg.34.8.656

Ritt, D. A., Daar, I. O., & Morrison, D. K. (2006). KSR regulation of the Raf-MEK-ERK cascade. *Methods Enzymol, 407*, 224-237. doi:10.1016/S0076-6879(05)07019-9

Rivers, J. K. (2004). Is there more than one road to melanoma? *Lancet, 363*(9410), 728-730. doi:10.1016/S0140-6736(04)15649-3

Robinson, J. T., Thorvaldsdottir, H., Winckler, W., Guttman, M., Lander, E. S., Getz, G., & Mesirov, J. P. (2011). Integrative genomics viewer. *Nat Biotechnol, 29*(1), 24-26. doi:10.1038/nbt.1754

Roczniak-Ferguson, A., Petit, C. S., Froehlich, F., Qian, S., Ky, J., Angarola, B., . . . Ferguson, S. M. (2012). The transcription factor TFEB links mTORC1 signaling to transcriptional control of lysosome homeostasis. *Sci Signal, 5*(228), ra42. doi:10.1126/scisignal.2002790

Roh, M. R., Eliades, P., Gupta, S., & Tsao, H. (2015). Genetics of melanocytic nevi. *Pigment Cell Melanoma Res, 28*(6), 661-672. doi:10.1111/pcmr.12412

Romeo, Y., Moreau, J., Zindy, P. J., Saba-El-Leil, M., Lavoie, G., Dandachi, F., . . . Roux, P. P. (2013). RSK regulates activated BRAF signalling to mTORC1 and promotes melanoma growth. *Oncogene, 32*(24), 2917-2926. doi:10.1038/onc.2012.312

Rubinsztein, D. C., Marino, G., & Kroemer, G. (2011). Autophagy and aging. *Cell, 146*(5), 682-695. doi:10.1016/j.cell.2011.07.030

Russell, R. C., Tian, Y., Yuan, H., Park, H. W., Chang, Y. Y., Kim, J., . . . Guan, K. L. (2013). ULK1 induces autophagy by phosphorylating Beclin-1 and activating VPS34 lipid kinase. *Nat Cell Biol, 15*(7), 741-750. doi:10.1038/ncb2757

Saito, H., Yasumoto, K., Takeda, K., Takahashi, K., Fukuzaki, A., Orikasa, S., & Shibahara, S. (2002). Melanocyte-specific microphthalmia-associated transcription factor isoform activates its own gene promoter through physical interaction with lymphoid-enhancing factor 1. *J Biol Chem, 277*(32), 28787-28794. doi:10.1074/jbc.M203719200

Saito, H., Yasumoto, K., Takeda, K., Takahashi, K., Yamamoto, H., & Shibahara, S. (2003). Microphthalmia-associated transcription factor in the Wnt signaling pathway. *Pigment Cell Res, 16*(3), 261-265.

Salo, J., Lehenkari, P., Mulari, M., Metsikko, K., & Vaananen, H. K. (1997). Removal of osteoclast bone resorption products by transcytosis. *Science, 276*(5310), 270-273.

Samie, M., & Cresswell, P. (2015). The transcription factor TFEB acts as a molecular switch that regulates exogenous antigen-presentation pathways. *Nat Immunol, 16*(7), 729-736. doi:10.1038/ni.3196

Sancak, Y., Peterson, T. R., Shaul, Y. D., Lindquist, R. A., Thoreen, C. C., Bar-Peled, L., & Sabatini, D. M. (2008). The Rag GTPases bind raptor and mediate amino acid signaling to mTORC1. *Science, 320*(5882), 1496-1501. doi:10.1126/science.1157535

Sancak, Y., Thoreen, C. C., Peterson, T. R., Lindquist, R. A., Kang, S. A., Spooner, E., . . . Sabatini, D. M. (2007). PRAS40 is an insulin-regulated inhibitor of the mTORC1 protein kinase. *Mol Cell, 25*(6), 903-915. doi:10.1016/j.molcel.2007.03.003

Sarbassov, D. D., Guertin, D. A., Ali, S. M., & Sabatini, D. M. (2005). Phosphorylation and regulation of Akt/PKB by the rictor-mTOR

complex. *Science, 307*(5712), 1098-1101. doi:10.1126/science.1106148

Sardiello, M., Palmieri, M., di Ronza, A., Medina, D. L., Valenza, M., Gennarino, V. A., . . . Ballabio, A. (2009). A gene network regulating lysosomal biogenesis and function. *Science, 325*(5939), 473-477. doi:10.1126/science.1174447

Sato, M., Morii, E., Takebayashi-Suzuki, K., Yasui, N., Ochi, T., Kitamura, Y., & Nomura, S. (1999). Microphthalmia-associated transcription factor interacts with PU.1 and c-Fos: determination of their subcellular localization. *Biochem Biophys Res Commun, 254*(2), 384-387. doi:10.1006/bbrc.1998.9918

Sato, S., Roberts, K., Gambino, G., Cook, A., Kouzarides, T., & Goding, C. R. (1997). CBP/p300 as a co-factor for the Microphthalmia transcription factor. *Oncogene, 14*(25), 3083-3092. doi:DOI 10.1038/sj.onc.1201298

Schepsky, A., Bruser, K., Gunnarsson, G. J., Goodall, J., Hallsson, J. H., Goding, C. R., . . . Hecht, A. (2006). The microphthalmia-associated transcription factor Mitf interacts with beta-catenin to determine target gene expression. *Mol Cell Biol, 26*(23), 8914-8927. doi:10.1128/MCB.02299-05

Schioth, H. B., Phillips, S. R., Rudzish, R., Birch-Machin, M. A., Wikberg, J. E., & Rees, J. L. (1999). Loss of function mutations of the human melanocortin 1 receptor are common and are associated with red hair. *Biochem Biophys Res Commun, 260*(2), 488-491. doi:10.1006/bbrc.1999.0935

Settembre, C., & Ballabio, A. (2014). Lysosomal Adaptation: How the Lysosome Responds to External Cues. *Cold Spring Harbor Perspectives in Biology, 6*(6). doi:ARTN a016907

10.1101/cshperspect.a016907

Settembre, C., De Cegli, R., Mansueto, G., Saha, P. K., Vetrini, F., Visvikis, O., . . . Ballabio, A. (2013). TFEB controls cellular lipid metabolism through a starvation-induced autoregulatory loop. *Nat Cell Biol, 15*(6), 647-658. doi:10.1038/ncb2718

Settembre, C., Di Malta, C., Polito, V. A., Garcia Arencibia, M., Vetrini, F., Erdin, S., . . . Ballabio, A. (2011). TFEB links autophagy to lysosomal biogenesis. *Science, 332*(6036), 1429-1433. doi:10.1126/science.1204592

Settembre, C., Zoncu, R., Medina, D. L., Vetrini, F., Erdin, S., Erdin, S., . . . Ballabio, A. (2012). A lysosome-to-nucleus signalling mechanism senses and regulates the lysosome via mTOR and TFEB. *EMBO J, 31*(5), 1095-1108. doi:10.1038/emboj.2012.32

Shain, A. H., Yeh, I., Kovalyshyn, I., Sriharan, A., Talevich, E., Gagnon, A., . . . Bastian, B. C. (2015). The Genetic Evolution of Melanoma from Precursor Lesions. *N Engl J Med, 373*(20), 1926-1936. doi:10.1056/NEJMoa1502583

Sheen, J. H., Zoncu, R., Kim, D., & Sabatini, D. M. (2011). Defective regulation of autophagy upon leucine deprivation reveals a targetable liability of human melanoma cells in vitro and in vivo. *Cancer Cell, 19*(5), 613-628. doi:10.1016/j.ccr.2011.03.012

Shi, H., Hugo, W., Kong, X., Hong, A., Koya, R. C., Moriceau, G., . . . Lo, R. S. (2014). Acquired resistance and clonal evolution in melanoma during BRAF inhibitor therapy. *Cancer Discov, 4*(1), 80-93. doi:10.1158/2159-8290.CD-13-0642

Shibahara, S., Takeda, K., Yasumoto, K., Udono, T., Watanabe, K., Saito, H., & Takahashi, K. (2001). Microphthalmia-associated transcription factor (MITF): multiplicity in structure, function, and regulation. *J Investig Dermatol Symp Proc, 6*(1), 99-104. doi:10.1046/j.0022-202x.2001.00010.x

Sigvaldadóttir, I. (2016). *Functional analysis of the dREQ MITF mutant. Determination of the nuclear localization and transcription activation potential of an MITF mutant lacking three amino acids.* (BSc), University of Iceland,

Smith, S. D., Kelley, P. M., Kenyon, J. B., & Hoover, D. (2000). Tietz syndrome (hypopigmentation/deafness) caused by mutation of MITF. *Journal of Medical Genetics, 37*(6), 446-448. doi:DOI 10.1136/jmg.37.6.446

Son, J., Kim, M., Jou, I., Park, K. C., & Kang, H. Y. (2014). IFN-gamma inhibits basal and alpha-MSH-induced melanogenesis. *Pigment Cell Melanoma Res, 27*(2), 201-208. doi:10.1111/pcmr.12190

Sonnenblick, A., Levy, C., & Razin, E. (2004). Interplay between MITF, PIAS3, and STAT3 in mast cells and melanocytes. *Mol Cell Biol, 24*(24), 10584-10592. doi:10.1128/MCB.24.24.10584-10592.2004

Sosman, J. A., Kim, K. B., Schuchter, L., Gonzalez, R., Pavlick, A. C., Weber, J. S., . . . Ribas, A. (2012). Survival in BRAF V600-Mutant Advanced Melanoma Treated with Vemurafenib. *New England Journal of Medicine, 366*(8), 707-714. doi:DOI 10.1056/NEJMoa1112302

Stanchina, L., Baral, V., Robert, F., Pingault, V., Lemort, N., Pachnis, V., . . . Bondurand, N. (2006). Interactions between Sox10, Edn3 and Ednrb during enteric nervous system and melanocyte development. *Dev Biol, 295*(1), 232-249. doi:10.1016/j.ydbio.2006.03.031

Steffan, J. J., Dykes, S. S., Coleman, D. T., Adams, L. K., Rogers, D., Carroll, J. L., . . . Cardelli, J. A. (2014). Supporting a role for the GTPase Rab7

in prostate cancer progression. *PLoS One, 9*(2), e87882. doi:10.1371/journal.pone.0087882

Steingrimsson, E., Copeland, N. G., & Jenkins, N. A. (2004). Melanocytes and the Microphthalmia transcription factor network. *Annual Review of Genetics, 38*, 365-411. doi:DOI 10.1146/annurev.genet.38.072902.092717

Steingrimsson, E., Moore, K. J., Lamoreux, M. L., Ferre-D'Amare, A. R., Burley, S. K., Zimring, D. C., . . . et al. (1994). Molecular basis of mouse microphthalmia (mi) mutations helps explain their developmental and phenotypic consequences. *Nat Genet, 8*(3), 256-263. doi:10.1038/ng1194-256

Steingrimsson, E., Tessarollo, L., Pathak, B., Hou, L., Arnheiter, H., Copeland, N. G., & Jenkins, N. A. (2002). Mitf and Tfe3, two members of the Mitf-Tfe family of bHLH-Zip transcription factors, have important but functionally redundant roles in osteoclast development. *Proc Natl Acad Sci U S A, 99*(7), 4477-4482. doi:10.1073/pnas.072071099

Steingrimsson, E., Tessarollo, L., Reid, S. W., Jenkins, N. A., & Copeland, N. G. (1998). The bHLH-Zip transcription factor Tfeb is essential for placental vascularization. *Development, 125*(23), 4607-4616.

Stemig, M., Astelford, K., Emery, A., Cho, J. J., Allen, B., Huang, T. H., . . . Jensen, E. D. (2015). Deletion of histone deacetylase 7 in osteoclasts decreases bone mass in mice by interactions with MITF. *PLoS One, 10*(4), e0123843. doi:10.1371/journal.pone.0123843

Stolt, C. C., Lommes, P., Hillgartner, S., & Wegner, M. (2008). The transcription factor Sox5 modulates Sox10 function during melanocyte development. *Nucleic Acids Res, 36*(17), 5427-5440. doi:10.1093/nar/gkn527

Strub, T., Giuliano, S., Ye, T., Bonet, C., Keime, C., Kobi, D., . . . Davidson, I. (2011). Essential role of microphthalmia transcription factor for DNA replication, mitosis and genomic stability in melanoma. *Oncogene, 30*(20), 2319-2332. doi:10.1038/onc.2010.612

Syn, N. L., Teng, M. W. L., Mok, T. S. K., & Soo, R. A. (2017). De-novo and acquired resistance to immune checkpoint targeting. *Lancet Oncol, 18*(12), e731-e741. doi:10.1016/S1470-2045(17)30607-1

Tachibana, M., Kobayashi, Y., & Matsushima, Y. (2003). Mouse models for four types of Waardenburg syndrome. *Pigment Cell Res, 16*(5), 448-454.

Takamura, A., Komatsu, M., Hara, T., Sakamoto, A., Kishi, C., Waguri, S., . . . Mizushima, N. (2011). Autophagy-deficient mice develop multiple liver tumors. *Genes Dev, 25*(8), 795-800. doi:10.1101/gad.2016211

Takebayashi, K., Chida, K., Tsukamoto, I., Morii, E., Munakata, H., Arnheiter, H., . . . Nomura, S. (1996). The recessive phenotype displayed by a dominant negative microphthalmia-associated transcription factor mutant is a result of impaired nucleation potential. *Mol Cell Biol, 16*(3), 1203-1211.

Takeda, K., Takemoto, C., Kobayashi, I., Watanabe, A., Nobukuni, Y., Fisher, D. E., & Tachibana, M. (2000). Ser298 of MITF, a mutation site in Waardenburg syndrome type 2, is a phosphorylation site with functional significance. *Hum Mol Genet, 9*(1), 125-132.

Takeda, K., Yasumoto, K., Kawaguchi, N., Udono, T., Watanabe, K., Saito, H., . . . Shibahara, S. (2002). Mitf-D, a newly identified isoform, expressed in the retinal pigment epithelium and monocyte-lineage cells affected by Mitf mutations. *Biochim Biophys Acta, 1574*(1), 15-23.

Takeda, K., Yasumoto, K., Takada, R., Takada, S., Watanabe, K., Udono, T., . . . Shibahara, S. (2000). Induction of melanocyte-specific microphthalmia-associated transcription factor by Wnt-3a. *Journal of Biological Chemistry, 275*(19), 14013-14016. doi:DOI 10.1074/jbc.C000113200

Takemoto, C. M., Yoon, Y. J., & Fisher, D. E. (2002). The identification and functional characterization of a novel mast cell isoform of the microphthalmia-associated transcription factor. *J Biol Chem, 277*(33), 30244-30252. doi:10.1074/jbc.M201441200

Tassabehji, M., Read, A. P., Newton, V. E., Harris, R., Balling, R., Gruss, P., & Strachan, T. (1992). Waardenburg's syndrome patients have mutations in the human homologue of the Pax-3 paired box gene. *Nature, 355*(6361), 635-636. doi:10.1038/355635a0

Thirlwell, C., & Nathan, P. (2008). Melanoma—Part 2: management. *BMJ, 337*. doi:10.1136/bmj.a2488

Thomas, A. J., & Erickson, C. A. (2009). FOXD3 regulates the lineage switch between neural crest-derived glial cells and pigment cells by repressing MITF through a non-canonical mechanism. *Development, 136*(11), 1849-1858. doi:10.1242/dev.031989

Thorvaldsdottir, H., Robinson, J. T., & Mesirov, J. P. (2013). Integrative Genomics Viewer (IGV): high-performance genomics data visualization and exploration. *Brief Bioinform, 14*(2), 178-192. doi:10.1093/bib/bbs017

Torra, A., Parent, A., Cuadros, T., Rodriguez-Galvan, B., Ruiz-Bronchal, E., Ballabio, A., . . . Bove, J. (2018). Overexpression of TFEB Drives a Pleiotropic Neurotrophic Effect and Prevents Parkinson's Disease-Related Neurodegeneration. *Mol Ther*. doi:10.1016/j.ymthe.2018.02.022

Tran, N. H., & Frost, J. A. (2003). Phosphorylation of Raf-1 by p21-activated kinase 1 and Src regulates Raf-1 autoinhibition. *J Biol Chem, 278*(13), 11221-11226. doi:10.1074/jbc.M210318200

Tran, N. H., Wu, X., & Frost, J. A. (2005). B-Raf and Raf-1 are regulated by distinct autoregulatory mechanisms. *J Biol Chem, 280*(16), 16244-16253. doi:10.1074/jbc.M501185200

Tshori, S., Sonnenblick, A., Yannay-Cohen, N., Kay, G., Nechushtan, H., & Razin, E. (2007). Microphthalmia transcription factor isoforms in mast cells and the heart. *Mol Cell Biol, 27*(11), 3911-3919. doi:10.1128/MCB.01455-06

Tulsiani, D. R., Abou-Haila, A., Loeser, C. R., & Pereira, B. M. (1998). The biological and functional significance of the sperm acrosome and acrosomal enzymes in mammalian fertilization. *Exp Cell Res, 240*(2), 151-164. doi:10.1006/excr.1998.3943

Vachtenheim, J., Novotna, H., & Ghanem, G. (2001). Transcriptional repression of the microphthalmia gene in melanoma cells correlates with the unresponsiveness of target genes to ectopic microphthalmia-associated transcription factor. *J Invest Dermatol, 117*(6), 1505-1511. doi:10.1046/j.0022-202x.2001.01563.x

Vachtenheim, J., & Ondrusova, L. (2015). Microphthalmia-associated transcription factor expression levels in melanoma cells contribute to cell invasion and proliferation. *Experimental Dermatology, 24*(7), 481-484. doi:10.1111/exd.12724

Valero, T. (2014). Mitochondrial biogenesis: pharmacological approaches. *Curr Pharm Des, 20*(35), 5507-5509.

Valverde, P., Healy, E., Jackson, I., Rees, J. L., & Thody, A. J. (1995). Variants of the melanocyte-stimulating hormone receptor gene are associated with red hair and fair skin in humans. *Nat Genet, 11*(3), 328-330. doi:10.1038/ng1195-328

Van Allen, E. M., Wagle, N., Sucker, A., Treacy, D. J., Johannessen, C. M., Goetz, E. M., . . . Dermatologic Cooperative Oncology Group of, G. (2014). The genetic landscape of clinical resistance to RAF inhibition in metastatic melanoma. *Cancer Discov, 4*(1), 94-109. doi:10.1158/2159-8290.CD-13-0617

Vega-Rubin-de-Celis, S., Pena-Llopis, S., Konda, M., & Brugarolas, J. (2017). Multistep regulation of TFEB by MTORC1. *Autophagy, 13*(3), 464-472. doi:10.1080/15548627.2016.1271514

Verastegui, C., Bertolotto, C., Bille, K., Abbe, P., Ortonne, J. P., & Ballotti, R. (2000). TFE3, a transcription factor homologous to microphthalmia, is a potential transcriptional activator of tyrosinase and Tyrpl genes. *Mol Endocrinol, 14*(3), 449-456. doi:10.1210/mend.14.3.0428

Vlckova, K., Vachtenheim, J., Reda, J., Horak, P., & Ondrusova, L. (2018). Inducibly decreased MITF levels do not affect proliferation and phenotype switching but reduce differentiation of melanoma cells. *J Cell Mol Med, 22*(4), 2240-2251. doi:10.1111/jcmm.13506

Wan, P. T., Garnett, M. J., Roe, S. M., Lee, S., Niculescu-Duvaz, D., Good, V. M., . . . Cancer Genome, P. (2004). Mechanism of activation of the RAF-ERK signaling pathway by oncogenic mutations of B-RAF. *Cell, 116*(6), 855-867.

Webster, D. E., Barajas, B., Bussat, R. T., Yan, K. J., Neela, P. H., Flockhart, R. J., . . . Khavari, P. A. (2014). Enhancer-targeted genome editing selectively blocks innate resistance to oncokinase inhibition. *Genome Res, 24*(5), 751-760. doi:10.1101/gr.166231.113

Weilbaecher, K. N., Hershey, C. L., Takemoto, C. M., Horstmann, M. A., Hemesath, T. J., Tashjian, A. H., & Fisher, D. E. (1998). Age-resolving osteopetrosis: a rat model implicating microphthalmia and the related transcription factor TFE3. *J Exp Med, 187*(5), 775-785.

Welinder, C., Jonsson, G. B., Ingvar, C., Lundgren, L., Baldetorp, B., Olsson, H., . . . Marko-Varga, G. (2014). Analysis of alpha-synuclein in malignant melanoma - development of a SRM quantification assay. *PLoS One, 9*(10), e110804. doi:10.1371/journal.pone.0110804

Wellbrock, C., & Arozarena, I. (2015). Microphthalmia-associated transcription factor in melanoma development and MAP-kinase pathway targeted therapy. *Pigment Cell Melanoma Res, 28*(4), 390-406. doi:10.1111/pcmr.12370

Wellbrock, C., Karasarides, M., & Marais, R. (2004). The RAF proteins take centre stage. *Nat Rev Mol Cell Biol, 5*(11), 875-885. doi:10.1038/nrm1498

Wellbrock, C., & Marais, R. (2005). Elevated expression of MITF counteracts B-RAF-stimulated melanocyte and melanoma cell proliferation. *J Cell Biol, 170*(5), 703-708. doi:10.1083/jcb.200505059

Wellbrock, C., Rana, S., Paterson, H., Pickersgill, H., Brummelkamp, T., & Marais, R. (2008). Oncogenic BRAF regulates melanoma proliferation through the lineage specific factor MITF. *PLoS One, 3*(7), e2734. doi:10.1371/journal.pone.0002734

Wen, H., Zhan, L., Chen, S., Long, L., & Xu, E. (2017). Rab7 may be a novel therapeutic target for neurologic diseases as a key regulator in autophagy. *J Neurosci Res, 95*(10), 1993-2004. doi:10.1002/jnr.24034

White, E., & DiPaola, R. S. (2009). The double-edged sword of autophagy modulation in cancer. *Clin Cancer Res, 15*(17), 5308-5316. doi:10.1158/1078-0432.CCR-07-5023

Whiteman, D. C., Green, A. C., & Olsen, C. M. (2016). The Growing Burden of Invasive Melanoma: Projections of Incidence Rates and Numbers of New Cases in Six Susceptible Populations through 2031. *J Invest Dermatol, 136*(6), 1161-1171. doi:10.1016/j.jid.2016.01.035

Wolfson, R. L., Chantranupong, L., Saxton, R. A., Shen, K., Scaria, S. M., Cantor, J. R., & Sabatini, D. M. (2016). Sestrin2 is a leucine sensor for the mTORC1 pathway. *Science, 351*(6268), 43-48. doi:10.1126/science.aab2674

Wu, M., Hemesath, T. J., Takemoto, C. M., Horstmann, M. A., Wells, A. G., Price, E. R., . . . Fisher, D. E. (2000). c-Kit triggers dual phosphorylations, which couple activation and degradation of the essential melanocyte factor Mi. *Genes Dev, 14*(3), 301-312.

Xie, X., Koh, J. Y., Price, S., White, E., & Mehnert, J. M. (2015). Atg7 Overcomes Senescence and Promotes Growth of BrafV600E-Driven Melanoma. *Cancer Discov, 5*(4), 410-423. doi:10.1158/2159-8290.CD-14-1473

Xie, Z., Nair, U., & Klionsky, D. J. (2008). Atg8 controls phagophore expansion during autophagosome formation. *Mol Biol Cell, 19*(8), 3290-3298. doi:10.1091/mbc.E07-12-1292

Xu, W., Gong, L., Haddad, M. M., Bischof, O., Campisi, J., Yeh, E. T., & Medrano, E. E. (2000). Regulation of microphthalmia-associated transcription factor MITF protein levels by association with the ubiquitin-conjugating enzyme hUBC9. *Exp Cell Res, 255*(2), 135-143. doi:10.1006/excr.2000.4803

Xue, G., Kohler, R., Tang, F., Hynx, D., Wang, Y., Orso, F., . . . Wicki, A. (2017). mTORC1/autophagy-regulated MerTK in mutant BRAFV600 melanoma with acquired resistance to BRAF inhibition. *Oncotarget, 8*(41), 69204-69218. doi:10.18632/oncotarget.18213

Yang, S., Wang, X., Contino, G., Liesa, M., Sahin, E., Ying, H., . . . Kimmelman, A. C. (2011). Pancreatic cancers require autophagy for tumor growth. *Genes Dev, 25*(7), 717-729. doi:10.1101/gad.2016111

Yasumoto, K., & Shibahara, S. (1997). Molecular cloning of cDNA encoding a human TFEC isoform, a newly identified transcriptional regulator. *Biochim Biophys Acta, 1353*(1), 23-31.

Yasumoto, K., Takeda, K., Saito, H., Watanabe, K., Takahashi, K., & Shibahara, S. (2002). Microphthalmia-associated transcription factor interacts with LEF-1, a mediator of Wnt signaling. *EMBO J, 21*(11), 2703-2714. doi:10.1093/emboj/21.11.2703

Yazdi, A. S., Palmedo, G., Flaig, M. J., Puchta, U., Reckwerth, A., Rutten, A., . . . Sander, C. A. (2003). Mutations of the BRAF gene in benign and

malignant melanocytic lesions. *J Invest Dermatol, 121*(5), 1160-1162. doi:10.1046/j.1523-1747.2003.12559.x

Yeh, J. E., Toniolo, P. A., & Frank, D. A. (2013). Targeting transcription factors: promising new strategies for cancer therapy. *Current Opinion in Oncology, 25*(6), 652-658. doi:10.1097/01.cco.0000432528.88101.1a

Yokoyama, S., Woods, S. L., Boyle, G. M., Aoude, L. G., MacGregor, S., Zismann, V., . . . Brown, K. M. (2011). A novel recurrent mutation in MITF predisposes to familial and sporadic melanoma. *Nature, 480*(7375), 99-103. doi:10.1038/nature10630

Yoshida, H., Kunisada, T., Grimm, T., Nishimura, E. K., Nishioka, E., & Nishikawa, S. I. (2001). Review: melanocyte migration and survival controlled by SCF/c-kit expression. *J Investig Dermatol Symp Proc, 6*(1), 1-5. doi:10.1046/j.0022-202x.2001.00006.x

Young, N. P., Kamireddy, A., Van Nostrand, J. L., Eichner, L. J., Shokhirev, M. N., Dayn, Y., & Shaw, R. J. (2016). AMPK governs lineage specification through Tfeb-dependent regulation of lysosomes. *Genes Dev, 30*(5), 535-552. doi:10.1101/gad.274142.115

Zhang, T., Zhou, Q., Ogmundsdottir, M. H., Moller, K., Siddaway, R., Larue, L., . . . Pignoni, F. (2015). Mitf is a master regulator of the v-ATPase, forming a control module for cellular homeostasis with v-ATPase and TORC1. *J Cell Sci, 128*(15), 2938-2950. doi:10.1242/jcs.173807

Zhao, G. Q., Zhao, Q., Zhou, X., Mattei, M. G., & de Crombrugghe, B. (1993). TFEC, a basic helix-loop-helix protein, forms heterodimers with TFE3 and inhibits TFE3-dependent transcription activation. *Mol Cell Biol, 13*(8), 4505-4512.

Zhu, J., Blenis, J., & Yuan, J. (2008). Activation of PI3K/Akt and MAPK pathways regulates Myc-mediated transcription by phosphorylating and promoting the degradation of Mad1. *Proc Natl Acad Sci U S A, 105*(18), 6584-6589. doi:10.1073/pnas.0802785105

Zoncu, R., Efeyan, A., & Sabatini, D. M. (2011). mTOR: from growth signal integration to cancer, diabetes and ageing. *Nat Rev Mol Cell Biol, 12*(1), 21-35. doi:10.1038/nrm3025

# Appendix I

## Buffers

### LTB

93.5 g Tris-HCl (pH 8.8)

2 g SDS

500 mL distilled water

### UTB

30.5 g Tris-HCl (pH 6.8)

2 g SDS

500 mL distilled water

### Running Buffer 1X

3.03 g Tris Base

14.4 g Glycine

1 g SDS

1L $H_20$

### Transfer Buffer 1X

3.03 g Tris Base

14.4 g Glycine

0.5 g SDS

200 mL Methanol

800 mL $H_20$

### TBS

10 mL 1M Tris-HCl (pH 7.4)

30 mL 5M NaCl

Fill to 1 L $H_2O$

# Appendix II

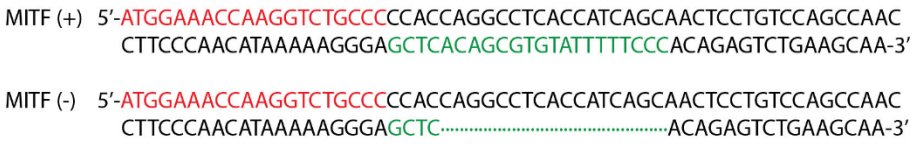


**Figure 38. MITF (+) primers aligned to the cDNA sequence of human MITF (+) or (-).** Primers are listed in Table 8. The sequence aligned by the forward primer is marked in red, whereas the (+) isoform-specific sequence aligned by the reverse primer is marked in green.

# Appendix III

**Table 15. List of pigmentation genes (GO:0043473)**

| Gene | Protein product |
|---|---|
| *ADAMTS20* | ADAM metallopeptidase with thrombospondin type 1 motif 20 |
| *ADAMTS9* | ADAM metallopeptidase with thrombospondin type 1 motif 9 |
| *AP1G1* | adaptor related protein complex 1 gamma 1 subunit |
| *AP1M1* | adaptor related protein complex 1 mu 1 subunit |
| *AP3B1* | adaptor related protein complex 3 beta 1 subunit |
| *AP3D1* | adaptor related protein complex 3 delta 1 subunit |
| *ARCN1* | archain 1 |
| *ARL6* | ADP ribosylation factor like GTPase 6 |
| *ASIP* | agouti signaling protein |
| *ATP6AP2* | ATPase H+ transporting accessory protein 2 |
| *ATP7A* | ATPase copper transporting alpha |
| *ATRN* | attractin |
| *BAX* | BCL2 associated X, apoptosis regulator |
| *BBS2* | Bardet-Biedl syndrome 2 |
| *BBS4* | Bardet-Biedl syndrome 4 |
| *BBS5* | Bardet-Biedl syndrome 5 |
| *BBS7* | Bardet-Biedl syndrome 7 |
| *BCL2* | BCL2, apoptosis regulator |
| *BCL2L11* | BCL2 like 11 |
| *BLOC1S1* | biogenesis of lysosomal organelles complex 1 subunit 1 |
| *BLOC1S3* | biogenesis of lysosomal organelles complex 1 subunit 3 |
| *BLOC1S4* | biogenesis of lysosomal organelles complex 1 subunit 4 |
| *BLOC1S5* | biogenesis of lysosomal organelles complex 1 subunit 5 |
| *BLOC1S6* | biogenesis of lysosomal organelles complex 1 subunit 6 |
| *C10orf11* | chromosome 10 open reading frame 11 |
| *C12orf10* | chromosome 12 open reading frame 10 |
| *CD63* | CD63 molecule |
| *CDH3* | cadherin 3 |
| *CITED1* | Cbp/p300 interacting transactivator with Glu/Asp rich carboxy-terminal domain 1 |
| *DCT* | dopachrome tautomerase |
| *DCTN1* | dynactin subunit 1 |
| *DCTN2* | dynactin subunit 2 |
| *DOCK7* | dedicator of cytokinesis 7 |
| *DRD2* | dopamine receptor D2 |

| | |
|---|---|
| *DTNBP1* | dystrobrevin binding protein 1 |
| *EDA* | ectodysplasin A |
| *EDAR* | ectodysplasin A receptor |
| *EDN3* | endothelin 3 |
| *EDNRB* | endothelin receptor type B |
| *EN1* | engrailed homeobox 1 |
| *FIG4* | FIG4 phosphoinositide 5-phosphatase |
| *GLI3* | GLI family zinc finger 3 |
| *GNA11* | G protein subunit alpha 11 |
| *GNAQ* | G protein subunit alpha q |
| *GPR143* | G protein-coupled receptor 143 |
| *HPS1* | HPS1, biogenesis of lysosomal organelles complex 3 subunit 1 |
| *HPS3* | HPS3, biogenesis of lysosomal organelles complex 2 subunit 1 |
| *HPS4* | HPS4, biogenesis of lysosomal organelles complex 3 subunit 2 |
| *HPS5* | HPS5, biogenesis of lysosomal organelles complex 2 subunit 2 |
| *HPS6* | HPS6, biogenesis of lysosomal organelles complex 2 subunit 3 |
| *IHH* | indian hedgehog |
| *KIF13A* | kinesin family member 13A |
| *KIT* | KIT proto-oncogene receptor tyrosine kinase |
| *KITLG* | KIT ligand |
| *LEF1* | lymphoid enhancer binding factor 1 |
| *LYST* | lysosomal trafficking regulator |
| *MAP2K1* | mitogen-activated protein kinase kinase 1 |
| *MC1R* | melanocortin 1 receptor |
| *MEF2C* | myocyte enhancer factor 2C |
| *MITF* | melanogenesis associated transcription factor |
| *MKKS* | McKusick-Kaufman syndrome |
| *MLPH* | melanophilin |
| *MREG* | melanoregulin |
| *MYO5A* | myosin VA |
| *MYO7A* | myosin VIIA |
| *NF1* | neurofibromin 1 |
| *OCA2* | OCA2 melanosomal transmembrane protein |
| *PAX3* | paired box 3 |
| *PMEL* | premelanosome protein |
| *POMC* | proopiomelanocortin |
| *RAB11A* | RAB11A, member RAS oncogene family |
| *RAB11B* | RAB11B, member RAS oncogene family |
| *RAB17* | RAB17, member RAS oncogene family |
| *RAB1A* | RAB1A, member RAS oncogene family |
| *RAB25* | RAB25, member RAS oncogene family |
| *RAB27A* | RAB27A, member RAS oncogene family |
| *RAB27B* | RAB27B, member RAS oncogene family |
| *RAB29* | RAB29, member RAS oncogene family |

| | |
|---|---|
| *RAB32* | RAB32, member RAS oncogene family |
| *RAB38* | RAB38, member RAS oncogene family |
| *SHROOM2* | shroom family member 2 |
| *SHROOM3* | shroom family member 3 |
| *SNAI2* | snail family transcriptional repressor 2 |
| *SNAPIN* | SNAP associated protein |
| *SOD2* | superoxide dismutase 2, mitochondrial |
| *SOX10* | SRY-box 10 |
| *SPNS2* | sphingolipid transporter 2 |
| *SZT2* | seizure threshold 2 homolog (mouse) |
| *TH* | tyrosine hydroxylase |
| *TYR* | tyrosinase |
| *TYRP1* | tyrosinase related protein 1 |
| *USP13* | ubiquitin specific peptidase 13 (isopeptidase T-3) |
| *VPS33A* | VPS33A, CORVET/HOPS core subunit |
| *VPS33B* | VPS33B, late endosome and lysosome associated |
| *ZEB2* | zinc finger E-box binding homeobox 2 |
| *ZIC2* | zic family member 2 |

**Table 16. List of lysosomal and autophagy-related genes**

| Gene | Protein product |
|---|---|
| *ACD* | shelterin complex subunit and telomerase recruitment factor |
| *AGA* | aspartylglucosaminidase |
| *ANPEP* | alanyl (membrane) aminopeptidase |
| *ARL8B* | ADP-ribosylation factor-like 8B |
| *ARSA* | arylsulfatase-peptidase A |
| *ARSB* | arylsulfatase-peptidase B |
| *ASAH1* | N-acylsphingosine amidohydrolase (acid cermidase) 1 |
| *ASNA1* | arsenite-stimulated ATPase component of the arsenite transporter |
| *ATG10* | autophagy related 10 homolog |
| *ATG12* | autophagy related 12 homolog |
| *ATG13* | autophagy related 13 homolog |
| *ATG14* | autophagy related 14 homolog |
| *ATG16L1* | autophagy related 16-like 1 |
| *ATG16L2* | autophagy related 16-like 2 |
| *ATG2A* | autophagy related 2 homolog A |
| *ATG2B* | autophagy related 2 homolog B |
| *ATG3* | autophagy related 3 homolog |
| *ATG4A* | autophagy related 4 homolog A |

| | |
|---|---|
| *ATG4B* | autophagy related 4 homolog B |
| *ATG4C* | autophagy related 4 homolog C |
| *ATG4D* | autophagy related 4 homolog D |
| *ATG5* | autophagy related 5 homolog |
| *ATG7* | autophagy related 7 homolog |
| *ATG9A* | autophagy related 9 homolog A |
| *ATG9B* | autophagy related 9 homolog B |
| *ATP13A2* | ATPase type 13A2 |
| *ATP6V0D2* | ATPase, H+ transporting, lysosomal 38 kDa V0 subunit d2 |
| *ATP6V1B1* | ATPase, H+ transporting, lysosomal 56/58 kDa V0 subunit B1 |
| *ATP6V1G3* | ATPase, H+ transporting, lysosomal 13 kDa V0 subunit G3 |
| *ATP6V0A1* | ATPase, H+ transporting, lysosomal V0 subunit a1 |
| *ATP6V0A2* | ATPase, H+ transporting, lysosomal V0 subunit a2 |
| *ATP6V0A4* | ATPase, H+ transporting, lysosomal V0 subunit a4 |
| *ATP6V0B* | ATPase, H+ transporting, lysosomal 21 kDa V0 subunit b |
| *ATP6V0C* | ATPase, H+ transporting, lysosomal 16 kDa, V0 subunit c |
| *ATP6V0D1* | ATPase, H+ transporting, lysosomal 38 kDa V0 subunit d1 |
| *ATP6V0E1* | ATPase, H+ transporting, lysosomal V0 subunit E1 |
| *ATP6V0E2* | ATPase, H+ transporting, lysosomal V0 subunit E2 |
| *ATP6V1A* | ATPase, H+ transporting, lysosomal 70 kDa, V1 subunit A |
| *ATP6V1B2* | ATPase, H+ transporting, lysosomal 56/58kDa, V1 subunit B2 |
| *ATP6V1C1* | ATPase, H+ transporting, lysosomal 42 kDa, V1 subunit C1 |
| *ATP6V1C2* | ATPase, H+ transporting, lysosomal 42 kDa, V1 subunit C2 |
| *ATP6V1D* | ATPase, H+ transporting, lysosomal 34 kDa, V1 subunit D |
| *ATP6V1E1* | ATPase, H+ transporting, lysosomal 31 kDa, V1 subunit E1 |
| *ATP6V1E2* | ATPase, H+ transporting, lysosomal V1 subunit E2 |
| *ATP6V1F* | ATPase, H+ transporting, lysosomal 14 kDa, V1 subunit F |
| *ATP6V1G1* | ATPase, H+ transporting, lysosomal 13 kDa, V1 subunit G1 |
| *ATP6V1H* | ATPase, H+ transporting, lysosomal 50/57 kDa, V1 subunit H |
| *BECN1* | beclin 1 (coiled-coil, myosin-like BCL2 interacting protein) |
| *CD63* | CD63 molecule (also known as LIMP1 or tetraspanin) |
| *CLCN5* | chloride channel 5 (nephrolithiasis 2, X-linked, Dent disease) |
| *CLCN6* | chloride channel 6 |
| *CLCN7* | chloride channel 7 |
| *CLN3* | ceroid-lipofuscinosis, neuronal 2, juvenille |
| *CREG1* | cellular repressor of E1A-stimulated genes 1 |
| *CTNS* | cystinosis, nephropathic |
| *CTSA* | cathepsin A |
| *CTSB* | cathepsin B |

| | |
|---|---|
| *CTSC* | catheptin C |
| *CTSD* | cathepsin D |
| *CTSF* | cathepsin F |
| *CTSH* | cathepsin H |
| *CTSK* | cathepsin K |
| *CTSL* | cathepsin L/L1 |
| *CTSV* | cathepsin V/L2 |
| *CTSO* | cathepsin O |
| *CTSS* | cathepsin S |
| *CTSZ* | cathepsin Z |
| *CTSE* | cathepsin E |
| *CTSG* | cathepsin G |
| *CTSW* | cathepsin W |
| *DNASE2* | deoxyribonuclease II, lysosomal |
| *DPP4* | dipeptydyl-peptidase 4 |
| *DPP7* | dipeptydyl-peptidase 7 |
| *FUCA1* | fucosidase, alpha-L 1, tissue |
| *GAA* | glucosidase, alpha |
| *GABARAP* | GABA(A) receptor-associated protein 2 |
| *GABARAPL1* | GABA(A) receptor-associated protein like 1 |
| *GABARAPL2* | GABA(A) receptor-associated protein like 2 |
| *GABARAPL3* | GABA(A) receptor-associated protein like 3 |
| *GALC* | galactosylceramidase |
| *GBA* | Glucosidase beta (Gaucher disease) |
| *GLB1L* | galactosidase, beta 1-like |
| *GM2A* | GM2 ganglioside activator |
| *GNS* | glucosamine (N-acetyl)-6-sulfatase (Sanfilippo disease IIID) |
| *HEXA* | hexosaminidase A (alpha polypeptide) |
| *HEXB* | hexosaminidase B (beta polypeptide) |
| *HGSNAT* | heparan-alpha-glucosaminide N-acetyltransferase |
| *HPS1* | Hermansky-Pudiak syndrome 1 |
| *HPS4* | Hermansky-Pudiak syndrome 4 |
| *IDS* | iduronate 2-sulfatase (Hunter syndrome) |
| *LAMP1* | lysosomal-associated membrane protein 1 |
| *LAMP2* | lysosomal-associated membrane protein 2 |
| *LAMTOR1* | late endosome/lysosomal adaptor, MAPK and MTOR activator 1 |
| *LAMTOR2* | late endosome/lysosomal adaptor, MAPK and MTOR activator 2 |
| *LAPTM4B* | lysosomal associated protein transmembrane 4 |
| *LIPA* | lipase A, lysosomal acid, cholesterol estarase |

| | |
|---|---|
| *MANBA* | mannosidase, beta A, lysosomal |
| *MAP1LC3A* | microtubule-associated protein 1 light chain 3 alpha |
| *MAP1LC3B* | microtubule-associated protein 1 light chain 3 beta |
| *MAP1LC3B2* | microtubule-associated protein 1 light chain 3 beta 2 |
| *MCOLN1* | mucolipin 1 (mucolipidosis type IV) |
| *MTCH1* | mitochondrial carrier 1 |
| *NAGA* | N-acetylgalactosaminidase, alpha |
| *NAGLU* | N-acetylglucosaminidase, alpha |
| *NPC1* | Neimann-Pick disease, type C1 |
| *NPC2* | Neimann-Pick disease, type C2 |
| *PIK3C3* | phosphoinositide-3-kinase, class 3 |
| *PIK3CG* | phosphoinositide-3-kinase,catalytic, gamma polypeptide |
| *PPT1* | palmytoyl-protein thioesterase 1 |
| *PSAP* | prosaposin |
| *SCARB2* | scavenger receptor class B, member 2 |
| *SFTPA1* | surfactant protein A1 |
| *SFTPA2* | surfactant protein A2 |
| *SGSH* | N-sulfoglucosamine sufohydrolase |
| *SLC11A2* | solute carrier family 11, member 2 |
| *SLC12A4* | solute carrier family 12, member 4 |
| *SLC17A5* | solute carrier family 17, member 5 |
| *SLC26A11* | solute carrier family 26, member 11 |
| *SLC29A3* | solute carrier family 29, member 3 |
| *SLC2A8* | solute carrier family 2, member 8 |
| *SLC36A1* | solute carrier family 36, member 1 |
| *SLC44A2* | solute carrier family 44, member 2 |
| *SMPD1* | sphingomyelin phosphodiesterase 1 |
| *SNCA* | synuclein, alpha |
| *SQSTM1* | sequestosome 1 |
| *TMEM175* | transmembrane protein 175 |
| *TMEM55A* | transmembrane protein 55A |
| *TMEM63A* | transmembrane protein 63A |
| *TPP1* | tripeptidyl peptidase I |
| *TTPA* | alpha tocopherol transfer protein |
| *ULK1* | unc-51-like kinase 1 |
| *ULK2* | unc-51-like kinase 2 |
| *UVRAG* | UV radiation resistance associated gene |
| *VAMP1* | vesicle-associated membrane protein 1 |
| *VPS8* | vacuolar protein sorting 8 homolog |

| | |
|---|---|
| *VPS11* | vacuolar protein sorting 11 homolog |
| *VPS18* | vacuolar protein sorting 18 homolog |
| *VPS33A* | vacuolar protein sorting 33 homolog A |
| *WIPI1* | WD repeat domain, phosphoinositide interacting 1 |

# Appendix IV

**Table 17. RT-qPCR analysis of the expression of MITF, TFEB and TFE3 in 501Mel and A375P cell lines.**

| | 501Mel Ct value ratio | A375P Ct value ratio |
|---|---|---|
| MITF/actin | 1.049 | 1.1465 |
| TFEB/actin | 1.323 | 1.4775 |
| TFE3/actin | 1.2645 | 1.299 |